INVESTIGATING NEUTROPHIL DYSFUNCTION IN COVID-19, UNDERLYING DISEASE MECHANISMS AND RELATIONSHIP TO CLINICAL OUTCOMES

by

ONN SHAUN THEIN

A thesis submitted to the University of Birmingham for the degree of

DOCTOR OF PHILOSOPHY

Supervisors:

Dr Dhruv Parekh, Dr Aaron Scott and Professor David Thickett

Institute of Inflammation and Ageing

College of Medical and Dental Sciences

University of Birmingham

December 2023

Abstract

Coronavirus disease 2019 (COVID-19) caused by the severe acute respiratory syndrome coronavirus 2 (SARS-CoV-2) caused a world-wide pandemic in March 2020. Since first identified, over 30 different variants have been identified, with dominant strains causing waves of infection mirrored in hospital admissions and mortality. Rapid collaborative research into understanding the host-virus interactions and to develop treatment strategies led to repurposing of several therapeutics to improve patient outcomes.

The innate immune system is the first-line cellular defence against pathogens, and responsible for the initiation, maintenance and recruitment and resolution of inflammation. Disruption to any point of this process can lead to an inadequate response, either with insufficient recruitment of cells or prolonged inflammation. Neutrophils are involved with all these processes and represent the largest leucocyte subpopulation.

This thesis aimed to investigate the role of neutrophils in COVID-19 infection, to determine how their function was altered in disease and how this correlated with clinical outcomes. By investigating the effect of inhibitory molecules and therapeutics, we investigated the potential pathways that may be disrupted leading to altered neutrophil function. Viral evolution and the changes to the clinical phenotype are important to note as this may affect therapeutic efficacy, and this thesis compared neutrophil effector functions between alpha, delta and omicron variant COVID-19 patients.

Neutrophil effector functions such as phagocytosis, migration and neutrophil extracellular trap formation were examined, in addition to surface marker expression. All experiments were adapted for investigator safety with a novel infectious disease, and these were validated to demonstrate equivalency. Clinical data and outcome measures (e.g. length of hospital stay, long- and short-term mortality) from recruited patients and age-matched controls were collected to correlate to any changes in neutrophil effector functions.

Compared to age matched controls and community acquired pneumonia patients, neutrophils isolated from alpha variant patients demonstrated decreased phagocytosis, with reduced

nuclear/ mitochondrial reactive oxygen species generation, increased migration, increased neutrophil extracellular trap formation (NETosis) and altered surface marker expression. This constellation of changes could suggest pseudopod dysfunction related to phosphoinositide 3-kinase (PI3K) signalling, but inhibition of PI3K did not restore function in COVID-19 neutrophils. Similarly, there was no improvement with the use of treatments affecting neutrophil elastase, which may account for increased migration.

Neutrophils isolated from patients with omicron COVID-19 demonstrated decreased migration and NETosis compared to alpha variant COVID-19. Surface marker expression was unique to omicron compared to alpha variant neutrophils and there was a decrease in circulating vascular endothelial growth factor and myeloperoxidase with increased interleukin-6.

The neutrophil dysfunction seen in alpha variant patients did not persist to omicron variant patients which correlates to the less severe clinical phenotype observed. This data presented in this thesis supports the hypothesis that neutrophil dysfunction COVID-19 contributes to the clinical symptoms observed. The treatments and pathway inhibitors investigated here did not restore neutrophil function, suggesting a mechanism separate to PI3K signalling and neutrophil elastase activity. The differences in function and clinical data seen between SARS-CoV-2 strains suggests further investigation into currently recommended COVID-19 treatments is required to determine their efficacy with the evolving disease.

For my family

Acknowledgements

I am incredibly grateful to everyone for the advice, laboratory help and emotional support that you have given me throughout my PhD. I am also grateful to the Birmingham Health Partners for providing me with a starter fellowship to allow to me to start this doctorate. There are so many people without whom I would not have been able to complete this thesis and I would like to highlight a few people.

Firstly to Dhruv – for the endless support and faith in me as a clinical academic. You not only supervised this PhD but have been a clinical mentor and someone who always made time for me despite your hectic schedule. I feel lucky and honoured to be your first of what will be many PhD students. Aaron – thank you for being the voice of reason of all laboratory work when I was stuck or needed advice. Your open office door might make it difficult for you to get work done, but I can't count the number of times I've been relieved you were there for me to ask you something. David – thank you for appointing me as an ACF all those years ago, and always being in my corner. Your support clinically and academically has always been unfaltering, and it has always been appreciated.

To Kylie – I couldn't have done this without your help. I'll always remember the months we spent locked doing experiments in the COVID lab and your no nonsense get on with it approach. Jon – thank you for all your help, advice and expertise with the experiments needed for this project. You've helped so much with reviewing manuscripts and are always so efficient with everything!

To the respiratory group – my friends – I can't begin to name everyone who is currently in the group or has been in the past. You have all contributed to me remaining sane and being able to complete this thesis. We've enjoyed celebrating the highs and being there for each other in the tough times as well; it's been an honour to be there through it all. Thank you to my friends who have encouraged me throughout my academic journey and supported me and my family.

To Mum and Dad, thank you for supporting me my entire life and giving me the education and tools to be able to get me this far. Thank you to my brother for always setting the bar high and inspiring me to be my best self.

Finally, thank you to my wife, Emma. You are the smartest, most caring person I know, and I am so lucky to walk side by side through life with you. You have always been my rock, my better half and the voice of common sense in my head. Throughout this PhD you have looked after me and our two children and kept me on track. I honestly couldn't have done this without you.

COVID-19 Declaration

This project was born from the COVID-19 pandemic, in a scientific environment which was rapidly evolving. The adjustments to scientific experimentation are described and validated in this thesis. Literature and similar studies conducted at the same time are discussed in the relevant chapter discussion sections and the general discussion as opposed to being reviewed in the introduction of this thesis.

Table of Contents

Contents

1 CHAPTER 1 21

1.1 Background/ Lay Summary 22
1.2 The respiratory immune system 23
1.3 Neutrophils 25
1.3.1 Overview of function 25
1.3.2 Neutrophils in disease 33
1.4 COVID-19 37
1.4.1 Epidemiology 37
1.4.2 Viral pathology and natural history 37
1.4.3 Evolution 39
1.4.4 Clinical considerations 42
1.4.5 Evolving therapies and vaccines 48
1.4.6 Vaccines 49
1.5 Neutrophils in COVID-19 50
1.5.1 Patient populations 51
1.5.2 Effector function alteration 52
1.6 Summary 58

2 CHAPTER 2 60

2.1 Hypothesis 61
2.2 Aims 61
2.3 Scope of thesis and research 62

3 CHAPTER 3 63

3.1 Materials 64
3.2 Methods 66
3.2.1 Subject selection 66
3.2.2 Sample processing 70
3.2.3 Cell isolation 71
3.2.4 Functional experiments 75
3.2.5 ELISA 82
3.2.6 Surface marker phenotyping 85
3.2.7 Western blotting 88
3.2.8 Phosphoinositide-3-kinase (PI3K) 89
3.2.9 Effect of selected pharmacological agents on neutrophil function 90
3.2.10 Clinical scoring systems 90
3.2.11 Statistical analysis 94
3.2.12 Power calculations 96

3.2.13 Method limitations 96
4 CHAPTER 4 99
4.1 Introduction 100
4.2 Fixation 101
4.2.1 Phagocytosis 102
4.2.2 Transwell migration 114
4.2.3 NETosis 116
4.3 PI3K inhibitor viability 118
4.4 Dexamethasone 118
4.4.1 Phagocytosis 120
4.4.2 Transwell migration 120
4.4.3 NETosis 121
4.5 Carbon dioxide incubation 123
4.5.1 Phagocytosis and viability 123
4.5.2 Transwell migration 125
4.5.3 NETosis 126
4.6 Bacterial fluorescence 127
4.7 Discussion 129
4.8 Summary of adaptations 131
5 CHAPTER 5 132
5.1 Introduction 133
5.2 Aims of Chapter 5 134
5.3 Clinical phenotype 134
5.3.1 Patient demographics 134
5.3.2 Biochemical correlations 136
5.3.3 Severity scoring correlations 138
5.4 Discussion 145
5.4.1 Demographics 145
5.4.2 Time from symptom onset to presentation 146
5.4.3 Conclusion 147
6 CHAPTER 6 148
6.1 Introduction 149
6.1.1 PI3K inhibition 149
6.1.2 Effect of selected pharmacological agents on neutrophil function 150
6.2 Aims of Chapter 6 154
6.3 Neutrophil effector functions 155
6.3.1 Phagocytosis 155
6.3.2 Neutrophil migration 157

6.3.3 NETosis ... 158
6.3.4 Circulating inflammatory mediators ... 161
6.3.5 Surface marker phenotype ... 162
6.3.6 Day 3-5 follow-up ... 163
6.4 Relationship of clinical phenotype to function ... 169
6.4.1 Clinical outcomes ... 169
6.4.2 4C score ... 172
6.4.3 Circulating inflammatory mediators ... 174
6.4.4 ARDS ... 175
6.5 PI3K inhibition ... 176
6.5.1 Clinical phenotype ... 176
6.5.2 Neutrophil effector functions ... 178
6.6 Effects of selected pharmacological agents on neutrophil function ... 180
6.7 Discussion ... 183
6.7.1 Cellular outcomes ... 183
6.7.2 PI3K inhibition ... 188
6.7.3 Effect of selected pharmacological agents ... 190
6.7.4 Limitations ... 191
6.7.5 Conclusion ... 193
7 CHAPTER 7 ... 194
7.1 Introduction ... 195
7.2 Aims of Chapter 7 ... 196
7.3 Additional patient recruitment ... 197
7.4 Clinical phenotype ... 198
7.4.1 Patient demographics ... 198
7.4.2 Biochemical correlations ... 200
7.5 Functional assays ... 204
7.5.1 Phagocytosis ... 204
7.5.2 Transwell migration ... 206
7.5.3 NETosis ... 207
7.5.4 Circulating inflammatory mediators ... 208
7.5.5 Surface marker phenotype ... 210
7.6 Relationship of clinical phenotype to function ... 212
7.6.1 Clinical outcomes ... 212
7.6.2 4C ... 217
7.6.3 Vaccination status ... 219
7.7 Omicron comparison to AMC and CAP ... 221
7.8 Discussion ... 227
7.8.1 Clinical outcomes ... 227

7.8.2 Cellular outcomes 227
7.8.3 Compared to AMC and CAP 229
7.8.4 Limitations 232
7.8.5 Conclusion 232
8 CHAPTER 8 234
8.1 Overall findings 235
8.1.1 Clinical 236
8.1.2 Neutrophil effector functions 237
8.1.3 Surface marker expression 238
8.1.4 Mechanisms and treatments 239
8.2 What does this study contribute to the field? 239
8.3 Clinical implications 240
8.4 Study strengths 240
8.5 Study limitations 241
8.6 Future directions 243
8.7 Conclusions 245
9 REFERENCES 246

Papers published from the work in this thesis:

- *'Dysregulated neutrophil phenotype and function in hospitalised non-ICU COVID-19 pneumonia'*, KBR Belchamber, **OS Thein**, J Hazeldine, FS Grudzinska, AA Faniyi, MJ Hughes, AE Jasper, LE Crowley, KP Yip, ST Lugg, E Sapey, D Parekh, David R Thickett, A Scott; 2022; Cells; PMID: 36139476 (joint 1st author)

Conference presentations from the work in this thesis:

- '*Dysfunctional neutrophil response in COVID-19 infection vary by subtype*', 2023, **OS Thein**, KBR Belchamber, J Hazeldine, FS Grudzinska, AA Faniyi, MJ Hughes, AE Jasper, LE Crowley, KP Yip, ST Lugg, E Sapey, D Parekh, DR Thickett, A Scott
  Association of Physicians of Great Britain and Ireland Annual Conference, Liverpool, Poster Presentation (Presenter)

- *'Dysfunctional neutrophil response in COVID-19 infection vary by subtype*', 2023, **OS Thein**, KBR Belchamber, J Hazeldine, FS Grudzinska, AA Faniyi, MJ Hughes, AE Jasper, LE Crowley, KP Yip, ST Lugg, E Sapey, D Parekh, DR Thickett, A Scott
  Royal College of Physicians Medicine 2023, London, Poster Presentation (Presenter)

- '*Prolonged neutrophil dysfunction and phenotype in elderly hospitalised community acquired pneumonia patients*', AA Faniyi, FS Grudzinska, **OS Thein,** KBR Belchamber, A Scott, D Parekh, E Sapey, DR Thickett
  British Thoracic Society Winter Meeting 2022, London, Oral Presentation S95

- *'Dysfunctional neutrophil response in COVID-19 infection vary by subtype'*, 2022, **OS Thein**, KBR Belchamber, J Hazeldine, FS Grudzinska, AA Faniyi, MJ Hughes, AE Jasper, LE Crowley, KP Yip, ST Lugg, E Sapey, D Parekh, DR Thickett, A Scott
  British Thoracic Society Winter Meeting 2022, London, Oral Presentation S94 (Presenter)

- '*Neutrophils in elderly hospitalised community acquired pneumonia older patients are immature and migrate inaccurately*', 2022, AA Faniyi, FS Grudzinska, **OS Thein,** KBR Belchamber, A Scott, D Parekh, E Sapey, DR Thickett
  European Respiratory Society Congress 2022, Barcelona, Oral Presentation 4411 (Presenter)

- *COVID-19 neutrophils show elevated migration and NETosis, which is reduced by PI3K inhibition'*, 2022, KBR Belchamber, **OS Thein**, J Hazeldine, FS Grudzinska, AA Faniyi, MJ Hughes, AE Jasper, LE Crowley, KP Yip, ST Lugg, E Sapey, D Parekh, DR Thickett, A Scott
  European Respiratory Society Congress 2022, Barcelona, Oral Presentation 3778 (Presenter)

- *'Elevated NETosis and migration but impaired anti-microbial responses in COVID-19 neutrophils*', 2021, **OS Thein,** KBR Belchamber, J Hazeldine, FS Grudzinska, MJ Hughes, AE Jasper, LE Crowley, KP Yip, ST Lugg, E Sapey, D Parekh, David R Thickett, A Scott
  British Association for Lung Research 2021 Virtual Conference, Virtual, Oral Presentation - PGR Competition

List of Figures

Figure 1.1 Types of neutrophil granules.. 29
Figure 1.2 Neutrophil extracellular trap formation (NETosis). 30
Figure 1.3 Neutrophil functions. 32
Figure 1.4 Neutrophil contributions to viral clearance and pathology.. 36
Figure 1.5 Phylogenetic tree showing the diversification and relationship of the COVID-19 variants to both each other and the wild-type virus as of December 2023 39
Figure 1.6 Graphical description of the SARS CoV-2 virion, with attachment to ACE2 receptor. 41
Figure 1.7 Summary of changes to neutrophil function in COVID-19 infection 58
Figure 3.1 Neutrophil isolation process, after Percoll® centrifugation. 72
Figure 3.2 Neutrophil effector function experiment flow cytometry gating strategy. 78
Figure 3.3 Diagrammatic representation of Transwell migration experiment 79
Figure 3.4 Gating strategy for neutrophil surface receptor expression by flow cytometry. 86
Figure 3.5 Approach used for statistical analysis for single comparisons in this thesis 95
Figure 4.1 Table detailing the introduction of various novel therapies for COVID-19 during the pandemic until the end of patient recruitment (December 2022). 101
Figure 4.2 Isolated neutrophil phagocytosis of labelled *S. pneumonia*, demonstrated as % phagocytosis 103
Figure 4.3 Isolated neutrophil phagocytosis of labelled S. pneumonia, demonstrated as median fluorescent intensity (MFI) 105
Figure 4.4 Isolated neutrophil cytoplasmic reactive oxygen species (cROS) production expressed as median fluorescent intensity (MFI) 107
Figure 4.5 Isolated neutrophil cytoplasmic reactive oxygen species (cROS) production after *S. pneumoniae* phagocytosis expressed as fold change in median fluorescent intensity (MFI) 109
Figure 4.6 Isolated neutrophil nuclear/ mitochondrial reactive oxygen species (n/mROS) production expressed as median fluorescent intensity (MFI) 111
Figure 4.7 Isolated neutrophil nuclear/ mitochondrial reactive oxygen species (n/mROS) production expressed as fold change in median fluorescent intensity (MFI) 112
Figure 4.8 Percentage of labelled *S. aureus* phagocytosed by isolated neutrophils at 30 minutes comparing ice and 4% (v/v) PFA as method of termination of phagocytosis .. 114
Figure 4.9 Comparison of neutrophil migration through a transwell membrane between fixed and unfixed samples. 115
Figure 4.10 Neutrophil extracellular trap production after stimulation with PMA or vehicle control (VC) 117
Figure 4.11 Viability of neutrophils after 30 minutes incubation with pan PI3K inhibitor 118
Figure 4.12 Percentage of neutrophil phagocytosis of labelled *S. pneumoniae* after dexamethasone treatment. 120
Figure 4.13 Comparison of neutrophil migration through a transwell pore between samples treated with dexamethasone and IL-8 (Dexamethasone) and IL-8 only (IL-8). 121
Figure 4.14 Neutrophil extracellular trap formation after PMA stimulation, compared between cells treated with dexamethasone and untreated. 122
Figure 4.15 Comparison of neutrophil incubation in 5% controlled CO_2 (5% CO_2) and atmospheric CO_2 (Atm CO_2) throughout the experiment 124
Figure 4.16 Comparison of neutrophil migration at atmospheric CO_2 (Atm CO_2) and 5% controlled CO_2 (5% CO_2) 125
Figure 4.17 Fluorescence (in reference units (RFU)) recorded of neutrophil extracellular trap production after PMA stimulation in atmospheric CO_2 (Atm CO_2) and 5% controlled CO_2 (5% CO_2) environments 126
Figure 4.18 Comparison over time of bacterial fluorescence of phagocytosed *S. pneumoniae*. 128

Figure 6.1 Phagocytosis assays carried out on neutrophils from AMC, COVID-19 and CAP participants. 156
Figure 6.2 Neutrophil migration through a transwell membrane towards CXCL8, compared between age matched controls (AMC), COVID-19 patients and community acquired pneumonia (CAP) patients.. 157
Figure 6.3 NETosis in COVID-19 after stimulation with PMA. 159
Figure 6.4 Western blot detection of CitH3 in plasma samples from COVID-19 patients and age matched controls (AMC). 160
Figure 6.5 Circulating inflammatory markers in COVID-19 as measured by serum ELISA, ... 161
Figure 6.6 Serial changes in clinical phenotype for COVID-19 patients followed up at day 3-5 after recruitment 164
Figure 6.7 Neutrophil phagocytosis compared between baseline (Day 1) and follow-up (Day 3-5) of labelled *S. pneumoniae* 165
Figure 6.8 Neutrophil transwell migration and NETosis from COVID-19 patients compared between baseline (Day 1) and follow-up (Day 3-5) 166
Figure 6.9 Measured circulating inflammatory mediator expression from lithium-heparin serum taken at Day 1 compared to Day 3-5 after COVID-19 admission 167
Figure 6.10 Neutrophil effector functions in COVID-19 patients when stratified by in-hospital patient mortality. 170
Figure 6.11 Circulating inflammatory mediators compared in COVID-19 patients who survived and died during hospital admission 171
Figure 6.12 Neutrophil effector functions in COVID-19 patients when mortality is stratified using the 4C score. 173
Figure 6.13 Circulating inflammatory mediators in COVID-19 patients stratified by disease severity by 4C score 174
Figure 6.14 Circulating inflammatory mediators in COVID-19 patients stratified by the presence of ARDS defined by SpO2/FiO2 conversion 175
Figure 6.15 Isolated neutrophil phagocytosis from COVID-19 patients of *S. pneumoniae* (SP) after 30 minutes 178
Figure 6.16 Neutrophil transwell migration towards CXCL8 chemoattractant after 90 minutes from COVID-19 patients CXCL8 179
Figure 6.17 COVID-19 neutrophils NET release measured in response to PMA stimulation. 180
Figure 6.18 Neutrophil phagocytosis of *S. pneumoniae* (SP) after 30 minutes. 181
Figure 6.19 Viability of isolated neutrophils after 30 minutes incubation with treatments prior to 30 minutes phagocytosis of labelled *S. pneumoniae*. 181
Figure 6.20 Effect of treatments on neutrophil migration and NETosis on COVID-19 samples 182
Figure 6.21 Summary of changes to cellular function. 184
Figure 7.1 Isolated neutrophil phagocytosis of labelled S. pneumonia after 30 minutes compared between COVID-19 variants 205
Figure 7.2 Neutrophil migration through a transwell membrane compared between variants 206
Figure 7.3 NETosis and circulating cfDNA compared between COVID-19 variants 207
Figure 7.4 Circulating inflammatory mediators, measured by serum ELISA, compared between COVID-19 variants 209
Figure 7.5 Neutrophil effector functions when stratified by length of stay, split between below median (<6 days) and above median (≥6 days) hospital admission for COVID-19 patients with different variant infection. 213
Figure 7.6 Differences in neutrophil effector functions from different COVID-19 variant infections when stratified by time from symptom onset to presentation. 215

Figure 7.7 Differences in circulating inflammatory mediators from different COVID-19 variant infections when stratified by time from symptom onset 216
Figure 7.8 Differences in neutrophil effector functions from different COVID-19 variant infections when stratified by 4C in-hospital mortality risk, split 4C score <9 and ≥9..... 218
Figure 7.9 Neutrophil phagocytosis of labelled *S. pneumoniae* and reactive oxygen species (ROS) generation compared between omicron COVID-19, AMC and CAP 223
Figure 7.10 Neutrophil transwell migration, NETosis after PMA stimulation and serum cfDNA comparison between omicron COVID-19, AMC and CAP 224
Figure 7.11 Summary of changes to cellular function. 230

List of Tables

Table 1.1 Table showing the predominant dates for major strains beyond the wild-type virus. 40
Table 1.2 Berlin criteria for acute respiratory distress syndrome (ARDS). 42
Table 1.3 WHO clinical severity scale. 46
Table 1.4 4C mortality score with interpretation of in-hospital mortality. 47
Table 3.1 Inclusion and exclusion criteria for recruitment of admitted COVID-19 patients. 67
Table 3.2 Table of prioritisation of isolated neutrophil experiments and number of cells required 74
Table 3.3 Lower and upper limits of detection pre-dilution of samples as per manufacturer datasheets for ELISA kits used. 83
Table 3.4 Antibodies used for surface receptor expression detection by flow cytometry. 87
Table 3.5 Final concentrations of PI3K inhibitors used in the functional neutrophil experiments. 89
Table 3.6 Final concentrations of treatments applied in the functional neutrophil experiments. 90
Table 3.7 National Early Warning Score2 (NEWS2) scoring criteria and appropriate response 92
Table 3.8 quick Sequential Organ Failure Assessment (qSOFA). 93
Table 3.9 CURB-65 score with parameters and related 30-day mortality risk 93
Table 3.10 4C score with scoring criteria and breakdown to in-hospital mortality risk groups and percentage risk.. 94
Table 5.1 Recruited patient and AMC demographics 135
Table 5.2 Recruited COVID-19 and CAP patient biochemical results 137
Table 5.3 Disease severity scores calculated based on clinical observations and blood tests done on admission. 139
Table 5.4 Table showing demographics and comorbidity data when COVID-19 and CAP patients are stratified by 4C score <9 and ≥9. 140
Table 5.5 Table showing biochemical clinical measures and severity scores when COVID-19 and CAP patients are stratified by 4C score <9 and ≥9. 140
Table 5.6 COVID-19 and CAP patient clinical outcome data, with follow up outcomes at 28 days, 3, 6, and 9 months after discharge.. 141
Table 5.7 Recruited COVID-19 and CAP patients split by in-hospital mortality with demographics. 142
Table 5.8 Recruited COVID-19 and CAP patients split by in-hospital mortality with biochemical clinical measures and severity scores. 142
Table 5.9 Table showing demographics and comorbidities of COVID-19 and CAP patients split by presentation <7 or ≥7 days (median time from symptom onset to presentation). 144
Table 5.10 Table showing biochemical clinical measures and severity scoring of COVID-19 and CAP patients split by presentation <7 or ≥7 days 144
Table 6.1 Percentage of cells expressing and MFI of isolated neutrophil cell surface markers as measured by flow cytometry 162
Table 6.2 Median fluorescent intensity (MFI) of isolated neutrophil cell surface markers as measured by flow cytometry compared between D1 and D3-5. 168
Table 6.3 Table of patients recruited for investigation of PI3K inhibition and inhibitor experimentation collected at the time of enrolment. 177
Table 7.1 Demographics from recruited patients for alpha, delta and omicron COVID-19 variants, collected at time of enrolment. 199
Table 7.2 Biochemical data from recruited patients, collected at time of enrolment for alpha, delta and omicron COVID-19 patients. 201

Table 7.3 Clinical data from recruited patients, collected at time of enrolment for alpha, delta and omicron COVID-19 patients. 202
Table 7.4 COVID-19 patient clinical outcome data for alpha, delta and omicron COVID-19 patients. 203
Table 7.5 Fold change of omicron COVID-19 surface receptor expression compared to alpha COVID-19. 211
Table 7.6 Table showing demographics of vaccinated vs unvaccinated patients. 219
Table 7.7 Table showing biochemical and severity scoring data for vaccinated and unvaccinated COVID-19 patients. 220
Table 7.8 Demographic data for omicron, AMC and CAP with significance shown. 221
Table 7.9 Biochemical data for omicron and CAP patients with significance shown..... 222
Table 7.10 Disease severity scoring and length of stay for omicron and CAP patients. 222
Table 7.11 Circulating inflammatory mediators in omicron COVID-19, AMC and CAP as measured by ELISA. 225
Table 7.12 Fold change of omicron COVID-19 surface receptor expression compared to AMC of percentage of cells expressing and MFI of isolated neutrophil cell surface markers 226

List of abbreviations

ACE2	Angiotensin converting enzyme 2
AMC	Age matched controls
ANOVA	Analysis of Variance
ARDS	Acute respiratory distress syndrome
BAFF	B-cell activating factor
BAME	Black, Asian and minority ethnic
BHI	Brain Heart Infusion
BMI	Body mass index
BSA	Bovine serum albumin
CAP	Community acquired pneumonia
CD62-L	L-selectin
CDC	US Centre for Disease Control
cfDNA	Cell free DNA
CFS	Clinical frailty score
CitH3	Citrullinated histone 3 protein
CO_2	Carbon dioxide
CoA	Certificate of Analysis
COPD	Chronic obstructive pulmonary disease
COVID-19	Coronavirus disease 2019
cROS	Cytoplasmic reactive oxygen species
CRP	C-reactive protein
CXCL	CXC-chemokine ligand
CXCR	CXC-chemokine receptor
CXR	Chest radiograph
DAD	Diffuse alveolar damage
DAMP	Danger-associated molecular pattern
DMSO	Dimethylsulfoxide
DNA	Deoxyribonucleic acid
DPP-1	Dipeptidyl peptidase 1
EDTA	Ethylenediaminetetraacetic acid
ELISA	Enzyme linked immunosorbent assay
f/s	Filter/sterilised
FACS	Fluorescence activated cell-sorting
FcR	Fc receptors
FGF-23	Fibroblast growth factor-23
fMLP	N-formylmethionine-leucyl-phenylalanine
GCP	Good Clinical Practice
GCS	Glasgow Coma Score
G-CSF	Granulocyte-colony stimulating factor
GDPR	General Data Protection Regulation
Gfi-1	Growth factor independent transcription repressor
GFP-SA	Green fluorescent protein- *Staphylococcus aureus*
GM-CSF	Granulocyte macrophage- colony stimulating factor
GTP	Guanosine-5'-triphosphate
HIV	Human immunodeficiency virus
HS Troponin I	High sensitivity troponin I
HSE	Health and Safety Executive
HSV	Herpes simplex virus
ICU	Intensive care unit
IL-	Interleukin-
IMV	Invasive mechanical ventilation
IQR	Interquartile range

IV	Intravenous
LFA1	Lymphocyte function-associated antigen 1
LFTs	Lateral flow tests
LoS	Length of stay
LPS	Lipopolysaccharide
MAPK	p38 mitogen-activated protein kinase
MERS-CoV	Middle East respiratory syndrome coronavirus
MFI	Median fluorescence intensity
MMP	Metallomatrix proteinases
MPO	Myeloperoxidase
n/m ROS	Nuclear/ mitochondrial reactive oxygen species
NADPH	Nicotinamide adenine dinucleotide phosphate
NE	Neutrophil elastase
NET	Neutrophil extracellular trap
NETosis	Neutrophil extracellular trap formation
NEWS2	National Early Warning Score 2
NF-kB	Nuclear factor kB
NICE	National Institute for Health and Care Excellence
NIR	Near infra-red
NLR	Neutrophil to lymphocyte ratio
NP	Nasopharyngeal
NSP	Neutrophil serine proteases
ONS	UK Office of National Statistics
PAD4	Peptidylarginene deiminase 4
PAMP	Pathogen-associated molecular pattern
PBMC	Peripheral blood mononuclear cells
PBS	Phosphate buffered saline
PCA	Principle component analysis
PCR	Polymerase chain reaction
PFA	Paraformaldehyde
PI3K	Phosphoinositide-3-kinase
PIP3	Phosphoinositol 3,4,5-triphosphate
PMA	Phorbol 12-myristate 13-acetate
PO	Per oral
PR3	Proteinase 3
PRR	Pattern recognition receptors
QEHB	Queen Elizabeth Hospital Birmingham
qSOFA	Quick Sepsis related Organ Failure Assessment Score
REC	Research ethics committee
RNA	Ribonucleic acid
ROS	Reactive oxygen species
RPMI medium	Roswell Park Memorial Institute medium
RSV	Respiratory syncytial virus
RT-PCR	Reverse transcriptase polymerase chain reaction
S. pneumoniae	*Streptococcus pneumoniae*
SARS-CoV-2	Severe acute respiratory syndrome coronavirus 2
SDF-1	Stromal cell-derived factor-1
SEM	Standard error of the mean
SIRS	Systemic inflammatory response syndrome
SIV	Simian immunodeficiency virus
sTNFR1	Soluble tumour necrosis factor receptor 1
TBS	Tris buffered saline
TLR	Toll like receptors
TNF	Tumour necrosis factor
UTC	Untreated control

v/v	Volume per volume concentration
VEGF	Vascular endothelial growth factor
w/v	Weight per volume concentration
WCC	White cell count
WHO	World Health Organisation
α1AT	Alpha-1 antitrypsin
α2M	Alpha-2 macroglobulin

CHAPTER 1
INTRODUCTION

1.1 Background/ Lay Summary

Coronavirus disease 2019 (COVID-19) caused by infection with the virus severe acute respiratory syndrome coronavirus 2 (SARS-CoV-2) has shaped all areas of daily life since it was declared a world-wide pandemic by the World Health Organisation in March 2020. Treatments to help people were quickly investigated at the same time as research into how the virus affected cells. This was a necessary approach, but for most diseases, treatments are based on how the disease affects cells. Therefore, the cell research is done well before any treatments are trialled.

Neutrophils are the most common white blood cell in the blood. They help with inflammation after an injury or infection, recruiting other white blood cells to the correct location. If they do not work properly, this can cause more severe infections. COVID-19 can cause too much inflammation and build-up of fluid in the lung. This is unlike other viral infections. We wanted to investigate if the virus was affecting the way neutrophils function and adding to the disease. If so, determining the affected parts of the cell might lead to more treatments, and explain why some treatments did not work in the way we expected.

Viruses are very simple organisms and can mutate quickly to form new strains. This can mean treatments that originally worked may not work as well with new strains. The SARS-CoV-2 virus has evolved since the first time it was discovered, and people with COVID-19 display very different symptoms in subsequent strains compared to 2020. We wanted to see if there was a difference in the way neutrophils function between strains.

1.2 The respiratory immune system

The mammalian respiratory system is a closed end mucosal interface with the external environment. Despite defences such as nasal hair follicles and the epiglottis, the system is exposed to several antigens, particles, pollutants and microbes on a regular basis through inhalation. Some defence is required to prevent damage and infection (Nicod, 2005).

Defence mechanisms range from macro- to microscopic. Macroscopic defences start at the nasal mucosa, where hair follicles trap larger debris and particulate matter in conjunction with secreted nasal mucous. Abundant mucosal associated lymphoid tissue lines the mucosa, with high concentrations of antigen presenting cells to mount appropriate immune responses. The epiglottis serves to prevent inhalation of food matter into the lungs, and when ineffective can lead to aspiration of food into the lungs, precipitating infection. Beyond the epiglottis, the muco-ciliary escalator of the conducting airways acts to further trap particulate matter in mucous secreted by goblet cells of the pseudostratified epithelium (Kuek and Lee, 2020). Part of this epithelium are ciliated epithelial cells, which beat in a co-ordinated fashion to move the mucous towards the epiglottis where it is swallowed and destroyed in hydrochloric acid produced by the stomach.

Microscopically, immune cells within the non-conducting portion of the respiratory system (e.g. alveoli) present the mainstay of antigen defence. Resident alveolar macrophages (“dust cells”) act as antigen presenting cells and contribute to pathogen clearance (Belchamber et al., 2020). Pathogen recognition through damage-associated molecular pattern (DAMP) and pathogen-associated molecular pattern (PAMP) receptors lead to release of pro-inflammatory cytokines, leading to vascular endothelial wall changes necessary for the targeted recruitment of circulating immune cells such as peripheral blood mononuclear cells and neutrophils. Neutrophils contribute to immune cell recruitment through release of proteases from intracellular azurophilic granules, like neutrophil elastase (NE), proteinase 3 (PR3) and metallomatrix proteinases (MMPs). These enzymes act on substrates such as elastin (Janoff and Scherer, 1968) and collagen (Kafienah et al., 1998). Breakdown of these proteins allows

for increased and rapid translocation of immune cells to the site of tissue injury. In order to contain the immune mediated host tissue damage to the areas of injury, anti-proteinases such as alpha-1 antitrypsin (α1AT) and α2-macroglobulin (α2M) inhibit proteinase activity.

Resolution of inflammation after clearance of acute injury/ infection is important to prevent ongoing damage leading to chronic disease. Apoptotic leukocytes including neutrophils must be cleared by macrophages in a process known as efferocytosis. This phagocytic process prevents the release of internal cellular compounds which can be toxic and cause a local pro-inflammatory process in the tissue (Allard et al., 2018). Two distinct phases of inflammatory resolution have been described. The first involves release of anti-inflammatory cytokines (interleukin (IL)-4, IL-10) and reduction of nuclear factor kB (NF-kB). Both IL-4 and IL-10 have been shown to inhibit the cyclooxygenase-2 expression in neutrophils, a key component of prostanoid synthesis in neutrophils (Niiro et al., 1997). This is followed by a resolution phase, where further leucocyte recruitment is inhibited (Levy and Serhan, 2014) and release of pro-resolving mediators (lipoxins, resolvins, protectins and maresins). These actively clear inflammatory exudates to allow for restoration of normal tissue architecture (Bannenberg and Serhan, 2010).

The role that neutrophils play in both initiation and resolution of inflammation is a fine balance between host tissue damage and cessation of these processes. Disruption of the homeostatic balance can lead to diseases, such as bronchiectasis, asthma, α1AT deficiency, cystic fibrosis, pneumonia and sepsis (Jasper et al., 2019, Patel et al., 2018, Crisford et al., 2021, Bedi et al., 2018, Houston et al., 2013). Many chronic lung conditions are characterised by pulmonary neutrophilia (Jasper et al., 2019). Dysfunction of neutrophil function can progress disease and the severity of disease correlates to the degree of dysfunction (Sapey et al., 2011, Thompson et al., 1989). Although neutrophils are involved with the disease process, progression and severity, it is difficult to determine if dysfunctional neutrophils are the cause or result of the underlying disease process.

1.3 Neutrophils

1.3.1 Overview of function

1.3.1.1 Production, release and activation

Neutrophils are the most abundant circulating white blood cell, derived from the common myeloid progenitor cell. Terminal differentiation to mature neutrophils occurs before release from the bone marrow, reliant on the expression of specific growth factors such as Growth factor independent transcription repressor (Gfi-1) (Hock et al., 2003, Karsunky et al., 2002). Circulating neutrophils, which are terminally differentiated but inactive have an average lifespan between 5 and 135 hours (Tak et al., 2013, Pillay et al., 2010). Circulating levels of neutrophils are balanced between a population within the vascular system and a bone marrow population that can be mobilised when required. Neutrophils are derived from long-term haematopoietic progenitors which mature to granulocyte-macrophage progenitors. Further differentiation occurs to immature neutrophils before mature neutrophils are formed, ready for release into the circulation. During this process, neutrophil nuclei develop a characteristic multi-lobular shape ('banding'). It is thought that this morphology allows for rapid migration and neutrophil extracellular trap production (Manley et al., 2018). Membrane expression of CXC-chemokine receptor (CXCR)2 induced by CXC-chemokine ligand (CXCL)1 and CXCL2 on bone marrow cells, leads to the release of neutrophils to the circulation (Eash et al., 2010, Christopher et al., 2009). Expression of CXCR4 induced by CXCL12 acts to retain neutrophils in the bone marrow (Eash et al., 2010, Hernandez et al., 2003). Maturation of neutrophils leads to decreased expression of CXCR4 and increased expression of CXCR2 (Suratt et al., 2004). This leads to their release. As neutrophils approach senescence, the converse expression of surface receptors occurs, with CXCR4 increasing and CXCR2 decreasing, leading to these cells being removed from the circulation.

Macrophages and other antigen presenting cells aid recruitment and mobilisation of neutrophils into the circulation through the production of IL-23, and subsequent IL-17 release from activated T-helper 17 cells (Ley et al., 2006, Schwarzenberger et al., 2000). IL-17 leads

to the release of Granulocyte colony stimulating factor (G-CSF), in turn increasing CXCR1 and CXCL12 expression in the bone marrow (Eash et al., 2010). This skews surface expression of CXCR2/4 towards CXCR2, leading to neutrophil release. Conversely, at inflammation resolution macrophage efferocytosis causes reduces IL-23 release and thus downstream granulocyte-colony stimulating factor (G-CSF) signalling, reducing neutrophil release from the bone marrow to circulation.

As part of the innate immune system, neutrophils are recruited to sites of injury or infection rapidly after insult (Dancey et al., 1976). They have several effector functions including phagocytosis and production and release of neutrophilic extracellular traps (NET)osis (Kolaczkowska and Kubes, 2013). Pro-inflammatory states such as autoimmune conditions, malignancy and infections can cause a neutrophilia.

Activation of circulating neutrophils is required for cells to become functional immune cells, which leads to a shift in state. There are three states described; quiescent, primed and activated (Sapey and Stockley, 2014). Circulating neutrophils in health exist in the quiescent phase, with low adherence, low response to antigen signalling and suppressed transcription. This prevents host-mediated tissue damage (Miralda et al., 2017, Sheppard et al., 2005).

Priming occurs after interaction with pro-inflammatory cytokines, activated endothelial cells or antigens from infection (e.g. lipopolysaccharide (LPS)). Activated endothelial cells lead to priming through altered surface receptor expression, as an indication of where infection or injury has occurred. Surface adhesion molecules such as P-selectin, intracellular adhesion molecule (ICAM) are upregulated in response to the accumulation of bacterial molecules such as LPS (Borregaard, 2010, Phillipson and Kubes, 2011). Neutrophils express P-selectin glycoprotein ligand-1 (PSGL-1) which along with the subsequent activation of intracellular kinases (e.g. p38 mitogen-activated protein kinase (MAPK)) interacts and tethers the neutrophil to the vessel wall (Kansas, 1996, Yago et al., 2010, Ley et al., 2007). Cell rolling across the luminal surface occurs as sheer stress from blood flow leads to sequential detachment and reattachment of selectin-mediated bonds (Pospieszalska and Ley, 2009, Yago et al., 2010). Firm attachment is induced though the interaction of β2-integrin interaction

and lymphocyte function-associated antigen 1 (LFA1) with the endothelial cell surface, leading to the cessation of rolling (Phillipson et al., 2006, Ley et al., 2007, Mócsai et al., 2015).

1.3.1.2 Migration

Neutrophils are required to migrate through the vascular endothelium to sites of injury. Following firm adhesion, Ras signalling leads to guanosine-5'-triphophate (GTP) activation (Phillipson et al., 2006). This induces actin polymerisation to form a lamellipodium, extending along the endothelial wall (Goldfinger et al., 2003). Myosin filament contraction at the opposite end leads to a propulsive movement to the site of transmigration (Van Keymeulen et al., 2006). At this point, neutrophils migrate between endothelial cells (Woodfin et al., 2009). Progression through the vessel basement membrane is aided by the release of azurophilic granules containing serine proteases such as NE, leading to enzymatic breakdown of the basement membrane matrix (Borregaard, 2010).

Migration to the site of infection beyond the basement membrane is along a chemotactic gradient to chemokines secreted by the initial response to injury (e.g. CXCL-8, IL-17) or bacterial components (LPS) (Wang, 2009). As per migration along the endothelial wall, the combination of actin polymerisation and myosin filament contraction moves the neutrophil along the chemotactic concentration gradient (Wang, 2009, Ley et al., 2007).

1.3.1.3 Phagocytosis

Engulfment of foreign particles into an intracellular phagosome is part of the bactericidal functions of the neutrophil. Pattern recognition receptors (PRRs) such as Toll like receptors (TLRs) respond to foreign bacterial material or opsonic receptors such as Fc receptors (FcRs) which recognise host-derived molecules, causing downstream signalling to initiate the phagocytosis process (Kobayashi et al., 2018, Uribe-Querol and Rosales, 2020). Localised pseudopod formation consequently occurs at the site of the particle, extending until there is complete engulfment (Uribe-Querol and Rosales, 2020). Internally, fusion of azurophilic

granules with the phagosome occurs, leading to the release of immune active molecules into the phagosome lumen. These include myeloperoxidase (MPO) and lactoferrin (Kobayashi et al., 2018, Häger et al., 2010). Further antimicrobial activity through the formation of hypochlorous acid, through the generation of hydrogen peroxide (H_2O_2) and subsequently reaction with chloride (Cl^-) ions (Uribe-Querol and Rosales, 2020, Babior, 2004). The creation of a physiologically highly acidic environment (pH around 6.0) leads to the destruction of the bacteria, as well as creating the optimal environment for MPO activity (Segal et al., 1981, Jankowski et al., 2002).

Neutrophils contain an array of granules as part of the antimicrobial response. These can be subdivided into azurophilic (primary), specific (secondary) and gelatinase (tertiary). The contents of these granules are shown in **Figure 1.1**. Azurophilic granules are mobilised once the neutrophil is activated, leading to fusion with the phagosome and creation of the phagolysosome, as discussed above. Specific granules are required for adhesion and migration (Jasper et al., 2019). Activation of azurophilic granules only occur in response to infection of injury as inappropriate activation and content release can lead to host-tissue damage and unregulated inflammation e.g. septic shock (Lacy, 2006). There is some evidence that CD54 (ICAM-1) is involved with supporting reactive oxygen species (ROS) generation, with murine knockout models demonstrating impaired zymosan particle phagocytosis (Woodfin et al., 2016)

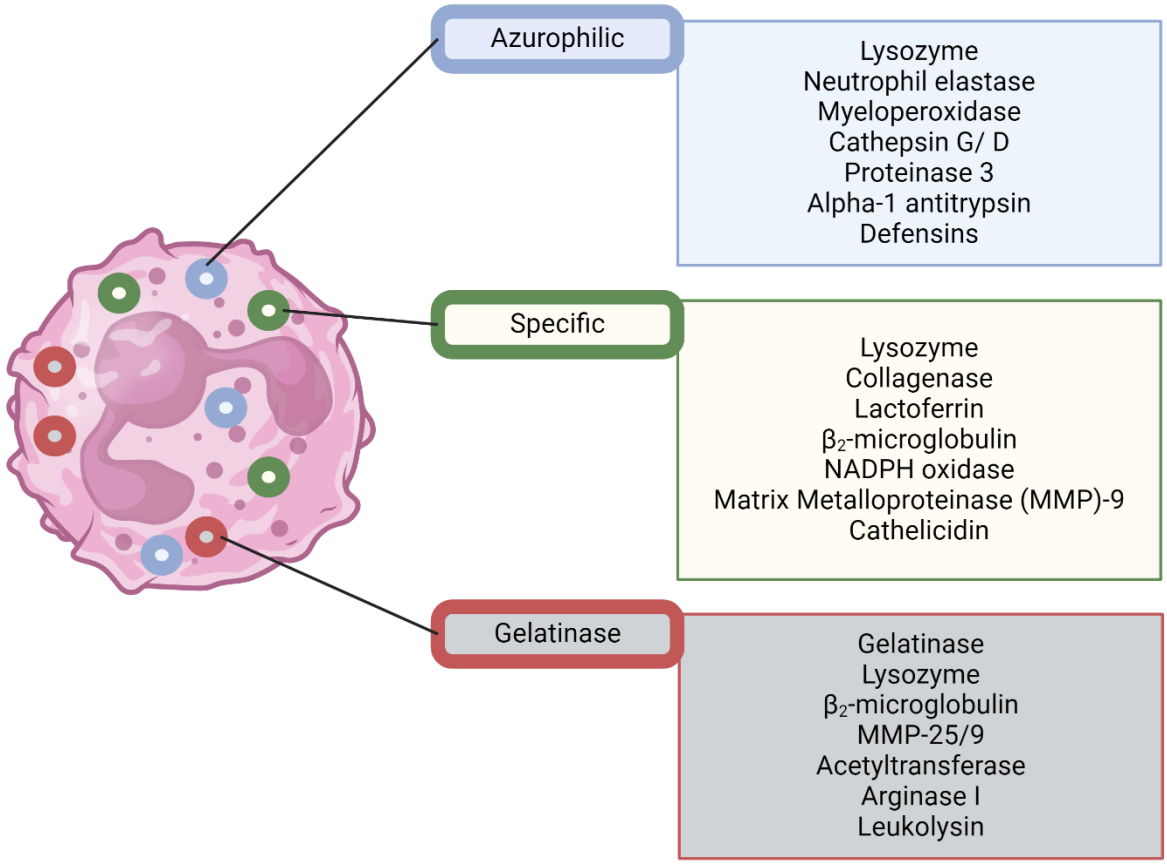

Figure 1.1 Types of neutrophil granules. Granules can be classified into azurophilic, specific, and gelatinase. Listed matrix proteins are contained within the granules. They are released to fuse with the phagosome to form the phagolysosome, or to the cell surface membrane for release to extracellularly. Release is dependent on situation and activation. Adapted from (Jasper et al., 2019, Vols et al., 2017).

1.3.1.4 NETosis

As an extreme response to severe infection, neutrophils are able to release deoxyribonucleic acid (DNA) as a web-like structure. This consists of a histone-DNA backbone with attached enzymes and antimicrobial proteins, known as NETs (**Figure 1.2**) (Brinkmann et al., 2004). NETosis is the process in which NETs are generated, and ultimately leads to neutrophil cellular death. This cell death pathway is separate to apoptosis or necrotic processes.

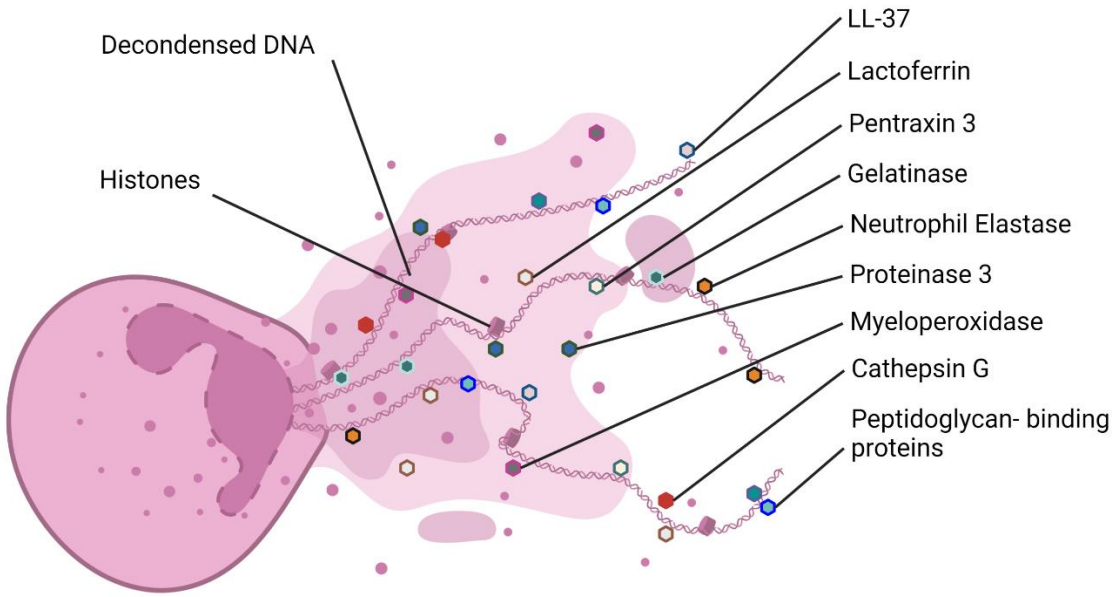

Figure 1.2 Neutrophil extracellular trap formation (NETosis). NETs are released to trap bacteria and pathogenic components to reduce spread. Constituent components, including several antimicrobial peptides of NETs are shown (Delgado-Rizo et al., 2017). NETosis represents a non-apoptotic and non-necrotic mode of neutrophil death, adapted from (Jasper et al., 2019)

The web-like structure of the NETs immobilises bacteria to prevent further spread (Brinkmann 2004). ROS generation can cause NE translocation to the nucleus, leading to chromatin decondensation (Papayannopoulos et al., 2010). ROS presence then causes the breakdown of the nuclear membrane, releasing the decondensed chromatin into the cytoplasm prior to extrusion to the extracellular environment (Delgado-Rizo et al., 2017). Total cell lysis follows. Whilst NETs function to prevent progression of infection in the host, excessive formation is associated with host damage processes. The extracellular exposure to DNA can lead to auto-antibody formation and consequent autoimmune conditions such as systemic lupus erythematosus and rheumatoid arthritis (Papayannopoulos et al., 2010). NETs have been implicated in the formation of immunothromboses in the vasculature and formation of microemboli (Whyte et al., 2020, Zhang et al., 2020b, Middleton et al., 2020). In lung related inflammatory conditions and infections, blockage of pulmonary capillaries can cause ventilation-perfusion mismatch. This leads to systemic hypoxia and can be potentially fatal.

1.3.1.5 Phenotypes

Neutrophils can be characterised or 'phenotyped' by a pattern of surface receptor expression. This phenotype is determined by unique state and function of that cell and can be indicative of the prevailing position of the neutrophil population in terms of activation and cell death.

In inflammation, there is evidence of non-segmented (immature) banded nucleus neutrophils being released from the bone marrow (Seebach et al., 1997). These immature neutrophils have lower surface expression of CD10 compared to neutrophils with a multi-lobular nucleus (Orr et al., 2005, Marini et al., 2017), with higher levels of CD10, CD11b and CD15 expression observed on activated neutrophils (Orr et al., 2005, van Lochem et al., 2004, Ssemaganda et al., 2014). Immature neutrophils released from the bone marrow have high levels of CD62L with low CXCR4 expression (Drew et al., 2018). As neutrophils age, the surface expression of CXCR4 increases with the stromal cell-derived factor-1 (SDF-1) receptor. This leads to migration to tissues with high SDF-1 expression where apoptosis then occurs (Martin et al., 2003).

Patients with systemic inflammatory response syndrome (SIRS) have demonstrated an increased population of $CD11c^{+}CD64^{+}$ neutrophils compare to age matched controls. This persisted in patients with a diagnosis of sepsis (Patel et al., 2018). Other studies have suggested that there is upregulation of CD11b and downregulation of CD62L, commonly associated with cell activation as both these (CD11b as surface integrin and CD62L as L-selectin endothelial carbohydrate receptor) are involved with neutrophil firm adhesion (Lin et al., 1993, Rosenbloom et al., 1999, Muller Kobold et al., 2000, Chishti et al., 2004). Surface expression of CD66b is also a marker of neutrophil endothelial adhesion and activation (Opasawatchai et al., 2019)

These dominant phenotypes observed in sepsis, senescence and immaturity are indicative of disease states, and differ from the surface expression of these molecules on healthy circulating neutrophils.

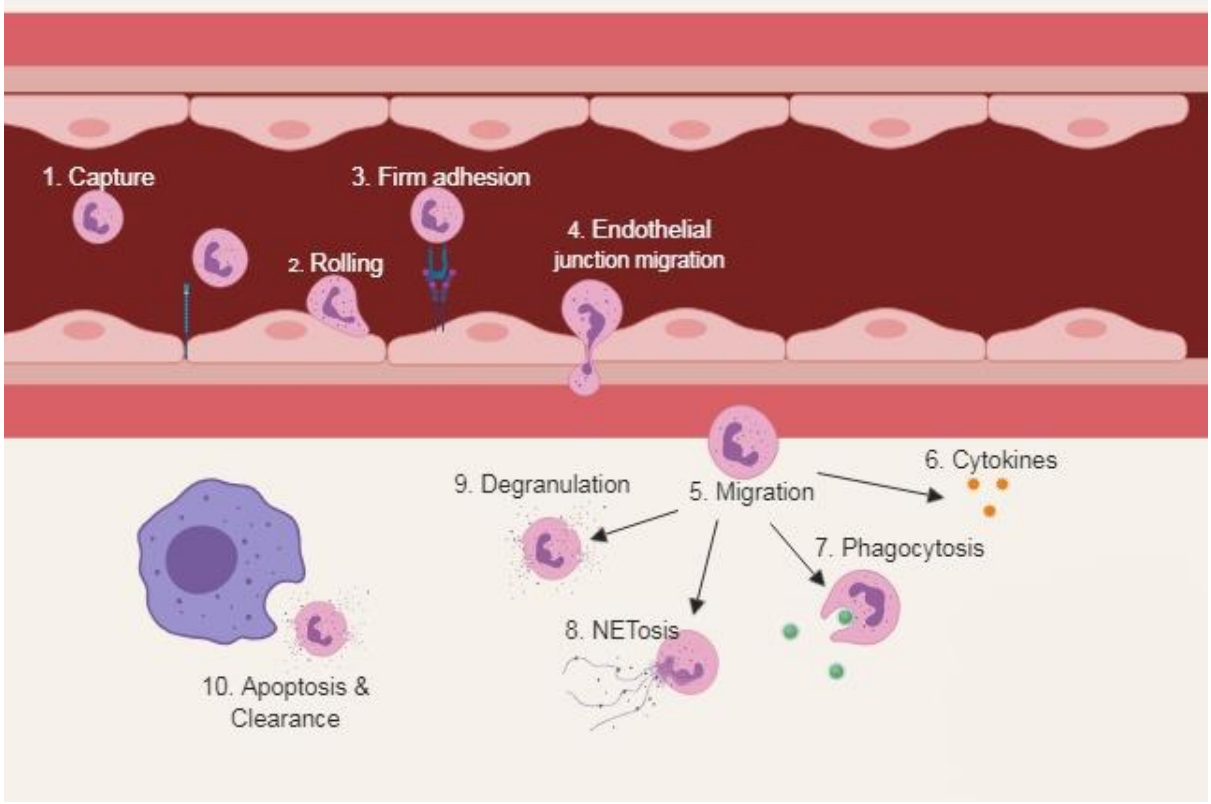

Figure 1.3 Neutrophil functions. 1) Capture: Active patrolling of systemic circulation allows for detection of host- and pathogen- associated pro-inflammatory signals through interaction with endothelial cells. 2) Rolling: On recognition of pro-inflammatory signals, neutrophils become tethered and roll along the endothelial wall in a selectin dependent manner. 3) Firm adhesion: Activation of integrins leads to firm adhesion. 4) Endothelial junction migration: Neutrophils undergo cytoskeletal rearrangement to allow for migration through endothelial cell junctions. 5) Migration: interstitial migration occurs due to the chemoattractants released from the site of injury. Neutrophils migrate down a chemokine gradient towards site of injury 6) Cytokines: cytokine release has a role in directing and recruitment of further immune cells and the subsequent response. 7) Phagocytosis: Bacterial clearance occurs through neutrophil phagocytosis – bacteria are trapped and submitted to antimicrobial peptides and reactive oxygen species. 8) NETosis: Generation of neutrophil extracellular traps. Here decondensed chromatin is released into the extracellular space, covered in antimicrobial peptides. 9) Degranulation: protease release is required for migration through dense extracellular spaces. 10) Apoptosis and clearance: Neutrophil clearance is required for resolution of inflammation; this occurs in a process known as macrophage efferocytosis. Incomplete clearance and persisting inflammatory response can lead to unnecessary host-mediated tissue damage. Figure adapted from (Grudzinska et al., 2020)

1.3.1.6 Resolution

Activation must be controlled and limited to the site of infection/ injury. Once this has been resolved, clearance of activated and dead cells must occur to prevent host tissue damage. Clearance occurs through processes such as efferocytosis by tissue resident macrophages and dendritic cells (Borregaard, 2010).

In vivo and in health, circulating neutrophils have a half-life of 6-8 hours, and a production rate of $5x10^{10}$ to $10x10^{10}$ cells per day (Summers et al., 2010). Activation and translocation to sites of infection can prolong their lifespan (Robinson et al., 1994). However, bactericidal processes such as NETosis can lead to this being shortened (Lee et al., 1993). Non-activated neutrophils undergo apoptosis at the end of their life and are cleared by haematopoietic organs e.g. spleen, bone-marrow, liver (Sadik et al., 2011).

1.3.2 Neutrophils in disease

1.3.2.1 Bacterial infection

In community acquired pneumonia (CAP) neutrophils and macrophages demonstrate a stereotyped response (as described in **Figure 1.3**) in response to chemotactic agents released at the site of injury. Activated neutrophils in the lung parenchyma demonstrate increased nicotinamide adenine dinucleotide phosphate (NADPH) oxidase activity and increased proteolytic enzyme release. Together these are likely to be responsible for collateral damage to the respiratory tissue. In addition to the role in clearance of bacteria, fungi, and yeast infections there is evidence suggesting that neutrophils have an important role in viral infections. Firstly, viral infections can impair the host immune response which can allow additional opportunistic infection from bacteria and fungi through excessive activation and host tissue damage. Similarly to classic pneumococcal infection, influenza A related inflammation leads to increased concentrations of CXCL8 both locally and systemically. In turn, this initially causes neutrophil recruitment and activation (Gotts et al., 2019, Shah and Wunderink, 2017,

Aulakh, 2018). Higher levels of circulating CXCL8 correlate to increased disease severity (Hayden et al., 1998). This increase in circulating neutrophils has been shown in mice and human models post viral infection (Long et al., 2013). Neutrophils play a key role in the resolution of inflammation (El Kebir and Filep, 2010). Depleting neutrophil populations in a murine models leads to decreased recovery from severe influenza A infection (Tate et al., 2011).

In COVID-19 disease changes to neutrophils have been reported including increased neutrophil counts, neutrophil to lymphocyte ratio (NLR), MPO levels, and circulating NET markers (Aschenbrenner et al., 2021, Schulte-Schrepping et al., 2020, Meizlish et al., 2021, Vitte et al., 2020, Wilk et al., 2020).

1.3.2.2 Viral infection

As part of the innate immune system, neutrophils play a key role in the initial response to viral infection. There is evidence of recruitment to the site of other viral infection in the fashion described above, such as cutaneous varicella zoster, cerebrospinal fluid in viral meningitis and after influenza and respiratory syncytial virus (RSV) infection (Shackelford and Feigin, 1973, Ratcliffe et al., 1988, Perrone et al., 2008). The volume of neutrophil recruitment appears to correlate to the severity of infection in influenza (Perrone et al., 2008, Tate et al., 2011). Neutrophil depletion studies using anti-Gr-1 monoclonal antibodies in influenza A H3N2 challenge leads to increased disease severity (Tumpey et al., 2005). There is further evidence of increased influenza replication and spread when neutrophils are depleted (Tate et al., 2009).

Prolongation of neutrophil lifespan demonstrates a degree of activation; delayed apoptosis has been shown in RSV infection through phosphoinositide-3-kinase (PI3K) and NF-kB pathway activation. Systemic cytokines such as tumour necrosis factor (TNF)-α and G-CSF can prolong survival as well as act as chemoattractants (Basu et al., 2002).

It is thought that neutrophils have multiple roles in viral infections, from immune cell recruitment to engulfment of viral particles as shown in **Figure 1.4** (Amulic et al., 2012). Phagocytosis of

herpes simplex virus (HSV) virions and infected fibroblasts by electron microscopy has been observed (Van Strijp et al., 1989). Blockade of phagocytosis using Annexin V increased mortality in a mouse model of influenza A infection (Watanabe et al., 2005). The components of neutrophil granules such as defensins and cathelicidin (LL-37) are able to neutralise viral infections through disruption of glycoproteins (Hazrati et al., 2006, Howell et al., 2004, Tripathi et al., 2014, Currie et al., 2016). Unregulated release may cause host-tissue damage and viral-associated lung injury, through both degranulation and pro-inflammatory cytokine release (Okrent et al., 1990, Tjabringa et al., 2005). Neutrophil ROS production can lead to viral DNA damage and infection with viruses such as influenza, RSV and rhinovirus have been shown to increase ROS production (Peterhans, 1997). Viral antigens are strong triggers of the pattern recognition receptors (PRRs) such as TLR3, TLR7 and TLR8. These TLRs are involved in the recognition of foreign nucleic acids within endosomes, including single stranded RNA (TLR7) and double stranded RNA (TLR3). In conjunction with a systemic increase in platelet production and activation, this can trigger NETosis (Lisman, 2018). Excessive NETosis is associated with increased inflammation leading to damage to tissue structure (Narasaraju et al., 2011, Narayana Moorthy et al., 2013).

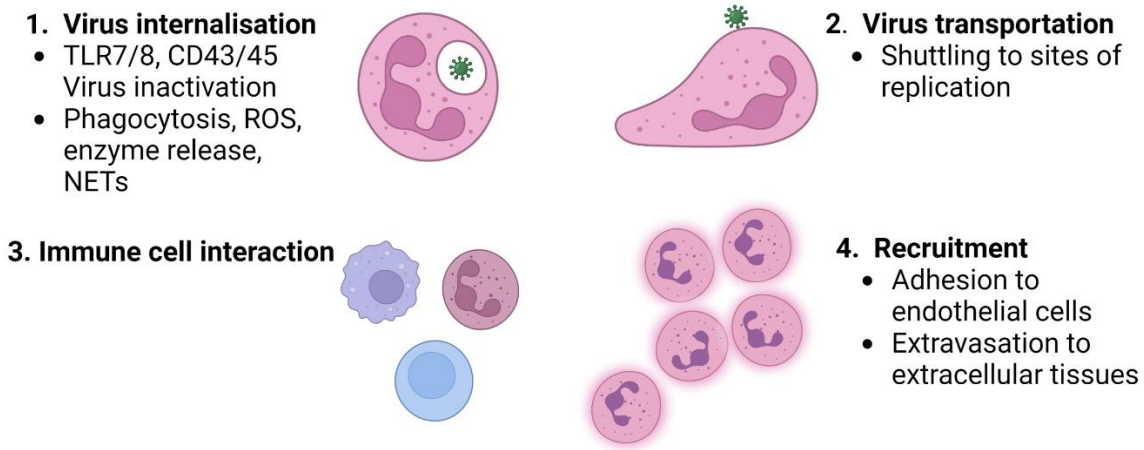

Figure 1.4 Neutrophil contributions to viral clearance and pathology. **1.** Virus internalisation through phagocytosis and trapping in neutrophil extracellular traps (NETs). Neutrophils can contribute to host protection through destruction via reactive oxygen species (ROS) and enzyme release, but some viruses use neutrophils as a vessel for replication. **2.** Attachment to surface receptors can lead to transport to sites of replication as neutrophils migrate. **3.** Neutrophils interact with the adaptive immune system via chemokine signalling to activate host responses. **4.** Neutrophils are recruited to sites of infection or injury as part of the innate immune system response. Adapted from (Naumenko et al., 2018).

The interaction between neutrophils and the adaptive immune system is also a key process in response to viral infection. Neutrophils are able to migrate to peripheral lymph nodes and act as antigen-presenting cells triggering a CD8+ T-cell response through the expression of major histocompatibility complex class II (MHC/ HLA-DR) (Yang et al., 2010, Beauvillain et al., 2011, Hufford et al., 2012),. This process may represent a form of viral pathogenicity in certain infections such as human immunodeficiency virus (HIV), where the combination of phagocytosis and migration to lymphoid tissue allows for transportation to susceptible cells (Schönrich and Raftery, 2016). This exploitative viral pathogenicity is less relevant in respiratory infections, but viral particles have been found in the neutrophils in the spleen, intestine and placenta (Pan et al., 2013).

1.4 COVID-19

1.4.1 Epidemiology

Coronavirus disease 2019 (COVID-19) caused by the severe acute respiratory syndrome coronavirus 2 (SARS-COV-2) was first reported in December 2019. The first case outside of Wuhan, China was confirmed in Thailand on 14th January 2020. On 29th January 2020, two people from the same family tested positive for COVID-19 in York, UK. On 11th March 2020, the World Health Organisation declared a global pandemic. From then, global transport was shut down to limit the spread and number of cases overwhelming healthcare systems.

1.4.2 Viral pathology and natural history

Coronaviruses from the family *Coronaviridae* commonly cause upper respiratory tract infections in humans and animals. Three significant zoonotic *Coronaviridae* have transferred from animal reservoirs to cause human disease; severe acute respiratory syndrome coronavirus (SARS-CoV), Middle East respiratory syndrome coronavirus (MERS-CoV) and SARS-CoV-2. Each of these can cause an acute respiratory distress syndrome (ARDS) and acute pneumonitis.

SARS-CoV-2 is an enveloped virus of the beta *Coronaviridae* subgroup, containing positive-sense, single stranded RNA coding for 29 proteins. The SARS-CoV-2 virus is transmitted via respiratory droplets, with the majority of infected people presenting with mild symptoms or being asymptomatic following a mean incubation period of 5-6 days (Van Doremalen et al., 2020, Cevik et al., 2020). Asymptomatic individuals can still transmit the virus. Those patients who develop severe symptoms can potentially develop respiratory failure and death.

Following viral entry, an innate immune response is triggered by activation of TLRs leading to the formation of an inflammasome and the subsequent maturation of and release of IL-1β and IL-18 (Park and Iwasaki, 2020). In addition, production of IL-6, IL-10, IL-17, myeloid differentiation primary response 88 (MyD88) and TNFα are triggered through distinct TLR

subsets (Manik and Singh, 2022). The activation of MyD88 leads to initiation of NF-κB and thus production of interferons (IFN) (Hartenian et al., 2020). IFN signalling is an important pathway of defence, eventually leading to the expression of MHC class I, facilitating CD8 T cell cellular clearance. Antibody production through a CD4 T cells and B-cell mediated response is important to prevent disease progression, and antibodies persist for around 6 months after vaccination and 12 months after infection (Kim et al., 2022, Qi et al., 2022, Sette and Crotty, 2021). The surface spike glycoprotein of SARS-CoV-2 determines host-virion interaction. It is formed of the S1 subunit, which binds to the angiotensin converting enzyme 2 (ACE2) receptor and the S2 subunit, involved in membrane fusion (Zhou et al., 2020). Once binding has occurred, spike protein cleavage occurs, mediated by TMPRSS2, a transmembrane serine protease. Cleavage triggers the S2 subunit to fuse host and viral cell membranes, releasing positive sense viral ribonucleic acid (RNA) into the host cell (Barnes et al., 2020). There is some evidence that host-viral fusion may occur through spike protein cleavage mediated by surface cathepsins, but it is unlikely this is the primary mode of entry in epithelial cells (Beumer et al., 2021, Lamers et al., 2021).

Viral protein replication occurs in modified endoplasmic reticulum from the positive sense SARS-CoV-2 RNA (Ogando et al., 2020). Transcribed double stranded RNA intermediates are shielded from cytoplasmic immune responses through PRRs by the modified endoplasmic reticulum forming a bubble-like structure. The cytoplasmic PRR MDA5 responds to long strands of double stranded DNA, triggering an internal cascade leading to production of type I and III IFNs. Interferon signalling causes chemokine release through further extracellular signalling cascades, leading to innate immune cell recruitment and inflammation. Cytokine production causes a B- and T-cell response and further host-tissue damage through the inflammatory response. Dissemination of the infection into the lower respiratory tract can impair gaseous exchange and lead to respiratory failure. There is evidence of SARS-CoV-2 primarily infecting type 2 pneumocytes (Katsura et al., 2020, Salahudeen et al., 2020). Damage to the lower respiratory tract prevents appropriate surfactant secretion and reduce

the regenerative capability of the lung tissue as type 2 pneumocytes are the progenitors for type 1 pneumocytes.

1.4.3 Evolution

Coronaviruses mutate frequently, and since the identification of the wild-type virus, there have been several strains identified. **Figure 1.5** shows the diversification from the wild-type virus as a phylogenetic tree up to the time of writing this thesis.

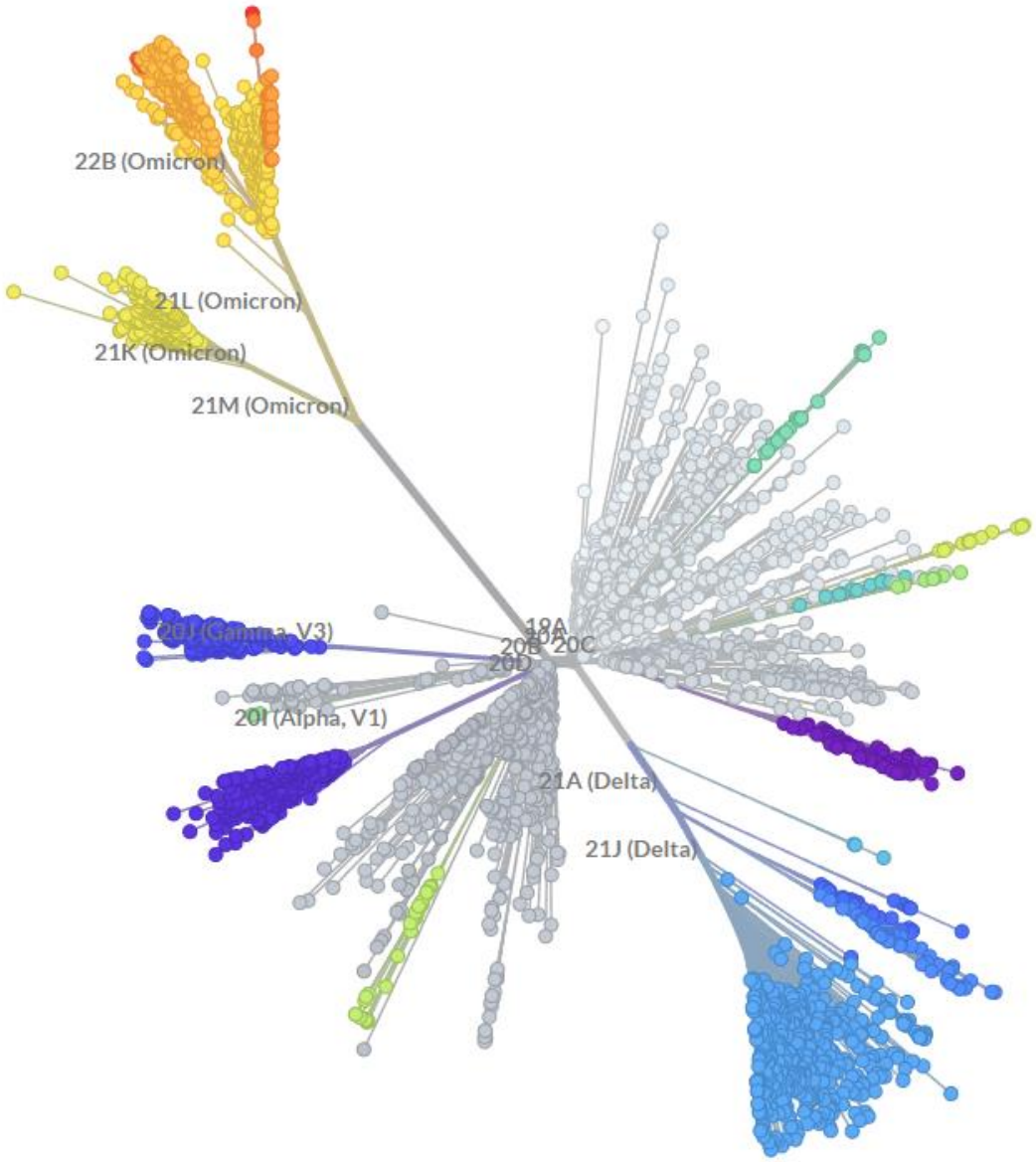

Figure 1.5 Phylogenetic tree showing the diversification and relationship of the COVID-19 variants to both each other and the wild-type virus as of December 2023. Variants of interest

and related to infections in the United Kingdom include Alpha (B.1.1.7), Delta (B.1.617.2), Omicron (B1.1.529 - BA.1, BA.2, BA.3) Source: (NextStrain, 2023)

As shown in **Figure 1.5**, there have been three waves of COVID-19 infection in the UK causing an increase in either cases or deaths. There will have been more variants but have not routinely been tested for in the UK since the reduction of severe cases and mortality. These correspond to predominant strains of Alpha, Delta and Omicron COVID-19. The trend demonstrates increased case numbers with a proportional reduction in deaths. This may be explained for two different reasons: 1) availability and use of lateral flow tests (LFTs) by the general public to record cases; 2) increased transmissibility with decreased severity of evolving strains. The first reason is the main reason for the discrepancy seen in the alpha deaths vs recorded cases as described above. Lateral flow testing (LFT) and routine hospital testing for all patients was established and thus testing availability is unlikely to be a factor in the mortality changes between Delta and Omicron variants.

The UK Office of National Statistics (ONS) reported a lower risk of death of 67% after Omicron infection relative to Delta (Statistics, 2022). **Table 1.1** shows the rates of cases to deaths during each wave and the corresponding dominant strain, relevant to the timing of samples collected for this body of work.

Date	Predominant strain	Cases	Deaths	Case: Death	ICU admission/ 100000 cases
January 2021	Alpha (B.1.1.7)	700,000	12,300	56.91	0.96
September 2021	Delta (B.1.617.2)	600,000	9,500	63.16	0.57
April 2022	Omicron (B1.1.529)	1,500,000	4,095	355.30	0.32

Table 1.1 Table showing the predominant dates for major strains beyond the wild-type virus. Reported cases to the nearest 100,000 are shown with deaths, case to death ratio and the number of intensive care unit (ICU) admissions. Cases reported for alpha infections are likely to be inaccurate due to the limited availability of lateral flow tests to the general public.

.

The US Centre for Disease Control (CDC) reported double the spread of Delta variant compared with Alpha (CDC, 2021). In the UK, the risk of hospitalisation was double that of Alpha variant infection with more rapid spread through schools (Torjesen, 2021). Rapid transmission leads to increased replication and the likelihood of further mutations conferring viral penetration.

RNA viruses are more susceptible to mutations due to the lack of genetic repair and proofreading activity (Fitzsimmons et al., 2018, Duffy, 2018).

Mutations affecting the transmissibility and pathogenicity of the virus occur in the surface spike protein. The two components of the spike protein S1 and S2 are involved with the binding and internalisation of the virus respectively, as shown in **Figure 1.6** (Huang et al., 2020). Mutations in the spike protein are responsible for the increased transmissibility observed in the Delta variant compared to Alpha. The L452R spike protein mutation (arginine- leucine substitution), leads to increased binding affinity to ACE2 (Starr et al., 2021).

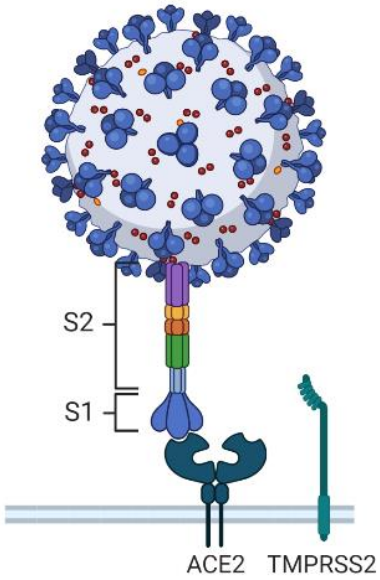

Figure 1.6 Graphical description of the SARS CoV-2 virion, with attachment to ACE2 receptor. Following binding, cleavage of the S protein occurs at the S1/S2 interface. This is facilitated by TMPRSS2. Cleavage activates the S2 domain for fusion with the cell membrane. Lipid bilayers fuse and viral positive-sense, single-stranded RNA is deposited into the cell. Viral replication leads to the production of double stranded RNA.

1.4.4 Clinical considerations

Transfer of SARS-CoV-2 between humans is via aerosol spread, with a median incubation time of four to five days before presentation with symptoms (Guan et al., 2020). Following symptoms, severe illness related to hypoxia begins one week later, which can progress to respiratory failure in patients that develop ARDS. ARDS is classically defined by the Berlin Criteria, see **Table 1.2**. Characteristic pulmonary inflammation and vascular leak causes hypoxia and stereotypical radiological changes.

Timing		Within 1 week of known clinical insult or worsening respiratory symptoms
Radiology		Bilateral opacities – not fully explained by pleural effusions, lung or lobar collapse or nodular changes
Origin of oedema		Respiratory failure not fully explained by cardiac failure, fluid overload
Oxygenation	**Mild**	200mmHg < PaO_2/FiO_2 ≤ 300mmHg with PEEP/CPAP ≥5cm H_2O
	Moderate	100mmHg < PaO_2/FiO_2 ≤ 200mmHg with PEEP ≥ 5cmH_2O
	Severe	PaO_2/FiO_2 ≤ 100mmHg with PEEP ≥ 5cmH_2O

Table 1.2 Berlin criteria for acute respiratory distress syndrome (ARDS). Conversion of PaO_2/FiO_2 ratio to SpO_2/FiO_2 ratio has been calculated for equivalency. 200mmHg PaO_2/FiO_2 = 235mmHg SpO_2/FiO_2; 300mmHg PaO_2/FiO_2 = 315mmHg SpO_2/FiO_2 (Rice et al., 2007).

1.4.4.1 Acute Respiratory Distress Syndrome (ARDS)

Histologically, patients with ARDS demonstrate a pattern of changes described as diffuse alveolar damage (DAD) (Katzenstein et al., 1976). This term describes “endothelial and alveolar lining cell injury which leads to fluid and cellular exudation and in some cases progression to extensive interstitial fibrosis. Some patients progress to a further fibrosis of the alveoli. Early post-mortem sampling of patients with COVID-19 demonstrated DAD (Carsana et al., 2020, Menter et al., 2020). Hyaline membrane formation and fibrin thrombus formation occurs here as there is disruption to the homeostasis of the coagulation cascade. Increased

activation and prevention of fibrinolysis leads the formation of hyaline membranes, helping to prevent the alveolus from further oedema, but consequently leading to impaired gaseous exchange. Similarly, there is an increase in formation of fibrin thrombi; immunothrombotic disease is a key feature of severe COVID-19 disease (Vorobjeva and Chernyak, 2020, Hazeldine et al., 2014, Zuo et al., 2021).

It is not clear what triggers the disruption of the coagulation cascade. However, damage to the endothelium leads to release of tissue factor to the extracellular space. This triggers both the intrinsic and extrinsic coagulation pathway (Owens and Mackman, 2010, Kenawy et al., 2015). NETs can directly activate factor XII (Skendros et al., 2020b). It has been shown that in severe COVID-19, neutrophils release NETs covered with tissue factor, a potent activator of the clotting cascade (Skendros et al., 2020b). In addition, NET accumulation can lead to platelet recruitment, which in turn can cause further NET release. This cascading process can help establish clot formation in areas of tissue injury. Georg et al demonstrated that CD16+/+ T cells can increase endothelial damage in COVID 19 (Georg et al., 2022). This T cell population released chemoattractants IL-8 and CCL2, furthering damage and clot formation through recruitment of innate immune cells. The overall systemic inflammatory state of patients with COVID-19 also contributes to immunothrombosis, with raised IL6 correlated with poor outcomes (Del Valle et al., 2020, Galván-Román et al., 2021).

Release of proinflammatory cytokines such as IL-1, IL-6, IL-8, TNF-α lead to systemic inflammation and subsequent production of downstream effector molecules. This includes C-reactive protein, ferritin and d-dimer. Many of these molecules are routinely measured as part of clinical practice and are markers of systemic inflammation, rather than being specific for pulmonary disease. High admission serum IL-6, IL-8, and TNF-α were correlated to predict patient survival (Del Valle et al., 2020).

ARDS has a mortality rate of up to 40% (Pham and Rubenfeld, 2017, Sigurdsson et al., 2013). Infiltration of neutrophils into the lung parenchyma is classically seen in acute respiratory distress syndrome. As with infective causes of inflammation, neutrophil activation leads to release of cytokines, proteases, and NETs. Excess neutrophil enzyme activity and oxidative

activity contributes to the damage to the respiratory tissues characterised in ARDS. As expected, decreased neutrophil recruitment decreases the production of cytotoxic mediators, compared to the increased tissue damage seen with increased neutrophil counts (Chen et al., 2018a, Baudiß et al., 2016). However, neutropenia in both human and animal studies has led to poorer outcomes in ARDS (Yacoub et al., 2014, Mokart et al., 2012). This suggests dysfunctional or inappropriately cleared neutrophils are responsible in disease propagation and the requirement of an adequate neutrophil response to aid viral and inflammatory resolution. Programmed death ligand-1 (PD-L1) may play a role in the neutrophil contribution to lung injury in ARDS. In vivo and in vitro PD-L1 blockade reduced NET release and reduced autophagy through PI3K signalling (Zhu et al., 2022).

Comparisons between COVID-19 patients with ARDS compared to those with non-infectious ARDS demonstrated differences in the minute ventilation and higher ventilatory dead space fraction observed in COVID-19. Additionally, COVID-19 ARDS patients were intubated for a longer period. Microscopically, microthrombi were more prevalent in COVID-19 ARDS, suggesting a significantly different enough disease to further investigate and treat this as a separate clinical entity (Auriemma et al., 2020, Yatim et al., 2021, Bain et al., 2021, Sinha et al., 2020). Systemic manifestations of COVID-19 disease include thromboembolic events, arrhythmias, acute kidney injury, hepatic injury and shock. There is evidence of SARS-CoV-2 presence in extrapulmonary organs, but severe disease manifestations may be caused by distant viral-host interactions rather than local effects of SARS-CoV-2 replication (Lindner et al., 2020, Bhatnagar et al., 2021, Puelles et al., 2020).

From an early point in the global pandemic, correlating disease severity and outcomes (e.g. mortality) to routine clinical measures was of paramount importance. The ability to determine which patients may require increased levels of care and respiratory support would allow for healthcare systems to triage and plan. Demographic distinctions such as age, obesity, and gender (male) were established as higher risk of developing severe disease along with comorbidities affecting all major organ systems.

1.4.4.2 Scoring systems

Scoring systems used in COVID-19 can be broadly classed into one of two categories: 1) those used to describe the severity of disease; 2) those used to predict mortality, progression or outcome of patients with COVID-19.

The World Health Organisation (WHO) clinical progression scale was widely adopted to classify disease severity, shown in **Table 1.3**. The 4C score was developed during the pandemic to predict patient mortality based on history, admission observations and biochemical measures (**Table 1.4**).

Patient State	Descriptor	Score
Uninfected	Uninfected; no viral RNA detected	0
Ambulatory mild disease	Asymptomatic; viral RNA detected	1
	Symptomatic; independent	2
	Symptomatic; assistance required	3
Hospitalised: moderate disease	Hospitalised; no oxygen therapy*	4
	Hospitalised; oxygen by mask or nasal cannulae	5
Hospitalised: severe disease	Hospitalised; oxygen by NIV or high flow	6
	Intubation and mechanical ventilation, pO2/FiO2 >=150 or SpO2/FiO2 >=200	7
	Mechanical ventilation pO2/FiO2 <150 or SpO2/FiO2 <200 or vasopressor support required	8
	Mechanical ventilation pO2/FiO2 <150 or SpO2/FiO2 <200 and vasopressor/ dialysis or ECMO support required	9
Dead	Dead	10

Table 1.3 WHO clinical severity scale. * If hospitalised for oxygen only then patients are recorded as for an ambulatory patient only. Adapted from WHO clinical severity scale (WHO, 2020)

Variable		Points
Age (years)	<50	0
	50-59	2
	60-69	4
	70-79	6
	≥80	7
Sex at birth	Female	0
	Male	1
Number of comorbidities	0	0
	1	1
	≥2	2
Respiratory rate (breaths/min	<20	0
	20-29	1
	≥30	2
Peripheral oxygen saturation on room air	≥92%	0
	<92%	2
Glasgow Coma Scale	15	0
	<15	2
Serum urea (mmol/L)	≥7 to ≤14 mmol/L	1
	>14 mmol/L	3
C-reactive protein	<50 mg/L	0
	50-99 mg/L	1
	≥ 100mg/L	2

4C Score	Risk	In-hospital mortality
0-3	Low	1.2-1.7%
4-8	Intermediate	9.1-9.9%
9-14	High	31.4-34.9%
≥15	Very high	61.5-66.2%

Table 1.4 4C mortality score with interpretation of in-hospital mortality. Co-morbidities include chronic cardiac disease, chronic respiratory disease (excluding asthma), chronic renal disease (estimated glomerular filtration rate ≤30 mL/min), mild to severe liver disease, chronic neurological conditions (including dementia), connective tissue disease, diabetes mellitus, HIV or AIDS and malignancy (Gupta et al., 2021).

Clinical severity scores are used in a multitude of diseases to help stratify patient care. These are validated over several patient cohorts to determine the highest sensitivity and specificity. National Early Warning Score 2 (NEWS2) is routinely used to identify in-patients at risk of deterioration. However, it is non-specific and is not able to identify those patients who are at risk of deteriorating on admission. Similarly, evidence and testing of established scores of respiratory disease e.g. CURB-65 in community acquired pneumonia (CAP) demonstrates poor correlation with disease outcomes (Ahmed et al., 2022). These scores were also used in the early days of the pandemic to predict the risk of deterioration, resource requirement and outcomes.

1.4.5 Evolving therapies and vaccines

Therapy for COVID-19 evolved with the understanding of the virus. Platform trials such as RECOVERY and REMAP-CAP (Abani et al., 2021, Anthony Gordon, 2021), provided healthcare professionals with the evidence base treat patients more effectively with COVID-19. Since the beginning of the pandemic to current practice, there are several therapeutics which have been shown to improve patient outcomes. These are approved by the National Institute for Health and Care Excellence (NICE) for treating patients with COVID-19, dependent on severity of disease. Treatments discussed as part of this thesis relate to those available at the time of patient recruitment.

The first drugs with proven improvement in outcomes were corticosteroids. Patients on dexamethasone with severe COVID-19 mechanically ventilated or on supplemental oxygen showed lower 28-day mortality compared to those not treated with dexamethasone or hydrocortisone in severe disease (Group, 2021, Anthony Gordon, 2021). There was no significant difference between treated and untreated if patients were not requiring respiratory support.

Remdesivir was investigated in its role as a broad-spectrum antiviral agent. Addition to COVID-19 treatment initially showed a reduced recovery time in patients with mild to moderate COVID-19 (Beigel et al., 2020). However, further trials demonstrated that there was little to no effect on mortality, initiation of mechanical ventilation or length of admission (Zhang and Mylonakis, 2021).

Anti-IL-6 agents Tocilizumab and Sarilumab which were previously used in rheumatological disease have been approved for the treatment of COVID-19. Tocilizumab is licenced by NICE in COVID-19 for the treatment of those patients on systemic corticosteroids or on supplemental oxygen treatment. The REMAP-CAP trial demonstrated increased survival and the number of organ support-free days in those on an IL-6 inhibitor compared to control in severe COVID-19 (Anthony Gordon, 2021, Abani et al., 2021). The RECOVERY trial demonstrated similar

improvements in patient survival in patients with hypoxia and systemic inflammation (CRP ≥75 mg/L) (Abani et al., 2021). One randomised control trial (COVACTA) of Tocilizumab did not demonstrate significant improvement in patient outcomes such as mortality or intubation rates compared to placebo (Rosas et al., 2021). Sarilumab as a treatment for COVID-19 did not show significant clinical benefit in terms of clinical course or mortality outcomes for those patients not admitted to critical care (Lescure et al., 2021).

After the completion of this work there have been subsequent therapies which have also shown benefit in patients with severe COVID-19 including baricitinib, an inhibitor of janus kinase (JAK), an intracellular enzyme of tyrosine-protein kinase family, which modulates signals from cytokines and growth factor receptors (Manoharan and Ying, 2022). Paxlovid (nirmatrelvir/ ritonavir) remains as part of recommendation for reducing hospital admission in COVID-19 patients with moderate to high risk of deterioration (Agarwal et al., 2020).

1.4.6 Vaccines

Vaccination as a treatment for COVID-19 was rapidly developed in response to the pandemic, in an attempt to prevent transmission, protect vulnerable patients and reduce the likelihood of further waves requiring national lockdown. However, rapid mutations in the viral proteins used to generate antibody responses after vaccination have the potential to cause decreased efficacy in vaccine protection. There is evidence of different vaccine efficacy against evolving COVID-19 strains. A single dose of the BNT162b2 (Pfizer BioNTech) or ChAdOx1 nCoV-19 had similar efficacy against alpha (48.7%) and delta (30.7%) infection (Bernal et al., 2021). Two doses of BNT162b2 conveyed 93.7% efficacy against alpha and 88% efficacy against delta, whilst two doses of ChAdOx1 nCoV-19 conveyed 74.5% efficacy against alpha and 67% efficacy against delta (Bernal et al., 2021). Similar results have been obtained from international studies (Abu-Raddad et al., 2021). This suggests evolution and different behaviours of the virus with the host-immune system.

In terms of systemic infection and COVID-19, there is a subset of patients who do not mount an effective antibody response. This would explain why viral titres of patients with breakthrough infections are similar to those who have not been vaccinated (Argyropoulos et al., 2020).

The innate immune system continues to play an important role in the body's response to infection after vaccination. A study depleting neutrophils during vaccination demonstrated that even after a period of recovery, mice had lower survival rates after infection challenge (Tchalla et al., 2020). B-cells challenged with replication-competent adenovirus-simian immunodeficiency virus (SIV) recombinants showed improved responses in terms of antibody generation and class switching when co-cultured with neutrophils from vaccinated rhesus macaques compared to vaccine naïve (Musich et al., 2018a). Post vaccination, neutrophils are recruited to the vaccination site where there is increased B-cell activating factor (BAFF) expression in these cells, leading to B-cell recruitment (Wang et al., 2022). Post vaccination, the role of neutrophils in interfacing with the adaptive immune system has a clear shift, but there is no evidence indicating innate neutrophil effector functions are altered by the vaccination.

Uptake in COVID-19 vaccinations in the UK shows that a total of 110.87 million initial protocol doses have been administered in the UK, with a further 40.37 million booster doses (total 151.25 million COVID-19 vaccinations administered as of 4th September 2022), this represents 50.76 million people completing the recommended COVID-19 vaccine protocol (OurWorldInData, 2022).

1.5 Neutrophils in COVID-19

The role of neutrophils in COVID-19 inflammatory states began to be investigated from the onset of the pandemic. Their role in acute lung injury including acute respiratory distress syndrome and other respiratory inflammatory pathologies suggests that a dysfunctional

neutrophil response may play a key role in both perpetuation and initial injury (Galani and Andreakos, 2015, Grudzinska et al., 2020, Patel et al., 2018, Juss et al., 2016b). Initial focus of research centred on the production of NETs and the role this may play in COVID-19. This may be in part due to NET associated with immunothrombosis, with COVID-19 patients demonstrating a higher rate of thrombotic events compared to non-COVID-19 hospitalised patients (Hazeldine et al., 2014, Vorobjeva and Chernyak, 2020).

More clinically, the importance of neutrophils was established early in the pandemic, with an elevated NLR identified as a marker for severe COVID-19 infection (Yang et al., 2020, Kerboua, 2021, Citu et al., 2022). This is reflected in the current neutrophil studies published. Masso-Silva et al. and Morrissey et al. demonstrated a higher NLR compared to controls and Leppkes showed a higher NLR in more severe disease (Masso-Silva et al., 2021, Morrissey et al., 2021, Leppkes et al., 2020). However, it is unclear if neutrophils are in themselves drivers of disease progression or implicated due to their inappropriate clearance in COVID-19 is yet to be discerned.

1.5.1 Patient populations

It is important to consider the populations that were studied as part of understanding the clinical phenotype of infected COVID-19 patients. Research initially was focussed on the most unwell patients; those admitted to intensive care units. Whilst these patients had the highest clinical risk of deterioration, the majority of hospitalisations secondary to COVID-19 consisted of patients who were cared for on normal in-patient hospital wards (level 1 care). This was due to either being deemed not suitable for advanced organ support or escalation to invasive mechanical ventilation not being indicated clinically (on the grounds of co-morbidities, frailty and futility). Indeed, even clinical treatments varied between treatment centres and countries, meaning patients were admitted to ICUs with different clinical needs. Most studies combined patients on invasive mechanical ventilation (IMV) although this did not correlate to admission

to ICU. Middleton et al. reported 50% of patients on ICU requiring IMV whilst Zuo et al 32% (Zuo et al., 2020, Middleton et al., 2020). Zuo et al. separated patients based on requirement of IMV support as severe disease, whilst Busch et al. classified severe patients as requiring supplemental oxygen deliver via face mask or IMV (Busch et al., 2020). There is not enough data published in demographics tables of these studies to calculate a retrospective 4C score, validated for in-hospital mortality secondary to COVID-19.

During the pandemic, the treatment landscape of COVID-19 was rapidly evolving, with new drugs being tested in multi-national platform trials. Several of these drugs were repurposed anti-inflammatory treatments e.g. Dexamethasone /Tocilizumab (Abani et al., 2021). These affect systemic biomarkers of inflammation, of which many form key parts of inflammatory signalling cascades e.g. IL-6. Some studies combined the results of patients given these novel treatments with treatment naïve (Masso-Silva et al., 2021, Zuo et al., 2020). Longitudinal follow up in studies did not document if patients received novel treatments after initial recruitment, which may have biased results.

Circulating levels of all degranulated granulocytes have been reported to be higher in COVID-19 infection, as evidenced by CD63+ surface marker in neutrophils, eosinophils and basophil populations (Borella et al., 2022). This was also seen in the ICU patients studied by Loyer et al. which demonstrated higher levels of neutrophil granule derived proteins such as NE and LTB4 (Loyer et al., 2022). Degranulation is a key effector function of neutrophils.

1.5.2 Effector function alteration

1.5.2.1 Phagocytosis

Phagocytic dysfunction can lead to impaired responses and more severe bacterial infections. Bacterial infection following COVID-19 has been associated with increased severity of lung disease and poorer outcomes (Feldman and Anderson, 2021, Buehler et al., 2021). Although a cohort of severe ICU COVID-19 disease neutrophils were demonstrated to have increased

phagocytosis to labelled bioparticles compared to controls and, the poor clinical outcomes were thought to be due to increased neutrophil host-tissue damage rather than directed to bacterial infection (Masso-Silva et al., 2021). In a pHrodo *Staphylococcus* model, a subset of predominant neutrophils in severe COVID-19 patients had increased phagocytic capacity compared to healthy controls (Morrissey et al., 2021). Investigation into bacterial proliferation using a green fluorescent protein- *Staphylococcus aureus* (GFP-SA) model measuring lag time to exponential growth demonstrated that neutrophils from COVID-19 were less efficient at reducing the lag time compared to healthy controls (Nomani et al., 2021). This led to increased bacterial growth with COVID-19 neutrophils. The increased phagocytic activity combined with increased bacterial growth suggests these activated neutrophils are not reaching the site of infection or are unable to function properly if migration is successful.

Decreased ROS production in COVID neutrophils was reported in a cohort of ICU patients compared to healthy controls and CAP patients. Neutrophils primed with TNFα or TLR4 agonists were exposed to bacterial peptide N-formylmethionine-leucyl-phenylalanine (fMLP) and there was significantly lower ROS production (Loyer et al., 2022). Decreased nuclear mitochondrial ROS (n/mROS) production was reported in the non-ICU cohort of patients. This has been predominantly associated with differentiation and migration, as opposed to phagocytic capacity, classically related to cytoplasmic ROS. However, pre-COVID-19 work has demonstrated that hypoxic states can lead to a decreased n/mROS production (Willson et al., 2022). Masso-Silva et al. also demonstrated an increase in ROS compared to healthy controls after Phorbol 12-myristate 13-acetate (PMA) stimulation (Masso-Silva et al., 2021). This may reflect the method of oxygenation and relatively low state of hypoxia in comparison to the previously described ward-based cohort, limited to conventional oxygen delivery devices.

1.5.2.2 Migration

Migration accuracy is important to limit host-tissue damage. Impaired migration can lead to the presence of immune cells in non-diseased tissues and subsequent cellular activation. The resulting damage from inflammation can then cause increased endothelial leak, more severe illness and release of chemokines leading to further immune cell recruitment. Several enzymes are involved in the migration process, including NE. Increased levels of NE, neutrophil gelatinase and MMP9 were measured in COVID-19 patients compared to controls (Metzemaekers et al., 2021, Aschenbrenner et al., 2021). Overall, there was excessive release of activating and mobilising factors in cells isolated from COVID-19 patients. Elevated serine protease activity in COVID-19 has been previously demonstrated, with associated changes in dipeptidyl peptidase 1 (DPP-1), required for neutrophil serine protease activation (Metzemaekers et al., 2021). Thus investigation of DPP-1 inhibition using brensocatib through a randomised control trial was carried out showing there was no improvement in clinical status at day 29 after administration (Keir et al., 2022). It is not clear if the lack of improvement was due to minimal NE involvement in COVID-19, or if systemic dysfunction in COVID-19 was responsible for the migration inaccuracy. Investigation of the ex vivo effect of brensocatib has not been done to determine if it is effective at a cellular level. The randomised control trial investigating DPP-1 inhibition using Brensocatib showed there was no improvement in clinical status at day 29 after administration (Keir et al., 2022).

RNA sequencing in nine post-mortem patients showed upregulation of genes related to leucocyte migration, although Wu et al. associated these changes with the inflammatory response (Wu et al., 2020). In conjunction with increased migration compared to controls, increased gene expression of cathepsin B and L in COVID-19, and increased expression of genes associated with membrane formation and fibrosis (*MMP7, MMP8, MMP9, MUC5B, GDF15*) were seen. This would be congruent with dysregulated and misdirected migration contributing to host-mediated tissue damage and degree of inflammation seen in COVID-19 infection (Aschenbrenner et al., 2021). This suggests there is a role of neutrophils in the COVID-19 disease process.

1.5.2.3 NETosis

Neutrophil extracellular traps (NETs) have been of particular interest in COVID-19 disease. Associated with the formation of immune thrombus and subsequent thromboembolic disease, potentially correlating with higher levels of thrombotic events in COVID-19 patients (Hazeldine et al., 2019, Vorobjeva and Chernyak, 2020). Studies investigating NET production correlate this to several outputs, including but not limited to levels of citrullinated histone 3 protein (citH3), cell free DNA (cfDNA), direct NET staining, and MPO-DNA. There have been several studies measuring NET levels in post-mortem samples (Radermecker et al., 2020, Leppkes et al., 2020). These show increased NET deposition within the lung parenchyma.

Higher NET production has been reported in COVID-19 compared to healthy controls in several studies (Masso-Silva et al., 2021, Zuo et al., 2020, Veras et al., 2020). This includes both unstimulated production and those stimulated with varying concentrations of PMA. Zuo et al compared 11 COVID-19 patients who developed thrombotic events to 33 hospitalised COVID-19 controls (Zuo et al., 2020). There were higher levels of cfDNA, MPO-SDNA and citH3 in patients with recorded thrombotic events. Circulating D-dimer levels correlated to NET production. Leppkes correlated citH3 and cfDNA to leucocyte counts; and in their post-mortem samples, pulmonary vessels were occluded by aggregated NETs (Leppkes et al., 2020). Previous evidence suggests a propensity of neutrophils to form NETs at higher cellular densities (Schauer et al., 2014). Surface phenotyping of pulmonary endothelial cells near aggregated NETs showed a decreased CD31+ population, suggesting endothelial barrier dysfunction. Infection of healthy neutrophils with inactive SARS-CoV-2 caused NET release and damage to an A459 epithelial cell line, which was abrogated after addition of rhDNAse enzyme (Veras et al., 2020). Similar vascular post-mortem findings were noted in capillary beds in the glomeruli and hepatic periportal fields (Leppkes et al., 2020), indicating a potential role of NETs causing systemic organ dysfunction in severe disease. NET levels were reported to be higher in patients with more severe disease, those on IMV had increased cfDNA levels (Leppkes et al., 2020, Middleton et al., 2020). Exposure to non-activated virus led to increased

NET production in one study, but static levels of cellular and supernatant viral RNA in another, with no change in cell death (Metzemaekers et al., 2021, Veras et al., 2020). This may reflect fundamental changes to the viral spike protein and interaction with the ACE2 receptor expressed on neutrophils.

Addition of COVID-19 serum to healthy neutrophils induced NET production compared to controls, in two separate studies (Zuo et al., 2020, Middleton et al., 2020). Exposure to the virus increased the release of NETs in an infection dependent manner (Veras et al., 2020). This was abrogated by the addition of Cl-amidine, a peptidylarginine deiminase 4 (PAD4) inhibitor. citH3 production through PAD4 dependent signalling is thought to be required for NET formation as there was no correlation to MPO-DNA in COVID-19 serum (Zuo et al., 2020). ROS production required for NET release may function through an alternative PAD4 independent pathway in addition to conventional signalling (Kenny et al., 2017). However, RNA sequencing studies demonstrated upregulation of PAD4 in COVID patients (Aschenbrenner et al., 2021). NETosis was inhibited after supplementation with tenofovir (RNA polymerase inhibitor) in an ex vivo neutrophil infection model (Veras et al., 2020). This suggests that the SARS-CoV-2 virus may be triggering NETosis in COVID-19.

1.5.2.4 Phenotype

Surface protein expression of markers can be indicative of neutrophil reaction to infection or insult. CD62L (L-selectin) is shed after neutrophil adhesion with low levels signifying activation (Kuhns et al., 1995). $CD62L^{low}$ neutrophils have been reported across several COVID-19 studies, in keeping with increased activation. Low density neutrophils appear to be prevalent in COVID-19 infection (Leppkes et al., 2020). These are classically predominant in auto-immune inflammatory conditions and have a high propensity to form NETs, a feature reported throughout COVID-19 neutrophil studies.

Surface markers in keeping with increased levels of reverse transmigration of neutrophils into the endothelial space been shown with higher CD54+ neutrophils. Increased proteolytic

cleavage of junctional adhesional molecule-C (JAM-C) promotes in vivo neutrophil reverse transmigration. JAM-C is important for neutrophil polarisation (Woodfin et al., 2011). Movement of neutrophils back to the vascular space should suggest reduced tissue damage from activated neutrophils. However, the clinical phenotype of pneumonitis and ARDS contradicts this. Patients recruited in these studies represent severely unwell patients in intensive care, and increased reverse transmigration by this point may be too late to reduce ARDS. Investigation of disease state before patients require critical care intervention is therefore key (Loyer et al., 2022).

Three distinct subsets of neutrophil populations have been described depending on CD16 expression levels. $CD16^{int}$ subset was predominantly high in severe COVID-19 infection, and had associated lower expression of CD44 extracellular matrix adhesion molecule (Morrissey et al., 2021). In bacterial pneumonia, downregulated CD44 was associated with neutrophilic lung inflammation. Compared to $CD16^{high}$, $CD16^{int}$ neutrophils displayed increased CD38/ CD40/ CXCR5/ CD69 expression. These molecules suggest an inflammatory, activation phenotype of the neutrophils isolated from COVID-19 patients. CD38 is necessary for extracellular calcium efflux affecting neutrophil chemotaxis (Partida-Sanchez et al., 2001). Platelet interaction and driven inflammation enhanced through neutrophil CD40 interactions, with CD40L neutrophil priming as a potential cofactor has been demonstrated in transfusion related acute lung injury (Khan et al., 2006, Vanichakarn et al., 2008).

Reported changes to neutrophils in COVID-19 infection have been summarised in **Figure 1.7**

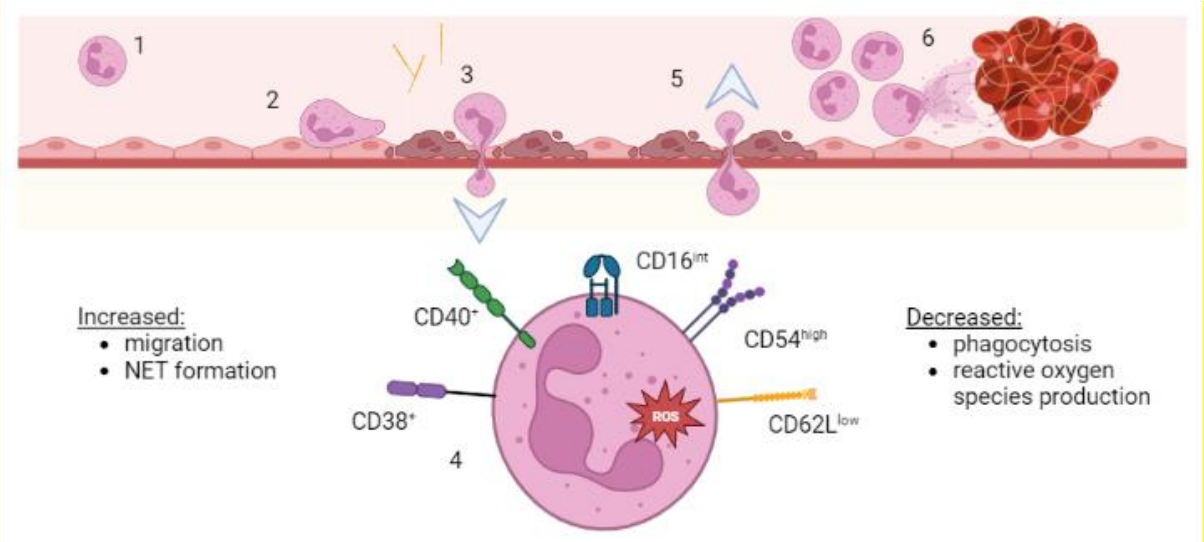

Figure 1.7 Summary of changes to neutrophil function in COVID-19 infection. **1.** Chemotaxis increased through upregulation of CXCR2. **2.** Adhesion alterations with decreased CD44 expression, with shed of CD62L on activation. **3**. Migration through endothelium, with increased damage secondary to increased serine protease expression, leading to increased inflammatory fluid leakage to lung parenchyma. **4**. Altered neutrophil phenotype: CD38/ CD40/ CD54 expression increased, decreased CD62L and dominant $CD16^{int}$ population. **5**. Increased reverse transmigration, with increased CD54 expression and JAM-C proteolytic cleavage. **6**. Increased return to circulation of potentially more rigid neutrophils, leading to subsequent aggregation, neutrophil extracellular trap (NET) release and increased propensity of thrombus formation.

1.6 Summary

Neutrophil population and function described in COVID-19 infection does not correspond to expected behaviours in sepsis or bacterial infections (Masso-Silva et al., 2021). There is conflicting evidence regarding COVID-19 replication and direct effect on neutrophils (Kermani et al., 2021, Chaudhry et al., 2020). Poor outcomes in viral disease are associated with secondary bacterial infections after inflammatory damage to the lung parenchyma (Brundage 2006). The increased neutrophil phagocytosis in one study and ROS described would suggest increased activation and improved bacterial clearance (Masso-Silva et al., 2021). However, decreased bacterial lag time would suggest that there is some dysfunction preventing bacterial clearance, which may be related to changes in ROS production (Nomani et al., 2021). Migration has been described as increased, which may represent migration beyond sites of

infection rather than more rapid migration (Belchamber et al., 2021, Wu et al., 2020). In conjunction with increased NETosis, this would lead to inflammation and immunothromboses beyond the sites of injury. Together, the neutrophil changes in COVID-19 would suggest that they contribute to disease severity.

One of the key considerations of the COVID-19 studies described above is that the patient population sampled mainly included patients admitted to intensive care (Zuo et al., 2020, Middleton et al., 2020). In the United Kingdom, the majority of COVID-19 admissions were on the non-intensive care wards (Sapey et al., 2020). These patients included those with severe comorbidity, frailty and poor pre-morbid state. Similar levels of mortality were observed in this cohort and due to the higher overall volume of patients, this cohort represented the majority of inpatient hospital deaths (Belchamber et al., 2021). In addition to this, patients who were initially treated on non-intensive care units who deteriorated may have had their care escalated.

Investigation of the disease in ward-based, non-intubated patients is therefore crucial. Changes to innate immune function that are noted in severe disease may be irreversible. Knowledge of traits that may lead to poor outcomes will help to target research to treatable traits that could prevent deterioration and death. Dysfunctional neutrophil responses early in disease could cause feed forward changes which lead to the catastrophic pneumonitis and ARDS seen in severe COVID-19.

CHAPTER 2
HYPOTHESIS AND AIMS

2.1 Hypothesis

The clinical symptoms and mortality observed in COVID-19 infection are partly due to a dysfunctional effector neutrophil response compared to that expected in bacterial pneumonia.

2.2 Aims

This thesis aims to:

1) To validate laboratory techniques for isolation of potentially hazardous samples (**Chapter 4**)
2) To describe the population of ward-based COVID-19 patients and identify clinical biomarkers for poor outcomes (**Chapter 5**)
3) To investigate differences in neutrophil effector functions in ward-based patients compared to age-matched controls correlating to clinical measures (**Chapter 6**)
4) To determine if there are differences in neutrophil function between SARS-CoV-2 variants which may account for the different clinical phenotypes observed (**Chapter 7**)
5) To postulate a mechanism by which neutrophil function is altered in COVID-19 (**Chapter 6**, **Chapter 7**)

2.3 Scope of thesis and research

COVID-19 is such a wide-reaching disease that it is important to define the scope of the research possible in this thesis. The patients investigated here are ward-based COVID-19 patients, defined as those admitted to an acute hospital but not requiring intensive care admission or not eligible to intensive care or ventilatory support (including non-invasive ventilation). This population was chosen for several reasons. Patients requiring ward-based care represented the highest burden in terms of absolute numbers of hospital admissions during the pandemic. They represent a population that either recovered with supportive care or deteriorated and required escalation to intensive care. Determining risk factors for deterioration or recovery of these patients and linking these to the underlying cellular mechanism is therefore crucial, potentially identifying a targetable cellular dysfunction. Therefore, this population is more representative of the majority of hospitalised COVID-19 patients.

CHAPTER 3
MATERIALS & METHODS

3.1 Materials

Material	Supplier
4% paraformaldehyde	Avantor, UK product no. PRC/R/3PRC/R/3
96-well flat bottom clear plates	Sigma-Aldrich, Poole, UK product no. PHZ1063
AlexaFluor 488	Invitrogen, UK product number A56021
Antibodies (CXCR4, CD10, CD62L, CD11b, CXCR2, CD54, PD-L1, CD11c, CD66b)	BioLegend, UK
BD Fortessa X20	Becton Dickinson and Company; Franklin Lakes, USA
BioTek Synergy 2 fluorometric plate reader	NorthStar Scientific Ltd, UK
Blood tube - clotted (SST)	Becton Dickinson and Company; Franklin Lakes, USA UK product no. 367977
Blood tube - EDTA	Becton Dickinson and Company; Franklin Lakes, USA UK product no. 367861
Blood tube - lithium heparin (6mL)	Becton Dickinson and Company; Franklin Lakes, USA, UK product no. 367886
Bovine serum albumin	Sigma-Aldrich, Poole, UK product no. A8412
CellROX Deep Red	Thermofischer, UK product no. C10444
CellROX Green	Thermofischer, UK product no. C10422
Centrifuge tube – 15mL	Appleton woods, Birmingham, UK product no. BF032
Centrifuge tube – 50mL	Appleton woods, Birmingham, UK product no. BF034
CitH3 antibody	Abcam, Cambridge, UK product no. ab5103
CXCL8 (Interleukin 8, E. Coli derived)	R&D Systems, USA UK product no 208-IL-050/CF
Cytochalasin D	Sigma-Aldrich, Poole, UK product no. PHZ1063
Dextran	Sigma-Aldrich, Poole, UK product no. 31392
Eppendorf tubes	Sigma-Aldrich, Poole, UK product no. AXYMCT150CS
Fast-read slide	Biosigma, Cona, Italy product no. BVS100
Fibroblast Growth Factor 23 Duoset ELISA	R&D Systems, UK product no DY2604-05
Fine tipped pipette – sterile	Alpha Labs, Eastleigh, UK product no. LW4238
FlowJo v10.8.0	Becton Dickinson and Company; Franklin Lakes, USA
Frosted microscope slides	Fisher Scientific, Loughborough, UK product no. 12362098
Granulocyte Macrophage-Colony Stimulating Factor Duoset ELISA	BioTechne, USA, UK product no DY215-05
GraphPad Prism v9.2	GraphPad Software, Boston, USA
Hanks' Balanced Salt Solution	Gibco, Sigma Life Sciences, UK
Interleukin-6 Quantikine ELISA	BioTechne, USA, UK product no D6050
MACSQuant® Flow Cytometer	Miltenyi BioTec, Surrey, UK

MACSQuant® Washing Solution	Miltenyi BioTec, Surrey, UK product no 130-092-749
MACSQuant® Wash buffer	Miltenyi BioTec, Surrey, UK product no 130-092-747
Myeloperoxidase Quantikine ELISA	BioTechne USA, UK product no MPO-DMYE00B
Penicillin/ streptomycin	Sigma-Aldrich, Poole, UK product no. P4333
Percoll®	Sigma-Aldrich, Poole, UK product no. P4937
Phorbol 12-myristate 13-acetate (PMA)	Sigma-Aldrich, Poole, UK product no. P1585
Phosphate Buffered Saline (PBS)	Sigma-Aldrich, Poole, UK product no. P4417
REASTAIN® Quick-Diff Kit	REAGENA, Finland product no. 102164
RPMI media	Sigma-Aldrich, Poole, UK product no. R8758
Sodium chloride	Sigma-Aldrich, Poole, UK product no. S9888
SPSS Statistics	IBM, USA
Sytox Green	Thermofischer, USA, UK product no. S7020
Transwell plates	Fisher Scientific, Loughborough, UK product no. 40627
TRIzol Reagent	Ambion, UK product no. 15596018
Tween-20	Sigma-Aldrich, Poole, UK product no. P1379
Vascular Endothelial Growth Factor Quantikine ELISA	BioTechne, USA, UK product no. DVE00
Venepuncture vacutainer system	Becton Dickinson and Company; Franklin Lakes, USA
Zombie Near Infrared Live/Dead stain	Thermofischer, USA, UK product no. L34976

3.2 Methods

Methods described in this chapter are universal for experiments throughout this thesis.

3.2.1 Subject selection

3.2.1.1 Validation experiments

Healthy volunteers of varying ages were recruited from within the Institute of Inflammation and Ageing, University of Birmingham, in accordance with ethics REC ref: ERN 12-1184R2. Written informed consent was obtained, and all volunteers had no acute medical illness in the last two weeks prior to recruitment.

3.2.1.2 COVID-19 patients

Patients were recruited between 19th January 2021 and 22nd April 2022, from the Queen Elizabeth Hospital Birmingham (QEHB) under the studies “Neutrophil function in Pneumonia and Sepsis” and “Neutrophil Bioenergetics and function in Pneumonia and Sepsis” in accordance with ethics REC ref: 19/WA/0299 and 20/WA/0092. Written informed consent was obtained from all patients. In cases where this was not possible (e.g. patients lacked capacity due to illness or chronic neurological impairment), next of kin was contacted as personal consultee. In the instances where the next of kin was not contactable or there was no next of kin listed, a designated consultee (Consultant responsible for inpatient care) was sought for discussion of consent.

Patients were screened by a single researcher from patients who had been inpatients for less than 48 hours, had radiological changes on chest radiograph, not been treated as part of a drug trial, and at least one of: 1) positive point of care (antigen) COVID-19 test on admission;

or 2) positive polymerase chain reaction (PCR) COVID-19 test result. Full inclusion and exclusion criteria are listed in **Table 3.1**.

Inclusion Criteria	**Exclusion Criteria**
>18 years old	Declines consent OR personal consultee OR designated consultee declines consent
Diagnosis of pneumonia (clinical or radiological evidence)	Patient treatment palliative in nature
Positive COVID-19 test (antigen OR PCR), either in community or on admission	Patient currently pregnant
Recruitment within 48 hours of admission to Queen Elizabeth Hospital Birmingham	Patient does not meet inclusion criteria
	Patient enrolled in an interventional research study of a novel drug/ unlicensed therapy
	Patient is immunocompromised (prior oral systemic corticosteroid therapy within the last 3 months and prior to acute episode; known regular therapy with other immunosuppressive medication (e.g. azathioprine); known acquired immunodeficiency syndrome
	Active malignancy
	Diagnosis of COPD or asthma

Table 3.1 Inclusion and exclusion criteria for recruitment of admitted COVID-19 patients

Sensitivity of reverse transcriptase PCR (RT-PCR) testing has been reported at 98% for nasopharyngeal (NP) swabs and 69% for salivary samples compared to that of rapid antigen testing, reported at 35-47% depending on site and dry swabbing (Kritikos et al., 2021). PCR tests were used as per contemporaneous NHS supply to acute NHS trusts at the time of the

pandemic. To avoid recruitment of patients without active pulmonary COVID-19 infection (e.g. those with incidental positive COVID-19) who may have been admitted for other illnesses, we reviewed chest radiographs to ensure there was a radiological diagnosis of COVID-pneumonitis. This was carried out by a respiratory specialist doctor. Patients were physically examined after consent at recruitment to confirm biochemical and imaging data.

Age, height, weight, smoking history, co-morbidities, clinical frailty score, ethnicity, and presenting symptoms were collected from the patient and electronic records. Clinical observational data including NEWS2 parameters and biochemical data from blood results was collected for each patient. Data was stored anonymously on local NHS Trust servers. Sufficient clinical data was recorded in order to calculate clinical severity scores e.g. 4C score for COVID-19 pneumonia mortality, CURB-65 score for community acquired pneumonia mortality. In accordance with General Data Protection Regulation (GDPR) and Good Clinical Practice (GCP) guidance, only sufficient data was collected for analysis.

As per ethical approval, patients were followed up in hospital if they remained an inpatient between day 3-5 after recruitment. Remote follow up was carried out at 28 days for mortality and readmission, and at 3, 6 and 12 months for mortality, readmission and radiological changes.

3.2.1.3 Age matched controls (AMC)

AMC were recruited between 1st February 2021 and 19th July 2021. These were either patients attending pre-booked face-to-face outpatient appointments (ophthalmology clinic) under the study “Neutrophil function in Pneumonia and Sepsis”, ethics REC ref:19/WA/0299, or from hospital staff under ethics REC ref: ERN 12-1184R2. Written informed consent was obtained from all AMC.

AMC displayed no clinical signs of acute illness, including COVID-19 within the previous 2 weeks, as assessed by a respiratory physician. Exclusion criteria matched those for COVID-19 patients as shown in table 1.

Age, smoking history, vaccination status, co-morbidities, ethnicity, and clinical frailty score were collected from the patient and electronic records. Data was stored anonymously on local NHS Trust servers. No NHS clinical routine biochemical and haematological blood samples or biochemical measurements (e.g. height, weight, oxygen saturations, respiratory rate, blood pressure, temperature, heart rate) were recorded due to constraints during the recruitment process in a busy NHS outpatient clinic. This avoided delays in patient care.

3.2.1.4 Community acquired pneumonia (CAP)

Community acquired pneumonia (CAP) patients were recruited between 19th January 2021 and 3rd March 2021 under the study "Neutrophil function in Pneumonia and Sepsis", in accordance with ethics REC ref: 19/WA/0299. Patients admitted to the QEHB were screened for a clinical diagnosis of CAP as defined by the British Thoracic Society Guidelines on the Management of Community Acquired Pneumonia 2009: 1) "symptoms and signs consistent with an acute lower respiratory tract infection associated with new radiographic shadowing for which there is no other explanation (e.g. not pulmonary oedema or infarction") and 2) "the illness is the primary reason for hospital admission and is managed as pneumonia" (Lim et al., 2009). Patients were required to have either a negative 1) point of care (antigen) COVID-19 test on admission; or 2) PCR COVID-19 test result. Incidental COVID-19 infection (e.g. patients who were admitted with another infection but were incidentally found to be COVID-19 disease positive) were included only if there were pulmonary radiological changes present. Written informed consent was obtained from all patients. In cases where this was not possible (e.g. patients lacked capacity due to illness or chronic neurological impairment), next of kin was contacted as personal consultee. In the instances where the next of kin was not

contactable or there was no next of kin listed, a designated consultee (Consultant responsible for inpatient care) was sought for discussion of consent.

Chest radiographs were reported by a radiologist 3-7 days after admission. These were corroborated with the recruiting researcher's review.

Age, height, weight, smoking history, co-morbidities, clinical frailty score, ethnicity, and presenting symptoms were collected from the patient and electronic records. Clinical observational data including NEWS2 parameters and biochemical data from blood results was collected for each patient. Data was stored anonymously on local NHS Trust servers. Sufficient clinical data was recorded in order to calculate clinical severity scores e.g. 4C score for COVID-19 pneumonia mortality, CURB-65 score for community acquired pneumonia mortality. In accordance with GDPR and GCP guidance, only sufficient data was collected for analysis.

As per ethical approval, patients were followed up in hospital if they remained an inpatient between day 3-5 after recruitment. Remote follow up was carried out at 28 days for mortality and readmission, and at 3, 6 and 12 months for mortality, readmission and radiological changes.

3.2.2 Sample processing

Samples from COVID-19 patients were collected under risk assessment AG 20_65. Under the conditions of this assessment all samples were processed under aerosol free conditions and inactivated before leaving containment as SARS-CoV-2 is a hazard group 3 pathogen. As such, techniques used in processing of these samples have been modified to meet the specific requirements of Health and Safety Executive (HSE) guidance. Samples in AMC and CAP control groups have been collected and processed under matched conditions to ensure parity in analysis.

A total of 45mL of peripheral blood was taken by venepuncture by a clinician, using a BD vacutainer system (Becton Dickinson and Company; Franklin Lakes, USA). This was in the form of 5x 6mL lithium heparin blood tubes, 1x 6mL clotted sample tube, 1x 9mL EDTA blood tube. Where possible and appropriate for inpatients, routine clinical bloods for inpatient stay were collected concurrently to avoid repeated venepuncture. Routine serum/ blood clinical measures such as WCC, Neutrophil count, and CRP were obtained from samples processed in the Queen Elizabeth Hospital Birmingham NHS laboratory on admission to hospital.

Samples were taken for processing to the University of Birmingham Institute of Inflammation and Ageing laboratories on site at the Queen Elizabeth Hospital Birmingham within one hour. Samples were then processed for neutrophil isolation and collection of serum and plasma for storage and further experiments. Serum and plasma were obtained from lithium heparin, EDTA tubes and clotted sample tubes as appropriate (Becton Dickinson and Company; Franklin Lakes, USA). Tubes were left for 30 minutes upright for sedimentation, then centrifuged at 300 x *g*, 21°C, 5 minutes. Serum and plasma were pipetted into 1.5mL Eppendorf containers and stored at -80°C.

3.2.3 Cell isolation

Neutrophils were isolated following a laboratory standard and validated protocol. COVID-19 samples were processed and analysed as per COVID-19 processing guidance, in a separate laboratory environment to minimise the risk of infection.

In a sterile class II biological safety cabinet, 18mL of peripheral blood collected in lithium heparin vacutainer bottles (Becton Dickinson and Company; Franklin Lakes, USA)) was added to a 50mL Falcon centrifuge tube. 3mL of 2% (w/v) dextran (1g in 50mL 0.9% sodium chloride,

filter sterilised) was added to the blood. This was gently mixed by hand through rotation. Blood was incubated at room temperature for 30 minutes to allow erythrocyte sedimentation with remaining buffy coat on top.

A Percoll® (Merck, Darmstadt) gradient was used to separate both peripheral blood mononuclear cells (PBMCs) and neutrophils from the leucocytes in the buffy coat. 80% and 56% (v/v) Percoll® solutions were made using neat Percoll® and a combination of 10% and 1% (w/v) saline solutions. Percoll® gradient was made up in a single 15mL Falcon centrifuge tube, with a second tube used if the buffy coat volume was greater than 8mL from a single patient. 5mL of the 56% (v/v) Percoll® solution was added to the 15mL tube. A fine bore Pasteur pipette was used to layer 2-3mL of the 80% (v/v) Percoll® solution underneath the 56% solution.

The buffy coat was aspirated using a wide bore Pasteur pipette and gently layered on top of the Percoll® gradient at 45 degrees to avoid inadvertent mixing. When all the buffy coat had been transferred, the 15mL tube was centrifuged at 470 x *g* for 20 minutes (room temperature, minimum acceleration, minimum brake to prevent pelleting of PBMCs and neutrophils, through preserving Percoll® gradient. Tubes were carefully removed from the centrifuge (**Figure 3.1**).

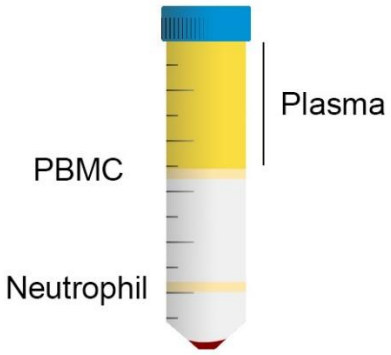

Figure 3.1 Neutrophil isolation process, after Percoll® centrifugation. Image depicts 15mL Falcon tube after removal from centrifuge. Demonstrates PBMC and neutrophil layers to be removed

The top layer of plasma, PBMCs and debris was aspirated using a wide bore Pasteur pipette and placed in a new 15mL Falcon centrifuge tube. This was topped up to 15mL with filter sterilised (f/s) phosphate buffered saline (PBS) solution. Cells were then centrifuged at 300 x *g* for 5 minutes (room temperature, maximum acceleration, maximum brake) for pelleting of cells.

Neutrophils form a layer at the interface between 80% and 56% (v/v) Percoll® layers. These were aspirated using a fine bore Pasteur pipette and transferred into a fresh 15ml tube containing 5mL of f/s PBS solution. Placing neutrophils gently into PBS solution rather than directly into the bottom of the tube reduces trauma, associated activation and consequent death of neutrophils. This was then topped up to 15mL with f/s PBS. Cells were then centrifuged at 300 x *g* for 5 minutes (room temperature, maximum acceleration, maximum brake) for pelleting of cells.

Resulting supernatant from PBMCs and neutrophils was discarded by tipping. The pellet was resuspended in 2-10mL media (RPMI 1640 media supplemented with 10mg/L 1% w/w Penicillin/Streptomycin). PBMCs and neutrophils were counted on a haemocytometer and conventional light microscope on a Fast Read slide (Biosigma, Cona, Italy). 5 million PBMCs and neutrophils were stored in 1mL TRIzol Reagent (Ambion, UK) for RNA analysis. The remaining neutrophil sample was diluted to either 1 million cells/mL or 10 million cells/mL depending on further experimentation. In the event of insufficient neutrophils, experiments were prioritised which is reflected in n for each experiment. Order of experiment prioritisation is detailed in **Table 3.2**.

Experiment in order of priority	Cells Required
Phagocytosis	3,000,000
Transwell migration	8,000,000
NETosis	3,000,000
Phenotyping	2,000,000
TRIzol treatment and storage for RNA/ protein analysis	5,000,000
Total cells required	21,000,000

Table 3.2 Table of prioritisation of isolated neutrophil experiments and number of cells required, including repeats.

Purity of neutrophils was assessed by cytospin. 100,000 neutrophils at a concentration of 1 million cells/mL were transferred to cytospin funnels clamped to a frosted microscope slide (Fisher Scientific, UK) and centrifuged at 300 rpm for 5 minutes (room temperature, maximum acceleration, maximum brake). Slides were fixed by immersion in 100% methanol for approximately 30 seconds followed by staining using the REASTAIN® Quick-Diff Kit (REAGENA, Finland) red (cytoplasmic) and blue (nuclear) stains for approximately 30 seconds each. Once dried, slides were reviewed under a light microscope at 45x magnification. Purity was determined by manual cell count in 4 distinct areas. 90% purity was used as a threshold for sample experimentation.

3.2.3.1 Neutrophil viability

Viability of isolated neutrophils was assessed with Zombie (near infra-red) NIR live/dead stain (BioLegend). 1µL of live/dead stain was added per 100µL of cell suspension. Cells were treated for 30 minutes at room temperature, in the dark. After incubation, 4% (v/v) PFA was added in equal volume to the cell suspension to stop further reagent reaction. Samples were

incubated for a further 5 minutes at room temperature. FACS tubes were centrifuged at 300 x *g* for 5 minutes (room temperature, maximum acceleration, maximum brake). Supernatant was discarded and pellet resuspended in 200µL of f/s (w/v) PBS. Samples were analysed on a Miltenyi BioTec MACSQuant 10 analyser, up to 10,000 neutrophil events per sample. Gating strategy for neutrophils is shown in **Figure 3.2**.

3.2.4 Functional experiments

3.2.4.1 Phagocytosis

Neutrophil phagocytic capacity was assessed using labelled heat-killed *Streptococcus pneumoniae (S. Pneumoniae*) bacteria, serotype 9V, strain 10692. Horse blood broth was prepared using 18.5g Brain Heart Infusion (BHI) in 500mL de-ionised (dH2O). Re-suspended broth was autoclaved at 121^{o}C and cooled prior to use. *S. pneumoniae* were obtained from agar plates, 3 colonies inoculated 25mL prepared broth. This was placed in an AnAerogen Jar with one packet of carbon dioxide generating charcoal. This was placed on a plate shaker at 150rpm for 8 hours. The inoculated 25mL was transferred to 500mL of media and incubated overnight. After 18 hours incubation, 16mL was removed and mixed with 4mL sterile Glycerol to be stored. The remaining 8mL was aliquoted into 4x 50ml Falcon centrifuge tubes and centrifuged at 2720 x *g* for 20 minutes (room temperature, maximum acceleration, maximum brake). Resulting pellet was resuspended in 2mL Hanks' Balanced Salt Solution (Sigma Life Sciences, UK), combined to a total volume of 20mL. This mixture was incubated at 70^{o}C for 2 hours to heat-kill bacteria. Efficacy of heat-treatment was determined by simple culture on an agar plate. Colony formation indicates insufficient heat-killing, indicating heat-treatment should be repeated.

To allow fluorescent labelling bacteria suspension was centrifuged at 5000 x *g* for 3 minutes (room temperature, maximum acceleration, maximum brake). The supernatant was aspirated and discarded, the pellet was resuspended in 1mL of $NaHCO_3$ buffer (0.84g sodium bicarbonate, 100mL dH_2O) and sonicated for 5 minutes. 10µL AlexaFluor 488 (A1101-[49656651 Invitrogen] (1mg lyophilised dye in 1mL DMSO) was added to each pellet. These

were placed on a windmill rotator overnight at room temperature in the dark. Eppendorfs were centrifuged at 2720 x *g* for 3 minutes (room temperature, maximum acceleration, maximum brake), supernatant aspirated and discarded. The pellet was resuspended in 1mL of Hanks' Balanced Salt Solution (Sigma Life Sciences, UK). This wash was repeated three times to thoroughly remove unbound stain. Bacteria were opsonised for 1 hour with 10% human albumin serum. Following this, bacteria were centrifuged at 5000 x *g* for 3 minutes to wash. Bacteria were resuspended in filter/sterilised PBS and sonicated for 5 minutes.

150,000 neutrophils at a concentration of 1 million cells/mL were added to FACS tubes. Experiments always included an untreated control (UTC), negative control and neutrophil viability stain. 1µL Cytochalasin D used as a negative control, incubated with the cells for 30 minutes prior to addition of labelled *S. pneumoniae*.

Following incubation, labelled 10µL *S. pneumoniae* was added to each FACS tube if required. 1µL CellROX green (Thermofischer), 1µL CellROX deep red (Thermofischer), or 1µL zombie NIR live/dead stain (BioLegend) were added to Neutrophils were incubated with *S. pneumoniae* for 30 minutes at a ratio of 1600:1 (bacteria: neutrophil). CellROX dyes allow assessment of reactive oxygen species generation by neutrophils during phagocytosis. 1µL live/Dead viability stain was added to the correct tube. Number of experiments varied depending on conditions and treatments tested. Cells were incubated at 37^{o}C for 30 minutes. Protocol used then varies depending if samples were fixed or unfixed.

<u>Fixed</u>

As per COVID-19 sample processing guidelines, 150µL 4% (v/v) PFA was added to each FACS tube. Samples were incubated at room temperature for 5 minutes. FACS tubes were centrifuged at 300 x *g* for 5 minutes (room temperature, maximum acceleration, maximum brake). Supernatant was discarded and pellet resuspended in 200µL of f/s (w/v) PBS.

Unfixed

Phagocytosis was stopped by placing FACS tubes on ice to cool to 4^{o}C for 10 minutes. FACS tubes were then centrifuged at 300 x *g* for 5 minutes (4^{o}C, maximum acceleration, maximum brake). Supernatant was discarded and pellet resuspended in 200µL of cold f/s PBS.

Samples were analysed on a Miltenyi BioTec MACSQuant 10 analyser, up to 10,000 neutrophil events per sample. Gating strategy for neutrophils is shown in **Figure 3.2**. Phagocytosis results are expressed as % phagocytosis (percentage of neutrophil population positive with fluorescent labelled *S. pneumoniae*), or median fluorescence intensity (MFI) of the positive neutrophil population. CellROX results (green and deep red) are expressed as MFI of the neutrophil population.

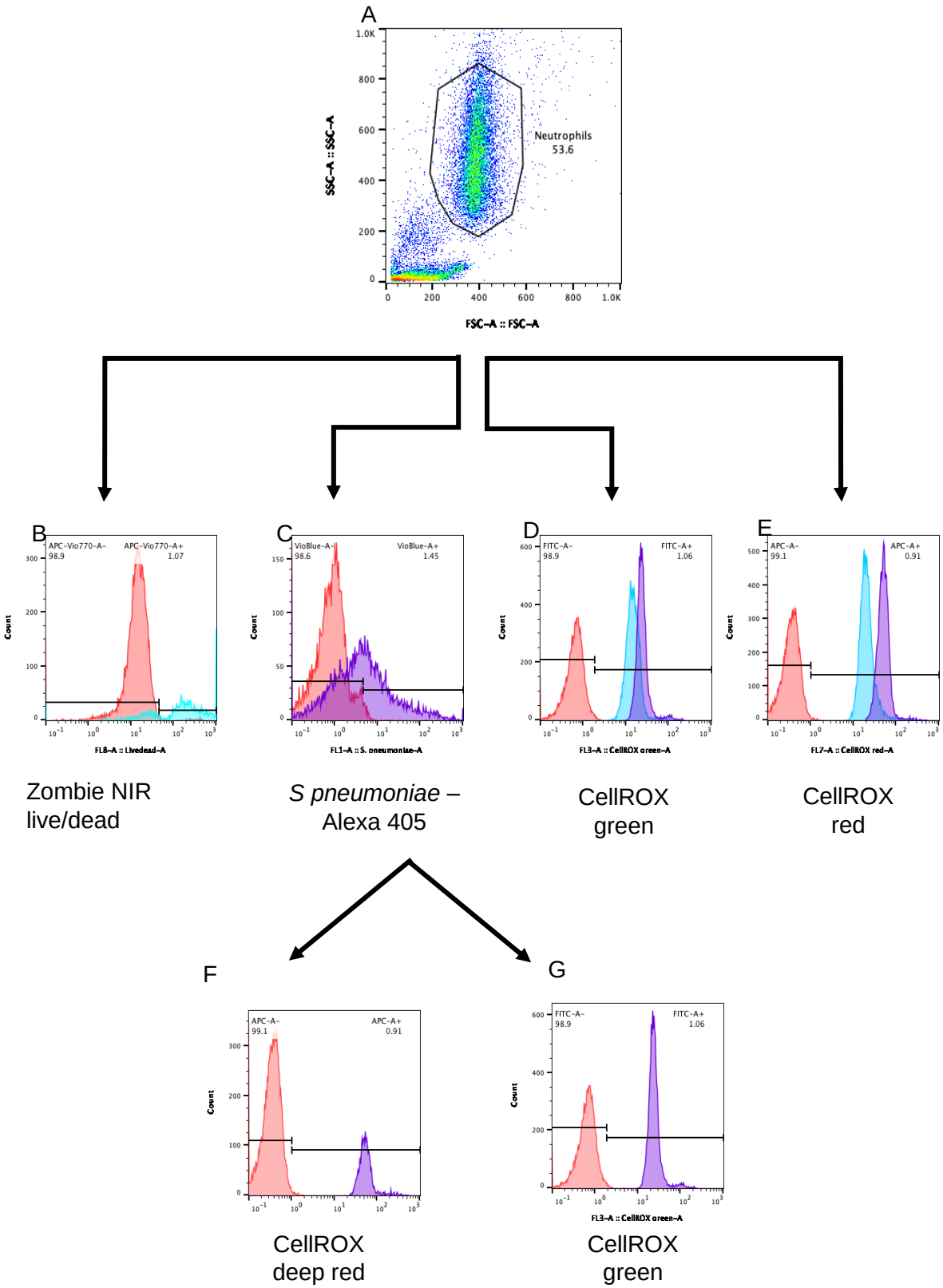

Figure 3.2 Neutrophil effector function experiment flow cytometry gating strategy. A. Neutrophil gating based on forward vs side scatter. Population then selected based on multiple parameters. B. Zombie near infra-red live/dead viability stain. C. Phagocytosis of labelled *S. pneumoniae* (AlexaFluor 405). D. CellROX Green staining for cytoplasmic ROS production. E. CellROX Red for nuclear/ mitochondrial ROS production. Both CellROX Green (F) and Red (G) were measured within the *S. pneumoniae* gate (C). Colours represent different labelling stains used to distinguish between populations.

3.2.4.2 Transwell migration

1 million neutrophils at a concentration of 10 M cells/mL were added to FACS tubes, and treatments added for 30-minute incubation at 37ºC as required. Each experiment included an untreated control (no CXCL8 added to media) and a positive control (only CXCL8 added to media, cells not incubated with any treatment) for comparison. 600µL of media (RPMI 1640 media supplemented with 10mg/L 1% w/w Penicillin/Streptomycin) was added to a 24 well plate for each condition tested. 100nM CXCL8 (Sigma) was added to each well. Transwell migration inserts (6.5mm Transwell with 3.0 μm pore, SLS Ltd) were carefully added to each well. **Figure 3.3** shows the setup for the Transwell experiments. Cells were transferred into the Transwell chamber with care not to directly add them to the media in the well. The plate was incubated at 37ºC, 5% CO_2 for 90 minutes.

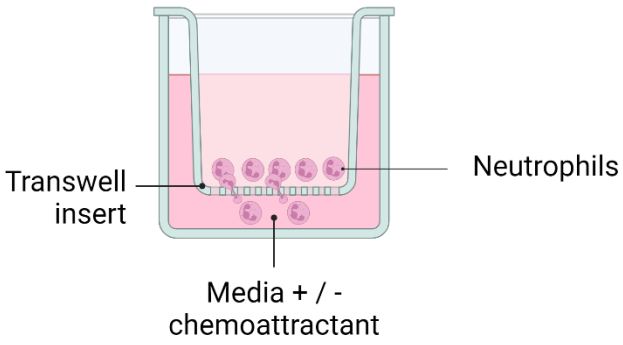

Figure 3.3 Diagrammatic representation of Transwell migration experiment. Media +/- chemoattractant was added to wells in a 24-well plate. Transwell inserts (6.5mm Transwell with 3.0µm pore, SLS Ltd) were subsequently inserted into the wells, and isolated neutrophils added. Neutrophils migrate towards chemoattractant through the pores and after 90 minutes the insert is removed and cells counted from the well.

At 90 minutes Transwell chambers were removed and discarded with care to not displace the remaining cells from the chamber to the media. Solution in the wells was then gently aspirated and then transferred into new FACS tubes.

Fixed

600µL of 4% (v/v) PFA was added to each FACS tube and left to incubate at room temperature for 15 minutes. Following incubation, tubes were centrifuged at 300 x *g* for 5 minutes (room temperature, maximum acceleration, maximum brake). Supernatant was discarded and pellet resuspended in 600µL of sterile PBS.

Unfixed

FACS tubes were transferred to ice to reduce temperature to 4°C. Tubes were centrifuged at 300 x *g* for 5 minutes (4°C, maximum acceleration, maximum brake). Supernatant was discarded and pellet resuspended in 600µL of cold sterile PBS.

Cells were analysed by flow cytometry on a Miltenyi Biotech MACSQuant analyser 10. Gating strategy as per **Figure 3.2**, however, no sub-gating analysis was required; count of neutrophils was used to compare between untreated control, positive control and treatments investigated. Fold change from RPMI negative control was calculated as per the following equation:

$$\frac{no.cells\ migrated\ to\ CXCL-8}{no.cells\ migrated\ to\ vehicle\ control}$$

3.2.4.3 Neutrophil extracellular trap (NET) measurement

227nM phorbol 12-myristate 13-acetate (PMA, Sigma-Aldrich) was used as a stimulant for NET production. 200,000 neutrophils at a concentration of 1 million cells/mL were added a 96-well plate, and treatments added for 30-minute incubation at 37°C, 5%CO_2 as required. Each experiment included an untreated control (no PMA added to cells) and a positive control (only PMA added to cells) for comparison. Experiments were duplicated for each treatment tested. 1µL of PMA was added to the wells and the plate was then incubated for 3 hours at 37°C, 5% CO_2.

Following incubation 150µL of supernatant from the 96-well plate was removed and transferred to FACS tubes.

Fixed

150µL of 4% (v/v) PFA was added to each FACS tube and left to incubate at room temperature for 15 minutes. Following incubation, tubes were centrifuged at 2,200 x *g* for 10 minutes (4°C, maximum acceleration, maximum brake).

Unfixed

100µL of supernatant from FACS tubes was carefully aspirated and transferred to a black sided 96-well plate. 1µM of Sytox green (Life Technologies) was added to each well. The 96-well plate was left to incubate at room temperature in the dark for 10 minutes. The plate was read on a BioTek Synergy 2 fluorometric plate reader (NorthStar Scientific Ltd, UK) with excitation set to 485nm and emission set to 528nm. Fold change from negative control was calculated as follows:

$$\frac{absorbance\ of\ PMA\ stimulated\ neutrophil\ supernatant}{absorbance\ of\ vehicle\ control\ neutrophil\ supernatant}$$

3.2.4.4 DNase activity

NETs isolated from healthy controls were used as the substrate to determine DNase activity. NETs were generated from 5 x10^4 neutrophils isolated from EDTA anti-coagulated blood. 100µL neutrophils at 1 M cells/mL were aliquoted into a 96-well flat-bottomed plate ((Becton Dickinson and Company; Franklin Lakes, USA) and then stimulated with 25nM PMA (Sigma-Aldrich) for 3 hours at 37°C, 5% CO_2. NETs were collected post-stimulation and incubated for 6 hours at 37°C, 5% CO_2 with 5% sera diluted in Hank's balanced salt solution, supplemented with calcium and magnesium ($HBSS^{+/+}$, Gibco, Life Technologies), or in $HBSS^{+/+}$ alone. Samples underwent fixation with 4% (v/v) PFA for 30 minutes. Three washes with sterile PBS followed (centrifuged at 300 x *g* for 5 minutes (21°C, maximum acceleration, maximum brake)

before a 10-minute incubation at room temperature in the dark with 1µM Sytox green (Life Technologies). Fluorescence was then measured using a BioTek Synergy 2 fluorometric plate reader (NorthStar Scientific Ltd, UK) with excitation set to 485nm and emission set to 528nm. NET degradation by 5% serum pooled from 4 healthy control participants was used as a control for 100% DNase activity.

3.2.4.5 Fluorometric analysis of plasma cell-free deoxyribonucleic acid (cfDNA)

cfDNA was measured from heparinised plasma samples using a fluorometric based assay. 10µL plasma was incubated with 1µM Sytox green (Life Technologies) for 10-minutes at room temperature in the dark. Following this, fluorescence was measured using a BioTek Synergy 2 fluorometric plate reader (NorthStar Scientific Ltd, UK) with excitation set to 485nm and emission set to 528nm. A λ-DNA standard curve (Fisher Scientific, UK) was used to determine cfDNA concentrations. Samples were replicated in duplicate and mean values were used to calculate concentrations from extrapolating the standard curve.

3.2.5 ELISA

Plasma biomarkers were measured by ELISA. BioTechne Quantikine kits were used for Myeloperoxidase (MPO – DMYE00B), IL-6 (D6050) and vascular endothelial growth factor (VEGF) (DVE00). BioTechne Duoset kits were used to measure granulocyte macrophage-colony stimulating factor (DY215-05). All kits were used according to manufacturing instructions. Lower and upper limits of detection are shown in **Table 3.3**.

ELISA Kit	Lower limit of detection	Upper limit of detection
MPO (DMYE00B)	0.156 ng/mL	10 ng/mL
VEGF (DVE00)	15.6 pg/mL	1000 pg/mL
GM-CSF (DY215-05)	15.6 pg/mL	1000 pg/mL
IL-6 (D6050)	3.13 pg/mL	100 pg/mL

Table 3.3 Lower and upper limits of detection pre-dilution of samples as per manufacturer datasheets for ELISA kits used (MPO – myeloperoxidase, VEGF – vascular endothelial growth factor, GM-CSF – granulocyte macrophage colony stimulating factor, IL-6 – interleukin 6).

R&D Systems Duoset ELISA kits

Duoset kits were prepared according to manufacturer instructions. Reagents were made in advance and autoclaved or f/s depending on component products: wash buffer 0.05% Tween® 20 in PBS, Reagent diluent 1% BSA in PBS, Colour Reagent A (H_2O_2), Colour Reagent B (tetramethylbenzidine), Stop solution (H_2SO_4). ELISA components pre-made were brought to room temperature at least 15 minutes before use: Streptavidin HRP made to working concentration as per individual certificate of analysis (CoA), Capture antibody made to working concentration as per individual CoA, Detection antibody, made to working concentration as per individual CoA, Recombinant standard, made to working concentration as per individual CoA and then underwent serial dilution as per manufacture instructions.

100µL of capture antibody was added to each well of a 96-well flat-bottomed plate to coat, then covered and incubated overnight at room temperature. The plate was washed three times using 400µL wash buffer dispensed through a squirt bottle. All liquid was removed between washes using a percussive method. 300µL Reagent diluent was added to each well and the plate was covered and incubated for one hour. Three washes as per previous method were carried out after this. 100µL of sample was added per well. Samples were diluted based on expected concentration of protein measured or based on previous sample results. 96-well plate was then covered and incubated for two hours at room temperature. Three washes as per previous method were carried out after this. 100µL of detection antibody was added, plate covered and incubated for two hours at room temperature. Three washes as per previous

method were carried out after this. 100µL of Streptavidin HRP was added to each well, plate covered and incubated for 20 minutes at room temperature in the dark. Three washes as per previous method were carried out after this. 100µL of substrate solution was added to each well, plate covered and incubated at room temperature in the dark. 50µL of Stop solution was added to each well, and gently mixed. Plates were then read on a plate reader set at 450nm with wavelength correction set to 540nm.

Biotechne Quantikine ELISA kits

Quantikine kits were prepared according to manufacture instructions. Reagents were made in advance: Wash buffer was mixed to dissolve the crystals and 20mL was added to 480mL of deionised water, Colour Reagents A+B were mixed prior to use and protected from light, Recombinant standard was made to working concentration and then underwent serial dilution as per manufacture instruction. The remaining reagents required for the ELISA assay were premade and supplied diluted to the correct concentration

Initially, the 96-well flat-bottomed plate was coated as per instructions, then covered and incubated overnight at room temperature. The following day, 100µL Assay diluent was added to each well, followed by 100µL sample per well. ELISA plate was covered and incubated for 2 hours at room temperature.. The plate was washed three times using 400µL wash buffer dispensed through a squirt bottle. All liquid was removed between washes using a percussive method. 200µL of target molecule conjugate antibody was added to each well. Plate was covered and incubated for 2 hours at room temperature. Three washes as per previous method were carried out after this. 200µL Substrate solution was added to each well and the plate was then incubated for 20 minutes in the dark. 50µL of Stop solution was added to each well, and gently mixed. Plates were then read on a plate reader set at 450nm with wavelength correction set to 540nm.

Samples were analysed in duplicate, and results averaged. A simple linear regression with line of best fit was calculated to determine target molecule concentration.

3.2.6 Surface marker phenotyping

Surface marker phenotyping was carried out by flow cytometry. Neutrophils at a concentration of 1 x10^6 cells/mL were fixed with 4% (v/v) PFA for 5 minutes before tubes were centrifuged at 300 x *g* for 5 minutes (room temperature, maximum acceleration, maximum brake). Supernatant was discarded and pellet resuspended in 100µL of sterile ACS buffer (sterile PBS with 1% bovine serum albumin (BSA). 100µL of cell suspension was then stained with mouse anti-human monoclonal antibodies or concentration-matched isotype controls on ice, in the dark. Gating strategy is show in **Figure 3.4**, materials used are shown in **Table 3.4**.

Table 3.4 Antibodies used for surface receptor expression detection by flow cytometry. All antibodies were sourced from BioLegend (UK).

.

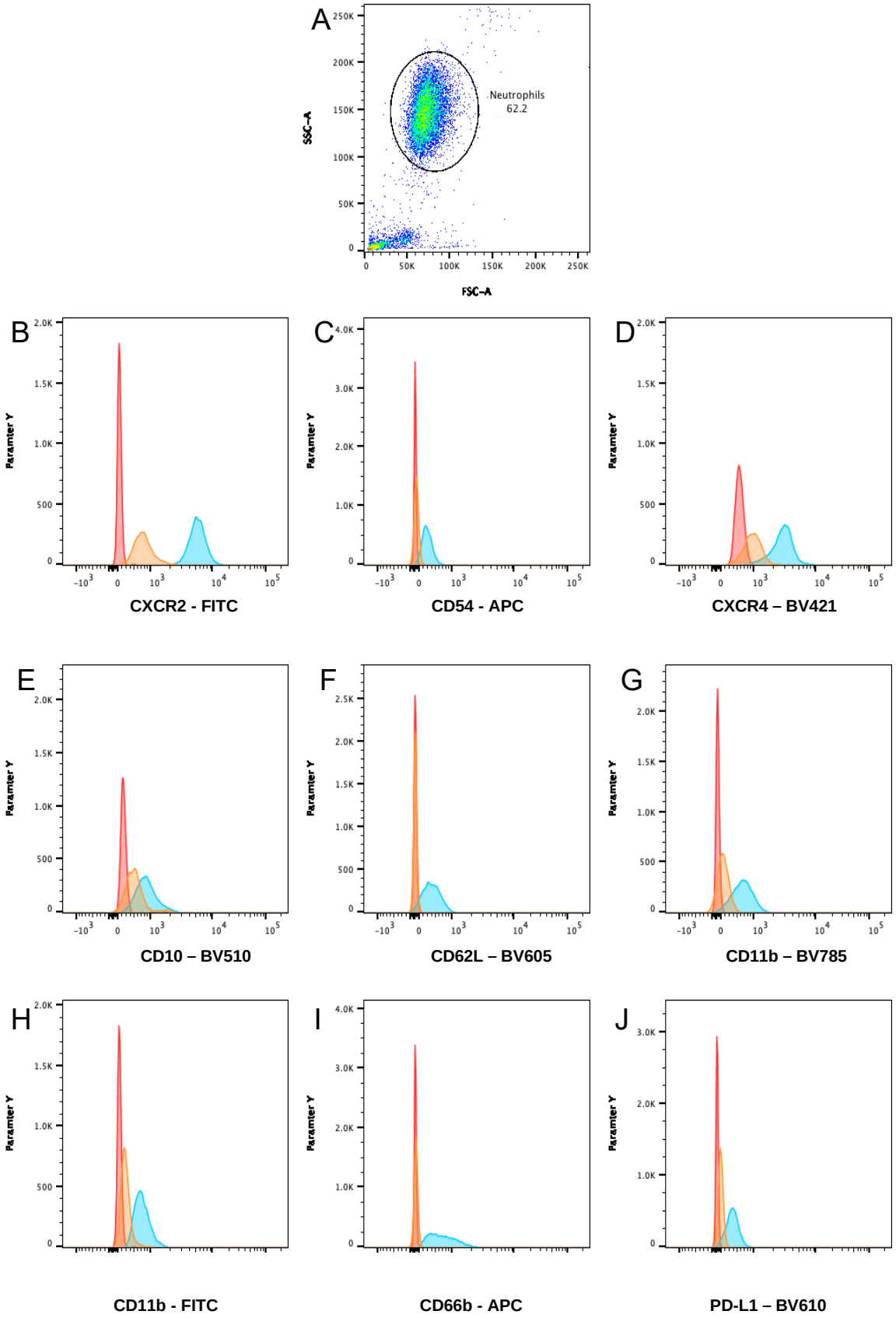

Figure 3.4 Gating strategy for neutrophil surface receptor expression by flow cytometry. Neutrophils were gated on forward vs side scatter. Receptor expression was analysed within this gate. Histograms show negative unstained control in red, isotype control in orange and the positive sample in blue.

Receptor	Cat no	Channel	Dilution
CXCR4	306518	BV421	1:20
CD10	312220	BV510	1:20
CD62L	304834	BV605	1:100
CD11b	301346	BV786	1:40
CXCR2	320704	FITC	1:40
CD54	322712	APC	1:100
PD-L1	329724	BV605	1:100
CD11c	371516	FITC	1:40
CD66b	305118	APC	1:100

Table 3.4 Antibodies used for surface receptor expression detection by flow cytometry. All antibodies were sourced from BioLegend (UK).

Flow cytometry analysis was performed on a BD Fortessa X20 (Becton Dickinson and Company; Franklin Lakes, USA), analysis of results carried out using FloJo (v10.8.0). 10,000 neutrophil events were recorded for each sample. Gating strategy used is displayed in **Figure 3.4**. Surface marker phenotype is presented as percentage of neutrophils antigen positive or median fluorescence intensity (MFI, concentration of surface marker per cell). MFI calculated as:

$$MFI\ sample - MFI\ isotype\ control$$

3.2.7 Western blotting

Western blots were carried out to determine CitH3 concentration in relation to NETosis. These were carried out by Dr Jon Hazeldine (Post-Doctoral Fellow), methods described below are for reference.

Samples were prepared from cell lysates obtained from lithium-heparin serum from COVID-19 patients, then loaded onto a pre-cast 15% SDS-polyacrylamide gel and run for 3 hours at 200 volts with appropriate pre-stained markers (Bio-Rad, Hertfordshire, UK). Proteins were transferred to methanol-activated 0.45 micron polyvinylidene difluoride using Bio-Rad turbo transfer technology (Bio-Rad). After blotting, membranes were incubated on an orbital shaker in 5% BSA/Tris buffered saline (TBS) containing 0.1% Tween®-20 (SigmaAldrich) for one hour at room temperature. Blots were then probed overnight at 4^{o}C with the CitH3 antibody (ab5103; Abcam, Cambridge, UK), diluted accordingly. Following a further three washes with 10ml TBST for 10 minutes after which blots incubated for one hour at room temperature with a HRP-linked anti-rabbit IgG antibody. Three washes with 10ml TBST for 10 mins were again performed, then incubated at room temperature in a chemiluminescence reporter solution (Geneflow, Staffordshire, UK). Proteins were visualised on a ChemiDoc (Bio-Rad). Equal loading of proteins was confirmed by Ponceau total protein stain. Densitometry was performed using the National institute of Health ImageJ software.

3.2.8 Phosphoinositide-3-kinase (PI3K)

PI3K inhibitors were used to block signalling; panPI3K (LY294002), PI3Kδ (CAL101), PI3Kγ (AS252434). For each functional experiment described in **Chapter 3**, isolated neutrophils were incubated with for 30 minutes with appropriate inhibitor to maintain desired concentration, **Table 3.5**. An additional neutrophil sample was treated with DMSO, the vehicle control for PI3k inhibitors.

Several studies examining the role of PI3K inhibition in neutrophil signalling have used 30-45 minute time points with documented effects to neutrophil phagocytic function (Sapey et al., 2014, Stockley et al., 2013, Giraldo et al., 2010). Concentrations of inhibitors used for experimentation were based on previous studies demonstrating effect of PI3K inhibitors (Giraldo et al., 2010, Stockley et al., 2013).

Patients recruited for investigation of PI3K inhibition were taken from the second recruited cohort of COVID-19 patients between August 2021 and September 2022. Ethics, recruitment procedure, inclusion and exclusion criteria, and sample processing are as described in **Chapter 3**. Variable numbers of samples were assessed with regards to PI3K inhibition due to prioritisation of experiments.

Treatment	Final concentration
PI3Ki (LY294002)	1μM
PI3Kγi (AS252434)	33nM
PI3Kδi (CAL101)	75nM

Table 3.5 Final concentrations of PI3K inhibitors used in the functional neutrophil experiments.

3.2.9 Effect of selected pharmacological agents on neutrophil function

Neutrophils isolated from COVID-19 patients were exposed to inhibitor compounds (brensocatib, metoprolol, and AZD9668). For each functional experiment described in **Chapter 3**, cells were incubated for 30 minutes with a single inhibitor compound. Compounds were used at the concentration expected in serum as per previously described in the literature or as advised by the manufacturing company (for AZD9668), shown in **Table 3.6** (Chalmers et al., 2017, Dunzendorfer and Wiedermann, 2000a).

Treatment	Final concentration
Brensocatib	100µM
Metoprolol	32nM
AZD9668	300nM

Table 3.6 Final concentrations of treatments applied in the functional neutrophil experiments.

Patients recruited for investigation of PI3K inhibition were taken from the second recruited cohort of COVID-19 patients between August 2021 and September 2022. Ethics, recruitment procedure, inclusion and exclusion criteria, and sample processing are as described in **Chapter 3.2**.

3.2.10 Clinical scoring systems

A number of scoring systems were used as part of stratifying disease severity in COVID-19 patients. Scores are validated for specific clinical outcomes in different underlying diseases. There are no specific scores that are validated for both COVID-19 and CAP outcomes, with the NEWS score generic for alerting medical personnel to unwell patients.

3.2.10.1 NEWS2

The National Early Warning Score 2 (NEWS2) is an updated version of the NEWS, designed to standardise the assessment and response to the acutely unwell patient (RCP, 2017). Higher scores based on clinical nursing observations indicate patients require more urgent review. There are caveats to using the NEWS2 in COVID-19, as rapid increase in oxygen requirement will not significantly change the score (Chikhalkar et al., 2022). Parameters for calculating a score along with expected responses are shown in **Table 3.7**.

Parameter	Range	Points
Respiratory Rate (breaths per minute)	≤8	3
	9-11	1
	12-20	0
	21-24	2
	≥25	3
Oxygen saturation (on room air or supplementation)	≤91%	3
	92-93%	2
	94-95%	1
	≥96%	0
Oxygen supplementation	Supplemental oxygen	2
	Room air	0
Temperature	≤35.0	3
	35.1-36.0	1
	36.1-38.0	0
	38.1-39.0	1
	≥39.1	2
Blood pressure (systolic)	≤90	3
	91-100	2
	101-110	1
	111-219	0
	≥220	3
Heart Rate	≤40	3
	41-50	1
	51-90	0
	91-110	1
	111-130	2
	≥131	3
Consciousness	Alert	0
	New-onset confusion/ responds to voice/ responds to pain/ unresponsive	3

Parameter	Range	Points
Oxygen saturation (if history of hypercapnic respiratory failure)	≤83%	3
	84-85%	2
	86-87%	1
	88-92% OR ≥93% on room air	0
	93-94% on supplemental oxygen	1
	95-96% on supplemental oxygen	2
	≥97% on supplemental oxygen	3

Score	Response
0	Continue routine NEWS monitoring
1-4 total	Inform registered nurse for assessment and escalation
3 in a single parameter	Registered nurse to escalate to medical team for assessment and escalation
5 or more total Urgent response threshold	Registered nurse to immediately inform medical team AND request urgent assessment by clinical team with core competencies Care to be provided in environment with monitoring facilities
7 or more total Emergency response threshold	Registered nurse to immediately inform medical team AND request emergency assessment by clinical team with core competencies + advanced airway skills Consider moving to level 2 or 3 care environment

Table 3.7 National Early Warning Score2 (NEWS2) scoring criteria and appropriate response as set out by the Royal College of Physicians (RCP, 2017)

3.2.10.2 qSOFA

The quick Sequential Organ Failure Assessment (qSOFA) score is a rapid scoring system used to identify patients with a suspected infection who are at greater risk from poor outcomes (Seymour et al., 2016). Parameters and prediction of in-hospital mortality are shown in **Table 3.8**

Parameter	Score
Altered mental state GCS <15	1
Respiratory rate ≥22 breaths/ min	1
Systolic blood pressure ≤100 mmHg	1

Score	Risk group
0-1	Not high risk for in-hospital mortality
2-3	High-risk for in-hospital mortality (3- to 14- fold increase)

Table 3.8 quick Sequential Organ Failure Assessment (qSOFA) score with clinical parameters and risk dependent on overall score (Seymour et al., 2016).

3.2.10.3 CURB-65

The CURB-65 score predicts mortality at 30 days, in patients diagnosed with a CAP (Lim et al., 2003), parameters and mortality prediction are shown in **Table 3.9**

Parameter	Score
Confusion (AMT <8)	1
Serum urea (>7 mmol/L)	1
Respiratory rate (≥30 breaths/ min)	1
Blood pressure (systolic <90 mmHg OR diastolic ≤60 mmHg)	1
Age ≥65 years	1

Score	Mortality risk
0	0.6%
1	2.7%
2	6.8%
3	14.0%
4 OR 5	27.8%

Table 3.9 CURB-65 score with parameters and related 30-day mortality risk (Lim et al., 2003)

3.2.10.4 4C

The 4C score predicts in-hospital mortality for patients with a positive COVID-19 test, parameters and mortality prediction is shown in **Table 3.10** (Knight et al., 2020).

Parameter	Range	Score
Age (years)	<50	0
	50-59	2
	60-69	4
	70-79	6
	≥80	7
Sex at birth	Female	0
	Male	1
Number of comorbidities	0	0
	1	1
	≥2	2
Respiratory rate (breaths/ min)	<20	0
	20-29	1
	≥30	2
Peripheral oxygen saturation on room air	≥92%	0
	<92%	2
Glasgow Coma Scale	15	0
	<15	2
Serum urea (mmol/L) or BUN (mg/dL)	Urea <7 BUN <19.6	0
	Urea 7-14 BUN 19.6-39.2	1
	Urea >14 BUN >39.2	3
C-reactive protein (mg/L)	<50	0
	50-99	1
	≥100	2

Score	Risk group	In-hospital mortality
0-3	Low	1.2-1.7%
4-8	Intermediate	9.1-9.9%
9-14	High	31.4-34.9%
≥15	Very high	61.5-66.2%

Table 3.10 4C score with scoring criteria and breakdown to in-hospital mortality risk groups and percentage risk. BUN – blood urea nitrogen as an alternative to serum urea measurement (Knight et al., 2020).

3.2.11 Statistical analysis

Statistical analysis was performed in Prism v9.2.0 (GraphPad Software Inc.; San Diego). Normal distribution was confirmed by performing a Shapiro-Wilk (<50 samples) or Kolmogorov-Smirnov (>50 samples) Test. Normally distributed data was analysed using a student's T-test. Mann-Whitney U, Wilcoxon matched pairs signed rank tests were used for analysis of not normally distributed data. Data in tables are presented as median with interquartile range (Q1-Q3). One-way analysis of variance (ANOVA) was used for multiple comparisons where data was normally distributed and Kruskal-Wallis for non-parametric data. No more than one

independent variable was examined in the statistical analysis. Significance was determined at $p<0.05$. Flow chart of decision making for statistical test used for single comparisons shown in **Figure 3.5**.

All graphs were generated using Prism v9.2.0 (GraphPad Software Inc.; San Diego). Data is presented as a Tukey box and whisker diagram (box representing median and IQR, whiskers as maximum and minimum points. Alternative graphical representation was used where data presentation is clearer in this format. Data is presented as aligned dot plots where there are fewer than 6 replicate values. Dots represent biological replicates with median and IQR values. Tables were generated in Microsoft Excel (Office 365 for Windows, Microsoft, USA).

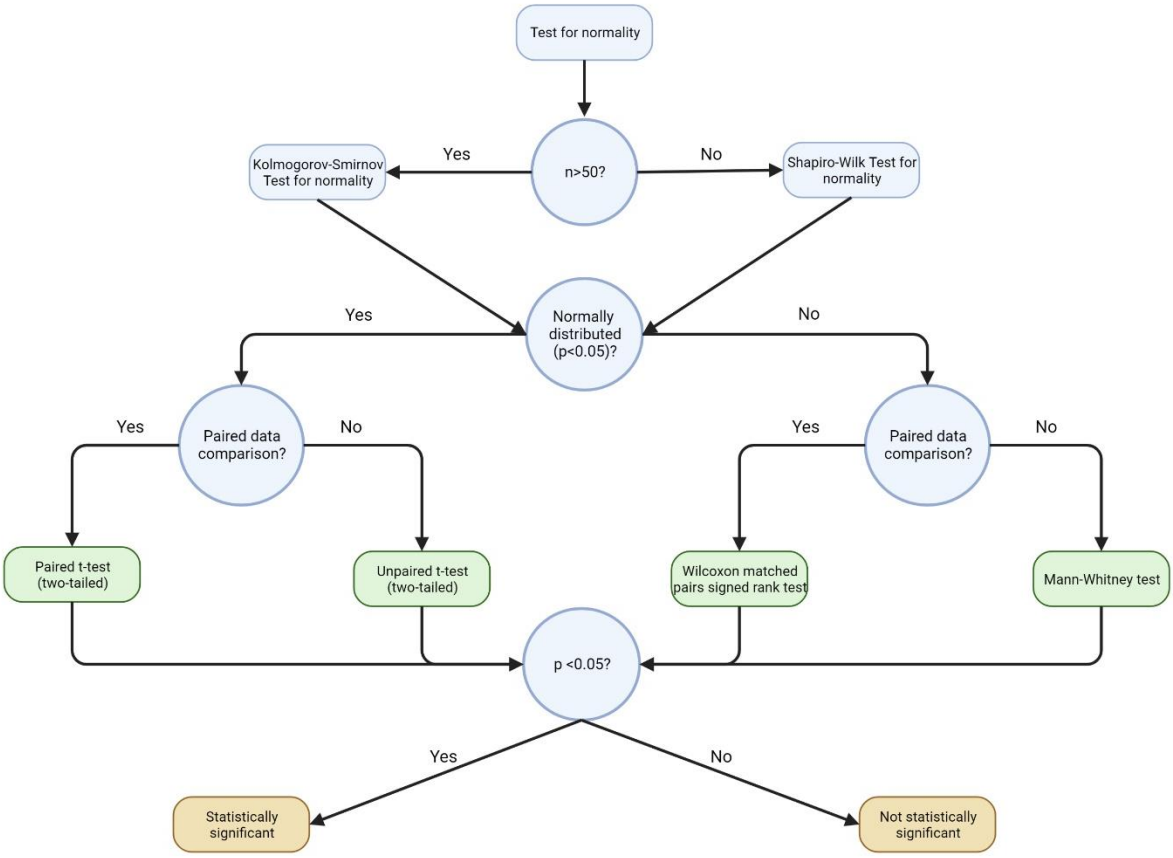

Figure 3.5 Approach used for statistical analysis for single comparisons in this thesis. Initial testing was carried out for normality of data, depending on the number of samples being analysed. For more than 50 samples, the Kolmogorov-Smirnov test was used, and for samples less than 50 samples, the Shapiro-Wilk test was used. If the data was normally distributed ($p<0.05$) then a paired t-test or un-paired t-test was used depending if the samples were paired. If the data was not normally distributed ($p>0.05$) then a Wilcoxon matched pairs signed rank test or Mann-Whitney test was used depending if the samples were paired. All tests were carried out in GraphPad Prism Version 9.2.0.

3.2.12 Power calculations

Power calculations for initial COVID-19, AMC, CAP data analysis were based on previously collected isolated neutrophil NETosis data (Group 1 mean=1.374, SD= 0.2876. Group 2 mean= 1.64) with 80% power, and alpha 0.05, revealed 18 participants were required in each group. Serum NETosis data was repeated which revealed that 6 participants were required in each group (Group 1 mean=26.32 SD= 32.1. Group 2 mean= 79.3) with 80% power, and alpha 0.05.

Subsequent power calculations were based on results from the initial analysis. Phagocytosis from isolated neutrophils from COVID-19 and AMC (Group 1 mean=33.53, SD=1.96. Group 2 mean = 31.21), with 80% power and alpha 0.05, 1:1 enrolment ratio demonstrated 11 participants were required for each group. Transwell migration from isolated COVID-19 neutrophils and AMC (Group 1 mean=24.97, SD=27.04. Group 2 mean =78.49), with 80% power and alpha 0.05, 1:1 enrolment ratio demonstrated 4 participants were required for each group. Isolated neutrophil NETosis data between COVID-19 and CAP patients (Group 1 mean=126.5, SD= 34.75. Group 2 mean= 164.0) with 80% power, and alpha 0.05, enrolment ratio 1:1 revealed 18 participants were required in each group. Further recruitment and analysis were based off these calculations.

3.2.13 Method limitations

The methods employed in this thesis were in part dictated by the nature of the COVID-19 pandemic environment and restrictions in place for safe working for researchers. Standard protocols were adapted to ensure that samples could be safely processed in non-isolated, shared equipment. Some of these measures have been explained earlier in **Chapter 3** (e.g.

fixation with 4% (v/v) PFA). Alternative methods used in replacement of those which are regularly used are explained below.

Neutrophil viability would be measured using an annexin V binding buffer (produced by diluting a 10 X concentrated buffer solution consisting of 0.2 µM sterile filtered 0.1 M 4-(2-hydroxyethyl)-1-piperazineethanesulfonic acid (HEPES) (pH 7.4), 1.4 M NaCl and 25 mM CaCl2 with distilled water 1:10) in combination with propidium iodide (PI) (Sigma-Aldrich, Poole UK, product no. P4864). This allows for increased discretion of neutrophil viability, distinguishing between live, early apoptotic, late apoptotic and necrotic neutrophils. However, cells cannot be fixed, and PI must be added immediately prior to flow cytometry analysis. Thus, viability data is limited to dichotomous live:dead using the Zombie staining as this allowed for cell fixation post staining with 4% (v/v) PFA.

Functional experiments on neutrophils are usually stopped at the appropriate time point through cooling by transfer to ice. Samples remain on ice until they are processed and analysed using the flow cytometer. This would breach safely processing samples on shared equipment. Therefore, 4% (v/v) PFA was used as an alternative to achieving a standardised timepoint for each sample.

Neutrophil chemotaxis can be quantified by use of an Insall chamber (modified Dunn Chamber), used previously in literature (Sapey and Stockley, 2014, Sapey et al., 2014, Muinonen-Martin et al., 2010). Neutrophils adhere to a coverslip which is then inverted and placed on the Insall chamber slide, before chemoattractant such as CXCL8 is applied. The resulting chamber with coverslip is then placed on a Leica DMI 6000B microscope with DFL350 FX camera. Filming then occurs for 12 minutes with images captured every 20 seconds. From these images, the speed, velocity, persistence and chemotactic index of the migrating cells can be calculated. Whilst more characteristics of the migrating neutrophil can be observed, this method requires leaving cells exposed to be filmed. Cells cannot be fixed in PFA for this

method. Therefore, neutrophil migration through a Transwell membrane was used as an alternative means of evaluating migration.

CHAPTER 4
VALIDATION

4.1 Introduction

Recruitment of COVID-19 patients for this thesis required enhanced, zero aerosol, safety measures to ensure safety of researchers and other laboratory group members. This was in part due to the evolving nature and knowledge early on in the pandemic. Samples were processed in a secure, isolated, category 2 laboratory according to the protocol developed by the institute and agreed with the University of Birmingham. Sample processing and experimentation required use of shared equipment outside of the secure environment. Due to the short half-life of neutrophils ex vivo, functional experiments on live cells are conducted within the shortest timeframe possible (Price and Dale, 1977). Delays in sample processing can decrease neutrophil viability and affect experiment outcomes (Buescher and Gallin, 1987). Isolation from whole blood can take up to two hours, and incubation for experimentation another three hours (NETosis). Alterations to established protocols were necessary, including, but not limited to cell fixation in 4% (v/v) paraformaldehyde (PFA) to ensure viral inactivation. Due to this requirement some assay outputs were limited.

In response to the increasing burden on clinical resources worldwide, many new therapies were introduced following outcomes from platform trials such as RECOVERY (Abani et al., 2021, Horby et al., 2021b). Treatment evolution occurred during recruitment as shown in **Figure 4.1**, and thus patients were recruited before administration of novel therapies. These may have significant influence on neutrophil function through disruption of signalling pathways, alterations to viral RNA processing and direct effects on neutrophils. At time of recruitment, dexamethasone was established as standard of care for those patients requiring supplemental oxygen. Recruitment of patients prior to administration was therefore unavoidable.

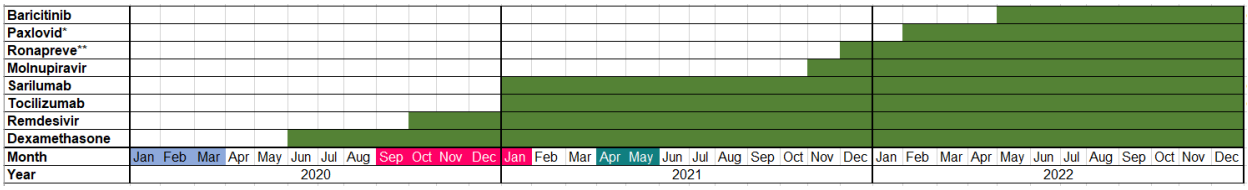

Figure 4.1 Table detailing the introduction of various novel therapies for COVID-19 during the pandemic until the end of patient recruitment (December 2022). Blue months denote alpha variant recruitment, pink months denote delta variant recruitment and green months denote omicron variant recruitment. Green bars indicate treatments being approved by NICE, but treatments may have been used earlier as part of a clinical trial. *Paxlovid = nirmatrelvir/ ritonavir, **Ronapreve = casirivimab/ imdevimab

For comparable results, we validated functional neutrophil experiments carried out in this environment. Experiments detailed in this chapter were carried out on paired healthy volunteer samples .

4.2 Fixation

During the initial outbreak of the COVID-19 pandemic several methods of inactivation and fixation were validated by PHE. The most appropriate reagent for viral inactivation and cellular fixation for our methodology, 4% (v/v) PFA for 15 minutes, was used throughout this thesis. Unfortunately, fixation by PFA precludes some functional experiments such as chemotaxis by Insall chamber, which require unfixed cells to be exposed to communal equipment.

4% (v/v) PFA cell fixation has been used in conjunction with quantitative flow cytometry cellular analysis on haematopoietic cells for several years (Lanier and Warner, 1981). Fixation occurs through formation of covalent bonds and cross-linking molecules. Functional experiments can be carried out in the secure laboratory and when using equipment designated solely for the use of infectious samples with appropriate isolation. Fixation occurs after these experiments and should not affect results.

Functional experiments can be halted by using rapid cooling by ice. Here incubation with 4% (v/v) PFA (15 minutes) was used for the same purpose as disposal of potentially contaminated ice was highlighted as a risk factor. This may affect experimental timepoint, change signal, and prevent comparison with samples not processed in this manner. In order to allow comparisons to be drawn between AMC, CAP and COVID-19 patients, all samples were processed with fixation.

4.2.1 Phagocytosis

Phagocytosis using fluorescently labelled *S. pneumoniae* was carried out on 5 paired samples (3M, 2F, mean age 28.8y) using the methods described in **Chapter 3.1.4.1**. Timepoints at 30 and 60 minutes were investigated initially with and without fixation to determine an appropriate experimental time course.

Fixed samples demonstrated significantly lower percentage phagocytosis compared to unfixed samples at both 30 (percentage phagocytosis fixed 20.50 vs unfixed 27.68, p=0.0013) and 60 (percentage phagocytosis fixed 22.30 vs unfixed 33.40, p=0.0183) minute incubation timepoints (**Figure 4.2A and B**). There was no significant difference in percentage phagocytosis between samples incubated for 30 or 60 minutes whether fixed or unfixed (fixed percentage phagocytosis 30 minutes 20.50 vs 60 minutes 22.30, p=0.1306) (unfixed percentage phagocytosis 30 minutes 27.68 vs 60 minutes 33.40, p=0.4405) (**Figure 4.2C and D)**. There was significant increase in percentage phagocytosis from 0 to 30 or 60 minutes for both fixed and unfixed samples (fixed percentage phagocytosis 0 minutes 5.23 vs 30 minutes 20.50 (p=0.0336) vs 60 minutes 22.30 (p=0.0153)), (unfixed percentage phagocytosis 0 minutes 4.87 vs 30 minutes 27.68 (p=0.0001) vs 60 minutes 33.40 (p<0.0001)), **Figure 4.2C and D**. There was no evidence of significant differences to MFI in paired samples between fixed and unfixed samples.

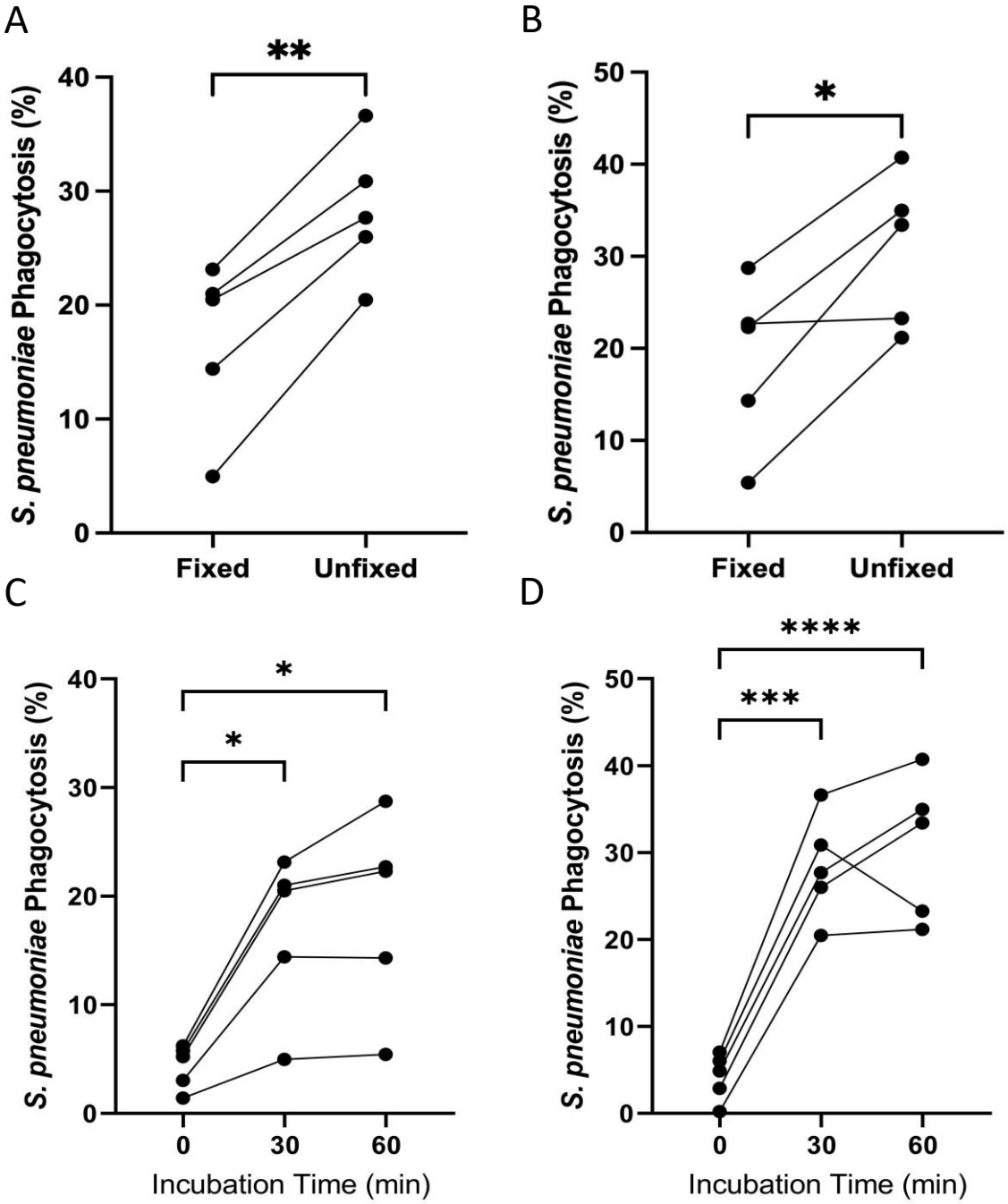

Figure 4.2 Isolated neutrophil phagocytosis of labelled *S. pneumonia*, demonstrated as % phagocytosis at timepoints 0, 30 and 60 minutes from addition of bacteria with comparison between fixed and unfixed samples with 4% (v/v) PFA. Fixed samples were treated with 4% (v/v) PFA post phagocytosis time point. Paired samples, fixed n=5, unfixed n=5. Statistics calculated using Wilcoxon matched pairs or Kruskal Wallis test for multiple comparisons, *p≤0.05, **p≤0.01, ***p≤0.001, ****p≤0.0001. **A**. Phagocytosis time = 30 minutes, compared between fixed and unfixed samples. **B** Phagocytosis time = 60 minutes, compared between fixed and unfixed samples. **C**. Percentage phagocytosis at 0, 30 and 60 minutes after bacteria addition for fixed samples. **D.** Percentage phagocytosis at 0, 30 and 60 minutes after bacteria addition for unfixed samples.

Medial fluorescent intensity (MFI) was measured for all samples. There was no significant difference in MFI between fixed and unfixed samples at 30 or 60 minutes (MFI 30 minutes fixed 5.77 vs unfixed 5.54, p=0.3807, **Figure 4.3A**), (MFI 60 minutes fixed 6.03, unfixed 6.25 p=0.9463, **Figure 4.3B**)**.** There was no significant difference in MFI between samples incubated for 30 or 60 minutes whether fixed or unfixed (fixed MFI 30 minutes 5.77 vs 60 minutes 6.03, p=0.7927) (unfixed percentage phagocytosis 30 minutes 5.54 vs 60 minutes 6.25, p=0.2144) (**Figure 4.3C and D)**. There was significant increase in MFI from 0 to 30 or 60 minutes for both fixed and unfixed samples (fixed MFI 0 minutes 3.99 vs 30 minutes 5.77 (p=0.0252) vs 60 minutes 6.03 (p=0.0078)), (unfixed MFI 0 minutes 3.08 vs 30 minutes 5.54 (p=0.0013) vs 60 minutes 6.250 (p<0.0001)), **Figure 4.3C and D**.

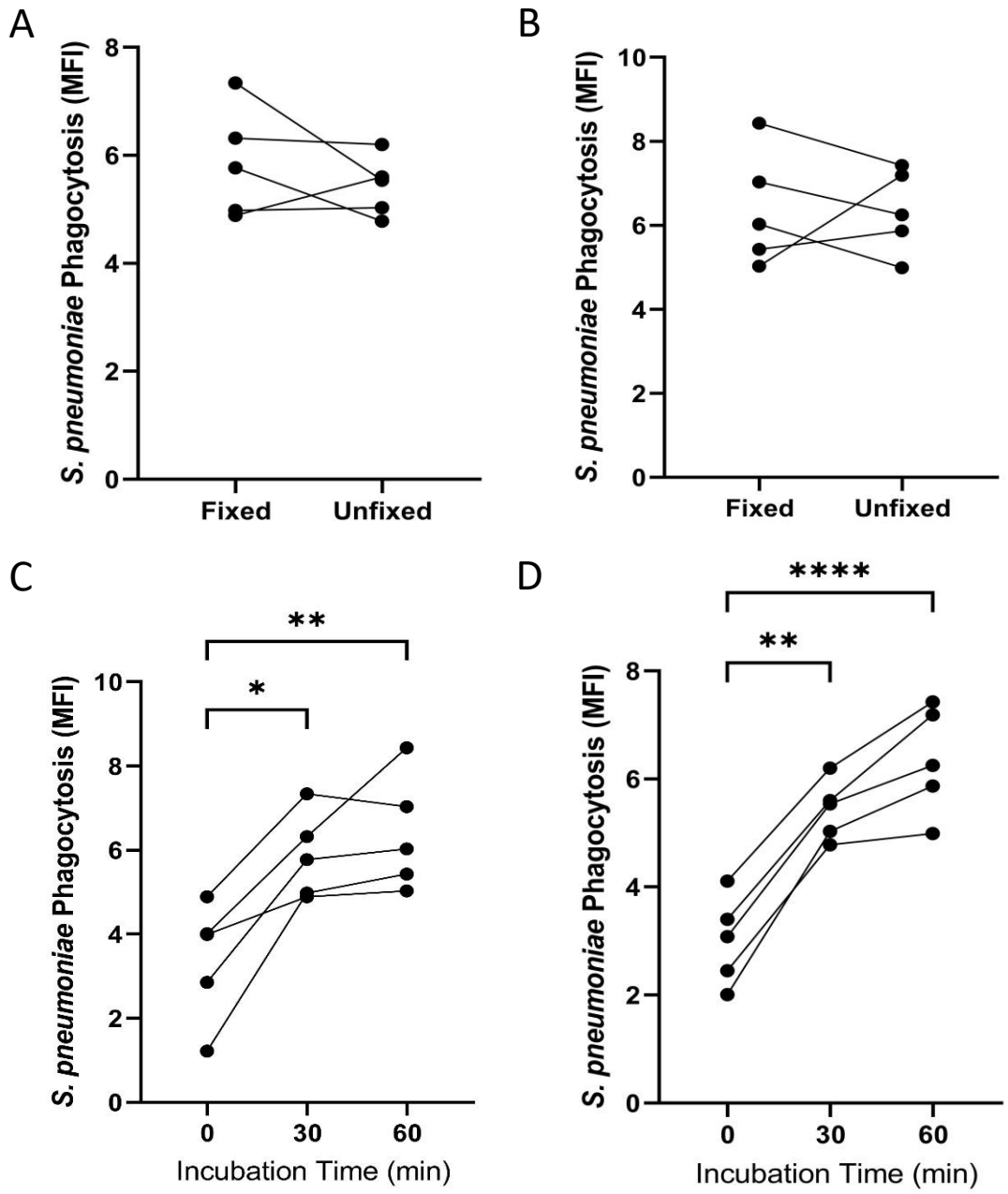

Figure 4.3 Isolated neutrophil phagocytosis of labelled S. pneumonia, demonstrated as median fluorescent intensity (MFI) at timepoints 0, 30 and 60 minutes from addition of bacteria with comparison between fixed and unfixed samples with 4% (v/v) PFA. Fixed samples were treated with 4% (v/v) PFA post phagocytosis time point. Paired samples, fixed n=5, unfixed n=5. Statistics calculated using Wilcoxon matched pairs or Kruskal Wallis test for multiple comparisons, *p≤0.05, **p≤0.01, ***p≤0.001, ****p≤0.0001. **A**. Phagocytosis time = 30 minutes, compared between fixed and unfixed samples. **B** Phagocytosis time = 60 minutes, compared between fixed and unfixed samples. **C**. MFI at 0, 30 and 60 minutes after bacteria addition for fixed samples. **D.** MFI at 0, 30 and 60 minutes after bacteria addition for unfixed samples.

As part of the neutrophil inflammatory response, cytoplasmic and nuclear/mitochondrial reactive oxygen species (cROS and n/mROS respectively) were measured using CellROX reagents.

cROS

There was no significant difference in cROS whether samples were fixed in 4% (v/v) PFA or unfixed at either 30 or 60 minutes (30 minutes cROS MFI fixed 30.36 vs unfixed 61.49, p=0.1087, **Figure 4.4A**) (60 minutes cROS MFI fixed 30 minutes 32.59 vs 60 minutes 75.70, p=0.0864, **Figure 4.4B**). There was no significant difference in cROS between 30 and 60 minute incubations whether samples were fixed in 4% (v/v) PFA or unfixed (cROS MFI fixed 30 minutes 30.36 vs 60 minutes 32.59, p>0.9999, **Figure 4.4C**) (cROS MFI unfixed 30 minutes 61.49 vs 60 minutes 75.70, p>0.9999, **Figure 4.4D**). There was significant increase in MFI from 0 to 30 or 60 minutes for both fixed and unfixed samples (fixed MFI 0 minutes 2.10 vs 30 minutes 30.36 (p=0.0327) vs 60 minutes 32.59 (p=0.0175), **Figure 4.4C**), (unfixed MFI 0 minutes 2.06 vs 30 minutes 61.49 (p=0.0318) vs 60 minutes 75.70 (p=0.0176), **Figure 4.4D**).

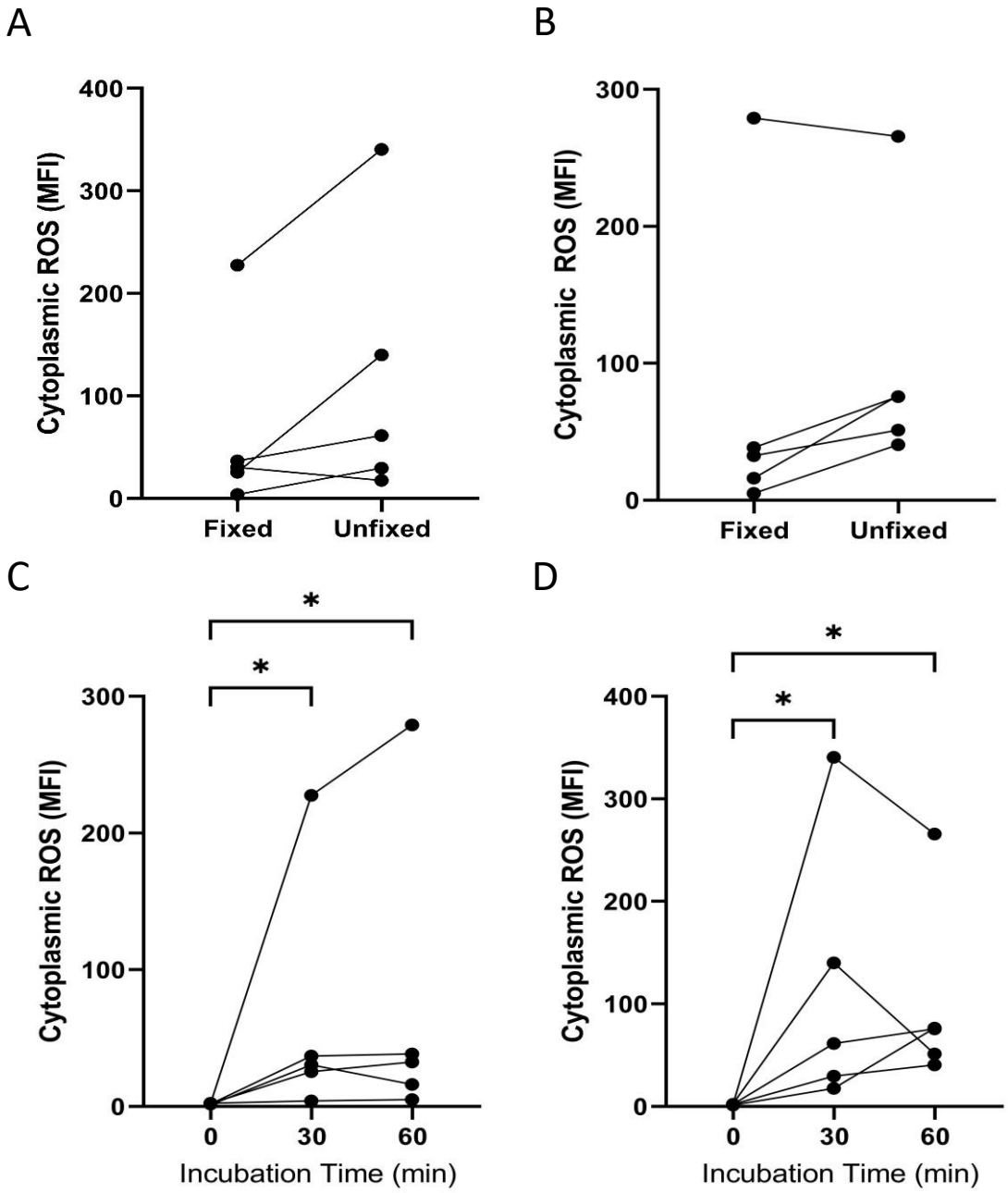

Figure 4.4 Isolated neutrophil cytoplasmic reactive oxygen species (cROS) production expressed as median fluorescent intensity (MFI) at timepoints 0, 30 and 60 minutes from addition of labelled *S. pneumoniae* with comparison between fixed and unfixed samples with 4% (v/v) PFA. Fixed samples were treated with 4% (v/v) PFA post phagocytosis time point. Paired samples, fixed n=5, unfixed n=5. Statistics calculated using Wilcoxon matched pairs or Kruskal Wallis test for multiple comparisons, *p≤0.05, **p≤0.01, ***p≤0.001, ****p≤0.0001. **A**. cROS production at 30 minutes compared between fixed and unfixed samples. **B.** cROS production at 60 minutes compared between fixed and unfixed samples. **C**. cROS production at time 0, 30 and 60 minutes for fixed samples. **D.** cROS production at time 0, 30 and 60 minutes for unfixed samples

Comparison on cROS production using fold change in MFI demonstrated a significant difference in cROS MFI was seen at 60-minute incubation between fixed and unfixed samples which was not replicated at 30 minute incubation (cROS MFI 30 minutes fixed 12.12 vs unfixed 27.70, p=0.0860, **Figure 4.5A**) (cROS MFI 60 minutes fixed 15.52 vs unfixed 19.71, p=0.0105, **Figure 4.5B**). Otherwise, there was no significant difference from baseline fold change between 30 or 60 minute incubation times for fixed or unfixed samples (MFI fold change fixed 30 minutes 19.51 vs 60 minutes 15.52, p=0.5730, **Figure 4.5C**), (MFI fold change unfixed 30 minutes 27.70 vs 60 minutes 34.10, p=0.7921, **Figure 4.5D**).

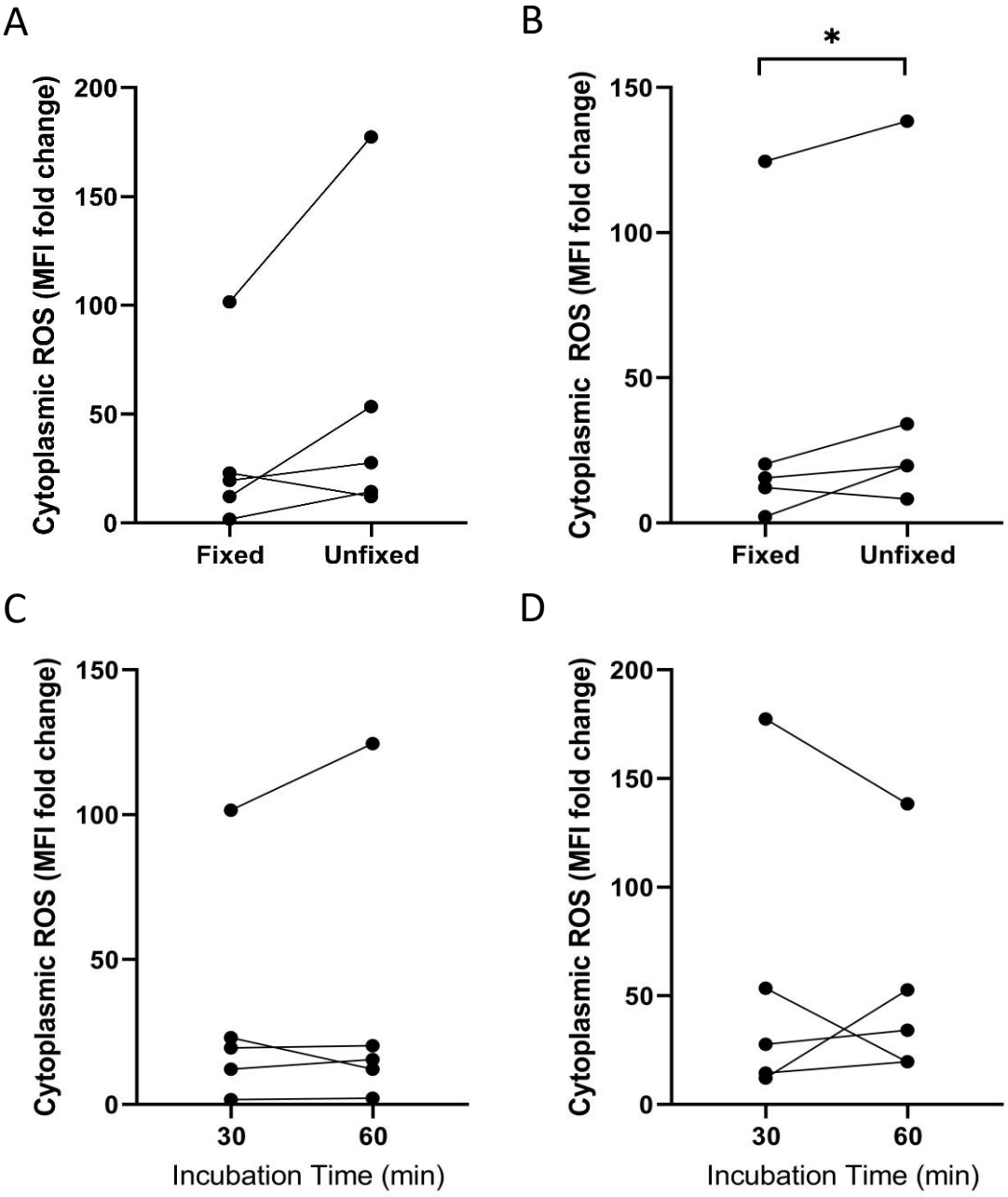

Figure 4.5 Isolated neutrophil cytoplasmic reactive oxygen species (cROS) production after *S. pneumoniae* phagocytosis expressed as fold change in median fluorescent intensity (MFI) from 0 minutes compared to 30 and 60 minutes, and between fixed and unfixed samples. Fixed samples were treated with 4% (v/v) PFA post phagocytosis time point. Paired samples, fixed n=5, unfixed n=5. Statistics calculated using Wilcoxon matched-pairs signed rank test or Kruskal Wallis test for multiple comparisons, *p≤0.05, **p≤0.01, ***p≤0.001, ****p≤0.0001. **A**. cROS production at 30 minutes compared between fixed and unfixed samples. **B.** cROS production at 60 minutes compared between fixed and unfixed samples. **C**. cROS production at time 30 and 60 minutes for fixed samples. **D.** cROS production at time 30 and 60 minutes for unfixed samples.

n/mROS

There was no significant difference in n/mROS whether samples were fixed in 4% (v/v) PFA or unfixed at either 30 or 60 minutes (30 minutes n/mROS MFI fixed 78.33 vs unfixed 294.9, p=0.21399, **Figure 4.6A**) (60 minutes n/mROS MFI fixed 30 minutes 294.7 vs 60 minutes 219.0, p=0.4207, **Figure 4.6B**). There was no significant difference in n/mROS between 30 and 60 minute incubations whether samples were fixed in 4% (v/v) PFA or unfixed (cROS MFI fixed 30 minutes 78.33 vs 60 minutes 294.7, p>0.9999, **Figure 4.6C**) (cROS MFI unfixed 30 minutes 294.9 vs 60 minutes 219.0, p>0.9999, **Figure 4.6D**). There was significant increase in MFI from 0 to 30 or 60 minutes for both fixed and unfixed samples (fixed MFI 0 minutes 1.890 vs 30 minutes 78.33 (p=0.05) vs 60 minutes 294.7 (p=0.0089), **Figure 4.6C**), (unfixed MFI 0 minutes 2.11 vs 30 minutes 294.9 (p=0.0112) vs 60 minutes 219.0 (p=0.0486), **Figure 4.6D**).

There was no significant difference in MFI fold change n/mROS production between fixed and unfixed samples at 30 or 60 minute incubation timepoints (MFI fold change 30 minutes fixed 38.97 vs unfixed 139.9, p=0.1806, **Figure 4.7A**), (MFI fold change 60 minutes fixed 157.6 vs unfixed 111.9, p=0.4235, **Figure 4.7B**). There was no baseline MFI fold change between 30 or 60 minute incubation times for fixed or unfixed samples (MFI fold change fixed 30 minutes 40.0 vs 60 minutes 157.6, p=0.498, **Figure 4.7C**), (MFI fold change unfixed 30 minutes 139.9 vs 60 minutes 111.9, p=0.1690, **Figure 4.7D**).

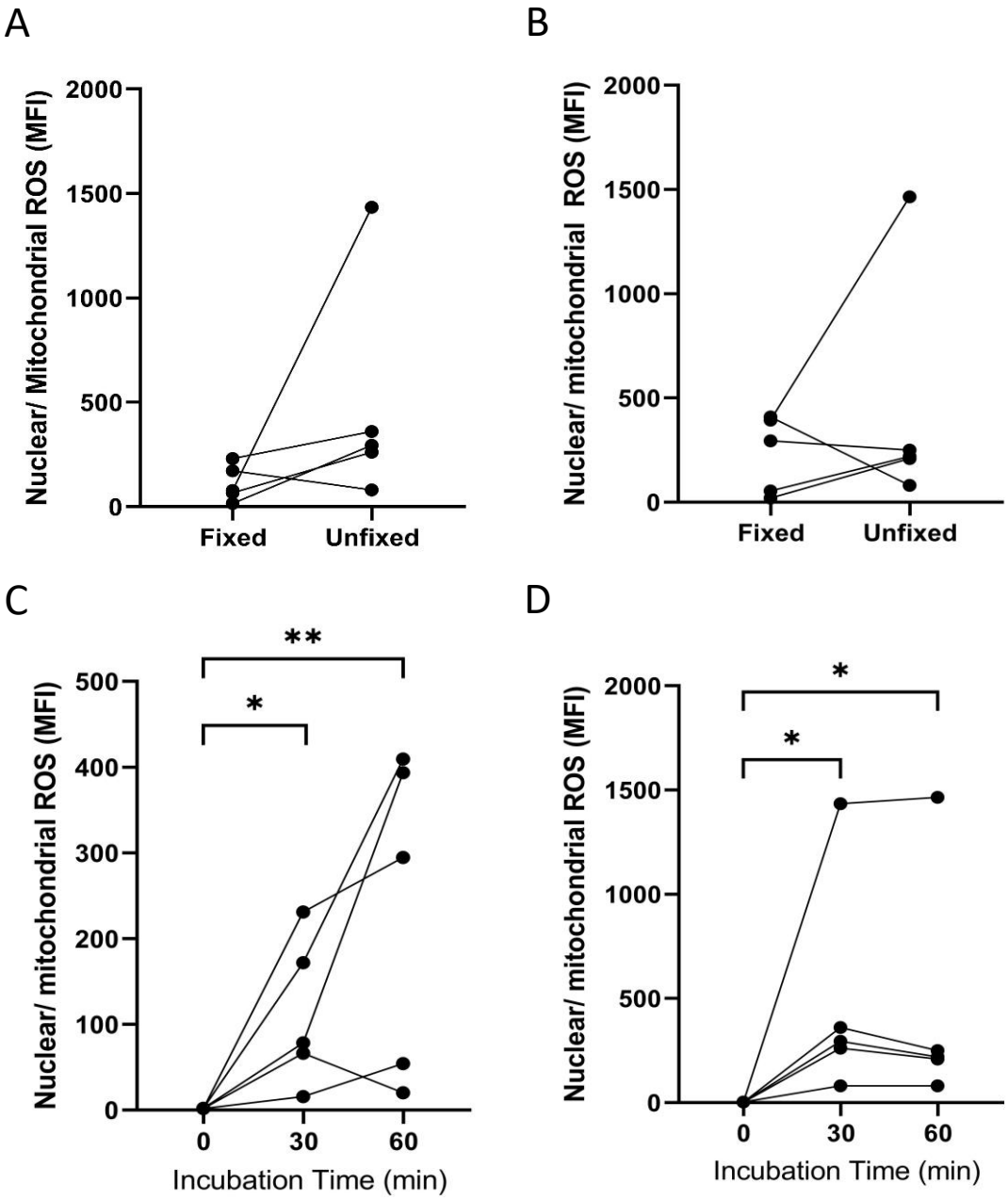

Figure 4.6 Isolated neutrophil nuclear/ mitochondrial reactive oxygen species (n/mROS) production expressed as median fluorescent intensity (MFI), at timepoints 0, 30 and 60 minutes from addition of labelled *S. pneumoniae* with comparison between fixed and unfixed samples with 4% (v/v) PFA. Fixed samples were treated with 4% (v/v) PFA post phagocytosis time point. Paired samples, fixed n=5, unfixed n=5. Statistics calculated using Wilcoxon matched pairs signed rank test or Kruskal Wallis test for multiple comparisons, *p≤0.05, **p≤0.01, ***p≤0.001, ****p≤0.0001. A. n/mROS production at 30 minutes compared between fixed and unfixed samples. B. n/mROS production at 60 minutes compared between fixed and unfixed samples. C. n/mROS production at time 0, 30 and 60 minutes for fixed samples. D. n/mROS production at time 0, 30 and 60 minutes for unfixed samples

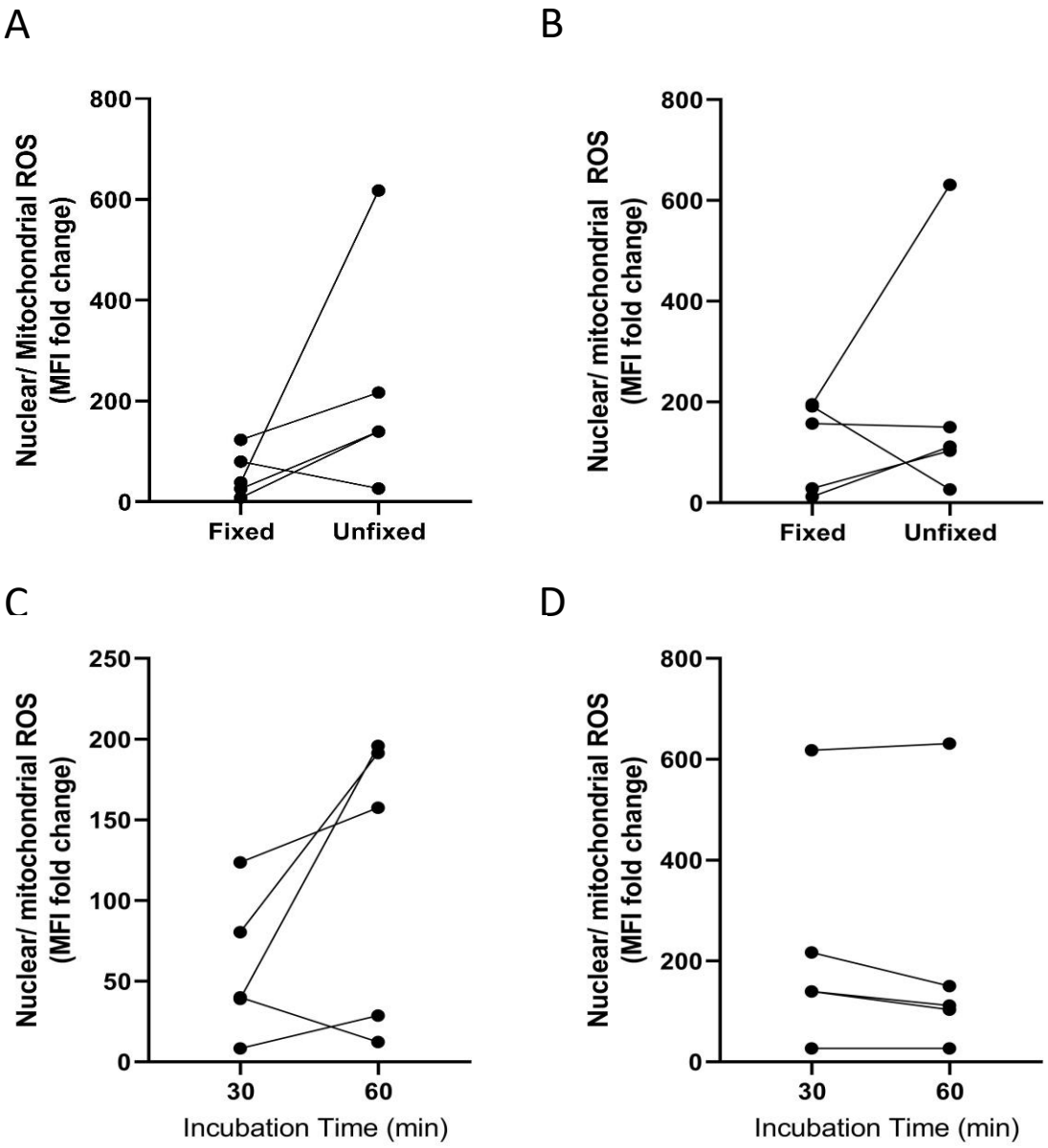

Figure 4.7 Isolated neutrophil nuclear/ mitochondrial reactive oxygen species (n/mROS) production expressed as fold change in median fluorescent intensity (MFI) from 0 minutes, compared to 30 and 60 minutes, and between fixed and unfixed samples after addition of labelled *S. pneumoniae*. Fixed samples were treated with 4% (v/v) PFA post phagocytosis time point. Paired samples, fixed n=5, unfixed n=5. Statistics calculated using Wilcoxon matched pairs signed rank test or Kruskal Wallis test for multiple comparisons, *p≤0.05, **p≤0.01, ***p≤0.001, ****p≤0.0001. **A**. n/mROS production at 30 minutes compared between fixed and unfixed samples. **B.** n/mROS production at 60 minutes compared between fixed and unfixed samples. **C**. n/mROS production at time 30 and 60 minutes for fixed samples. **D.** n/mROS production at time 30 and 60 minutes for unfixed samples

These results suggest that when using heat-inactivated fluorescently labelled SP, maximal phagocytosis is achieved within 30 minutes. Further, there was no significant increase in the generation of ROS in neutrophils at 30 minutes compared to 60-minutes. Based on these results a 30-minute timepoint was chosen for the phagocytosis assay as this minimises the time potentially infected cells are handled and incubated. Increases from baseline MFI demonstrate successful phagocytosis of bacteria and generation of both cROS and n/mROS. The percentage of cells which have undergone phagocytosis is within the range to allow for measurement of increased or decreased effects from patient samples. The significant change in phagocytosis between fixed and unfixed samples is noted, but due to the nature of COVID-19 it would be irresponsible and unsafe to use unfixed samples. Measurements and comparisons with AMC and CAP patients were only made between fixed samples.

Cessation of phagocytosis

Cessation of phagocytosis is routinely achieved by incubation on ice following the experimental time course. Samples must remain on ice until samples can be processed and analysed by flow cytometry. 4% (v/v) PFA was used as a surrogate for cessation of cellular activity.

Comparison between ice and 4% (v/v) PFA was carried out on 3 paired samples (3M, mean age (27), using the methods described in **Chapter 3**. The percentage of cells which have phagocytosed was not significantly different between ice control and PFA treated cells, suggesting equivalence in cessation of phagocytic function (mean ice control 38.2 vs 4% PFA 40.2, p=0.7500, **Figure 4.8**).

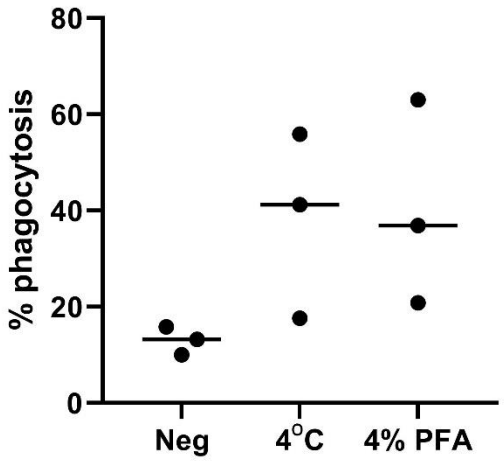

Figure 4.8 Percentage of labelled *S. aureus* phagocytosed by isolated neutrophils at 30 minutes comparing ice and 4% (v/v) PFA as method of termination of phagocytosis at the desired 30 minute timepoint. Paired samples, n=3. Neg indicates negative control using cytochalasin D. Kruskal-Wallis test used to compare groups.

4.2.2 Transwell migration

Migration through a transwell membrane was carried out on 5 paired samples (3M, 2F, mean age 28.8 years) using the methods described in **Chapter 3.1.4.2**. Number of cells migrating was calculated as per methods described previously. Results from cells fixed post 90-minute migration and unfixed samples were compared to determine differences and appropriate experimental plan.

Unfixed samples demonstrated significantly lower numbers of cells migrated compared to fixed (median no. cells migrated unfixed 4959 vs fixed 9277, p=0.0348, **Figure 4.9A**). To determine if there was a difference between stimulated and vehicle control, fold change to vehicle control was compared. There was no statistically significant difference, but there was decreased migration in unfixed samples (median fold change cells migrated fixed 35.45 vs unfixed 18.00, p=0.1250, **Figure 4.9B**).

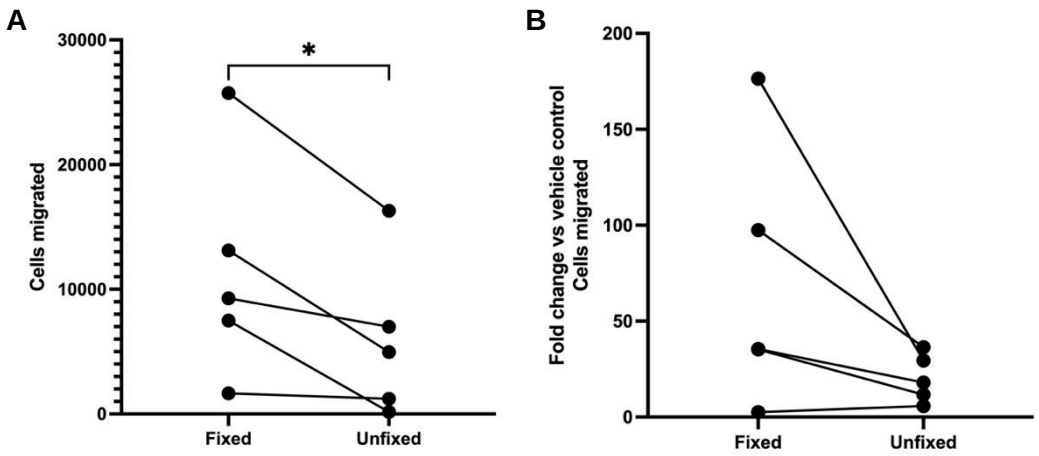

Figure 4.9 Comparison of neutrophil migration through a transwell membrane between fixed and unfixed samples**.** Paired samples, n=5. Wilcoxon matched pairs signed rank test carried out for statistical significance, *p≤0.05, **p≤0.01, ***p≤0.001, ****p≤0.0001. **A.** Number of cells migrated compared between fixed and unfixed samples. Vehicle control was negligible. **B.** Fold change of cells migrated compared to vehicle control compared to fixed vs unfixed.

Although absolute number of cells migrated is significantly lower in unfixed samples, changes will be reported as fold change compared to vehicle control. Comparisons between samples from COVID-19 patients, healthy controls and community acquired pneumonia patients will be valid as all samples will be processed with fixation.

4.2.3 NETosis

NET production after stimulation with PMA was carried out on 11 paired samples (4M, 7F, mean age 66.1 years) from a combination of healthy controls and community acquired pneumonia patients, using the methods described in **Chapter 3.1.4.3**. Absolute values in reference units (RFU) and percentage change from vehicle control were recorded after stimulation with PMA. Unfixed samples demonstrated no significant difference in NET production after stimulation compared to fixed samples (percentage change fixed 101.0 vs unfixed 116.1, p=0.1230, **Figure 4.10A**). There was a significant increase between vehicle control and PMA stimulated neutrophil NETosis (fixed VC 126RFU vs PMA 258RFU, p=0.0002), (unfixed VC 114RFU vs PMA 247RFU, p<0.0001), **Figure 4.10B**.

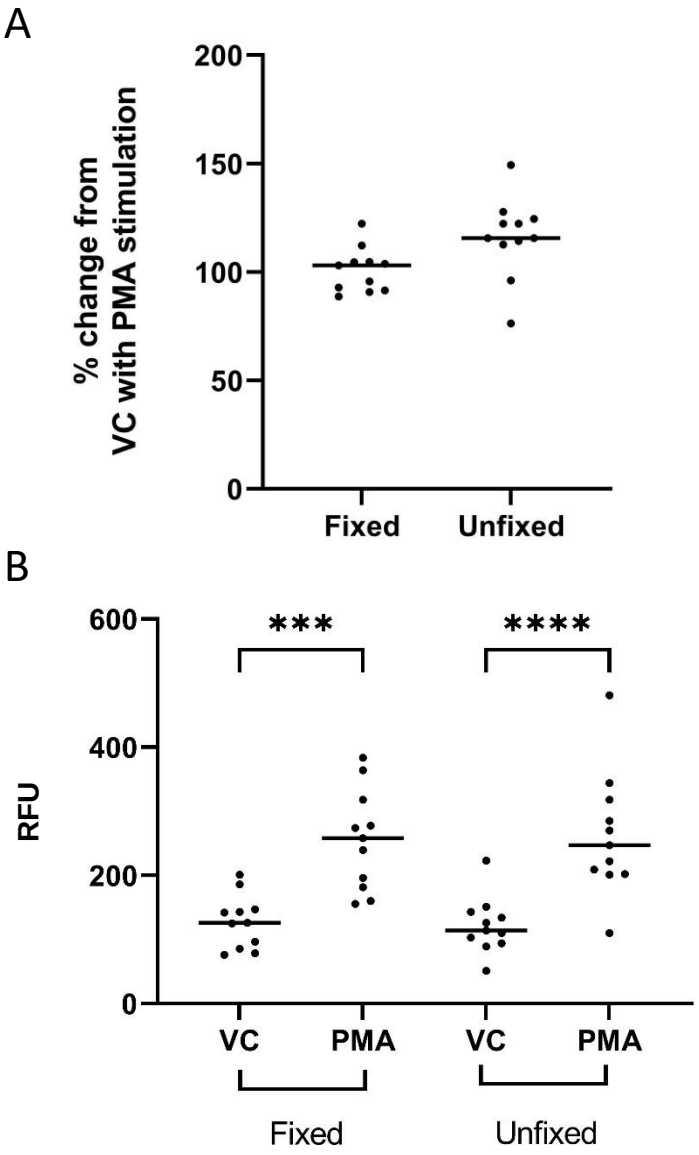

Figure 4.10 Neutrophil extracellular trap production after stimulation with PMA or vehicle control (VC) shown as **A**. Percentage change in neutrophil extracellular trap production compared to vehicle control after PMA stimulation and **B.** Increase in RFU compared between vehicle control and PMA stimulation of neutrophils. One-way ANOVA used for multiple comparisons and paired t-test used for single comparisons, n=11 for all groups, *p≤0.05, **p≤0.01, ***p≤0.001, ****p≤0.0001.

4.3 PI3K inhibitor viability

Addition of the pan PI3K inhibitor had no effect on the viability of the cells after isolation, 30 minutes incubation with the inhibitor and 30 minutes phagocytosis, **Figure 4.11**.

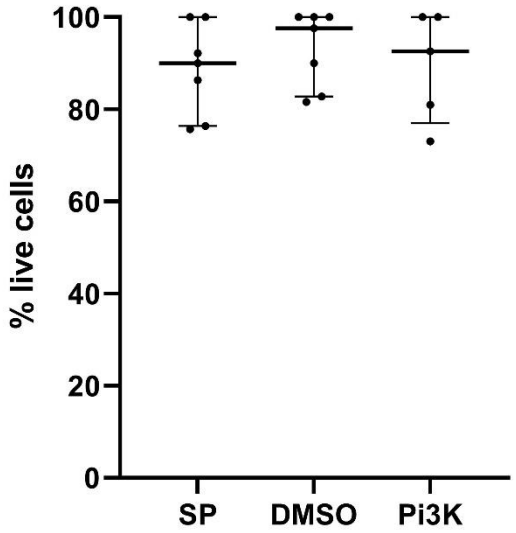

Figure 4.11 Viability of neutrophils after 30 minutes incubation with pan PI3K inhibitor or DMSO (vehicle control), or 30 minutes phagocytosis of labelled *S. pneumoniae* (SP), n=7, Kruskal-Wallis test used for comparisons.

4.4 Dexamethasone

Rapid development of COVID-19 treatment occurred throughout the pandemic and during patient recruitment. Patients were recruited prior to administration of novel repurposed therapies such as monoclonal antibodies. Dexamethasone, a synthetic glucocorticoid which has been commonly used since 1958 (Khan et al., 2005), was one of the first drugs to be investigated to determine if administration improved patient outcomes in COVID-19 disease. The RECOVERY trial showed improved clinical outcomes in severe disease (Johnson and Vinetz, 2020). Patients requiring supplemental oxygen to maintain peripheral saturations of >90% were prescribed dexamethasone either 6.6mg intravenously (IV) or 6mg orally (PO) as standard of care.

Previous studies have demonstrated inhibited neutrophil migration to inflammatory sites (van Overveld et al., 2003, Zentay et al., 1999). These studies used only neutrophils isolated from healthy controls. Dexamethasone related changes to neutrophil chemotaxis were documented to be recordable from within 2 hours after oral dosing of dexamethasone (Lomas et al., 1991). In order to determine the effect of dexamethasone on neutrophil function in an infective state, cells treated with dexamethasone were compared to those treated with vehicle control from CAP patients.

Neutrophils from CAP patients were supplemented *in vitro* with dexamethasone to replicate a peak plasma concentration of 60-100ng/mL (Weijtens et al., 1997). Phagocytosis of heat inactivated, labelled *S. pneumoniae*, transwell migration and NETosis were investigated. Cells were treated with dexamethasone for 30 minutes prior to functional experimentation, and all samples were fixed as per safety guidance for COVID-19 sample handling.

4.4.1 Phagocytosis

Phagocytosis using heat inactivated labelled *S. pneumoniae* was carried out on 6 paired samples (3M, 3F, mean age 26.5) using the methods described in **Chapter 3.1.4.1**. Dexamethasone was added to samples as detailed above. The percentage of bacterial phagocytosis was measured compared between vehicle control and dexamethasone.

There was no significant difference in the percentage of phagocytosis between those treated with dexamethasone and those with vehicle control (median percentage phagocytosis no dexamethasone 22.53 vs dexamethasone 20.24, p=0.6875, **Figure 4.12**).

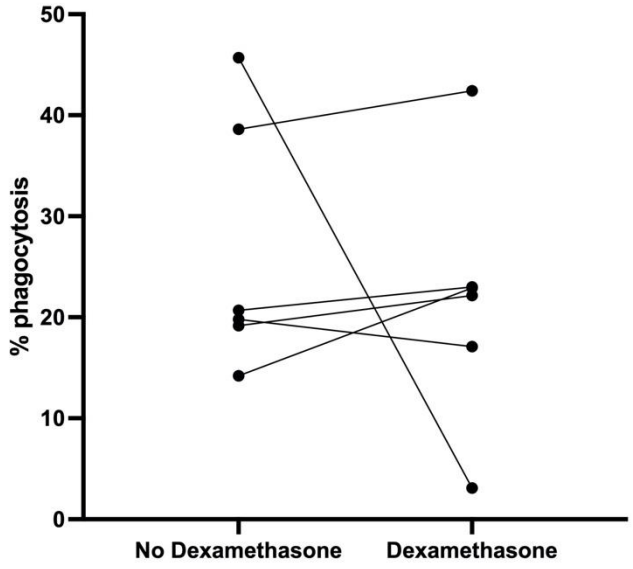

Figure 4.12 Percentage of neutrophil phagocytosis of labelled *S. pneumoniae* after dexamethasone treatment. Paired samples n=6, Wilcoxon matched-pairs signed rank test used for statistical analysis.

4.4.2 Transwell migration

Migration through a transwell chamber towards CXCL8 supplemented media was carried out on 16 paired samples (10M, 6F, mean age 72.5y) from a combination of healthy controls and

community acquired pneumonia patients, using the methods set out in **Chapter 3.1.4.2**. Cells migrated and fold change from vehicle control was measured.

There was no significant difference in number of cells migrated between those treated with vehicle control and supplemented dexamethasone (median no. cells migrated no dexamethasone 6471 vs dexamethasone 4134, p=0.3303,**Figure 4.13A**). As there was a difference demonstrated between fixed and unfixed samples as per **Chapter 4.2.2**, fold change in cells migrated was also compared. There was no significant difference between vehicle control and dexamethasone samples (fold change of cells migrated no dexamethasone 11.80 vs dexamethasone 11.08, p=0.4212, **Figure 4.13B**).

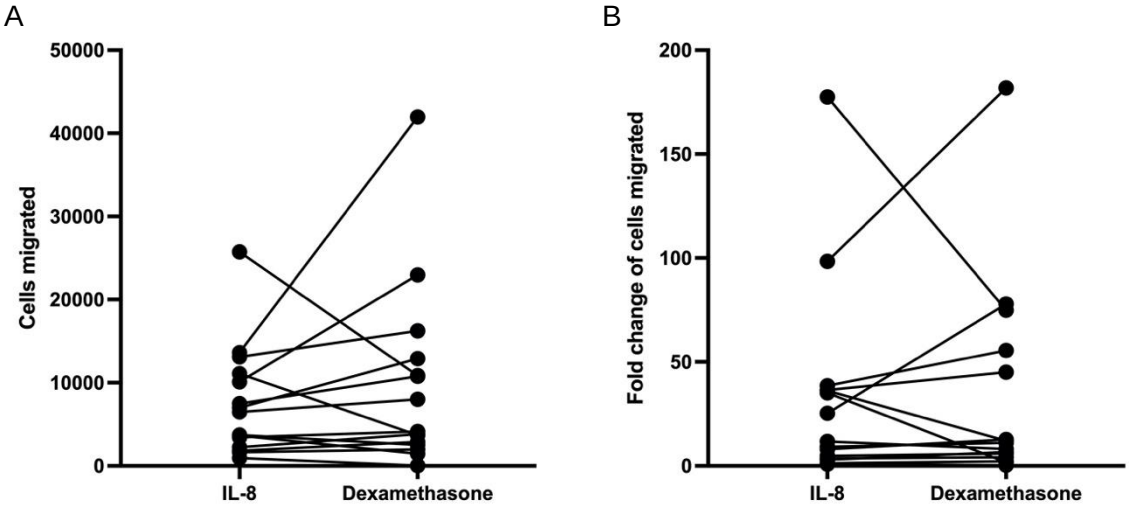

Figure 4.13 Comparison of neutrophil migration through a transwell pore between samples treated with dexamethasone and IL-8 (Dexamethasone) and IL-8 only (IL-8). Paired samples n=16, paired t-test used for statistical analysis. **A.** Total number of cells migrated with and without dexamethasone added . **B.** Fold change in cells migrated with and without dexamethasone added.

4.4.3 NETosis

NET production after stimulation with PMA was carried out on 9 paired samples (3M, 6F, mean age 76.8y) from a combination of healthy controls and community acquired pneumonia

patients, using the methods set out in **Chapter 3.1.4.3**. % change from vehicle control compared to additional dexamethasone was recorded after stimulation with PMA.

There was no significant difference in NET production after PMA stimulation between those treated with dexamethasone and those with vehicle control (percentage change in NET production no dexamethasone 99.19 vs dexamethasone 98.78, p=0.9300, **Figure 4.14**)

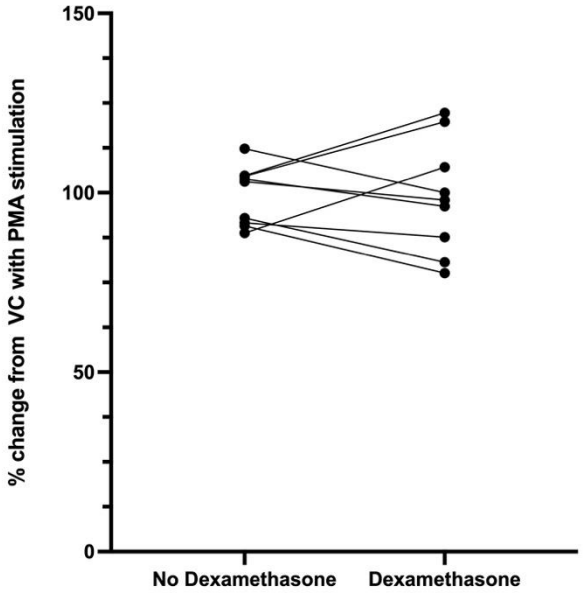

Figure 4.14 Neutrophil extracellular trap formation after PMA stimulation, compared between cells treated with dexamethasone and untreated. Paired samples n=9, paired t-test used for statistical analysis.

4.5 Carbon dioxide incubation

Communal incubators were unable to be used as part of COVID-19 safety protocols. These incubators are set up for optimal cell culture, including maintenance of a 5% CO_2 environment. Smaller incubators were used instead, which could be incorporated into the isolated laboratory. 5% CO_2 is important for media stability and prevention of disequilibrium of the carbonic acid pH buffering system. RPMI 1640 media was used for cell culture as laboratory standard. This is designed to buffer pH and counteract changes which may be induced by cellular respiration. Exposure to atmospheric CO_2 levels may therefore change the pH of the media, potentially affecting cellular function.

Comparison of neutrophil cellular function in an incubator capable of maintaining 5% CO_2 compared to atmospheric CO_2 was carried out.

4.5.1 Phagocytosis and viability

Phagocytosis and viability were carried out on 4 paired samples (3M, 1F, mean age 82.0y) using the methods described in **Chapter 3.1.4.1**. The percentage of bacterial phagocytosis of *S. pneumoniae* and percentage of cells alive were measured for these samples.

There was no significant difference seen in the percentage of phagocytosis or cell viability between those cells incubated in 5% controlled CO_2 or atmospheric CO_2 (percentage phagocytosis atmospheric CO_2 48.91 vs 5% CO_2 48.30, p=0.6250, **Figure 4.15A**) (percentage of cells alive atmospheric CO_2 96.00 vs 5% CO_2 99.00, p=0.2500, **Figure 4.15B**).

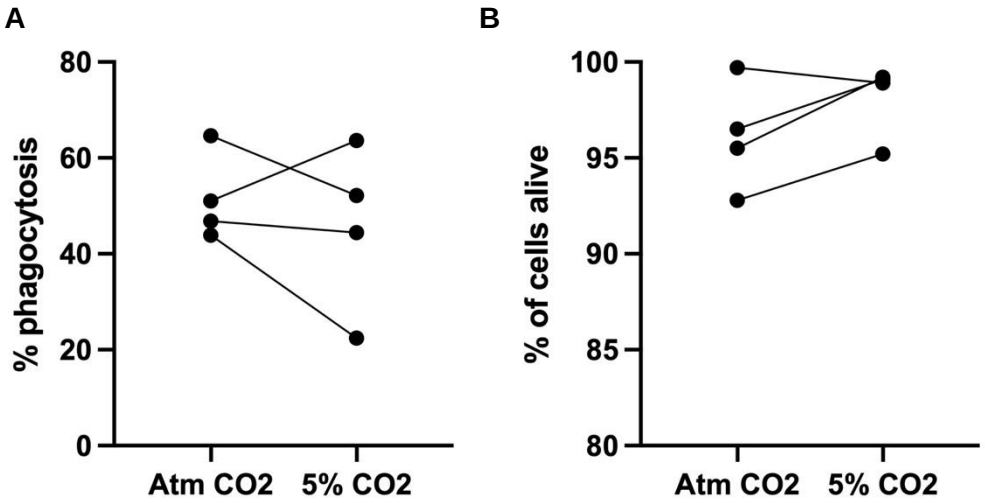

Figure 4.15 Comparison of neutrophil incubation in 5% controlled CO_2 (5% CO_2) and atmospheric CO_2 (Atm CO_2) throughout the experiment, for a total time of 1.5 hours. Paired samples n=4, Wilcoxon matched-pairs signed rank test used for statistical analysis. **A.** Percentage phagocytosis between atmospheric and 5% CO_2 environments **B.** Neutrophil viability comparison between atmospheric and 5% CO_2 environments

4.5.2 Transwell migration

Neutrophil migration through a transwell pore was carried out on 5 paired samples (4M, 1F, mean age 82.0y) using the methods described in **Chapter 3.1.4.2**. Number of cells migrated and fold change compared to untreated control was measured.

There was no significant difference in the fold change of cells migrated between CO_2 conditions (median fold change cells migrated atmospheric CO_2 5.333 vs 5% CO_2 4.361, p=0.6250, **Figure 4.16A**). There was a significant difference in the number of cells migrating between CO_2 conditions (median no. cells migrated atmospheric CO_2 1011 vs 5% CO_2 12-77, p=0.0042, **Figure 4.16B**). As described in **Chapter 4.2.2**, there was a significant difference in number of cells migrating between fixed and unfixed states.

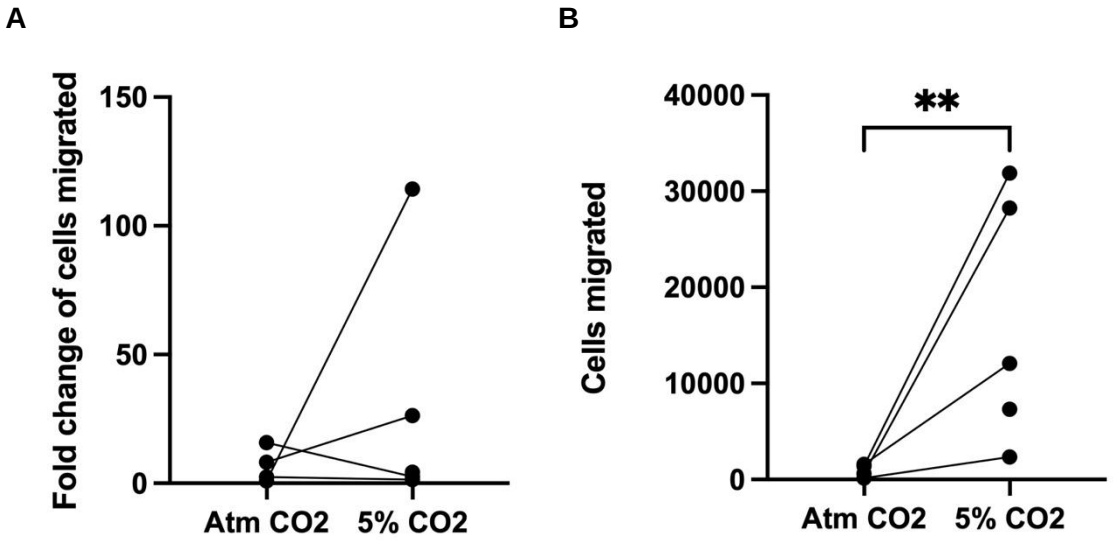

Figure 4.16 Comparison of neutrophil migration at atmospheric CO_2 (Atm CO_2) and 5% controlled CO_2 (5% CO_2). Paired samples n=5, Wilcoxon matched-paired signed rank test used for statistical analysis, *p≤0.05, **p≤0.01, ***p≤0.001, ****p≤0.0001. **A.** Fold change in number of cells migrated from control compared between atmospheric and 5% CO_2 environments . **B.** Total number of cells migrated compared between atmospheric and 5% CO_2 environments).

4.5.3 NETosis

NET formation after PMA stimulation was carried out on 3 paired samples (2M, 1F, mean age 85.0y) using the methods described in **Chapter 3.1.4.3**. Fold change of NET production compared to vehicle control was measured

There was no significant difference in NET production between the CO_2 conditions (median fluorescence atmospheric CO_2 1268 vs 5% CO_2 1332, p=0.7500, **Figure 4.17**).

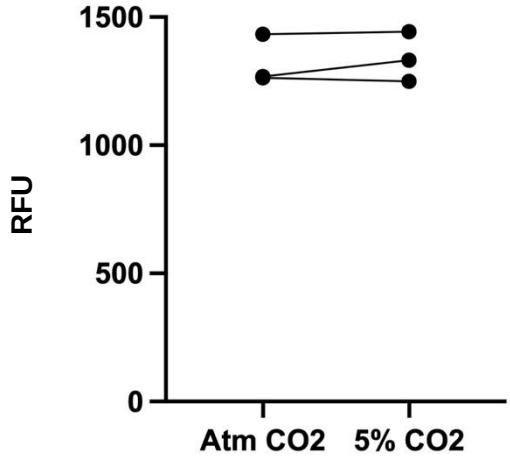

Figure 4.17 Fluorescence (in reference units (RFU)) recorded of neutrophil extracellular trap production after PMA stimulation in atmospheric CO_2 (Atm CO_2) and 5% controlled CO_2 (5% CO_2) environments. Paired samples n=3, Wilcoxon matched-pairs signed rank test used for statistical analysis.

4.6 Bacterial fluorescence

S. pneumoniae labelling with AlexaFluor 488 can degrade over time, decreasing intensity of bacterial fluorescence. To decrease potential batch variations that may occur with labelling, one batch of labelled bacteria was used across all phagocytosis experiments from January 2021 to May 2022. Comparisons made using this assay were internally controlled though fold change from baseline, but degradation of fluorescent intensity would lead to a reduction in median fluorescent intensity (MFI) for the same number of phagocytosed bacteria and reduce the ability of the assay to detect smaller changes. Theoretically degradation may not be equal across all labelled bacteria, introducing further bias.

Healthy young controls were analysed at the beginning at project start (January 2021), to represent neutrophils not affected by disease, age or other co-morbidities. 10 healthy young controls were recruited. Due to loss of follow up, 3 were available for repeat experiments at the conclusion of this project (November 2022). A total of 21 months had elapsed from bacterial labelling to final phagocytosis experiment. MFI of phagocytosed bacteria were compared to determine if degradation was significant.

There was no significant difference in recorded MFI or percentage of phagocytosis between experiments conducted in 2020 at the beginning of recruitment and 2022 at the end of patient recruitment (MFI 2020 7.880 vs 2022 7.330, p=0.4197, **Figure 4.18A**) (percentage phagocytosis 2020 54.80 vs 2022 29.90, p=0.0973, **Figure 4.18B**).

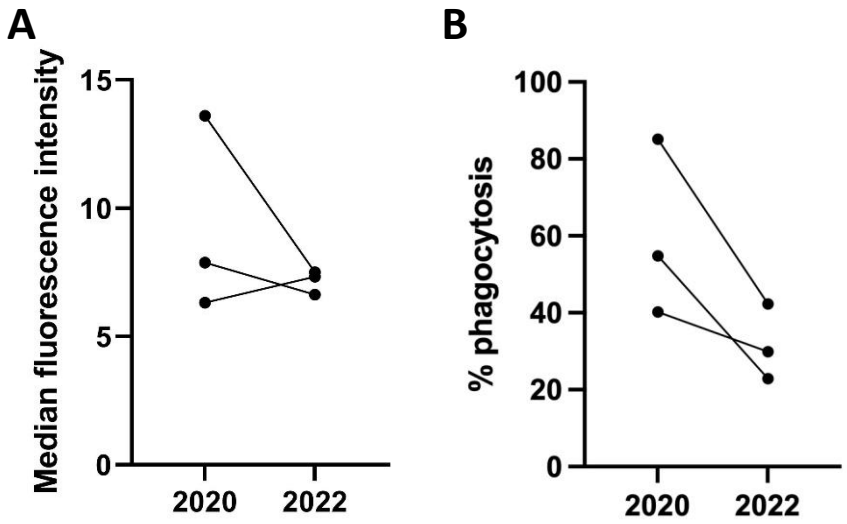

Figure 4.18 Comparison over time of bacterial fluorescence of phagocytosed *S. pneumoniae*. Paired samples n=3, Wilcoxon matched-paired signed rank test used for statistical analysis. **A**. Median fluorescent intensity (MFI) compared between phagocytosis experiments carried out in 2020 vs 2022. **B**. % phagocytosis of labelled bacteria compared between phagocytosis experiments carried out in 2020 vs 2022.

4.7 Discussion

The nature of a novel infectious disease requires careful manipulation of samples to ensure researcher safety. However, many established protocols for neutrophil effector function experiments are not designed or validated for this, including measurement of neutrophil viability and migration. Therefore, it was imperative to validate these experiments prior to patient recruitment. This enabled limitations to be evaluated and accounted for during data analysis. Fold change and percentage change for functional experiments were used in the analysis throughout this thesis especially between different variants of infection.

Our adapted methodology did not cause significant variance in functional neutrophil experiments; however, some differences were noted. Fixation significantly reduced the signal from the phagocytosis assay at both 30- and 60-minute timepoints. The results suggest that 30-minute incubation times for phagocytosis were appropriate for *S. pneumoniae*. Other neutrophil studies using labelled beads (e.g. pHrodo) are a less physiologically representative model of phagocytosis. The use of opsonised labelled *S. pneumoniae* was more physiologically relevant as well as reaching appropriate levels of phagocytosis at 30 minutes. There was decreased signal of phagocytosis in fixed samples, but sufficient to allow for changes to be detected. Total number of migrated cells decreased in unfixed samples, but there was no significant difference when fold change of migrated cells was compared. In order to accurately compare between samples, fold change to untreated control would be used in the first instance. No change in NET production was noted.

Avoiding dexamethasone treatment in patient recruitment was not be feasible for this study as it was given on admission to the Emergency Department and had quickly become standard of care. Delaying treatment could have detrimental effects on patient outcomes, and as such this was not ethical. Previous studies have documented changes to neutrophil function after steroid use (Burton et al., 1995, Dale et al., 1998, Zentay et al., 1999, Perretti and Flower, 1993, Fuenfer et al., 1975), but in this model, there were no significant differences in function recorded after treatment with dexamethasone. Previous studies have documented changes

to neutrophil function after 2 hours post oral dexamethasone administration (Lomas et al., 1991). Intravenous administration of dexamethasone should therefore have a reduced lag time. Glucocortiocosteroids have two main mechanisms of action on cells, mediated through the glucocorticosteroid receptor (GR). Genomic functions through GR signalling lead to induction or repression of gene expression, whilst more rapid responses occur through cytosolic or membrane GR through kinase enzyme activation (such as PI3K and mitogen-activated protein kinases (MAPKs) (Samarasinghe et al., 2012). Thus responses can occur within seconds to minutes of GR activation, with effects potentially lasting for days after administration. Patients were planned to be recruited within 24 hours of admission, with dexamethasone being administered from 0-24 hours before study recruitment. Assessing neutrophil changes beyond 30 minutes incubation would incur alterations to function due to ex vivo viability and would make interpretation and drawing conclusions unfeasible (Oh et al., 2008).

CO_2 concentrations can be responsible for changes to pH in the internal endovascular environment, when the natural carbonic anhydrase buffering system becomes overwhelmed. Exposure to different concentrations of CO_2 could theoretically alter function; studies have shown the effect of pH on neutrophil function in the past (Khan et al., 2018, Shimotakahara et al., 2008). We demonstrated a decreased neutrophil migration when neutrophils were incubated in atmospheric standard CO_2 compared to the controlled environment of a 5% controlled CO_2 incubator. There was no significant difference in fold change of cells migrated to vehicle control indicating the comparative effects remain constant.

Degradation in the fluorescent signal from heat-inactivated bacteria over time was observed during our study. Each model that could be used for phagocytosis has associated limitations. Inactivated bacteria suffer from decreased fluorescence; beads coated with bacterial fragments are a poorer physiological substitute; use of multiple batches of labelled bacteria can cause issues with inter-batch variability and labelling. Therefore, whilst this degradation of signal anticipated it was deemed preferable to potentially greater variance introduced from

the use of multiple cultures over a long period of time as relative comparisons to the untreated controls.

This chapter demonstrates some observed differences in output from our previously standardised methodology due to the requirement to fix samples before removal from a containment cabinet. Decreases in migration cell count may make detection of smaller fold changes more difficult but counts are not decreased to where they would be undetectable. These may be caused by clumping of cells during the fixation process (Kim and Sederstrom, 2015). However, all samples from disease and age-matched control groups underwent the same experimental protocol to unsure validity. Where possible, intra-patient controls were used and fold change analysed to ensure all comparisons were valid.

4.8 Summary of adaptations

1. Fixation with 4% (v/w) PFA

   Samples were fixed with 4% (v/w) PFA for researcher safety

2. Dexamethasone administration

   Patients who had dexamethasone administered were be included in recruitment as there was no significant difference in functional assay outcomes for isolated neutrophils compared to no dexamethasone administration

3. Carbon dioxide incubation at atmospheric pressures

   Due to safety protocols, incubation occurred in incubators at atmospheric carbon dioxide pressures. All experiments were conducted with the same protocol.

4. Bacterial fluorescence

   Use of percentage change in phagocytosis standardised to baseline of each patient helped to reduce the time sensitive effects of decreased fluorescence when comparing between patients infected with different SARS-CoV-2 strains.

CHAPTER 5
PATIENT PHENOTYPE IN COVID-19

5.1 Introduction

To date (December 2023), there have been 772 million recorded cases of COVID-19 worldwide (WHO, 2023a) and at the time of final recruitment for this project, 24.1 million cases in the UK alone. 80% of those infected develop a mild to moderate respiratory disease and 10-20% of these can manifest as pneumonitis (Sapey et al., 2020).

The clinical presentation and phenotype of COVID-19 patients varied significantly. In the early stages of the pandemic, it was not possible to discern why certain individuals developed a more severe disease course. It was thought that an exaggerated cytokine response, leading to overwhelming inflammation was a driver of severe disease and worse outcomes. Several routinely measured serum/ blood markers were thought to be associated with a poor outcome in COVID-19 such as ferritin and neutrophil: lymphocyte ratio (Aschenbrenner et al., 2021, Vitte et al., 2020, Wilk et al., 2020). To treat patients more effectively and triage patients earlier, scoring systems based on biochemical measurements, demographics and clinical observational data were developed. Traditional scores predicting mortality and disease outcomes in critical illness and bacterial CAP did not correlate to COVID-19 outcomes (Ahmed et al., 2022). The 4C score was validated for in-patient mortality outcomes in COVID-19, with patients being categorised into low, intermediate, high and very high scores (Gupta et al., 2021, Knight et al., 2020).

Increasing age was quickly recognised as a risk factor for severe COVID-19, including the development of acute respiratory distress syndrome (ARDS) (Zhang et al., 2020a, Printz, 2021). Neutrophil function has been shown to change with age; reduced phagocytic capacity, migration accuracy and NET production (Sapey et al., 2014, Butcher et al., 2001, Hazeldine et al., 2014). This in turn can delay pathogen clearance and increase bystander tissue injury. Any dysfunction is amplified in older adults who have severe infections where neutrophil functions are impaired even in younger adults (Patel et al., 2018, Grudzinska et al., 2020, Juss et al., 2016a, Sapey et al., 2017).

5.2 Aims of Chapter 5

1. To establish the clinical phenotype of the ward-based COVID-19 patients compared to community acquired pneumonia (CAP) and age matched controls (AMC)

5.3 Clinical phenotype

5.3.1 Patient demographics

41 COVID-19 patients (mean age 71.5 years, 26 male) were recruited alongside 23 healthy AMC (mean age 70 years, 10 male) and 26 CAP patients (mean age 67.5 years, 15 male). As described in **Chapter 3.2** BMI and comorbidity was also recorded, categorised into major organ systems. Patient demographics are shown in **Table 5.1.**

	AMC n=26	COVID-19 n=41	CAP n=26
Male: Female	10:16	26:15	15:11
White: Non-white	24:2	31:10	23:3
Died (%)	0 (0%)	10 (24%)	2 (8%)
Age	70 (61.0-78.0)	71.5 (58.0-84.0)	67.5 (54.5-85.0)
BMI (kg/m^2)		26.4 (24.2-32.8)	27.9 (23.3-41.1)
Comorbidities			
Cardiovascular	4 (15.3%)	12 (29.3%)	7 (26.9%)
Respiratory	0 (0%)	1 (2.4%)	4 (15.4%)
Endocrine	10 (38.4%)	16 (39.0%)	3 (11.5%)*
Hypertension	13 (50%)	19 (46.3%)	10 (38.5%)
Chronic Kidney Disease	1 (3.8%)	2 (4.8%)	5 (19%)
Other	10 (38.4%)	22 (53.7%)	10 (38.4%)
Smoking status			
Current	0 (0%)	1 (2.4%)	5 (19.2%)
Ex	8 (30.7%)	10 (24.4%)	3 (11.5%)
Never	18 (69.2%)	33 (80.5%)	18 (69.2%)

Table 5.1 Recruited patient and AMC demographics, collected at the time of enrolment. Height and weight measurements were not able to be collected to calculate a BMI measurement for the recruited AMC. Comparisons were calculated between cohorts of COVID-19 patients, AMC, or CAP patients. *p≤0.05, **p≤0.01, ***p≤0.001, ****p≤0.0001. Normally distributed results shown with mean (SEM), not normally distributed shown with median (IQR Q1-Q3). Statistical significance calculated using One-way ANOVA if parameter normally distributed and Kruskal-Wallis test if non-parametric parameter. Other comorbidities were included if they caused a significant impact on patient quality of life or regular medication – this included but not limited to: severe peripheral vascular disease with ulceration, dementia, stroke, childhood polio, obesity, diverticulosis, alcohol related liver disease, rheumatoid arthritis.

There was no significant difference in basic patient demographics between recruited AMC, COVID-19 and CAP patients. There was a lower incidence of endocrine comorbidities in the CAP group compared to either COVID-19 or AMC patients ($p<0.05$). There was no significant difference in the number of smokers vs ex- vs non-smokers between patient cohorts. No patients were transferred from ward-based care to intensive care.

Dexamethasone was prescribed for patients as per local and national guidelines. 92.6% (38/41) patients received at least one dose of dexamethasone during their COVID-19 admission. CAP patients were not treated with dexamethasone as this was not part of standard clinical care for pneumonia patients.

5.3.2 Biochemical correlations

Cell and biochemical markers of disease were collected and compared between COVID-19 and CAP patients, **Table 5.2.** There was a significantly raised white cell count (WCC) in CAP compared to COVID-19 patients (CAP 13.4 $x10^9$/L vs COVID-19 8.2 $x10^9$/L, $p<0.001$), as was neutrophil differential count (CAP 11.2 $x10^9$/L vs COVID-19 6.4 $x10^9$/L, $p<0.01$). Plasma ferritin was significantly raised in COVID-19 compared to CAP patients (COVID-19 1082µg/L vs CAP 110µg/L, $p<0.05$).

	COVID-19 n=41	CAP n=26
WCC ($x10^9$/L)	8.2 (6.3-12.0)	13.4 (10.7-16.4)***
Neutrophils ($x10^9$/L)	6.4 (4.4-8.6)	11.2 (7.8-13.6)**
CRP (mg/L)	103.0 (63.0-165.0)	119.0 (42.0-396.0)
NLR	5.4 (3.8-10.8)	8.5 (5.9-52.7)
HS Troponin I (ng/L)	14.5 (5.0-31.3)	17.5 (4.0-318.0)
D-dimer (ng/mL)	382.0 (218.0-829.5)	659.0 (270.5-1510.0)
Ferritin (µg/L)	1082 (428.3-1525.0)	110.0 (78.8-225.3)*
Vitamin D (nmol/L)	35.6 (23.0-51.8)	45.3 (23.8-73.2)

Table 5.2 Recruited COVID-19 and CAP patient biochemical results, recorded from admission blood tests and observations. WCC- white cell count; CRP- C-reactive protein; NLR- neutrophil lymphocyte ratio; HS Troponin I- high sensitivity troponin I. *p≤0.05, **p≤0.01, ***p≤0.001, ****p≤0.0001. Data shown as median (IQR Q1-Q3). Statistical significance calculated Wilcoxon matched pairs signed rank test for not normally distributed data.

5.3.3 Severity scoring correlations

Disease severity scores were compared between COVID-19 and CAP patients **Table 5.3**. 4C scores were calculated for CAP patients, but these have not been validated for mortality. They provide a useful comparison of biochemical measures between these cohorts. There was no significant difference between CAP and COVID-19 patient 4C scores. There was no significant difference in qSOFA (quick Sepsis-related Organ Failure Assessment Score) or CURB-65 (mortality score in community acquired pneumonia) scores. There was no significant difference observed in length of stay between COVID-19 and CAP patients observed. NEWS2 scores were not significantly different between COVID-19 and CAP patients. The worst score within 24 hours of admission was recorded for comparison.

	COVID-19 n=41	CAP n=26
Admission NEWS 2	6.0 (5.0-7.0)	5.0 (3.0-12.0)
4C	12.0 (9.0-14.0)	11.0 (5.3-13)
qSOFA	1.0 (1.0-1.5)	1.0 (1.0-1.0)
CURB-65	2.0 (1.0-3.0)	2.0 (2.0-2.0)
Length of stay (days)	5.5 (3.0-12.0)	4 (3.0-7.5)

Table 5.3 Disease severity scores calculated based on clinical observations and blood tests done on admission. qSOFA- quick Sepsis-related Organ Failure Assessment Score; CURB-65- Mortality in community acquired pneumonia. Data shown with median (IQR Q1-Q3). Statistical significance calculated Wilcoxon matched pairs signed rank test for not normally distributed data.

Stratifying patients by COVID-19 disease severity using the 4C score (<9 <9.9% mortality vs ≥9 mortality >31.4%) showed patients with 4C <9 had a significantly higher BMI than those with 4C ≥9 (p= 0.0155), and CAP patients with a 4C score ≥9 were significantly older (p=0.0001), **Table 5.4** There was no significant difference in mortality between COVID-19 patients with 4C <9 versus 4C ≥9 (p=0.1047). Patients with 4C ≥ 9 had significantly longer hospital length of stay than those with 4C score <9 (LoS p<0.0001). CAP patients stratified by 4C score demonstrated no significant difference in mortality (p=0.204) or length of hospital admission (p=0.1614), **Table 5.5**.

	COVID-19		CAP	
	4C <9 n=10	4C ≥9 n=31	4C <9 n=10	4C ≥9 n=16
Male: Female	7:3	18:13	6:4	9:7
White: Non-white	7:3	23:8	9:1	14:2
Age	78 (69.0-87.0)	71 (58.0-84.0)	50.0 (23.5-57.3)	83.5 (68.5-90.0)***
BMI (kg/m^2)	31.26 (30.0-36.9)	25.39 (23.3-31.9)*	27.4 (24.1-33.9)	27.9 (23.2-33.1)
Died	0 (0%)	10 (32%)	0 (0%)	0 (0%)
Comorbidities				
Cardiovascular	3 (30%)	9 (29.0%)	1 (10%)	6 (38%)
Respiratory	0 (0%)	1 (3.2%)	0 (0%)	1 (6%)
Endocrine	3 (30%)	13 (41.9%)	1 (10%)	2 (13%)
Hypertension	0 (0%)	19 (61.3)**	2 (20%)	8 (50%)
Other	1 (10%)	23 (74.2%)**	9 (90%)	10 (63%)

Table 5.4 Table showing demographics and comorbidity data when COVID-19 and CAP patients are stratified by 4C score <9 and ≥9 (<9 <9.9% mortality vs ≥9 mortality >31.4%). Normally distributed results shown with mean (SEM), not normally distributed shown with median (IQR Q1-Q3). Statistical significance calculated using One-way ANOVA if parameter normally distributed and Kruskal-Wallis test if non-parametric parameter. *p≤0.05, **p≤0.01, ***p≤0.001, ****p≤0.0001. Other comorbidities were included if they caused a significant impact on patient quality of life or regular medication – this included but not limited to: severe peripheral vascular disease with ulceration, dementia, stroke, childhood polio, obesity, diverticulosis, alcohol related liver disease, rheumatoid arthritis.

	COVID-19		CAP	
	4C <9 n=10	4C ≥9 n=31	4C <9 n=10	4C ≥9 n=31
WCC (x10^9/L)	7.1 (6.1-9.7)	8.8 (6.8-12.5)	13.8 (107-16.5)	13.4 (9.9-16.4)
Neutrophils (x10^9/L)	5.5 (4.3-8.0)	6.7 (4.6-8.8)	10.4 (7.8-13.6)	11.3 (6.4-14.5)
CRP (mg/L)	86.0 (44.3-158.3)	116.0 (72.0-170.0)	48.5 (16.8-109.5)	134 (103.0-196.0)
NLR	5.4 (3.7-7.5)	4.5 (3.9-13.3)	6.4 (4.5-7.7)	11.7 (7.2-20.1)
HS Troponin I (ng/L)	<5 (<5-5.0)	18.0 (9.0-37.0)	4.0 (4.0-21.5)	30 (16.3-64.5)
D-dimer (ng/mL)	267.0 (201.0-572.0)	408.5 (233.0-886.5)	254.0 (163.0-254.0)	915 (355.3-2001.8)
Ferritin (ug/L)	1169 (569.0-1377.0)	995 (394.0-2055.5)	98.0 (60.0-184.0)	163.0 (81.0-480.0)
Vitamin D (nmol/L)	25.3 (18.3-36.0)	45.0 (25.6-70.1)**	31.5 (22.5-51.4)	55.4 (23.4-77.6)
CFS	4.5 (2.5-6.0)	1.0 (1.0-2.0)**	0.0 (0.0-1.5)	4.0 (2.25-5.75)
Worst NEWS2	6.0 (5.3-7.0)	6.0 (4.3-7.0)	5.0 (2.5-6.3)	5.5 (3.0-8.0)
CURB65	2.0 (1.0-3.0)	2.0 (2.0-2.0)	0.0 (0.0-0.3)	2.0 (2.0-2.0)
qSOFA	1.0 (0.3-1.0)	1.0 (1.0-2.0)	1.0 (1.0-1.0)	1.0 (1.0-2.0)
Length of stay (days)	3.0 (2.0-4.0)	9.5 (4.3-12.0)*	3.0 (2.0-4.0)	5.5 (3.3-8.0

Table 5.5 Table showing biochemical clinical measures and severity scores when COVID-19 and CAP patients are stratified by 4C score <9 and ≥9 (<9 <9.9% mortality vs ≥9 mortality >31.4%). Normally distributed results shown with mean (SEM), not normally distributed shown with median (IQR Q1-Q3). Statistical significance calculated using One-way ANOVA if parameter normally distributed and Kruskal-Wallis test if non-parametric parameter, *p≤0.05, **p≤0.01, ***p≤0.001, ****p≤0.0001. WCC- white cell count; CRP- C-reactive protein; NLR- neutrophil lymphocyte ratio; HS Troponin I- high sensitivity troponin I

Patients were followed up for outcome at 28 days, 3 months, 6 months and 12 months from recruitment. Re-admissions at 28 days are shown in **Table 5.6** with reasons documented. 3 of the 5 patients from the CAP group readmitted were COVID-19 positive. In addition to patient outcome, radiological changes were reviewed at 6 months and 12 months to determine if any changes persisted.

COVID-19	In-hospital	28-day		3 month	6 month	12 month
		Mortality	Re-admission			
Additional mortality	10/41 (24%)	0/31	2/31 (1 non-related infection, 1 worsening of symptoms)	1/31 (3%)	2/29 (7%)	1/27 (4%)
Cumulative mortality	10/41 (24%)	10/41 (24%)		11/41 (27%)	13/41 (32%)	14/41 (34%)

CAP	In-hospital	28-day		3 month	6 month	12 month
		Mortality	Re-admission			
Additional mortality	2/26 (8%)	0/24	0/24	0/24 (0%)	2/24 (8%)	2/22 (9%)
Cumulative mortality	2/26 (8%)	2/26 (8%)		2/26 (8%)	4/26 (15%)	6/26 (23%)

Table 5.6 COVID-19 and CAP patient clinical outcome data, with follow up outcomes at 28 days, 3, 6, and 9 months after discharge. Mortality shown as additional deaths at each follow-up time point and cumulative mortality. Re-admission data was collected at 28 days only, with one patient being re-admitted for a non-related cellulitis infection and one re-admitted with worsening COVID-19 symptoms, and later that admission was transferred to ICU care. No CAP patients were readmitted at 28 days.

Clinical data for patients who survived versus those who died are shown in **Table 5.7**. Patients who did not survive were significantly older (median age survived 61 (56-78), median age died 87 (79-90), p=0.0006), and had increased cardiovascular comorbidity incidence (survived incidence 22.6%, died incidence 80%, p=0.002). Measured high sensitivity troponin I (median survived 7.0 (5.0-15.5), median died 17.5 (11.8-37.0), p=0.0048) and vitamin D3 (median survived 32.9 (21.4-56.9), median died 57.9 (29.6-86.5), p=0.0456) were lower in those who

survived compared to died, as in **Table 5.8**. Of those with COVID-19 who survived, 90% received dexamethasone and all who died received dexamethasone.

	COVID-19		CAP	
	Survived n=31	Died n=10	Survived n=24	Died n=2
Male: Female	19:12	7:3	14:10	1:1
White: Non-white	22:9	8:2	21:3	2:0
Age	61 (56-78)	87 (79-90)**	66.5 (51.5-84.8)	78.0 (71.0-85.0)
BMI (kg/m^2)	29.7 (24.3-33.3)	25.7 (23.8-28.5)	26.5 (23.1-33.2)	30.1 (29.9-31.9)
Comorbidities				
Cardiovascular	7 (22.6%)	8 (80%)*	6 (26.1%)	1 (50%)
Respiratory	2 (6.5%)	2 (20%)	3 (13.0%)	1 (50%)
Endocrine	12 (38.7%)	5 (50%)	4 (17.4%)	0 (0%)
Hypertension	10 (32.2%)	9 (90%)*	8 (34.8%)	1 (50%)
Other	8 (25.8%)	6 (60%)	14 (60.9%)	1 (50%)

Table 5.7 Recruited COVID-19 and CAP patients split by in-hospital mortality with demographics. Normally distributed results shown with mean (SEM), not normally distributed shown with median (IQR Q1-Q3). Statistical significance calculated using One-way ANOVA if parameter normally distributed and Kruskal-Wallis test if non-parametric parameter, *p≤0.05, **p≤0.01, ***p≤0.001, ****p≤0.0001. Other comorbidities were included if they caused a significant impact on patient quality of life or regular medication – this included but not limited to: severe peripheral vascular disease with ulceration, dementia, stroke, childhood polio, obesity, diverticulosis, alcohol related liver disease, rheumatoid arthritis

	COVID-19		CAP	
	Survived n=31	Died n=10	Survived n=24	Died n=2
WCC (x10^9/L)	8.2 (6.4-10.8)	8.3 (6.3-24.8)*	13.6 (10.7-16.8)	14.9 (14.1-15.7)
Neutrophils (x10^9/L)	6.5 (4.5-8.4)	5.8 (4.0-17.3)	10.6 (7.5-13.1)	13.4 (11.7-15.1)
CRP (mg/L)	98.0 (57.5-155.0)	139.0 (68.5-202.8)	87.0 (33.5-196.0)	146.5 (128.0-165.0)
NLR	6.3 (3.6-12.1)	4.9 (4.0-11.5)	7.8 (5.4-12.2)	18.5 (17.2-19.9)
HS Troponin I (ng/L)	7.0 (5.0-15.5)	17.5 (11.8-37.0)**	15.0 (4.0-63.0)	NA
D-dimer (ng/mL)	382.0 (242.5-825.0)	300.5 (182.8-3003.3)	659 (270.5-915.0)	NA
Ferritin (ug/L)	1260 (548.3-1531.0)	431 (371.0-2187.3)	110 (80.3-183.8)	NA
Vitamin D (nmol/L)	32.9 (21.4-56.9)	57.9 (29.6-86.5)**	45.3 (24.6-74.5)	40.6 (19.3-61.9)
Worst NEWS2	6.0 (4.5-7.0)	7.0 (7.0-9.5)	5.0 (3.0-8.0)	4.5 (3.0-6.0)
4C	10.0 (6.5-13.0)	16.0 (13.3-20.0)**	NA	NA
CURB65	1.0 (1.0-2.0)	3.0 (2.0-3.25)**	2.0 (2.0-2.0)	2.0 (2.0-2.0)
qSOFA	1 (0.5-1.0)	1.5 (1.0-2.0)	1.0 (1.0-1.5)	1.0 (1.0-1.0)
Length of stay (days)	4.0 (2.3-12.0)	9.5 (6.3-12.0)	4.0 (3.0-7.0)	15.5 (8.0-23.0)

Table 5.8 Recruited COVID-19 and CAP patients split by in-hospital mortality with biochemical clinical measures and severity scores. Normally distributed results shown with mean (SEM), not normally distributed shown with median (IQR Q1-Q3). Statistical significance calculated using One-way ANOVA if parameter normally distributed and Kruskal-Wallis test if non-parametric parameter, *p≤0.05, **p≤0.01, ***p≤0.001, ****p≤0.0001. WCC- white cell count;

CRP- C-reactive protein; NLR- neutrophil lymphocyte ratio; HS Troponin I- high sensitivity troponin I

Of the 12 patients who had follow up imaging done at 6 months, 3 demonstrated signs of persistent changes, with 2 patients being readmitted with signs of acute infection and the remaining 7 patients demonstrating resolution of initial pneumonitis. At 12 months, 5 patients had ongoing imaging, which demonstrated ongoing persistent changes that had not resolved from the imaging done at 6 months.

Patients were recruited within 48 hours of medical admission to hospital, but date of symptoms onset to presentation varied between patients, with a range between 0 and 19 days. Median time between symptom onset and presentation to hospital was 7 days for both CAP and COVID-19 patients. Patients who presented to hospital <7 days after symptom onset were significantly older than those who presented at ≥7 (mean age <7 days 76.3 (73.8-87.0); mean age ≥7 days 60.2 (55.3-76.3), p=0.026, **Table 5.9**). These patients also had a higher CFS (Clinical Frailty Scale score) (median CFS <7 4.5 (2.5-6.0), median CFS ≥7 days 1.0 (1.0-2.0), p<0.001, **Table 5.10**), higher measured vitamin D (mean vitamin D <7 54.8 (27.9-76.0), mean vitamin D ≥7 days 37.23 (21.0-54.3), p=0.05, **Table 5.10**), higher 4C score (median 4C score <7 14.0 (11.5-15.0), median 4C score ≥7 days 10.0 (7.5-11.0), p-0.004, **Table 5.10**). There was no significant difference in other measured clinical biochemical variables collected. There was no significant difference noted between CAP patients presenting less or more than 7 days after symptom onset.

	COVID-19		CAP	
	<7d symptoms n=20	≥7d symptoms n=21	<7d symptoms n=17	≥7d symptoms n=9
Male: Female	10:10	15:6	10:7	5:4
White: Non-white	16:4	13:8	15:2	8:1
Age	76.3 (73.8-87.0)	60.2 (55.3-76.3)*	70.0 (58.0-86.0)	61.0 (35.5-77.0)
BMI (kg/m^2)	25.2 (23.-31.3)	29.8 (23.1-34.3)	26.5 (23.3-31.2)	32.5 (23.2-34.4)
Comorbidities				
Cardiovascular	8 (40%)	4 (20%)*	5 (36%)	1 (11%)
Respiratory	2 (10%)	2 (10%)	1 (6 %)	0 (0%)
Endocrine	8 (40%)	11 (52%)	1 (6%)	2 (22%)
Hypertension	10 (50%)	9 (43%)*	5 (36%)	5 (56%)
Other	8 (40%)	6 (29%)	9 (53%)	4 (44%)

Table 5.9 Table showing demographics and comorbidities of COVID-19 and CAP patients split by presentation <7 or ≥7 days (median time from symptom onset to presentation). Normally distributed results shown with mean (SEM), not normally distributed shown with median (IQR Q1-Q3). Statistical significance calculated using One-way ANOVA if parameter normally distributed and Kruskal-Wallis test if non-parametric parameter, *p≤0.05, **p≤0.01, ***p≤0.001, ****p≤0.0001. Other comorbidities were included if they caused a significant impact on patient quality of life or regular medication – this included but not limited to: severe peripheral vascular disease with ulceration, dementia, stroke, childhood polio, obesity, diverticulosis, alcohol related liver disease, rheumatoid arthritis. BMI- Body Mass Index.

	COVID-19		CAP	
	<7d symptoms n=20	≥7d symptoms n=21	<7d symptoms n=20	≥7d symptoms n=21
WCC (x10^9/L)	7.6 (6.6-12.2)	8.4 (5.7-10.7)	13.3 (10.1-16.2)	14.2 (10.6-17.3)
Neutrophils (x10^9/L)	5.7 (5.1-8.4)	6.8 (4.1-8.6)	10.9 (7.1-13.1)	11.5 (7.6-15.0)
CRP (mg/L)	88 (64.5-170)	116.5 (48.0-156.8)	87.0 (25.0-173.0)	127.0 (33.6-192)
NLR	4.5 (3.6-9.1)	6.5 (3.8-12.2)	10.2 (6.7-19.5)	6.1 (3.8-10.0)
HS Troponin I (ng/L)	27.5 (13.8-154.8)	15 (8.5-29)	17.5 (4.0-41.3)	39.0 (4.0-157.0)
D-dimer (ng/mL)	386.5 (209.5-1029.8)	349.0 (195.5-870.5)	737.0 (254.0-2027.0)	480 (252.3-812.5)
Ferritin (ug/L)	569.0 (379.0-1522.0)	1169 (433.8-1513.5)	81.0 (60.0-301.0)	163.0 (98.0-246.0)
Vitamin D (nmol/L)	54.8 (27.9-76.0	37.2 (21.0-54.3)*	47.9 (26.9-75.1)	46.5 (21.9-61.0)
CFS	4.5 (2.5-6.0)	1.0 (1.0-2.0)**	4.0 (1.0-6.0)	3.5 (1.5-5.5)
Worst NEWS2	7.0 (4.5-7.0)	6 (5.0-7.0)	5.0 (2.5-8.0)	3.0 (3.0-7.5)
4C	14.0 (11.5-15.0)	10.0 (7.5-11.0)**	11.0 (4.0-13.0)	10.5 (4.75-13.0)
CURB65	2.0 (1.0-3.0)	2.0 (2.0-2.0)	2.0 (1.0-3.0)	2.0 (1.0-2.0)
qSOFA	1.0 (0.5-2.0)	1.0 (0.75-1.0)	1.0 (1.0-2.0)	1.0 (0.1-1.0)
Length of stay (days)	11.0 (2.0-15.0)	4.5 (3.0-9.5)	5.0 (3.0-7.8)	3.0 (2.0-14.0)

Table 5.10 Table showing biochemical clinical measures and severity scoring of COVID-19 and CAP patients split by presentation <7 or ≥7 days (median time from symptom onset to presentation). Normally distributed results shown with mean (SEM), not normally distributed shown with median (IQR Q1-Q3). Statistical significance calculated using One-way ANOVA if parameter normally distributed and Kruskal-Wallis test if non-parametric parameter, *p≤0.05, **p≤0.01, ***p≤0.001, ****p≤0.0001. WCC- white cell count; CRP- C-reactive protein; NLR- neutrophil lymphocyte ratio; HS Troponin I- high sensitivity troponin I, CFS- clinical frailty score, NEWS2- National Early Warning Score 2, qSOFA- quick Sequential Organ Failure Assessment.

5.4 Discussion

5.4.1 Demographics

Patients recruited to each comparative cohort for this work were demographically matched. A smaller proportion of CAP patients had endocrine co-morbidity, of which most were either disorders affecting the thyroid or diabetes mellitus. Diabetes was identified as a risk factor for poor outcomes after COVID-19 infection, but there is no evidence to suggest that those with diabetes are more likely to contract COVID-19 (Gangopadhyay, 2020). Patients were only recruited if they were not deemed suitable for escalation beyond ward-based care (e.g. level 2 and above or for intensive care – as defined as not for invasive respiratory support). The majority of COVID-19 hospitalisations and deaths occur in non-ICU wards which highlights the importance of investigating this cohort for potential therapeutic targets (Sapey et al., 2020). In addition, early intervention at this stage may help to improve trajectories, limit clinical deterioration and patients needing care escalated to organ support.

Cellularly there were significantly higher white cell count and neutrophil differential in CAP patients compared to COVID-19, which may reflect the immune response to a bacterial infection versus viral insult (Bhuiyan et al., 2019).

Clinical scoring systems used during COVID-19 were developed as the pandemic progressed. Previously published literature suggested the CURB-65 score had poor predictive value for mortality or disease severity, with more generic scores having better correlation to patient outcomes. Whilst our patients were managed on the ward, a median 4C disease severity score of 12 (IQR 9-14) suggests that these patients are in the high-risk group, with in-hospital mortality of 31.4-34.9% (Gupta et al., 2021). This is in keeping with previous evidence suggesting the reduced accuracy of the CURB-65 score in COVID-19 infection (Ahmed et al., 2022). Median CURB-65 score of 2 (IQR 1-3) would suggest 6.8% mortality; versus the 24% observed in this cohort. However, there was significantly higher length of hospital admission for COVID-19 patients stratified by either CURB-65 or 4C score, which is likely a reflection of the component parts of the score indicating patients being more unwell. Although the in-

hospital mortality for the ward-based patients recruited did not match the predicted 31.4-34.9% with a median 4C score of 12, the one-year mortality of this COVID-19 cohort matched this with 34% mortality.

Patients were followed up as part of gathering longer term data, and to determine if there were any markers of prediction to determine those patients who may have poorer long-term outcomes. The UK ONS sample of 20,000 COVID-19 positive participants found 13.7% had persistent symptoms and self-reported long-COVID post COVID-19 infection (UK, 2023). COVID-19 follow up imaging was not robust enough for us to determine if there were any persistent radiological changes, though there was evidence of some patients with persistent lung parenchymal changes and ongoing symptoms of shortness of breath and cough.

5.4.2 Time from symptom onset to presentation

Symptom onset to admission was calculated for all recruited patients, with a significant variance in time from onset to admission. A meta-analysis of 113 COVID-19 studies showed that viral load was highest at symptom onset, with a decrease seen within one to three weeks (Walsh et al., 2020). After 2 weeks, viral RNA was undetectable. Our patient cohort was comparable to other COVID-19 studies, with a median time from symptom onset to hospitalisation of 3-10 days (Faes et al., 2020) with a shorter time for older patients. Interestingly, the longest delay in patient admission was in the younger cohort, which may reflect the stress placed by the public health initiative highlighting older adults as being more vulnerable. Our patients who presented earlier demonstrated a higher CFS, in keeping with an older age at hospital admission. These patients had more severe disease when stratified by the 4C mortality score, which may have triggered seeking medical advice earlier rather than later. A meta-analysis of seven studies showed that CFS and mortality were linearly related (Pranata et al., 2021). There were no significant differences observed in the CAP cohort depending on the length of time between symptom onset and hospital admission. CAP

patients admitted more than 7 days after symptom onset had higher levels of circulating VEGF, but this could represent prolonged untreated infection.

5.4.3 Conclusion

The recruited CAP and COVID-19 cohorts in this chapter were well demographically matched. There were some significant differences in measured white cell differential, but not specific enough to be able to determine COVID-19 infection from CAP on routine blood tests alone. However, clinical outcomes are significantly different with a different disease course, which together supports the data that established scoring systems at the beginning of the pandemic were not suitable for COVID-19 patients (Ahmed et al., 2022).

CHAPTER 6
NEUTROPHILS IN COVID-19

Parts of this chapter have been published in: *'Dysregulated neutrophil phenotype and function in hospitalised non-ICU COVID-19 pneumonia'*, KBR Belchamber, **OS Thein**, J Hazeldine, FS Grudzinska, AA Faniyi, MJ Hughes, AE Jasper, LE Crowley, KP Yip, ST Lugg, E Sapey, D Parekh, David R Thickett, A Scott; 2022; Cells; PMID: 36139476 (joint 1st author)

6.1 Introduction

Between the COVID-19 and CAP cohorts, we demonstrated subtle differences in routinely measured clinical parameters. However, clinical scoring systems currently used do not demonstrate the same sensitivity or specificity for COVID-19 infection outcomes as for CAP (Ahmed et al., 2022). This suggests the underlying disease process and host immune response is different to that of a stereotypical CAP. Dysregulated host-immune responses are thought to be the main driver of COVID-19 disease (Dorward et al., 2021). Neutrophils play an important role in early inflammation. Distinct phenotypes have been described such as in sepsis, where altered migration and delayed apoptosis cause impaired pathogen clearance and poor clinical outcomes (Patel et al., 2018).

To determine if COVID-19 infection leads to production of a distinct neutrophil phenotype with an associated unique disruption to effector function, we compared samples obtained from COVID-19 patients to age matched controls (AMC) and patients with diagnosed community acquired pneumonia (CAP). The effect of altered neutrophil function on patient overall outcomes was then examined by comparing the clinical data to effector neutrophil function.

6.1.1 PI3K inhibition

To investigate potential mechanistic causes of altered neutrophil function, investigation into inhibition of the phosphoinositide 3-kinase (PI3K) pathway through inhibitory molecules was examined. PI3Ks are a family of enzymes which have a role in overall physiological homeostasis and have been studied as a therapeutic target in several diseases including cancer (Bilanges et al., 2019, Fruman et al., 2017, De Santis et al., 2019). Mammals have eight isoforms which can be subdivided into three classes (Domin and Waterfield, 1997). Class I PI3Ks lead to the generation of 3-phosphoinositide lipids, which in turn cause activation of signal transduction cascades through regulation of downstream membrane receptor signalling (Hawkins and Stephens, 2015, Vanhaesebroeck et al., 2010). Overactivation of PI3K has

been described in cancers (De Santis et al., 2019). Class II PI3Ks affect intracellular membrane dynamics and membrane traffic, leading to a direct effect on intracellular signalling (Braccini et al., 2015, Maffucci et al., 2005). There is only a single Class III PI3K (VPS34) which is involved with endosomal sorting, phagocytosis and autophagy (Backer, 2016, Ktistakis and Tooze, 2016).

PI3K signalling plays a key role in neutrophil function, including neutrophil migration. PI3K directs phosphoinositol 3,4,5-triphosphate (PIP3) to the leading edge of the cell following G-protein coupled receptor activation to allow for cytoskeletal mobilisation for movement (Stephens et al., 2002, Hannigan et al., 2004). Animal studies with PI3K γ -/- mice demonstrated no production of PIP3 and failure of the neutrophil oxidative burst and migration (Hirsch et al., 2000).

PI3K α , β , γ , and δ isoforms exist across the three classes of PI3K described by Waterfield, all of which are expressed by neutrophils (Fortin et al., 2011). These isoforms can be inhibited by a variety of available molecules which have varying specificity for each isoform. No PI3K δ isoforms have been identified in Class II to date, and PI3K γ has been described with a significant role in G-protein couple receptor regulation of cell signalling in health and disease (Lopez-Ilasaca et al., 1997, Bondeva et al., 1998). PI3K blockade prevents PIP3 accumulation to the leading edge of the cell, therefore disrupting cytoskeletal mobilisation.

6.1.2 Effect of selected pharmacological agents on neutrophil function

At the time of experimentation, focus on increasing the number of treatment options for patients with COVID-19 was key. In parallel with investigating potential disruption to the PI3K pathway, investigation of repurposing therapeutics with neutrophil activity was carried out to determine if these were potential viable treatment options.

Brensocatib is a selective inhibitor of dipeptidyl peptidase-1 (DPP-1/ cathepsin C). DPP-1 is involved with the activation of neutrophil serine proteases (NSPs), including NE, PR3 and cathepsin G. As described in Chapter 1.2.1, these enzymes are required for ease of neutrophil migration through the extracellular space to the site of infection or injury. These NSPs are held within azurophilic granules which fuse with the phagosome to form the phagolysosome, and are released during NETosis (Korkmaz et al., 2010). Uptake of NETs as part of the efferocytosis process is shown to promote type 1 interferon generation through NE mediating signalling (Apel et al., 2021). In chronic lung diseases such as non-cystic fibrosis bronchiectasis, neutrophil accumulation leads to increased serine protease activity and a state of chronic inflammation. Increased NE activity is related to a decline in lung function and mortality in bronchiectasis due to the increased degradation of the extracellular matrix by NSPs (Chalmers et al., 2017). Blockade of DPP-1 by brensocatib in these patients was shown to decrease the activity of these serine proteases, leading to normal levels of activation after a period of four weeks (Cipolla et al., 2023).

NE is a key NSP in azurophilic granules as part of migration through host tissues as well as for anti-microbial properties when attached to the NET backbone in NETosis. Specific NE inhibitors have been developed to determine if they have a role in the treatment of lung disease. NE inhibitors KRP-109 and sivelestat have been shown in animal models of lung infection to decrease inflammation histopathologically and enhance the clearance of bacteria respectively (Yamada et al., 2011, Hagio et al., 2008). In an animal acute lung injury model induced by LPS, addition of sivelestat showed a decrease in neutrophil migration to the lung parenchyma (Yasui et al., 1995). NE activation is DPP-1 dependent, and thus would be implicated in the mechanism of action of brensocatib. However, as other NSPs are activated by DPP-1, specific inhibition of NE activity leading to decreased neutrophil migration may help to prevent excessive damage.

Investigation into the use of brensocatib in non-cystic fibrosis bronchiectasis has progressed through phase 2 trials between placebo, and two different doses of brensocatib (10mg and 25mg) (Chalmers et al., 2020). This demonstrated an increased time to first exacerbation and

biochemically decreased NE activity in sputum samples. The use of brensocatib in COVID-19 patients has been investigated as part of the STOP-COVID-19 trial (ISRCTN30564012). Primary end point was clinical status at day 29 after drug administration. Compared to placebo, patients on brensocatib had worse clinical outcomes, with a 28-day mortality rate of 15% compared to 11%. Blood neutrophil NSP activity was reduced suggesting drug delivery efficacy. The beneficial effect of DPP-1 inhibition on reducing NSP activity affecting NETosis and migration may be masked by the wider implications of DPP-1 on the innate immune response (including cytotoxic T cells, natural killer cells and mast cells).

Metoprolol is a selective β1-receptor blocker, which has been used clinically since 1982 in the treatment of cardiovascular disease, including but not limited to: hypertension, supraventricular tachycardias and migraine prevention. There is evidence of the effect of metoprolol in affecting neutrophil function. In a chemotaxis model, neutrophil migration after formyl peptide-stimulation was inhibited in a dose dependent manner after metoprolol treatment. ROS production after PMA stimulation was decreased after metoprolol treatment, and along with migration affected neutrophils in a time dependent manner, with the greatest reduction in chemotaxis noted after 30 minutes of incubation with metoprolol (Dunzendorfer and Wiedermann, 2000b). Disruption of measured ROS production and protein kinase C inhibition may help in reducing elevated migration seen in our cohort through reduced downstream NADPH (nicotinamide adenine dinucleotide phosphate). Clinically, metoprolol administration post myocardial infarction has been shown to reduce the size of the infarcted tissue, in a neutrophil dependent manner. Depletion of neutrophils abrogated the effects of metoprolol administration post myocardial infarction in humans (García-Prieto et al., 2017).

Based on the ex vivo and clinical data on metoprolol effects on neutrophil function, a small randomised control trial of patients with severe COVID-19 on invasive mechanical ventilation (MADRID-COVID trial) (Clemente-Moragón et al., 2021). Compared to the placebo controls, there was reduced NETosis and Cit-H3 in those treated with metoprolol. In BAL samples from these patients, there was a reduction in measured MCP-1, a chemokine shown to promote fibrosis in ARDS (Rose Jr et al., 2003). Clinically, patients on metoprolol had improved

oxygenation compared to placebo. Reduced neutrophil recruitment and activation is thought to be related to the improved outcomes demonstrated.

A specific, reversible NE inhibitor AZD9668/ MPH966 was developed as part of a treatment strategy for chronic obstructive pulmonary disease and α1AT deficiency. The inhibitory effect achieved by AZD6998 is higher than that observed in silvelestat and has similar effects in animal models of pulmonary inflammation (Stevens et al., 2011).

Neutrophil functions disrupted by COVID-19 infection in comparison to AMC and CAP patients may be a contributing factor to the different clinical picture observed in **Chapter 5**. Restoration of expected neutrophil function in patients with COVID-19 infection may lead to improved clinical outcomes and less severe disease. The inhibitors and treatments discussed here for further investigation are medications which have an established record of use in modulating neutrophil function and are suitable for patient treatment. In addition, efficacy of these molecules may provide insight into potential mechanisms of neutrophil alterations in COVID-19. This was not designed as a comprehensive investigation of compounds which might directly impact neutrophil functions as many would not be suitable for human use.

Early therapeutic and observational studies of COVID-19 focused on the most critically ill patients to prevent death. However, only 12.9% of patients admitted to hospital with COVID-19 require intensive care admission (Sapey et al., 2020). The majority of patients are treated on standard hospital wards and it is here that most in-hospital mortality from COVID-19 occurs. Patients initially admitted to hospital may not require intensive care support clinically or may have co-morbidities which would preclude admission. Non-ICU patients can then further deteriorate to require ICU admission or illness can lead to death. Therefore, understanding how to prevent deterioration in this cohort is important. Sepsis studies have shown that cellular function is more therapeutically manipulable during early disease which highlights the key role timing plays in disease intervention.

We hypothesised that COVID19 infection causes neutrophil dysfunction that is different to that seen in bacterial CAP and that these cellular alterations in function may explain the differences seen in clinical phenotype.

6.2 Aims of Chapter 6

1. To determine alterations to neutrophil function from cells isolated from COVID-19 patients compared to AMC and CAP patients.
2. To explore any correlations between neutrophil function and clinical phenotype in this cohort.
3. To investigate a potential mechanism of neutrophil dysfunction observed in this cohort of patients through use of therapeutic molecules.
    a. To determine if blockade of the PI3K pathway will restore function to neutrophils isolated from COVID-19 patients.
    b. To determine if there is a direct or indirect effect of the inhibitor addition to neutrophil effector functions.

6.3 Neutrophil effector functions

Experiments in the following results were carried out using the methods described in **Chapter 3.**

6.3.1 Phagocytosis

Phagocytosis of labelled *S. pneumoniae* by neutrophils isolated from COVID-19 patients demonstrated was significantly reduced compared to both AMC (MFI 8.0 (4.2) vs. 6.6 (2.6) COVID-19, p=0.0332) and CAP (MFI 9.55 (23.7), p-=0.0332 vs COVID-19, **Figure 6.1**. There was no significant difference in percentage of cells phagocytosing bacteria.

Both cROS and n/mROS generation were measured in neutrophils at rest and after phagocytosis stimulation with labelled *S. pneumoniae*. cROS was elevated after phagocytosis in AMC (median MFI (Q3-Q1): 46.8 (28) baseline vs. 64.9 (51) 30 minutes, p=0.0091), CAP patients (median MFI (Q3-Q1): 285 (211) baseline vs. 357 (260) 30 minutes, p=0.038), and COVID-19 patients (median MFI (Q3-Q1): 44.1 (35) baseline vs. 65.3 (60) 30 minutes, p=0.134, **Figure 6.1C**). There was increased baseline cROS levels in CAP patients and after 30 minutes of phagocytosis stimulation compared to AMC (p<0.0001, **Figure 6.1C**)

Similarly, n/mROS was elevated after phagocytosis in AMC (median MFI (Q3-Q1): 21.8 (21) baseline vs. 32.0 (38), p<0.0001), but not in COVID-19 patients (median MFI (Q3-Q1): 18.9 (12) baseline vs. 21.2 (12), p=0.0329) or CAP patients (median MFI (Q3-Q1): 22.2 (21) baseline vs. 26.7 (17), p=0.989). At rest there was no significant difference in n/mROS production between all three groups prior to stimulation, but there were reduced n/mROS production after phagocytosis in CAP (p=0.0101) and COVID-19 (p<0.0001) cohorts compared to AMC (**Figure 6.1D**).

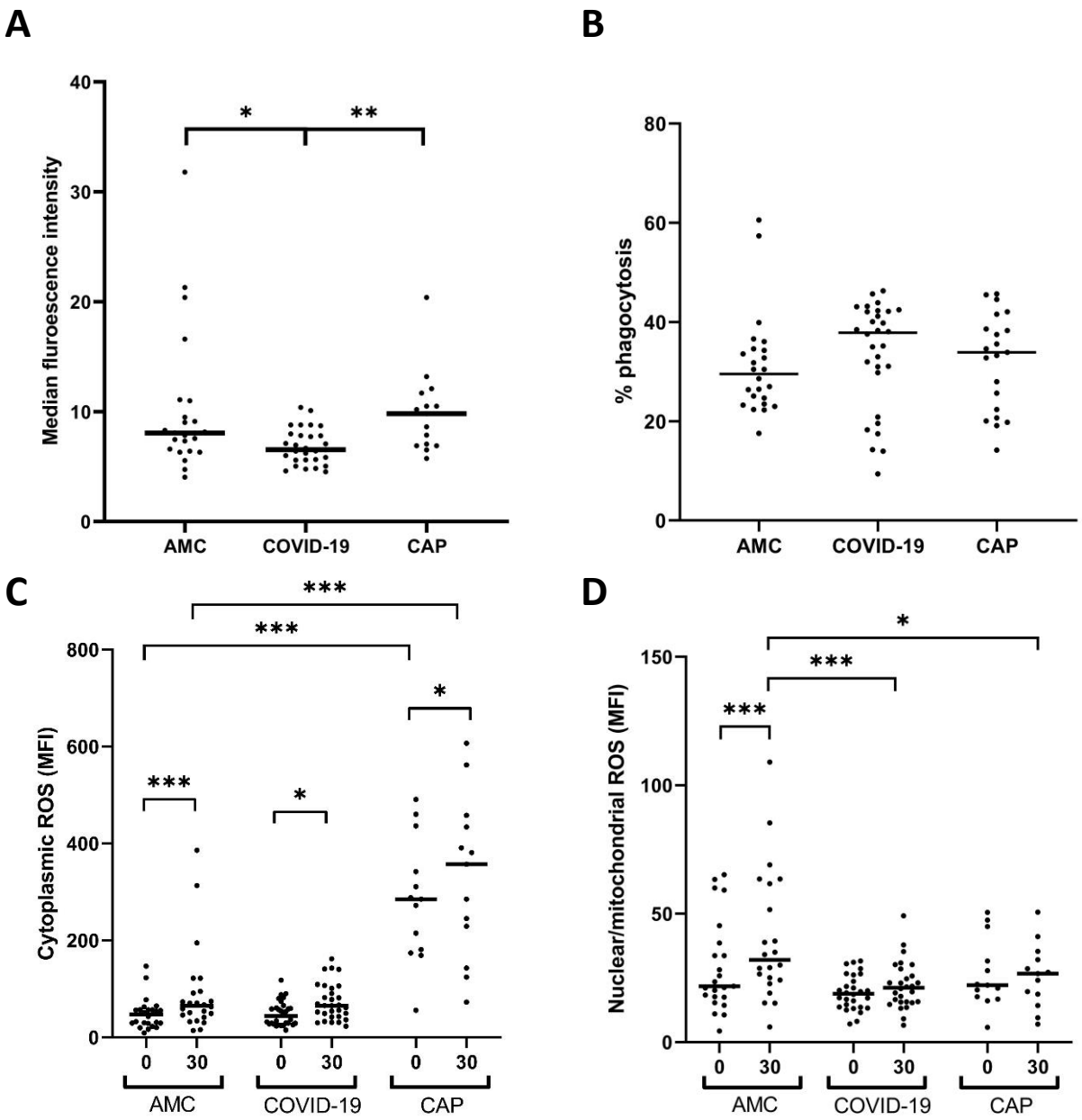

Figure 6.1 Phagocytosis assays carried out on neutrophils from AMC, COVID-19 and CAP participants. Results displayed as full data spread with median. Statistical significance calculated using a one-way ANOVA for multiple comparisons. **A**. Neutrophil phagocytosis of opsonised labelled *S. pneumoniae* after a 30-minute incubation. Data displayed as median fluorescence intensity (MFI) of positive neutrophils. AMC (n=24), COVID-19 (n=30), CAP (n=15) vs. COVID-19 (n=30). **B**. Neutrophil phagocytosis of opsonised labelled *S. pneumoniae* after a 30-minute incubation. Data displayed as percentage of cells phagocytosing. AMC (n=24) COVID-19 (n=30), CAP (n=21). **C**. Cytoplasmic ROS (cROS) generation at 0 minutes (baseline) and after 30-minute phagocytosis with opsonised labelled *S. pneumoniae*. AMC (n=24), CAP (n=13) COVID-19 (n=30). **D**. Nuclear/ mitochondrial ROS (n/mROS) generation at 0 minutes (baseline) and after 30-minute phagocytosis with opsonised labelled *S. pneumoniae*. AMC (n=24), CAP (n=13) COVID-19 (n=30). *p≤0.05, **p≤0.01, ***p≤0.001, ****p≤0.0001

6.3.2 Neutrophil migration

Neutrophils from COVID-19 patients demonstrated increased transwell migration towards chemoattractant CXCL8 compared to AMC (n=19) (median fold change of neutrophils migrated compared to vehicle control (Q3-Q1): 12.15 (51.4) AMC vs. 40.63 (115.2) COVID-19, p=0.0332). Increased neutrophil migration from COVID-19 patients compared to CAP (n=16) (median fold change of neutrophils migrated compared to vehicle control (Q3-Q1): 9.55 (23.7) CAP vs. 40.63 (115.2) COVID-19, p=0.0332, **Figure 6.2**).

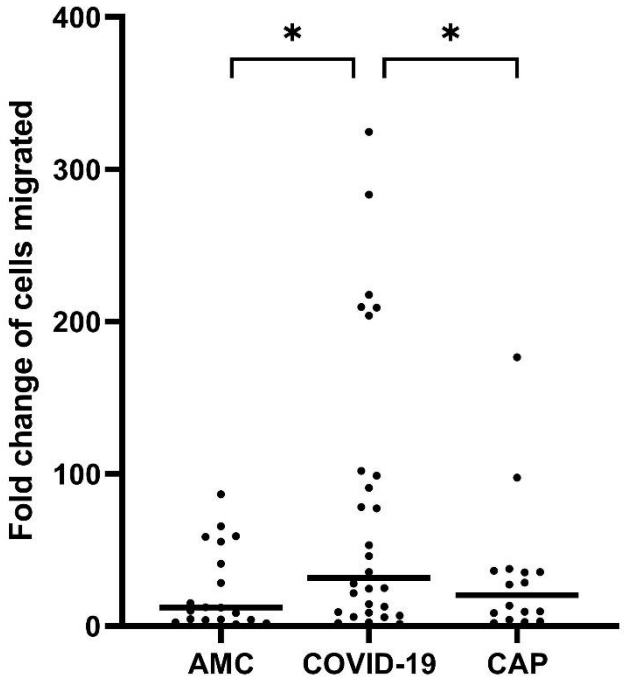

Figure 6.2 Neutrophil migration through a transwell membrane towards CXCL8, compared between age matched controls (AMC), COVID-19 patients and community acquired pneumonia (CAP) patients. Fold change in number of neutrophils shown compared to vehicle control (RPMI). AMC (n=18) vs. COVID-19 (n=28), CAP (n=16). Results displayed as full data spread with median. Kruskal-Wallis test used for statistical analysis. *p≤0.05, **p≤0.01, ***p≤0.001, ****p≤0.0001.

6.3.3 NETosis

At rest, there was no change in NET production between AMC, CAP and COVID-19 patients. Post stimulation with PMA, there was increased NET production in COVID-19 patients compared to AMC and CAP (median fold change after PMA (Q3-Q1): AMC 137.4 (5.996), COVID-19 164 (8.732), CAP 126.5 (6.815); AMC vs COVID-19 p=0.008, CAP vs COVID-19 p=0.0005, **Figure 6.3A**). Cell free DNA (cfDNA) was measured in the supernatants of samples obtained from all 3 cohorts. After PMA stimulation, there was a larger increase in cfDNA detected in COVID-19 patient samples compared to AMC (median fold change in absorbance of neutrophils stimulated with PMA vs. vehicle control (Q3-Q1): 1.29 (0.32) AMC vs. 1.53 (1.66) COVID-19, p=0.0394, **Figure 6.3B**).

COVID-19 patients presented with higher plasma cfDNA compared to AMC at time of admission to hospital (median cfDNA (Q3-Q1): AMC 621ng/ml (1324) vs. cfDNA COVID-19 1071ng/ml (856) COVID-19, COVID-19 vs AMC p=0.0396, vs CAP p=0.0322, **Figure 6.3C**). For the patients who were followed up as inpatients between day 3 and 5, this increased cfDNA persisted (p=0.0186, Figure. 3D). CAP patients demonstrated higher levels of plasma cfDNA compared to AMC (1220ng/ml (686), p=0.0322).

To confirm the cfDNA was a result of neutrophil release of NETs, plasma samples from patients were analysed for the presence of citrullinated-histone 3 (CitH3) protein. This is present on the DNA backbone of NETs (Liu et al., 2012). Western blotting demonstrated the presence of CitH3 in 6 of 8 analysed samples (**Figure 6.4**)

Serum DNase acts to breakdown NETs. Enzyme activity was measured using NETs produced from healthy donors. Serum DNase activity was lower in COVID-19 patients at hospital admission compared to AMC and CAP patients (median % degradation (Q3-Q1): AMC 88.4% (93), COVID-19 12.8% (49), CAP 77.45% (34), COVID-19 vs AMC p<0.0001, AMC vs CAP, p<0.0001, **Figure 6.3D**).

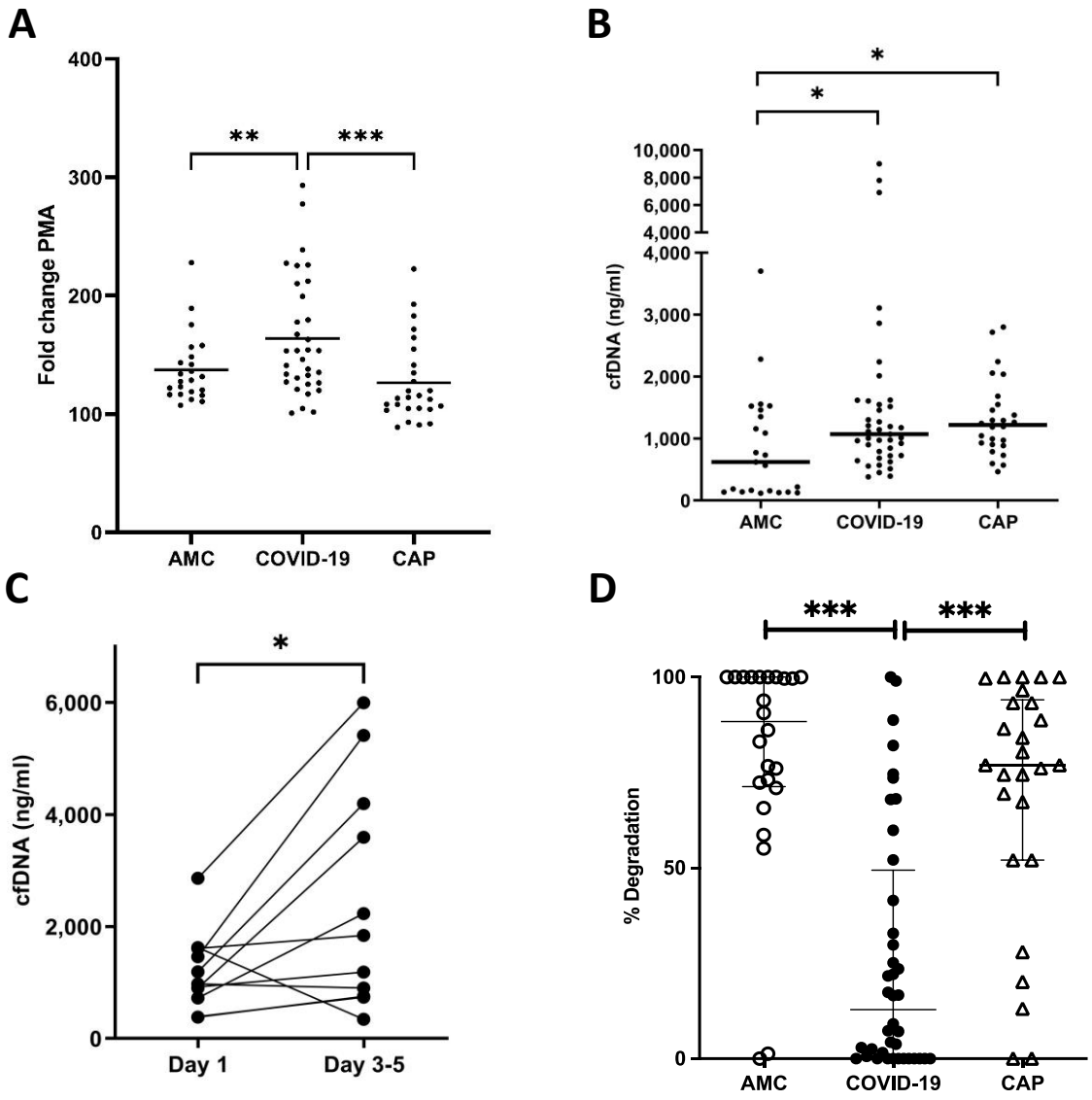

Figure 6.3 NETosis in COVID-19 after stimulation with PMA. Results displayed as full data spread with median, Kruskal-Wallis test used for multiple comparisons and Wilcoxon paired rank signed test for paired samples. **A**. NET release by neutrophils stimulated with PMA for 3 hours, measured as absorbance of cfDNA stained with Sytox green. Data shows fold change in absorbance of PMA stimulated neutrophils compared to vehicle control. (AMC n=26, COVID-19 n=39, CAP n=26). **B.** Plasma cfDNA levels measured by fluorometry (AMC n=23, COVID-19 n=39, CAP n=26). **C.** Comparison of cfDNA levels measured by fluorometry in COVID-19 (n=10) on day 1 and on day 3-5. **D.** DNA degradation by serum NETs (AMC n=23, COVID-19 n=39, CAP n=26). *p≤0.05, **p≤0.01, ***p≤0.001, ****p≤0.0001

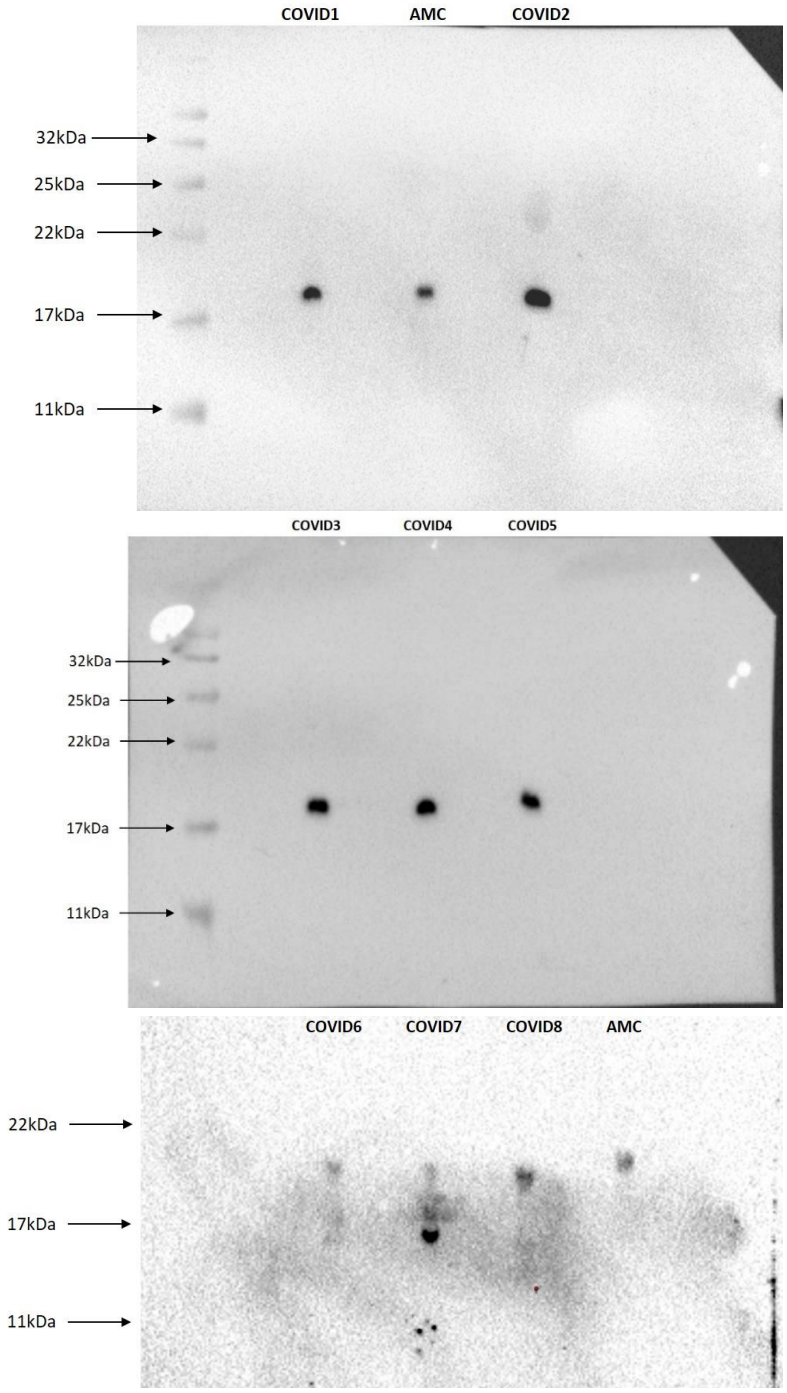

Figure 6.4 Western blot detection of CitH3 in plasma samples from COVID-19 patients and age matched controls (AMC). Plasma samples were electrophoresed and blotted for CitH3 (Abcam). Molecular weight markers are indicated with arrows.

6.3.4 Circulating inflammatory mediators

Circulating inflammatory mediators were measured in AMC, CAP and COVID-19 patients. Compared to AMC, there were elevated levels of IL-6 (COVID-19 p=0.0296, CAP p=0.0106, **Figure 6.5A**), VEGF (COVID-19 p<0.0001, CAP p=0.0032, **Figure 6.5B**), and sTNFRI (COVID-19 p<0.0001, CAP p<0.0001, **Figure 6.5C**). GM-CSF was decreased in CAP compared to AMC (p=0.0066) and between COVID and CAP patients (p=0.0187), **Figure 6.5D**. There were increased MPO levels in COVID-19 compared to AMC and CAP patients (p<0.0001, **Figure 6.5E**).

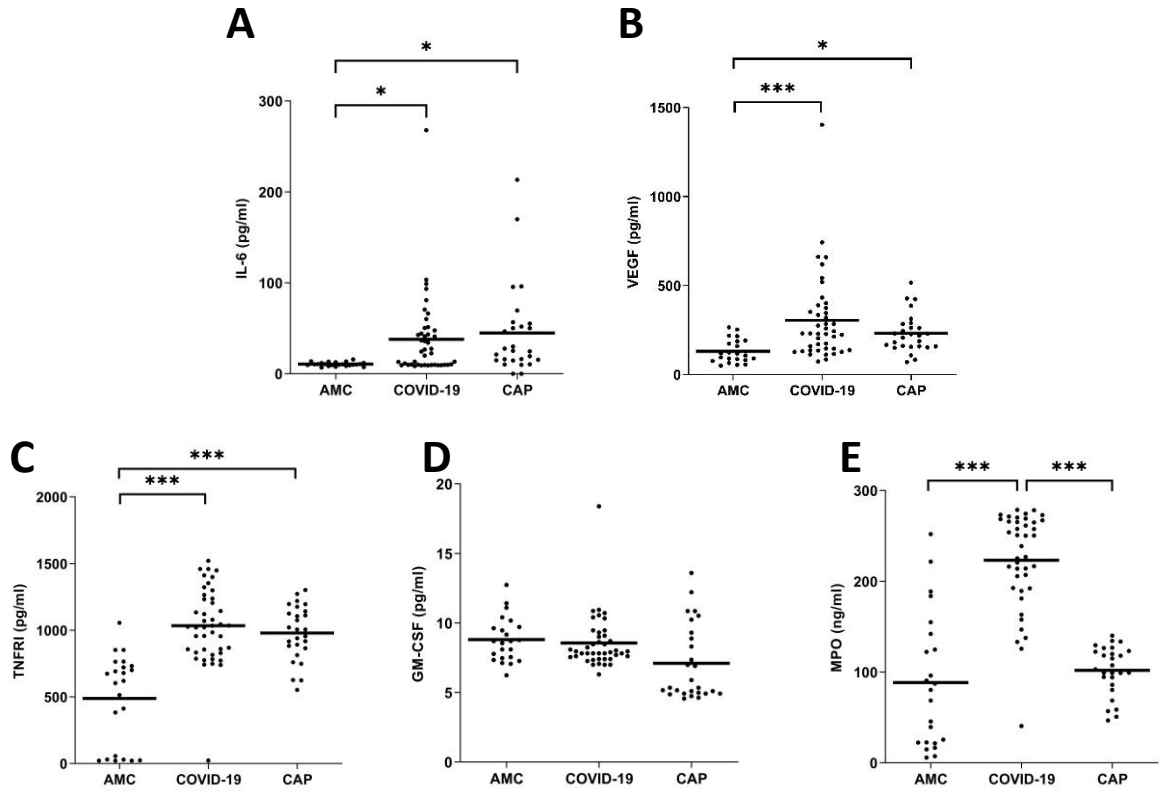

Figure 6.5 Circulating inflammatory markers in COVID-19 as measured by serum ELISA, COVID-19 n=41, CAP n=26, AMC n=23. Results displayed as mean with full data spread. One-way ANOVA used for statistical analysis**. A.** IL-6 **B.** VEGF **C.** sTNFR1 **D**. GM-CSF. **E.** MPO. *p≤0.05, **p≤0.01, ***p≤0.001, ****p≤0.0001

6.3.5 Surface marker phenotype

We investigated the expression of cell surface markers on neutrophils to determine if there was correlation with the observed functional changes. Comparisons were made with the recruited AMC and CAP cohorts. **Table 6.1** shows percent of receptor expression as well as MFI values for each.

Receptors	% Expression				MFI			
	COVID (n=34)	AMC (n=26)	CAP (n=16)	p value	COVID (n=34)	AMC (n=26)	CAP (n=16)	p value
CD10	95.3 (13.6)	94.3 (11.52)	74.7*# (60.6)	*<0.0006 #<0.0006	836 (518)	669 (511)	701 (486)	0.304
CD11b	67.8*$ (43.9)	81.6 (15.25)	83.9 (23.8)	*0.0014 $0.046	40*$ (223)	399 (331)	1701* (1268)	*0.0026 $<0.0001 *<0.0001
CD54	71.3*$ (21.2)	26.2 (37.0)	6.6 (10.9)	*<0.0001 $<0.0001	73 (58)	33 (48)	147*# (77)	*0.0001 #0.0012
CD62L	31.0 (15.3)	23.3 (58.8)	49.9 (41.4)	0.384	94 (121)	68 (400)	723*# (519)	*0.0005 #<0.0001
CXCR2	100 (0.2)	99.9 (0.1)	98.5 (1.6)	0.741	2031 (1600)	2482 (1415)	2839 (2839)	0.439
CXCR4	96.7 (9.07)	93.9 (16.4)	54.3*# (35.0)	*<0.0001 #<0.0001	1724$ (4177)	1917 (4039)	1090 (1376)	$0.028
CD66b	99.8 (0.3)	99.7 (0.5)	97.6 (1.6)	0.298	186 (161)	324 (367)	1631*# (1493)	*<0.0001 #<0.0001
CD11c	99.9 (1.05)	99.2 (2.9)	76.1*# (64.5)	*<0.0065 #<0.0001	1148 (670)	392 (2120)	4197*# (6040)	*<0.0001 #<0.0001
PD-L1	98 (27.9)	63.8 (32)	8.7*# (12.9)	*<0.0001 #<0.0001	70*$ (132)	193 (210)	524* (264)	*0.006 $<0.0001 *0.0006
HLA-DR	46.8*$ (38)	24.7 (29)	1.9*# (1.8)	*0.0024 #<0.0001 $0.0010	-122 (510)	-44 (387)	-22.5 (339)	0.6457

Table 6.1 Percentage of cells expressing and MFI of isolated neutrophil cell surface markers as measured by flow cytometry in AMC (n=26), COVID-19 patients (n=34) or CAP patients (n=16). Data displayed as median (IQR (Q3-Q1)). Data analysed by individual One Way ANOVA with multiple comparisons. Green square indicates significance where * vs. AMC, # vs. COVID-19 and $ vs. CAP.

There was a reduction in neutrophil expression of the activation marker CD11b (AMC 82% (15) vs. COVID-19 68% (44), p=0.0014), and its surface expression (median AMC MFI (Q3-Q1): 399 (331) vs. COVID-19 40 (223), p=0.0026,) in COVID-19 compared to AMC. There was a reduction in CD11b expression in COVID-19 patients compared to CAP patients (median CAP % expression (Q3-Q1): 83.9% (24), p=0.046; CAP MFI:1701 (1268), p<0.0001,).

There was an increased percentage of neutrophils expressing CD54, a marker of reverse transmigration in COVID-19 compared to both AMC and CAP neutrophils (median expression (Q3-Q1): AMC 26% (37) vs. COVID 71% (21), p<0.0001; vs. CAP 7% (11), p<0.0001,). There was increased expression HLA-DR, a major histocompatibility complex (MHC)-II cell surface receptor which interacts with the T-cell receptor (TCR), on COVID-19 compared to both AMC and CAP neutrophils (median expression (Q3-Q1): COVID-19 47% (38), vs. AMC 25% (29), p=0.0024; vs. CAP 1.9% (1.8), p<0.0001,)

We observed no change in the percentage of neutrophils expressing or the surface expression per neutrophil of CD66b, CD62L, CD10, CXCR2, CXCR4, orCD11c between AMC and COVID-19. PDL1 surface expression per neutrophil was significantly reduced in COVID-19 patients compared to AMC and CAP (median MFI (Q3-Q1): AMC 193 (210) vs. COVID-19 70 (132), p<0.006; vs. CAP 524 (264), p<0.0001,), but there was significantly increased percentage of neutrophils expressing PDL1 (median expression (Q3-Q1): COVID-19 98% (28) vs. AMC 8.7% (13), p<0.0001,).

6.3.6 Day 3-5 follow-up

6.3.6.1 Clinical phenotype

12 patients were followed up with clinical data, clinical biochemistry, and neutrophil function as they remained in-patients and consented to follow-up (n=12). There was a significant reduction in NEWS score for patients who remained inpatients at day 3-5 (D3-5) compared to day 1 (baseline), (median baseline NEWS2 7.0 (6-7.8), D3-5 4.0 (3.3-5.8), p=0.0098, **Figure 6.6A).**

There was a significant reduction in 4C score at follow-up (median baseline 4C 14.0 (13.3-15.8), D3-5 12.5 (10.0-14.0), p=0.0068, **Figure 6.6B**). There was no increase in 4C for patients that did not survive. There was no significant difference in vitamin D levels, NLR or CRP for patients followed up, **Figure 6.6C, D, E**. Other parameters were not indicated clinically for repeat measurement at D3-5, e.g. D-dimer.

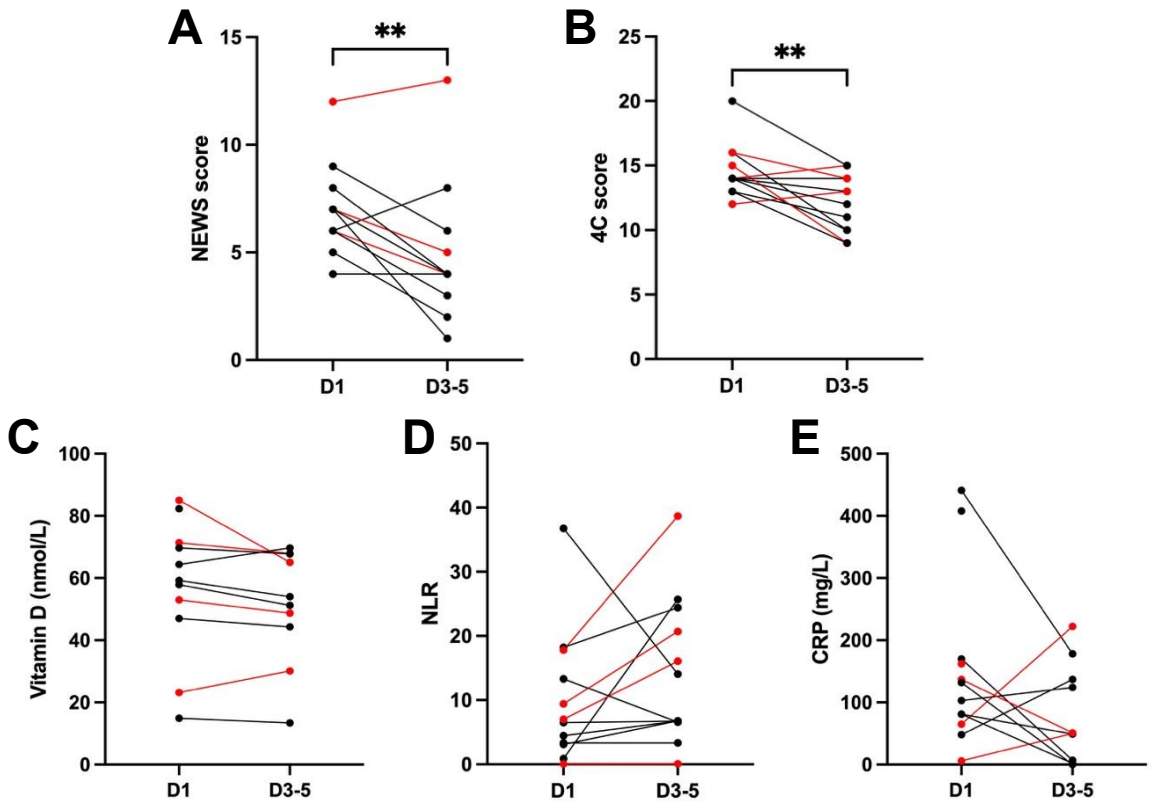

Figure 6.6 Serial changes in clinical phenotype for COVID-19 patients followed up at day 3-5 after recruitment, paired samples n=12, except CRP D3-5 n=10 and vitamin D baseline (D1) n=11, as not deemed necessary for repeat clinically. Red lines and dots indicate patients who did not survive hospital admission. Wilcoxon rank paired statistical analysis carried out. **A.** NEWS **B.** 4C score **C.** Vitamin D **D.** Neutrophil lymphocyte ratio (NLR) **E.** CRP . *p≤0.05, **p≤0.01, ***p≤0.001, ****p≤0.0001

6.3.6.2 Neutrophil function

There was no significant difference in phagocytic capacity at D3-5 compared to baseline in terms of MFI or % phagocytosis, **Figure 6.7A, B**. n/mROS production after PMA stimulation was not significantly different between D3-5 and baseline, but at D3-5 there was a greater but not significant difference in cROS production compared to at D1, **Figure 6.7C, D**.

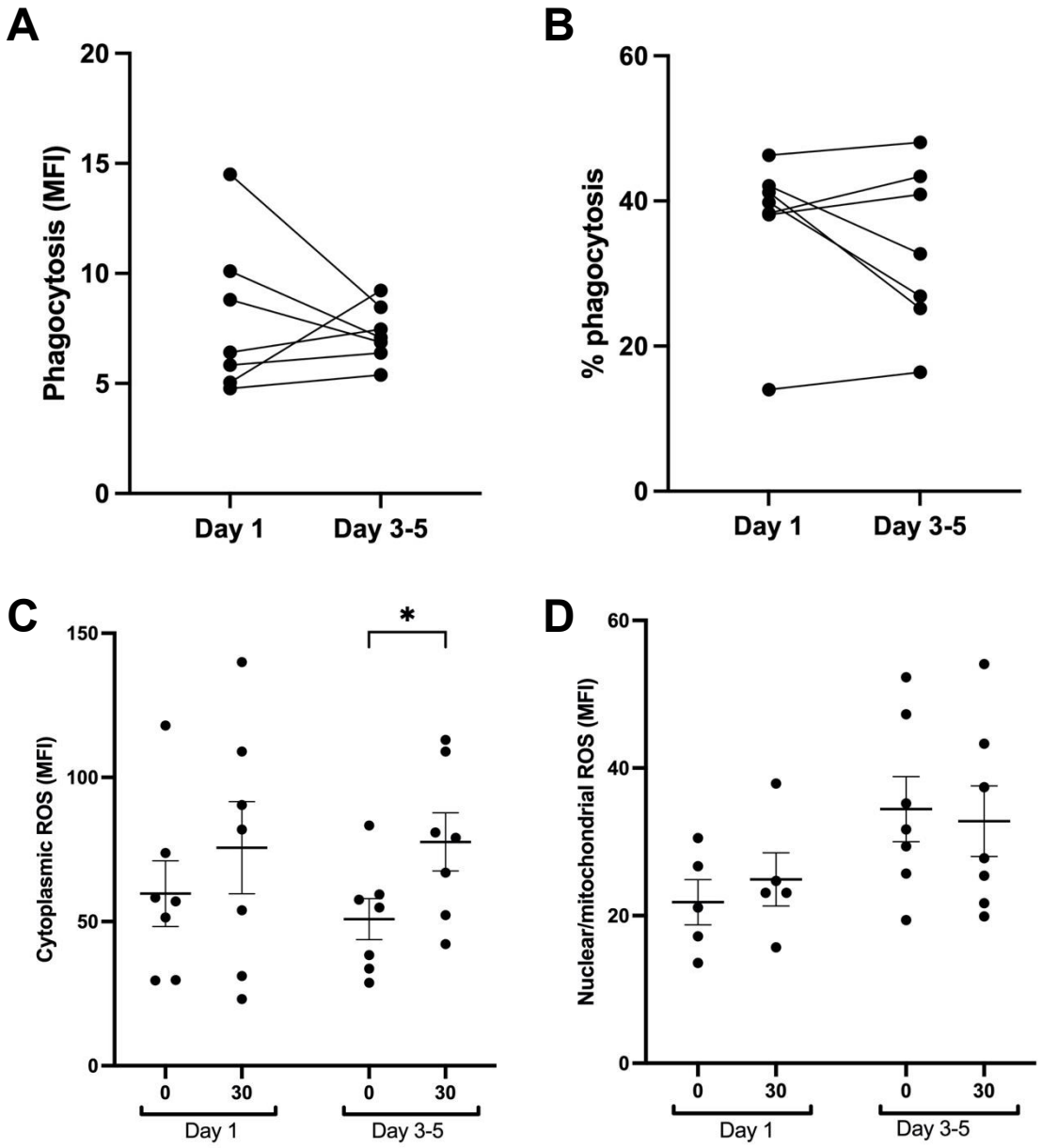

Figure 6.7 Neutrophil phagocytosis compared between baseline (Day 1) and follow-up (Day 3-5) of labelled *S. pneumoniae* after 30 minutes, n=7. Results displayed as median (IQR). Wilcoxon matched pairs signed rank test used for statistical significance as not normally distributed. **A.** phagocytosis MFI **B.** percentage of cells undergoing phagocytosis. **C.** cROS production after 30 minutes phagocytosis. **D.** n/mROS production after 30 minutes phagocytosis. *p≤0.05, **p≤0.01, ***p≤0.001, ****p≤0.0001

There was no significant difference in neutrophil migration between baseline and D3-5, **Figure 6.8A**. Serum cfDNA was significantly increased at D3-5 compared to baseline (median cfDNA D1 974 ng/mL (722.6-1609), D3-5 1841 ng/mL (752.7-4196), p=0.0186, **Figure 6.8D**). There were no significant changes to NETosis or DNase activity for patients followed up at D3-5, **Figure 6.8B, C**.

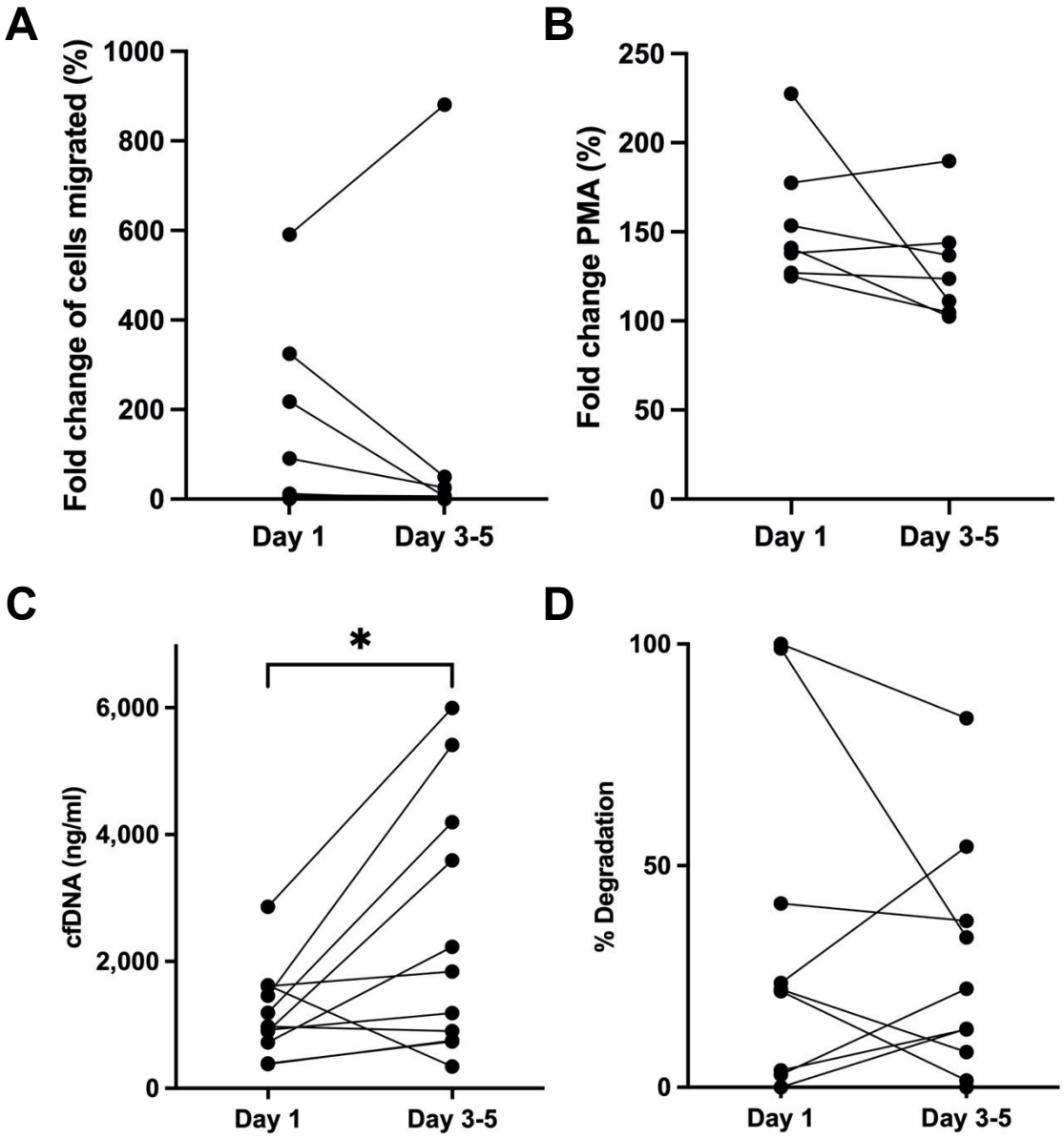

Figure 6.8 Neutrophil transwell migration and NETosis from COVID-19 patients compared between baseline (Day 1) and follow-up (Day 3-5), n=9, Wilcoxon matched-pairs rank test carried out for statistical analysis as not normally distributed. **A.** Neutrophil transwell migration **B.** Fold change in NET formation after stimulation with PMA for 3 hours **C.** Serum cfDNA **D.** DNase activity

6.3.6.3 Circulating inflammatory mediators

There were no significant differences in IL-6, VEGF, sTNFR1, GM-CSF or MPO for patients followed up at day 3-5 after hospital admission, **Figure 6.9**.

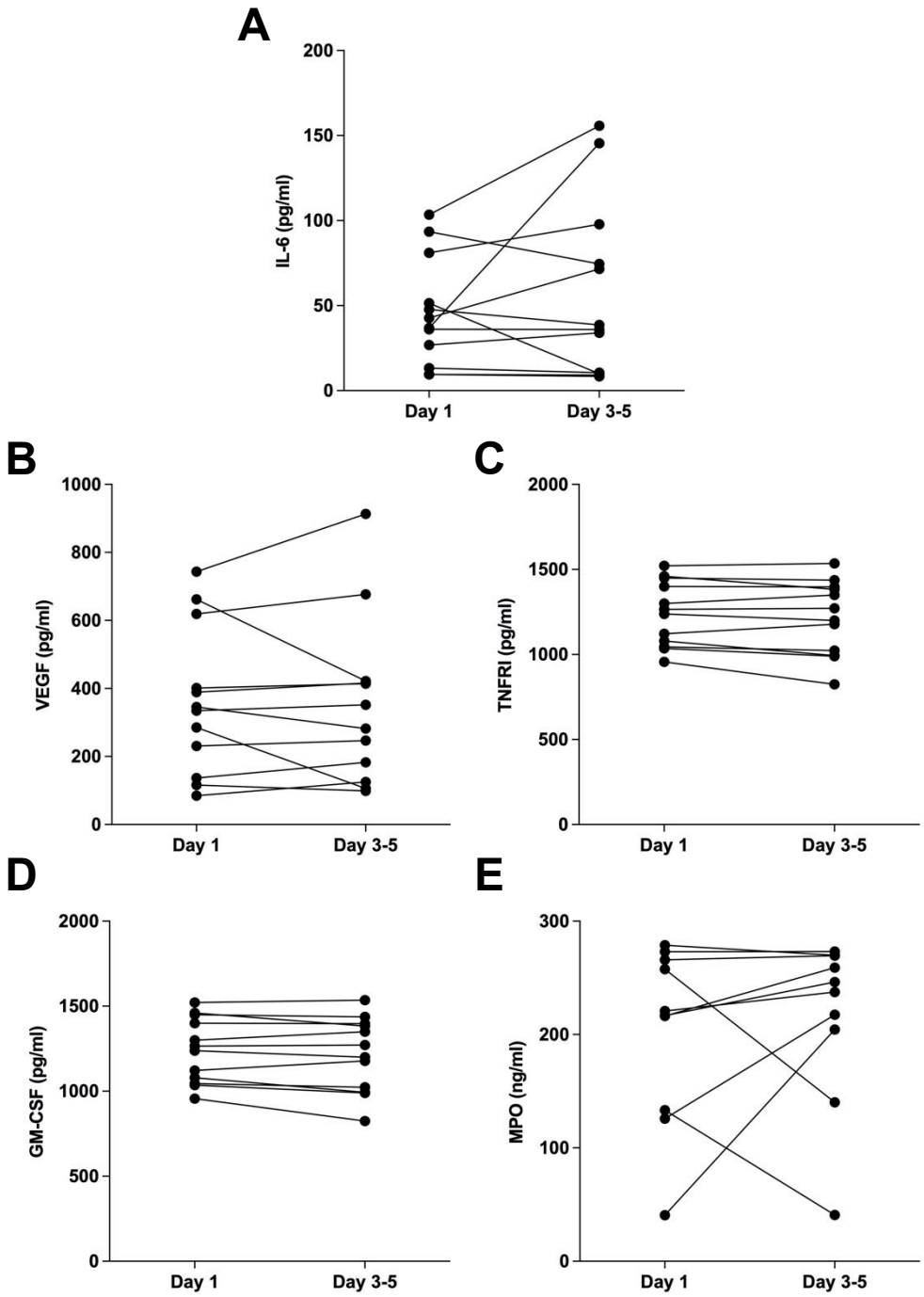

Figure 6.9 Measured circulating inflammatory mediator expression from lithium-heparin serum taken at Day 1 compared to Day 3-5 after COVID-19 admission for **A.** IL-6, **B**. VEGF, **C.** sTNFR1, **D.** GM-CSF, **E.** MPO. Samples are paired, analysed by ELISA, n=12 except for MPO n=10. Wilcoxon matched pairs-rank test carried out for statistical analysis as data not normally distributed.

6.3.6.4 Surface marker phenotype

There was a decrease in CXCR2 expression (median baseline CXCR2 MFI (Q3-Q1): 1960 (1601), D3-5 1126 (1262), p=0.0322, **Table 6.2**) and a significant increase in CXCR4 expression (median baseline CXCR4 MFI (Q3-Q1): 1785 (3951), D3-5 10248 (16483), p=0.0273, **Table 6.2**) between baseline and D-35 follow-up. Surface marker expression assays were not able to be carried out on all patient samples.

Receptors	MFI		
	D1 (n=11)	D3-5 (n=11)	p value
CD10	96.7 (7.0)	96.2 (24.2)	0.0229
CD11b	33.5 (68.3)	21.0 (97.9)	0.2475
CD54	76.9 (85.4)	45.0 (69.9)	0.1457
CXCR2	1960 (1601)	1126 (1262)	0.0322
CXCR4	1785 (3961)	10248 (16483)	0.0273
CD11c	1258 (1218)	1327 (1729)	0.9705

Table 6.2 Median fluorescent intensity (MFI) of isolated neutrophil cell surface markers as measured by flow cytometry compared between D1 and D3-5 paired samples (n=11). Data displayed as median (IQR). Data analysed by paired t-test. Green square indicates significance.

6.4 Relationship of clinical phenotype to function

6.4.1 Clinical outcomes

Clinical outcomes for patients are important to determine if neutrophil function influences course of patient admission. In-patient hospital mortality and length of stay were used as clinical endpoints. Median length of stay was 5.5 days (3.0-12.0) in the COVID-19 cohort. When compared to neutrophil effector functions, there was no significant difference in the % phagocytosis or transwell migration for those patients that survived or died, across the COVID-19 or CAP cohorts. There was no significant difference in NETosis or levels of serum cfDNA after PMA stimulation between those patients that survived or died.

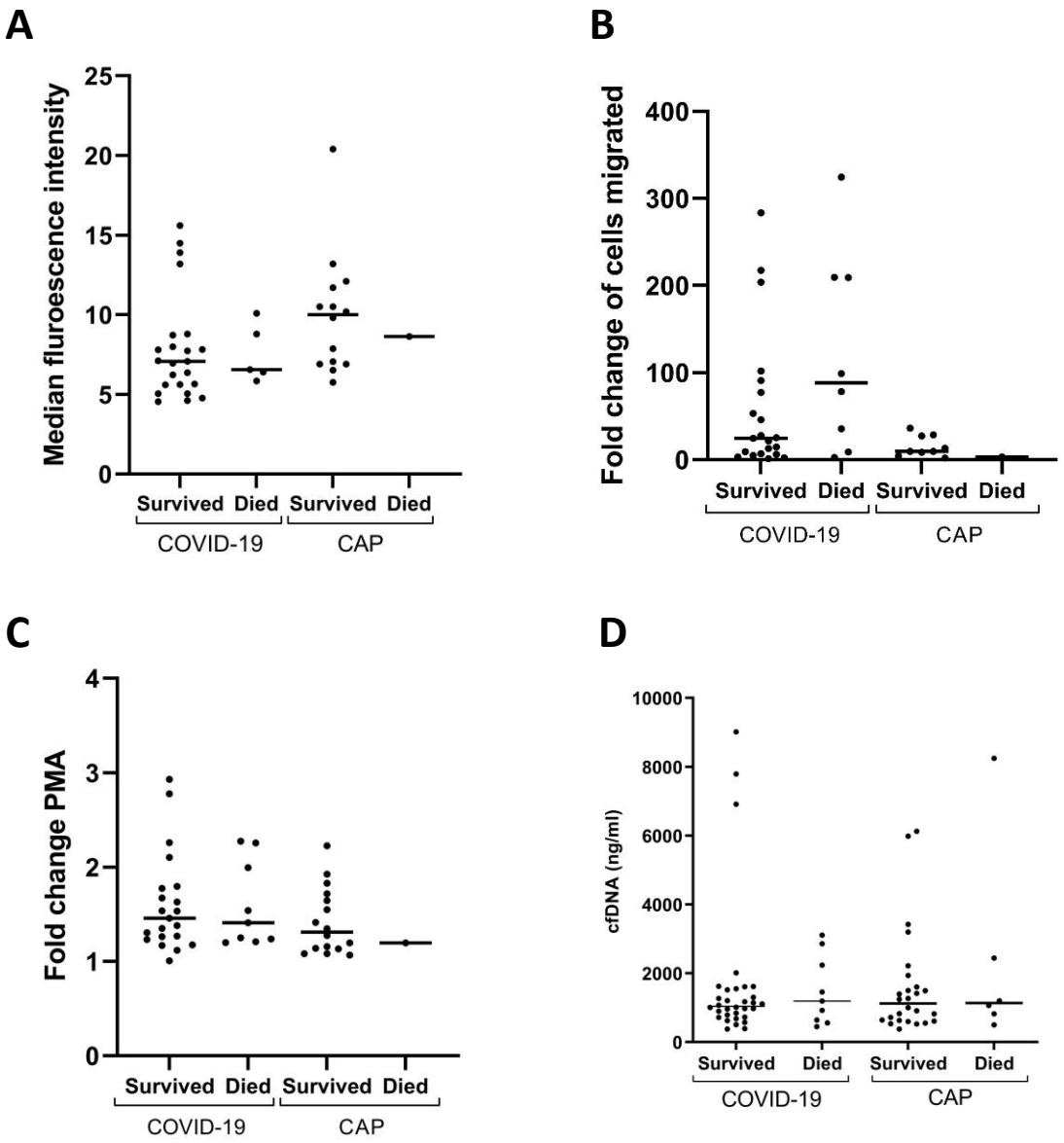

Figure 6.10 Neutrophil effector functions in COVID-19 patients when stratified by in-hospital patient mortality. Results displayed as full data spread with median. Statistical significance calculated using Mann Whitney U as not normally distributed **A**. Neutrophil phagocytosis of labelled opsonised *S. pneumoniae* after 30-minutes. (COVID-19 survived n=23, died n=5, CAP survived n=14, died n=1). **B**. Neutrophil transwell migration towards CXCL8 after 90 minutes. (COVID-19 survived n=21 died n=8 CAP survived n=9, died n=1). **C**. NETosis after PMA stimulation after 3 hours. (COVID-19 survived n=21, died n=9, CAP survived n=16, died n=1). **D**. Circulating cfDNA measured in serum. (COVID-19 survived n=32, died n=9, CAP survived n=26, died n=6)

Circulating inflammatory mediators

There were significantly higher levels of IL-6 in patients that died compared with those that survived admission (median survived IL-6 13.32 pg/mL (9.83-41.15), median died IL-6 60.19 pg/mL(38.49-87.26), p=0.0027, **Figure 6.11A**). sTNFR1 levels were significantly higher in patients who died compared to those that survived admission (median survived sTNFR1 1003 pg/mL (826.1-1137), median died sTNFR1 1300 pg/mL (977.7-1437), p=0.0311, **Figure 6.11C**). There was no significant difference between MPO, GM-CSF, or VEGF levels between patients that survived or died, **Figure 6.11B, D, E**.

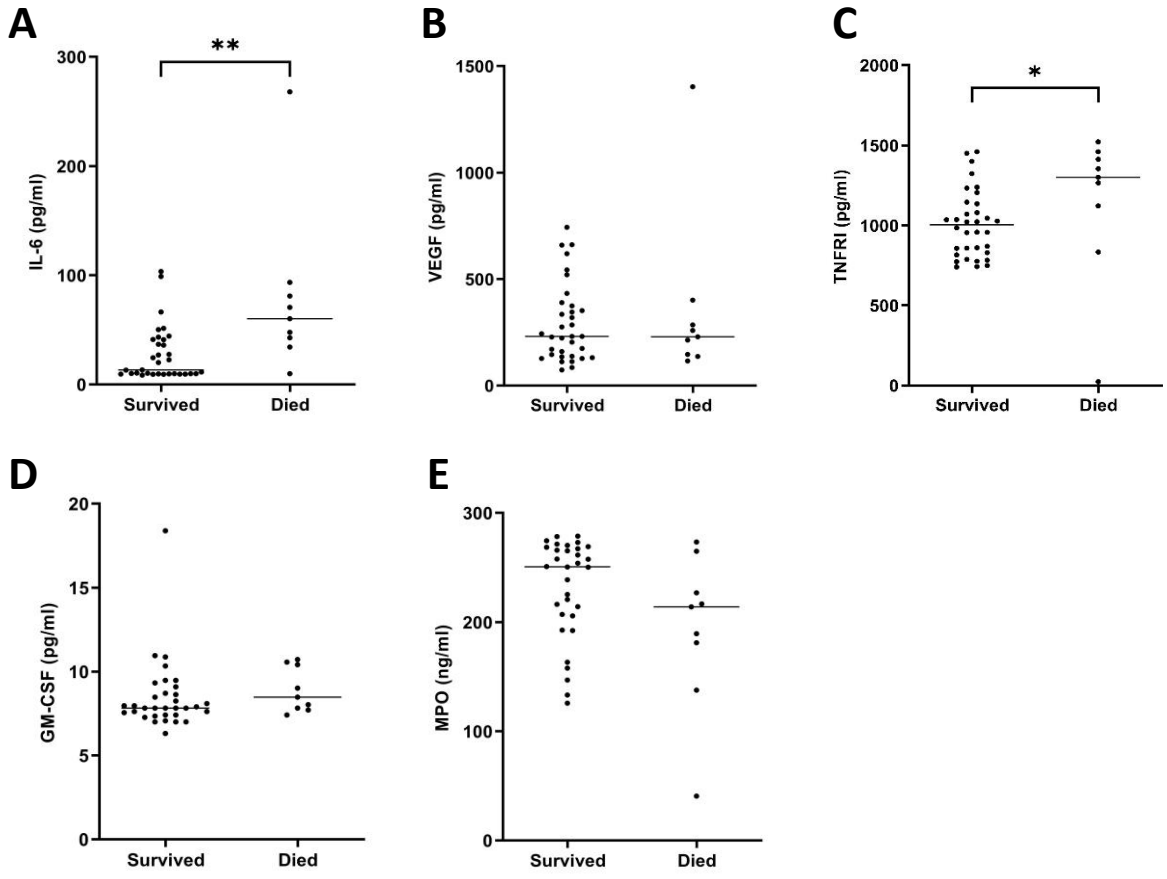

Figure 6.11 Circulating inflammatory mediators compared in COVID-19 patients who survived and died during hospital admission, survived n=33, died n=9. Full data spread shown with median. Mann Whitney U test used for statistical comparison as data is not normally distributed. **A**. IL-6 **B**. VEGF **C.** sTNRI1 **D**. GM-CSF **E.** MPO. *p≤0.05, **p≤0.01, ***p≤0.001, ****p≤0.0001

Time to admission

There was no significant difference in systemic inflammatory cytokines IL6, sTNFRI, VEGF, MPO or GM-CSF in COVID-patients admitted less than 7 days after symptom onset compared to those admitted beyond 7 days. There was no significant difference in neutrophil function between these groups across all experimental neutrophil functions. VEGF at admission was significantly higher in CAP patients who were admitted more than 7 days after symptom onset (<7 days VEGF 201.576 (19.142), ≥ 7 days VEGF 297.337 (44.661), p=0.030). There were no other significant differences in the CAP cohort noted.

6.4.2 4C score

Patients were stratified according to disease severity, using the validated 4C score. Patients were classified as either high or low risk mortality based on score, <9 low risk, ≥9 high risk. There was no difference in neutrophil phagocytosis between low and high 4C risk **Figure 6.12A**. There was no significant difference in neutrophil transmigration between low and high risk 4C, **Figure 6.12B**. There was no significant increase in NETosis in patients with a 4C score ≥9, and no significant difference in the serum cfDNA between these categories, **Figure 6.12C&D**.

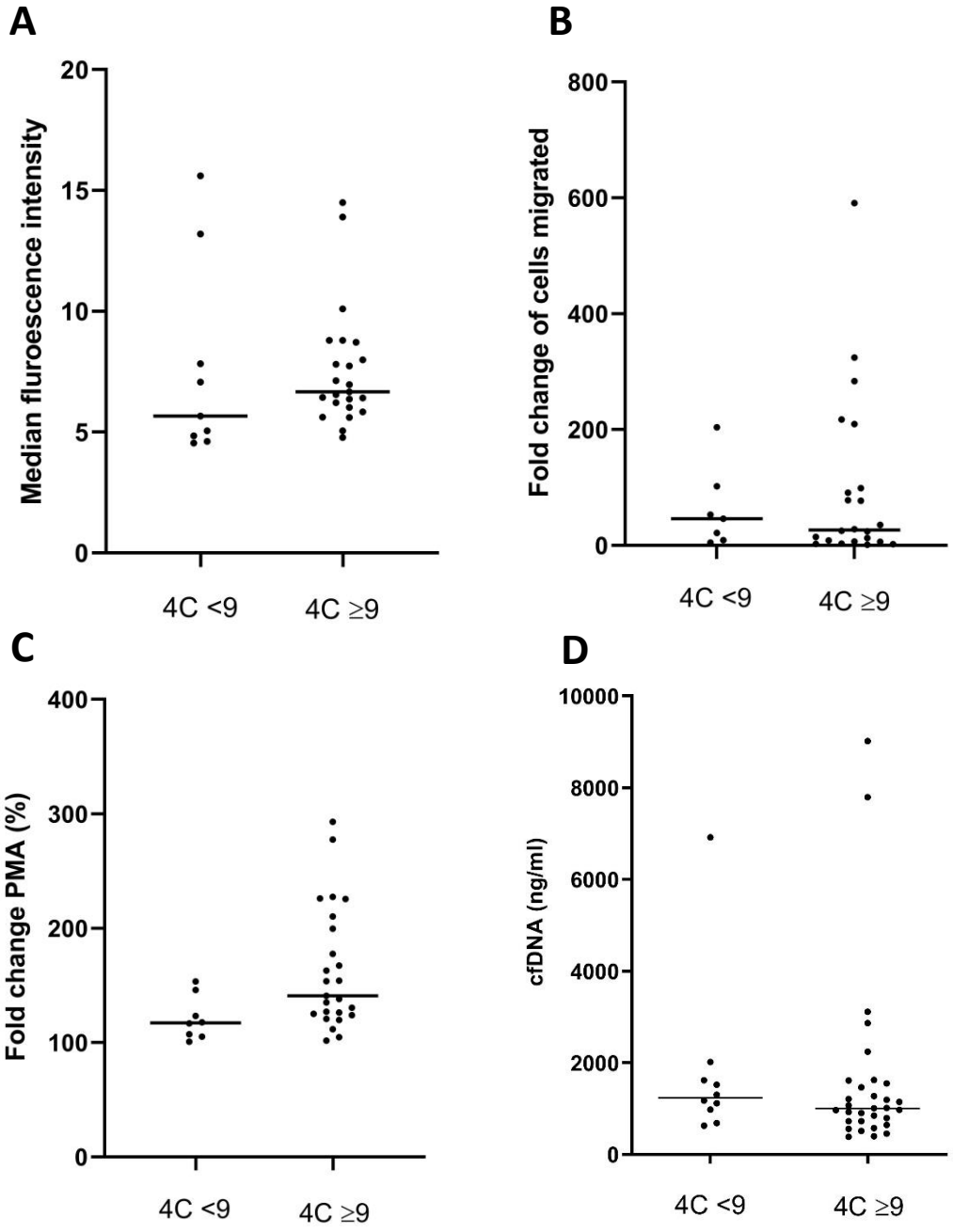

Figure 6.12 Neutrophil effector functions in COVID-19 patients when mortality is stratified using the 4C score. 4C score <9 relates to in-hospital mortality risk of 9.9%, scores ≥9 relate to in-hospital mortality of >31.4%. Data shown as full spread with median. Mann Whitney U test was used for statistical analysis as data not normally distributed. **A.** Neutrophil phagocytosis of labelled opsonised *S. pneumoniae* after 30-minutes. (4C <9 n=9 vs 4C ≥9 n=23). **B.** Neutrophil transwell migration towards CXCL8 after 90 minutes. (4C <9 n=7 vs 4C ≥9 n=22). **C.** NETosis after PMA stimulation after 3 hours. (4C <9 n= 7 vs 4C ≥9 n=22). **D.** Circulating cfDNA measured in serum. (4C <9 n=9 vs 4C ≥9 n=23). *p≤0.05, **p≤0.01, ***p≤0.001, ****p≤0.0001

6.4.3 Circulating inflammatory mediators

In COVID-19 patients with more severe disease stratified by 4C there were higher levels of circulating IL-6 (median IL-6 4C <9 9.87 pg/mL (9.499-13.12), 4C ≥9 35.15 pg/mL (10.98-57.99), p=0.0059), **Figure 6.13A**. There was significantly higher circulating sTNFR1 levels in more severe COVID-19 (median sTNFR1 4C <9 856.3 pg/mL, (780.1-1026), sTNFR1 4C ≥9 1070 (845.4-1311), p=0.0478), **Figure 6.13B**. There was no significant difference between the circulating levels of VEGF, GM-CSF or MPO between different levels of disease severity, **Figure 6.13C, D, E**.

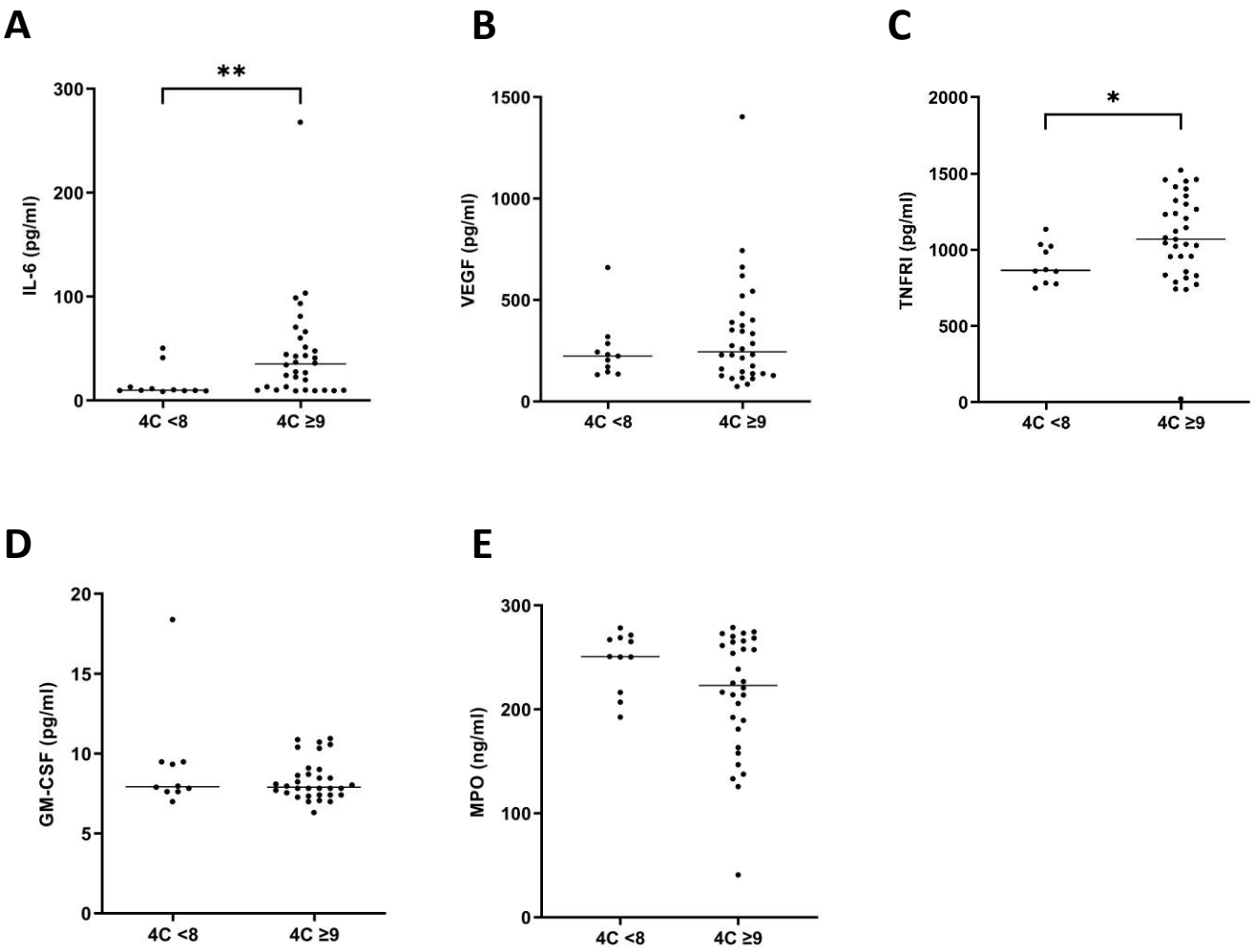

Figure 6.13 Circulating inflammatory mediators in COVID-19 patients stratified by disease severity by 4C score, low 4C <9 n=11, high 4C ≥9 n=30. Results displayed full data spread with median. Mann Whitney U test used for statistical analysis as data not normally distributed **A.** IL-6 **B.** VEGF **C**. sTNRF1 **D.** GM-CSF **E.** MPO. *p≤0.05, **p≤0.01, ***p≤0.001, ****p≤0.0001

6.4.4 ARDS

ARDS has been subdivided into those patients demonstrating a hyper-inflammatory phenotype in non-COVID-19 related lung injury. An algorithm was developed based on routinely measured clinical parameters (Sinha et al., 2020). Only 2/41 COVID-19 patients were categorised to the hyper-inflammatory group. In those patients with moderate to severe ARDS as defined by the Berlin Criteria, higher IL-6 levels were recorded compared to mild patients (median IL-6 ARDS 47.8 pg/mL (19.2-68.0), no ARDS 21.31 pg/mL (9.84-42.84), p=0.0468, **Figure 6.14**). There were no significant differences in the other measured circulating inflammatory mediators.

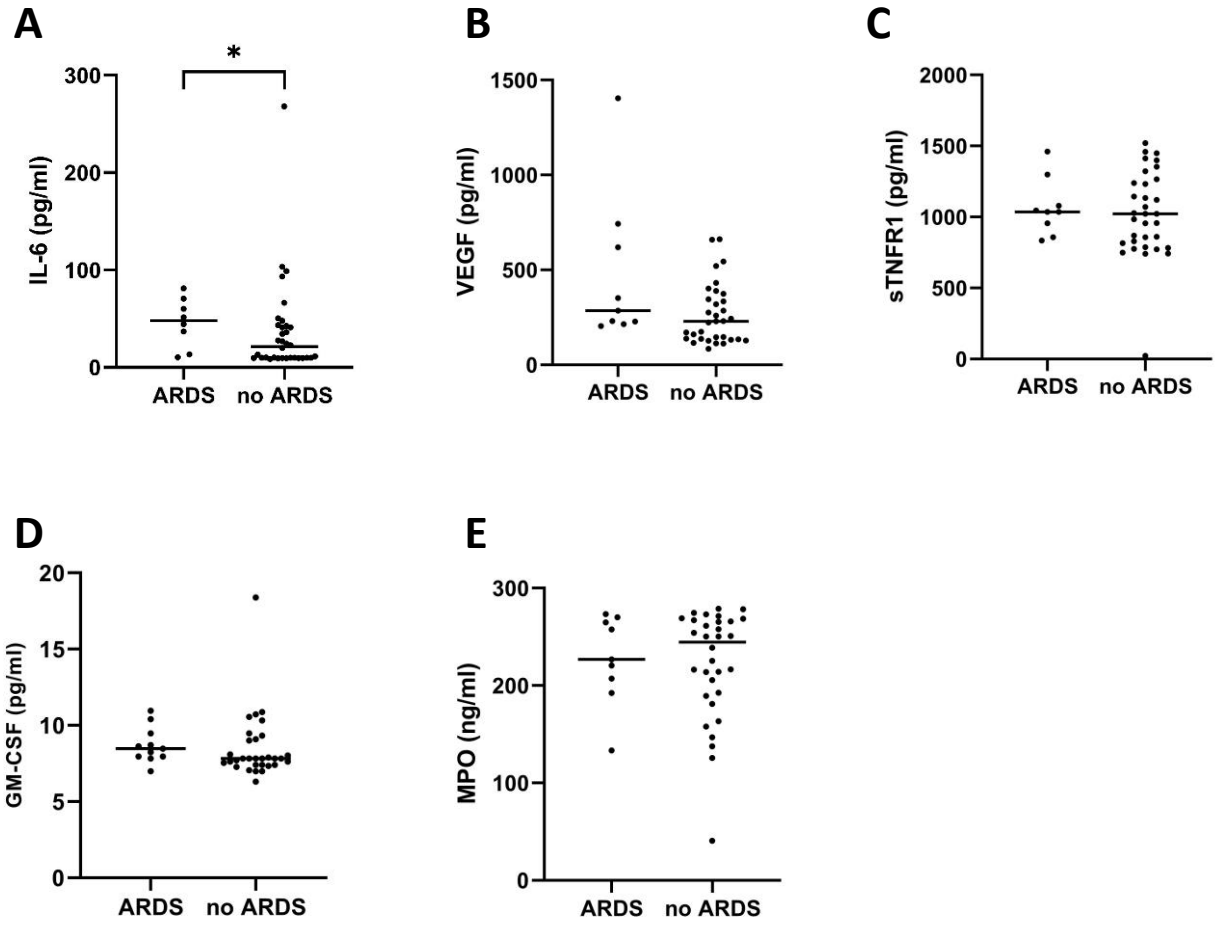

Figure 6.14 Circulating inflammatory mediators in COVID-19 patients stratified by the presence of ARDS defined by SpO2/FiO2 conversion (Rice et al., 2007) ARDS n=8, no ARDS n=34. Results displayed full data spread with median. Mann Whitney U test used for statistical analysis as data not normally distributed **A.** IL-6 **B.** VEGF **C**. sTNRF1 **D.** GM-CSF **E.** MPO. *p≤0.05, **p≤0.01, ***p≤0.001, ****p≤0.0001

6.5 PI3K inhibition

6.5.1 Clinical phenotype

For the investigation of PI3K inhibition on neutrophil effector function, a subsequent cohort of patients was required to be recruited as it was not possible to do the assays on the original cohort. Demographics between the original COVID-19 cohort and the subsequent recruitment after data analysis did not show any significant differences. This included biochemical data, severity of disease as well as outcome measures such as length of stay and mortality. We noted that treatment with dexamethasone was significantly decreased in the second cohort (COVID-19 92.6%, second cohort 55.6%, $p<0.05$), a reflection of the refinement in treatment protocols for hospitalised patients. The differences noted between the CAP and original COVID-19 cohort persisted to the further 18 patients recruited.

	AMC n=26	COVID-19 n=41	CAP n=26	COVID-19 PI3K n=18
Male: Female	10:16	26:15	15:11	9:9
White: Non-white	24:2	31:10	23:3	13:5
Died (%)	0 (0%)	10 (24%)	2 (8%)	5 (28%)
Age	70 (61.0-78.0)	71.5 (58.0-84.0)	67.5 (54.5-85.0)	70.7 (51.0-83.0)
BMI (kg/m^2)		26.4 (24.2-32.8)	27.9 (23.3-41.1)	30.1 (23.2-27.2)
Comorbidities				
Cardiovascular	4 (15.3%)	12 (29.3%)	7 (26.9%)	7 (38.9%)
Respiratory	0 (0%)	1 (2.4%)	4 (15.4%)	2 (11.1%)
Endocrine	10 (38.4%)	16 (39.0%)	3 (11.5%)*	9 (50.0%)
Hypertension	13 (50%)	19 (46.3%)	10 (38.5%)	9 (50.0%)
Other	11 (42.3%)	24 (58.5%)	15 (57.7%)	8 (44.4%)
Biochemistry				
WCC (x10^9/L)		8.2 (6.3-12.0)	13.4 (10.7-16.4)***	7.6 (4.6-11.9)
Neutrophils (x10^9/L)		6.4 (4.4-8.6)	11.2 (7.8-13.6)**	5.8 (2.9-9.4)
CRP (mg/L)		103.0 (63.0-165.0)	119.0 (42.0-396.0)	74 (24.3-161.3)
NLR		5.4 (3.8-10.8)	8.5 (5.9-52.7)	6.3 (2.4-10.2)
HS Troponin I (ng/L)		14.5 (5.0-31.3)	17.5 (4.0-318.0)	7.0 (4.0-31.5)
D-dimer (ng/mL)		382.0 (218.0-829.5)	659.0 (270.5-1510.0)	493.0 (247.0-890.0)
Ferritin (ug/L)		1082 (428.3-1525.0)	110.0 (78.8-225.3)*	251.5 (185.8-1230.3)
Vitamin D (nmol/L)		35.6 (23.0-51.8)	45.3 (23.8-73.2)	36.6 (22.6-60.1)
Admission				
Worst NEWS2		6.0 (5.0-7.0)	5.0 (3.0-12.0)	6.0 (3.0-8.0)
4C		12.0 (9.0-14.0)		13 (11.0-15.8)
qSOFA		1.0 (1.0-1.5)	1.0 (1.0-1.0)	1.0 (1.0-1.0)
CURB-65		2.0 (1.0-3.0)	2.0 (2.0-2.0)	2.0 (2.0-3.0)
Length of stay (days)		5.5 (3.0-12.0)	4 (3.0-7.5)	6.5 (3.3-14.8)

Table 6.3 Table of patients recruited for investigation of PI3K inhibition and inhibitor experimentation collected at the time of enrolment. Height and weight measurements were not able to be collected to calculate a BMI measurement for the recruited AMC. Comparisons were calculated between cohorts of COVID-19 patients, AMC, or CAP patients. Results shown with median (IQR Q1-Q3), statistical analysis performed using Kruskal-Wallis test as not normally distributed. Other comorbidities were included if they caused a significant impact on patient quality of life or regular medication – this included but not limited to: severe peripheral vascular disease with ulceration, dementia, stroke, childhood polio, obesity, diverticulosis, alcohol related liver disease, rheumatoid arthritis. WCC- white cell count; CRP- C-reactive protein; NLR- neutrophil lymphocyte ratio; NEWS2- National Early Warning Score 2, data collected was worst score in the 24 hours after admission; HS Troponin I- high sensitivity troponin I. . *p≤0.05, **p≤0.01, ***p≤0.001, ****p≤0.0001

6.5.2 Neutrophil effector functions

6.5.2.1 Phagocytosis

There was no significant effect with any of the PI3K inhibitors on phagocytosis of *S. pneumoniae* after 30 minutes. There was no change noted to the MFI or % phagocytosis **Figure 6.15**.

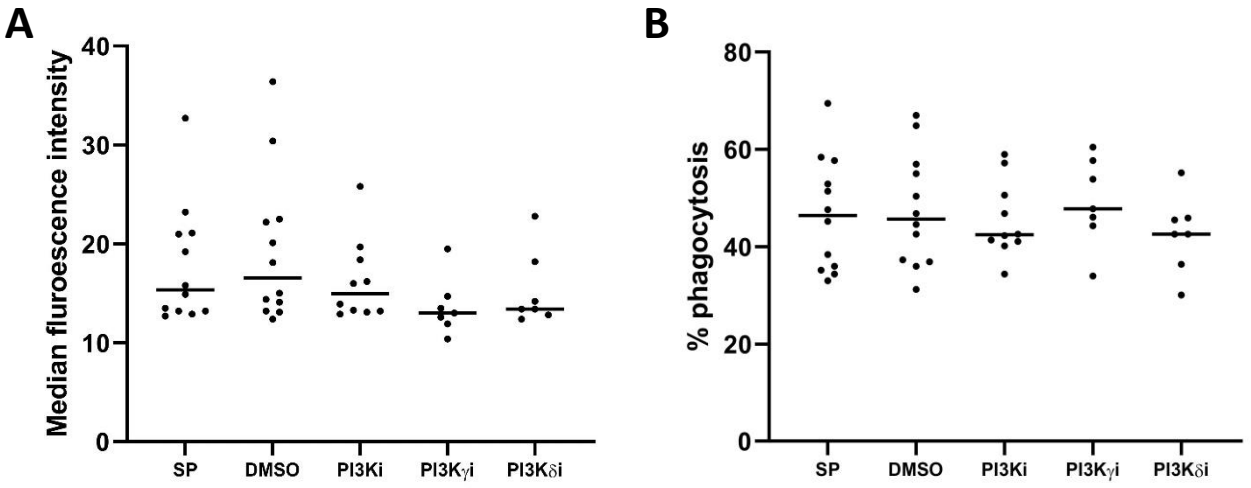

Figure 6.15 Isolated neutrophil phagocytosis from COVID-19 patients of *S. pneumoniae* (SP) after 30 minutes, n=12. Full data spread shown with median. Kruskal-Wallis test used for multiple comparisons as data not normally distributed. Cells were incubated with PI3K inhibitor for 30 minutes prior to exposure to labelled bacteria. Vehicle control of DMSO added. **A.** MFI and **B.** % phagocytosis

6.5.2.2 Transwell migration

There was no observed effect on neutrophil transwell migration towards CXCL8 with the addition of any PI3K inhibition for 30 minutes prior to neutrophil migration, **Figure 6.16**.

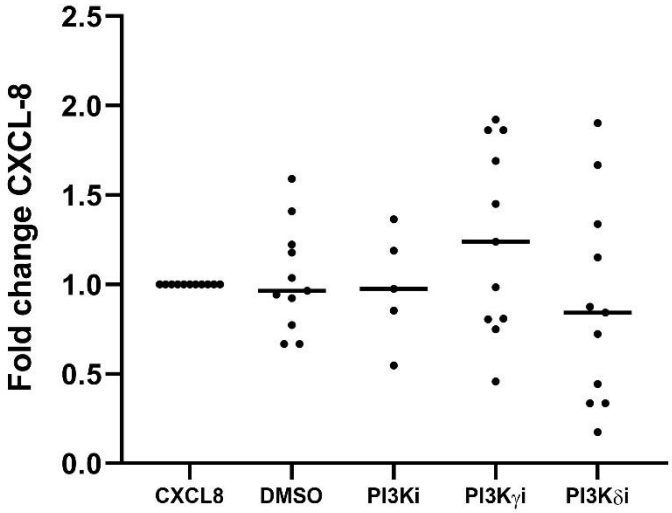

Figure 6.16 Neutrophil transwell migration towards CXCL8 chemoattractant after 90 minutes from COVID-19 patients CXCL8 n=12, DMSO n=12, PI3Ki (pan PI3K inhibitor) n=5, PI3Kγi (gamma PI3K inhibitor) n=11, PI3Kδi (delta PI3K inhibitor) n=12. Cells were incubated with PI3K inhibitor for 30 minutes prior to migration. Vehicle control of DMSO added. Number of neutrophils was measured by flow cytometry and then normalised to compare to neutrophils migrating to CXCL8 control. Kruskal Wallis test was used for statistical analysis of not normally distributed data.

.

6.5.2.3 NETosis

Incubation with PI3K delta (CAL101) and gamma (AS252434) inhibitors significantly decreased PMA induced NETosis (PMA RFU 247 (228.5) vs. delta 207.5 (242.5), p=0.0129, vs. gamma 216.5 (242), p=0.0156, **Figure 6.17**).

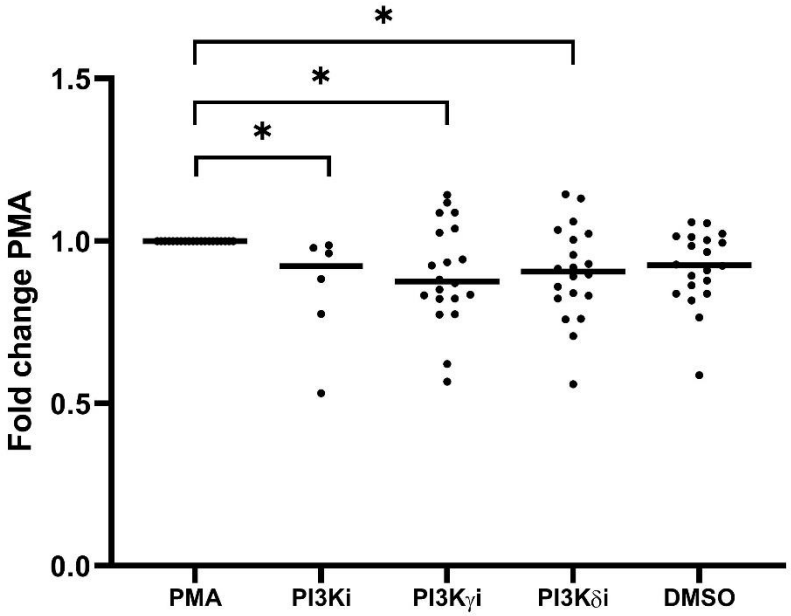

Figure 6.17 COVID-19 neutrophils were pre-incubated for 30 minutes with PI3Ks inhibitor, and NET release measured in response to PMA stimulation. Data shows fold change in absorbance of PMA stimulated neutrophils compared to PMA control, n=20, except PI3Ki (pan PI3K inhibitor) n=6. Full data spread shown with median. Kruskal-Wallis test used for statistical analysis.

6.6 Effects of selected pharmacological agents on neutrophil function

There was no significant difference in neutrophil phagocytosis of labelled *S. pneumoniae* after 30 minutes incubation with the treatments (metoprolol, brensocatib, AZD9668) followed by 30 minutes phagocytosis time, **Figure 6.18**.

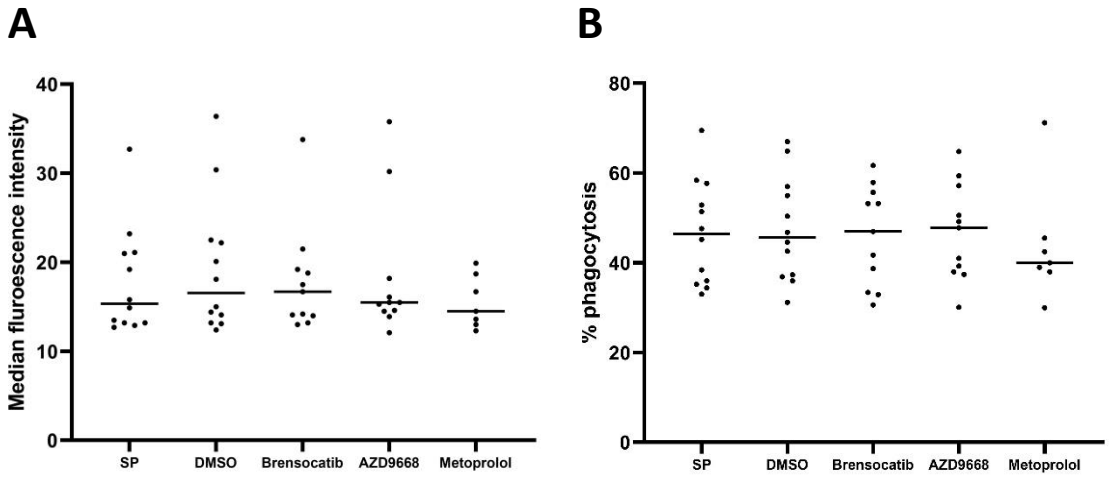

Figure 6.18 Neutrophil phagocytosis of *S. pneumoniae* (SP) after 30 minutes. Cells were incubated with inhibitor for 30 minutes prior to exposure to labelled bacteria. Vehicle control of DMSO added. *S. pneumoniae* (SP) n=11, DMSO n=11, Brensocatib n=11, AZD9668 n=11, Metoprolol n=7. Data shown as full data spread with median. Kruskal Wallis test used for multiple comparisons. **A.** median fluorescence intensity and **B.** % phagocytosis

There was no significant difference in viability after addition of treatments for 30 minutes,

Figure 6.19. There is no data for addition of metoprolol due to sample error.

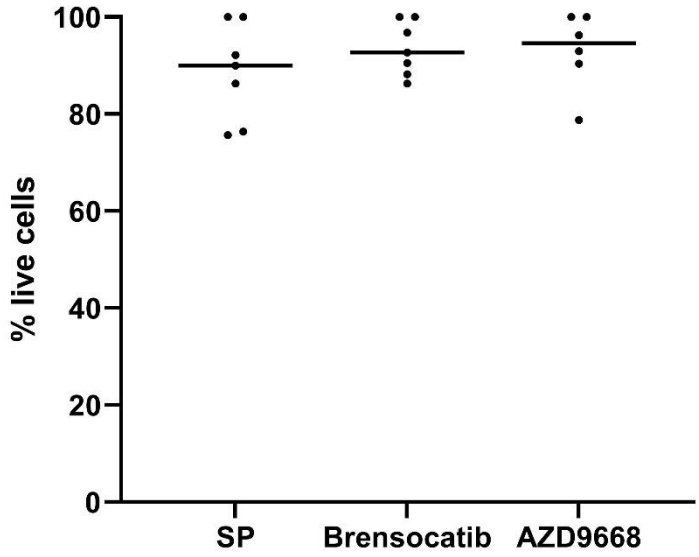

Figure 6.19 Viability of isolated neutrophils after 30 minutes incubation with treatments prior to 30 minutes phagocytosis of labelled *S. pneumoniae* (SP). There was no significant difference in viability. n=7. Data shown as full data spread with median. Kruskal-Wallis test use for statistical analysis of not normally distributed data.

There was no significant change to number of neutrophils migrated through the transwell membrane on addition of the treatments, **Figure 6.20A**. There was no change to NETosis after addition of the treatments for 30 minutes prior to addition of PMA for 3 hours, **Figure 6.20A**.

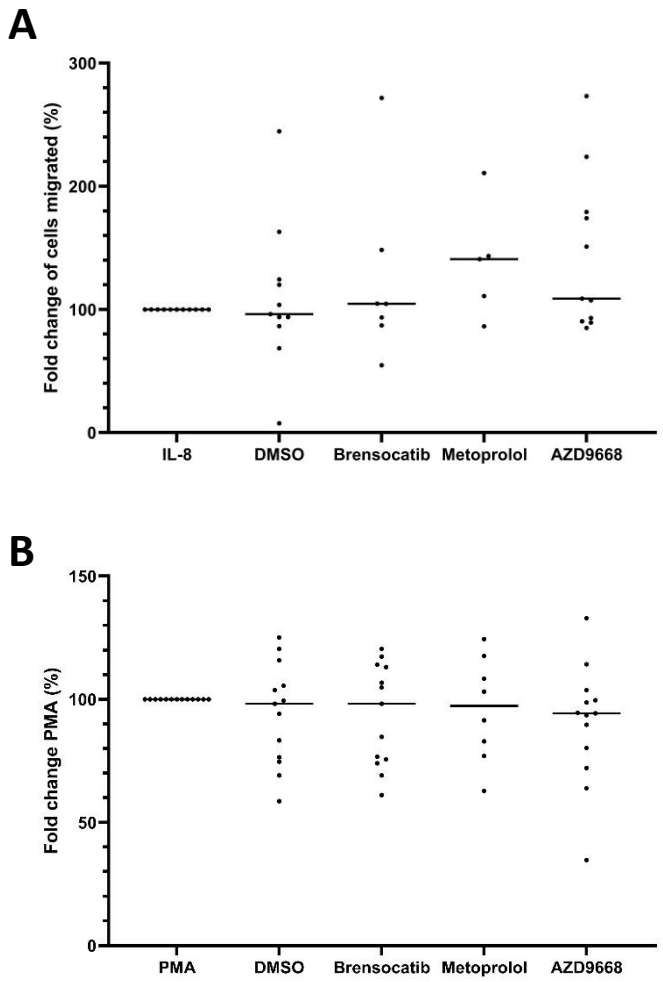

Figure 6.20 Effect of treatments (Brensocatib n=13, Metoprolol n=8, AZD9668 n=13) on neutrophil migration and NETosis on COVID-19 samples PMA/ IL8/ DMSO n=13. Results shown as full data spread with median. Kruskal-Wallis test used for statistical analysis. **A.** Neutrophil migration towards IL8 through a transwell membrane. **B.** Neutrophil NET formation after 3 hours stimulation with PMA.

6.7 Discussion

In summary, neutrophil changes observed in this ward based COVID-19 cohort are unique compared to previously described CAP and sepsis patients.

Neutrophils isolated from these patients demonstrated increased migration, impaired phagocytosis and n/mROS generation. There was an increase in NETosis with reduced DNase activity. A unique pattern of surface marker expression was found from COVID-19 patients suggesting a distinct effect of the virus on neutrophils.

Addition of PI3K inhibitors to neutrophils from COVID-19 patients demonstrated decreased NETosis but did not change other effector functions. There was no effect after addition of metoprolol, brensocatib or AZD9668.

6.7.1 Cellular outcomes

We present novel findings, unique to neutrophils isolated from COVID-19 patients. Neutrophil dysfunction affects all main effector functions compared to AMC and CAP patients. They demonstrate increased migration and impaired anti-microbial responses, including reduced phagocytosis and n/mROS generation after phagocytosis. Increased NETosis and decreased DNase activity represent an exaggerated late-stage response. In addition, the surface marker expression on neutrophils isolated from COVID-19 patients represents a distinct phenotype, different from those previously described in purely activated, immature, senescent or anti-inflammatory conditions. A summary of these changes is displayed in **Figure 6.21**. It is unlikely that there would be alterations to the underlying bio-energetics of cell function, given that there was an increase in some functions that require increased energy production (e.g. increased migration levels).

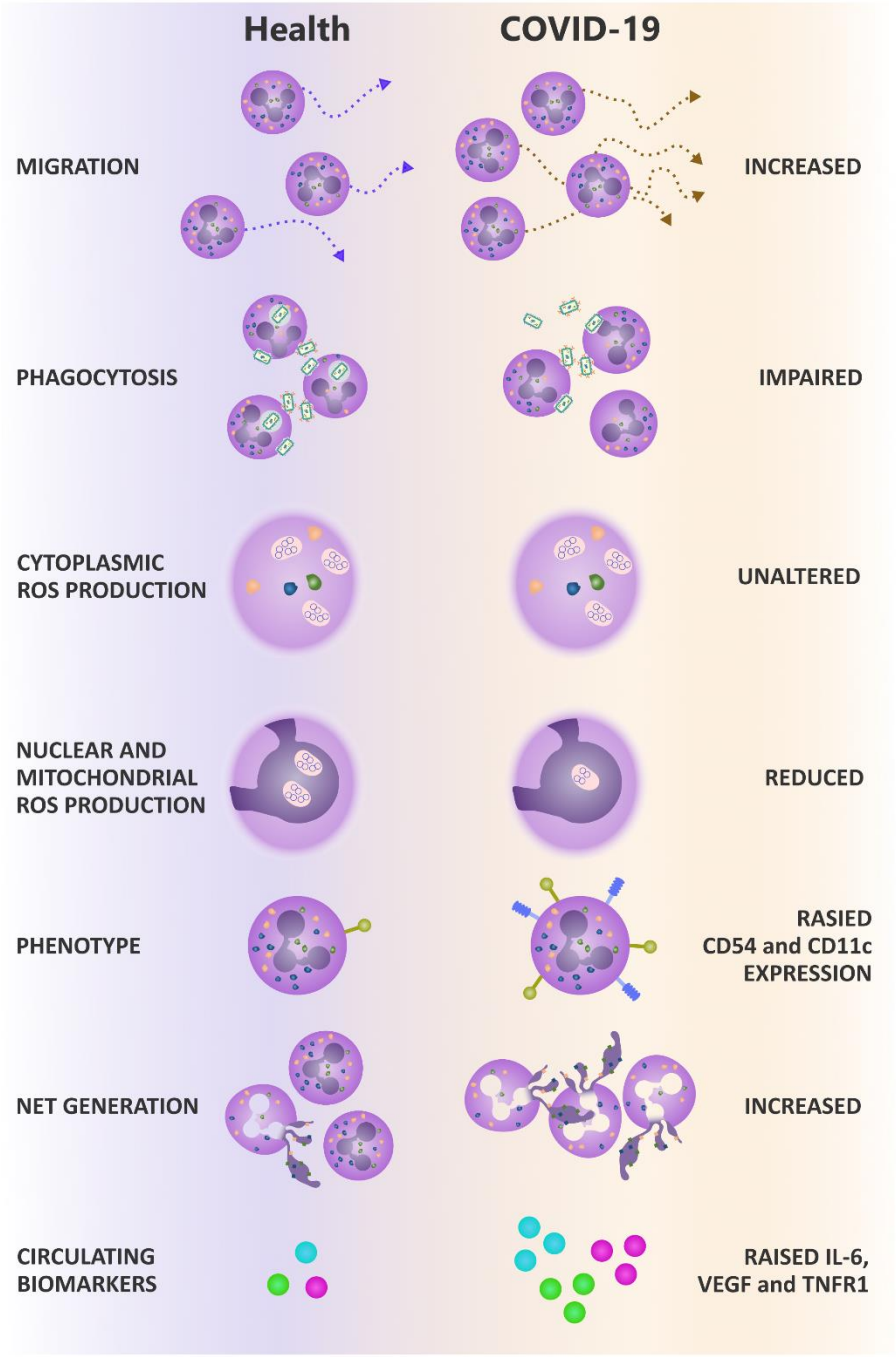

Figure 6.21 Summary of changes to cellular function. Compared to AMC, neutrophils from ward based COVID-19 patients demonstrate increased migration, impaired phagocytosis, and reduced nuclear/ mitochondrial ROS generation. An altered surface marker expression pattern present, with raised CD54 and CD11c expression (markers of migration). COVID-19 patient neutrophils display increased NETosis, and systemically increased pro-inflammatory cytokines.

Damage to lung parenchyma in viral infections can impair the physical barrier to further pathogens. Following viral infections, secondary bacterial infections are not uncommon and are associated with poorer outcomes and higher levels of mortality (Brundage, 2006). This has been reported in influenza associated pneumonias (Brundage and Shanks, 2008). Bacterial pneumonias in COVID-19 infection are associated with increased lung disease severity and poor outcomes (Feldman and Anderson, 2021, Buehler et al., 2021). Neutrophils isolated from COVID-19 patients here demonstrated impaired antimicrobial responses to exposure to *S. pneumoniae*; the most common bacteria isolated in secondary bacterial infection in COVID-19 (Zhu et al., 2020). In addition, decreased n/mROS generation in these cells suggest impaired phagosomal activity, a key element of bacterial killing in neutrophils. Together, this reduction in phagocytosis and bacterial killing may contribute to the increased incidence of secondary bacterial infection and poorer outcomes.

The release of NETs from neutrophils has been implicated in several diseases, causing local tissue damage and thrombotic disease events. Increased thrombotic events have been reported in COVID-19 patients throughout the pandemic. The increased NETosis and serum cfDNA that we report here has been reported in both COVID-19 and CAP patients before (Ebrahimi et al., 2018). Compounding an increase in NETosis, would be a reduction in the degradation of NETs through DNase activity. Our cohort of COVID-19 patients demonstrated decreased serum DNase activity compared to AMC and CAP cohorts which is corroborated in a previous study (de Buhr et al., 2022). Further, studies investigating the activity of DNase inhibitors showed decreased activity of gelsolin in COVID-19 serum. Geloslin acts to depolymerise filamentous actin, an inhibitor of DNase activity (Messner et al., 2020, Overmyer et al., 2021). Increasing the negative regulation of DNase could lead to the impaired DNase-1 activity that was observed in this cohort of patients here.

A study in rodents showed that the administration of disulfiram, usually used in the treatment of alcohol dependence, improved outcomes (Adrover et al., 2022). Disulfiram acts through gasdermin D blockade, which is vital for NETosis. Gasdermin D is a pore-forming protein, which when inhibited prevented NET formation (Chen et al., 2018b). Gasdermin D requires

proteolytic activation through neutrophil proteases, and consequently feeds forward to affect protease activation and genetic expansion for NETosis. Pulmonary manifestations such as hyaline membrane formation associated with acute lung injury were reduced, with a reduction in associated mortality. In rodents infected with SARS-CoV-2, there was a decrease in NET formation, perivascular pulmonary fibrosis and downregulated inflammatory immune pathways. Clinically, disulfiram has only been investigated as a COVID-19 treatment in a single study (Fillmore et al., 2021). In this retrospective cohort study of US veterans who were on a disulfiram prescription and diagnosis of alcohol use there were no deaths in the disulfiram group compared to the general population rate of 5-6%. There are clearly limitations to this study, with regards to design and population. However, this was not followed up further, and clinically, the side effects of disulfiram in the non-alcohol use disorder patients may be unacceptable.

Systemic circulating cytokine levels were altered in the COVID-19 cohort compared to AMC. There was generally increased expression of inflammatory cytokines, in keeping with an overall inflammatory state. Compared to CAP patients, there was only significantly increased MPO in COVID-19. MPO is a lysosomal protein which is primarily produced in neutrophils, although monocyte subsets are also capable of production (Thukkani et al., 2003). Given the massive expansion in the neutrophil subset of the leucocyte differential, this would be in keeping with an overall exaggerated neutrophil response. Overactivation of misdirected migration of neutrophils could be misdirected leading excessive host tissue damage with increased lung injury seen in COVID-19 infection.

Dexamethasone as a treatment in COVID-19 was established early in the pandemic (Horby et al., 2021a). There is previous evidence from neutrophils isolated in healthy controls suggesting that steroids can inhibit neutrophil migration towards inflammatory sites (van Overveld et al., 2003, Zentay et al., 1999). As dexamethasone was standard of care at the time of patient recruitment, over 90% of our patients were treated with dexamethasone on admission, prior to recruitment. Validation work in **Chapter 4** demonstrates that neutrophils isolated from healthy controls demonstrated no significant difference in function compared to those without

supplementation. Data from other studies investigating the effects of COVID-19 on neutrophils prior to the use of dexamethasone show similar results (Leppkes et al., 2020, Masso-Silva et al., 2021). This suggests that the results presented here are not solely the cause of treatment effect.

The pattern of neutrophil dysfunction described in this cohort may suggest disruption to the internal mechanosensing. Pseudopods are involved with migration and phagocytosis of neutrophils (Lee et al., 2003). A decrease in pseudopod extrusion could lead to increased migration and impaired phagocytosis. Previous studies have shown that reduced extrusion leads to increased migratory speed (Andrew and Insall, 2007), and they have a key role in the internal reorganisation of intracellular cytoskeleton for phagocytosis (Lee et al., 2003).

Phosphoinositide 3-kinase (PI3K) is an important intermediary intracellular signalling molecule in cytoskeletal rearrangement, superoxide generation, and NETosis (Stephens et al., 2002, Papayannopoulos, 2018). Disruption to PI3K signalling is linked to increased age; inhibition of PI3K increased migration accuracy in the elderly and reduced NET formation ex vivo (Erpenbeck et al., 2019). These findings in elderly neutrophils are similar to those described in the COVID-19 cohort. As some function can be restored through inhibiting PI3K signalling in these patients, it may be possible to achieve similar outcomes in COVID-19. Further examination into manipulation of the PI3K pathway is therefore needed to determine if this represents a treatable target.

Studies examining the effects of COVID-19 on neutrophil function to date have focused on patients requiring intensive care admission. The data describing cellular dysfunction here compliments this previously reported literature (Zuo et al., 2021, Skendros et al., 2020a). Elevated NETosis has been demonstrated in comparison to control patients (Skendros et al., 2020a, Middleton et al., 2020, Veras et al., 2020). One study demonstrated an overall increase in neutrophil phagocytosis in intensive care COVID-19 patients although serial samples from patients were combined to demonstrate this (Masso-Silva et al., 2021). Patients followed up here after 3-5 days admission showed a significant change in neutrophil phenotype and function, which suggests that evolution of the disease and host-response may occur on a more

acute basis. Separation of admission samples (representing the most unwell and highest viral load) and those from acute convalescence would therefore be indicated. Phenotype data from another ICU cohort showed increased CD11b expression and ROS production with decreased CD62L expression, suggestive of neutrophil exhaustion (Loyer et al., 2022).

6.7.2 PI3K inhibition

Based on our initial findings, we postulated that pseudopod dysfunction and aberrant activation of PI3K signalling pathways may contribute to this novel neutrophil phenotype. In a further cohort of COVID-19 patients PI3K blockade was investigated to determine if this could improve migration and decrease NET formation as previously reported (Erpenbeck et al., 2019). Focus for PI3K inhibition focused on an unselective pan-PI3K inhibitor, and two PI3K inhibitors with higher affinity to disrupt γ, and δ signalling.

Inhibition of PI3K signalling with delta and gamma inhibitors decreased ex vivo NET production in COVID-19 patients. As described previously, the increased incidence of thromboembolic events in COVID-19 patients may be partly attributed to an increased tendency to form NETs (Leppkes et al., 2020). Regulation of elevated NET production may help to prevent this and reduce COVID-19 associated morbidity. This would suggest further clinical assessment using established NETosis inhibitors (including methotrexate, prednisolone, diphenyleneiodonium chloride (DPI)) and a trial to determine if these inhibitors may have patient benefits (Palma et al., 2020).

PI3K signalling is involved with cytoskeletal rearrangement in neutrophils, which has a role in pseudopod extrusion, phagocytosis and superoxide generation – the key effector function roles. In the elderly, addition of PI3K inhibitors improved migration accuracy, restoring a decline in chemotaxis and chemotactic index observed from the third decade of life onwards. Neutrophil migration using a transwell model was dysregulated in COVID-19 patients compared to AMC suggesting a likely viral specific interaction leading to alterations in

migration. We were unable to alter the observed dysregulated migration by addition of PI3K inhibitors, suggesting another mechanism is driving this effect in COVID-19 infection.

There was no improvement in phagocytosis of labelled *S. pneumoniae* with the addition of PI3K inhibitors, which fits in with the lack of restoration of migration function with PI3K inhibition. These cytoskeletal rearrangement processes are linked, and thus, the alterations to both migration and phagocytosis are likely not underpinned by PI3K pathway disruption.

PI3K signalling disruption represented a potential mechanism to explain the neutrophil dysfunction observed in COVID-19. Whilst there were modest improvements in reducing NET formation after addition of PI3K inhibitors (pan-inhibitor, γ, and δ), these did not restore the other key disrupted neutrophil functions in COVID-19 infection. This suggests another mechanism affecting neutrophil dysfunction. The overall defects observed in neutrophils from COVID-19 patients is similar to that previously described in the elderly, with inaccurate migration, and impaired phagocytic function (Sapey et al., 2014). However, combined with the lack of restoration of function with PI3K inhibition and the different surface receptor expression this suggests a different underlying mechanism. Cellular phenotype representing underlying function has not been clearly studied (Faniyi et al., 2022).

Despite a study population in keeping with senescent neutrophils, PI3K inhibition was unable to restore function which suggests COVID-19 causes an overwhelming effect, either leading to synergistic functional impairment or a new neutrophil phenotype. It is possible that PI3K signalling is disrupted, but the PI3K pathway is altered beyond restoration by the point of symptom onset. Thus, in order to restore neutrophil function, manipulation of other neutrophil processes must be explored. For instance, increased systemic thrombotic events observed in COVID-19 suggest diffuse alveolar disease with fibrin thrombus formation (Carsana et al., 2020, Menter et al., 2020). Alterations to the vascular endothelium have been demonstrated, and in combination with alterations to circulating clotting factors such as NETs leads to an increased clotting tendency as per Virchow's triad (Dupont et al., 2021, Virchow, 2022). Neutrophil migration is dependent on interaction with endothelial marker expression including e-cadherin, L-selectin. Changes to expression can lead to altered migration, and abnormal

flow may further disrupt neutrophil adhesion and arrest. This has been seen in trauma and the blood brain barrier with neutrophil adhesion and COVID-19 has been shown to affect right and left ventricular function (Scholz et al., 2007, Baruch et al., 2022). Thus, the changes observed in migration may be as a response to microvascular disruption as opposed to intrinsic neutrophil migration dysregulation as part of viral infection.

6.7.3 Effect of selected pharmacological agents

There were no observed improvements with the addition of any treatment (brensocatib, metoprolol or AZD9668) on neutrophil function. This may indicate that neutrophil dysfunction seen in COVID-19 patients is not mediated by impaired enzymes such as neutrophil elastase. There has been improvement in COVID-19 patient outcomes with supplementation of these treatments but it is likely they have multiple systemic affects. Patients recruited to the MARID-COVID trial (metoprolol in COVID-19), were severely unwell, admitted to intensive care and treated with invasive mechanical ventilation (Clemente-Moragón et al., 2021). These patients with established ARDS in the context of COVID-19 may demonstrate more benefit from IV metoprolol. Furthermore, the beneficial effects seen in this study may be due to the cardiovascular effects of metoprolol over any postulated impact on cellular function. Compared to the ward-based patients recruited, the ongoing inflammatory response in established lung parenchymal damage may be indicative of more inherent neutrophil dysfunction. As a result, there would be more functional difference observed in this cohort.

Poorer outcomes with supplementation of brensocatib compared to placebo were seen in the STOP-COVID trial and were not explained by the effects to neutrophil function. We did not observe a significant change in neutrophil effector functions after supplementation with brensocatib. Patients recruited here were similar to the patients in the STOP-COVID trial (inclusion criteria: one risk factor for severe COVID-19 – radiographic infiltrates, clinical evidence of infection, peripheral blood oxygen saturation <94%, or lymphopenia) (Chalmers et

al., 2020). The difference in COVID-19 disease severity is unlikely to be the cause of the change in neutrophil activity.

Many of these treatments mediate NE activity, which is required for migration through connective tissue and the endothelium. There was no significant change in migration noted in this model, which may be due to a lack of an epithelial membrane. Addition of an epithelial membrane for migration may demonstrate decreased migration due to decreased NE activity. Immunomodulatory prostaglandin release is increased by NE activity, and cleaves receptors on T cells, monocytes and neutrophils to limit hyperinflammation (Domon et al., 2021, van den Berg et al., 2014, Perng et al., 2003). Blockade of NE activity may reduce prostaglandin release and then lead to increased inflammation and cytokine release. This may explain the poor outcomes in the STOP-COVID trial.

Neutrophil dysfunction in COVID-19 has been demonstrated compared to CAP and AMC patients recruited here. It is likely that neutrophil dysfunction plays a role in poor outcomes in hospitalised patients. To restore neutrophils to that of AMC has not demonstrated any significant improvement in function *in vivo*. Further research is required to determine what mechanism drives neutrophil dysfunction in COVID-19 patients.

6.7.4 Limitations

Method limitations regarding handling of COVID-19 samples have been discussed in **Chapter 3.**

Migration was measured through a transwell model. This can determine migration towards a chemoattractant through a 3.0 μm pore. Total number of cells migrated can be determined through flow cytometry. This method can determine the change in number of cells migrating but cannot quantify the overall neutrophil velocity. Rapid migration without accuracy presents a different neutrophil response compared to those with accuracy. Whilst the number of

migrated cells to the membrane suggests a degree of migrational directionality, this is only in a single, gravity assisted plane. The use of Insall chamber (modified Dunn Chamber) chemotaxis assay in determining migration would be a better model, as this is able to determine the speed, velocity, persistence and chemotactic index of the migrating cells (Sapey et al., 2014, Muinonen-Martin et al., 2010). The risk of exposing cells from COVID-19 patients to shared laboratory equipment was determined too high at time of experimentation. Transwell migration assay can be carried out in a self-contained tissue-culture hood in a category-3 laboratory prior to fixation with 4% (v/v) PFA.

Patients recruited were ward-based, and therefore may not be representative of the most severe COVID-19 patients. Although these represent the majority of hospital admissions, less severe disease may make teasing out cellular and clinical differences to AMC and CAP more difficult. However, as they represent the in-patient burden and are underrepresented in research and in our cohort had a significant proportion within the high risk 4C severity score. Prevention of deterioration of these patients could reduce the ICU admission and improve mortality.

AMC recruited for this study were recruited from hospital staff and elderly patients attending regular, routine outpatient hospital appointments. Whilst recruitment and investigation occurred before the rollout of COVID-19 vaccination, these AMC would have had exposure to COVID-19 in the past. In addition, data was not collected if AMC had previously been infected and symptomatic. Controlling for the time including severity, timescale from infection to recruitment and recovery would have not been possible, and at time of recruitment there was no established method of determining antibody response generated.

The patients recruited for the effects of PI3K inhibition on restoring neutrophil function in COVID-19 were well matched demographically to the patients initially recruited. Similarly, disease severity was not significantly different. However, due to the evolving nature of the disease patients recruited for further investigation were infected with the delta SARS-CoV-2 variant (B1.617.2) compared to infection with the alpha SARS-CoV-2 variant (B.1.1.7) described earlier in this chapter. There is insufficient published literature to determine if there

is significant difference in neutrophil function between the strain types. Clinical phenotype of delta COVID-19 would suggest a similar if not more severe disease (Torjesen, 2021).

6.7.5 Conclusion

Investigation into neutrophil function in COVID-19 shows that moderate-severe (WHO class 5) disease is associated with a unique pattern of dysfunction. Increased migratory capacity, NET formation, and impaired phagocytic capacity have been observed compared to both AMC and CAP patients. Expression of surface receptors suggests altered intracellular signalling and membrane trafficking leading to a pattern of expression which has not previously been documented in health or disease states. Inaccurate migration and increased NETosis can lead to increased inflammation which can cause host-mediated tissue damage and severe disease. Inhibition of PI3K did not significantly restore neutrophil function to that seen in AMC and treatments targeting NE and NSPs were also unable to do this. Targeting the underlying dysfunctional processes in neutrophils may highlight potential future treatments in COVID-19 to prevent patient deterioration, as well as further research into understanding the interaction between circulating neutrophils and altered microvascular endothelium. Isolated neutrophil dysfunction by SARS-CoV-2 is unlikely to be the primary driver of this unique inflammatory response, and a more systemic immune approach to treatment will be required.

CHAPTER 7
COVID-19 VARIANTS

7.1 Introduction

Since coronavirus disease 2019 (COVID-19) was declared a pandemic on 11th March 2020, prevention of disease spread has continued to present a challenge to the world's population. In the three years from the first emergence of the virus in Wuhan in November 2019, there have been eight significant variant changes with several subvariants. Major subvariant classification was changed from initial naming based on initial location origin to sequential Greek alphabet characters. Clinical phenotype observed in the NHS varied significantly between infection strains. Waves of infection for alpha and delta variants correlated more closely with mortality rates in comparison to the current prevailing omicron virus.

Outcomes reported from alpha variant infection ranged from mortality from acute respiratory distress syndrome to asymptomatic patients. Patients who required ventilatory support and therefore admission to intensive care accounted for 12% of all COVID-19 related hospital admissions (Sapey et al., 2020). This varied presentation and outcome persists across all COVID-19 variant subtypes, but the risk of death is lower in 2022 (at time of final patient recruitment) compared to the beginning of the pandemic. The UK Office of National Statistics (ONS) reported a 67% reduction in risk of death following infection with omicron variant COVID-19 compared to delta (Statistics, 2022). Worldwide mortality rates echo this picture seen in the UK with the 7 day average of new cases reported by the WHO was 700,000 worldwide to 12,300 deaths in January 2021 compared to September 2021 with 600,000 cases to 9,500 deaths and April 2022 with 1,500,000 new cases and 4096 deaths (WHO, 2023b). Several factors are likely to account for the mortality reduction, including vaccination strategy, national and local lockdown implementation, and novel therapy introduction. Novel therapies which involved repurposing of immunomodulatory drugs targeted common biochemical traits of underlying pathways of inflammation such as raised interleukin-6 (IL-6) observed in the first wave of patients.

However, the evolution of the virus and corresponding changes to mortality and clinical presentation have not been mirrored in the ongoing therapeutic research. Treatments leading

to significant patient symptom and outcome improvement in the first wave have been implemented into guidelines but follow up and update considering viral shifts and their potential differing host-immune responses have not. The change to clinical presentation suggests a different underlying host response to the virus compared to its emergence in November 2019, and therefore new treatment strategies may need to be considered. Similar to seasonal influenza infection, treatments and vaccination may need to reflect the antigenic shift and drift.

Our initial work on the dysfunctional neutrophil response in COVID-19 infection centred around patients recruited with the alpha variant (B1.1.7). We demonstrated in **Chapter 6** of this thesis that neutrophils in COVID-19 had increased migration, decreased phagocytic capacity, and increased NET production. Additionally, there was an altered surface phenotype compared to those previously characterised (Belchamber et al., 2022).

We hypothesised that the change in clinical phenotype of patients infected with subsequent dominant COVID-19 strains was in part driven by changes to neutrophil function.

7.2 Aims of Chapter 7

1. To establish if the clinical phenotype of COVID-19 patients differs between COVID-19 variants.
2. To determine if alterations to neutrophil function previously seen in COVID-19 are sustained with infection in less clinically severe variants.
3. To explore any correlations between neutrophil function and clinical phenotype in this cohort.

7.3 Additional patient recruitment

Patients were recruited as per the criteria in **Chapter 3**.

Additional patients were recruited for investigation for different COVID-19 variant strains. Patients were recruited from a single hospital site, at different times, with PCR COVID-19 swab carried out in certain in-patient admissions. Point of care testing was carried out for the remaining patients to confirm presence of COVID-19.

Recruited patients for each variant: January 2021 (Alpha variant - B1.1.7): Patients were recruited between 19th January 2021 and 3rd March 2021. September 2021 (Delta variant - AY4.2): Patients were recruited between 22nd September 2021 and 13th January 2022. April 2022 (Omicron variant - BA2): Patients were recruited between 6th April 2022 and 22nd April 2022.

7.4 Clinical phenotype

7.4.1 Patient demographics

87 non-ICU COVID-19 patients were recruited for this study. 41 patients with alpha COVID-19 (26M: 15F, mean age 71.5y (58.0-84.0)), 32 patients with delta variant COVID-19 (17M: 15F, mean age 72.0y (51.8-83.0) and 14 patients with omicron variant COVID-19 (5M: 9F, mean age 82.0y (72.5-93.8).

There were no significant differences between recruited variant groups in terms of BMI, ethnicity or comorbidities recorded, as shown in **Table 7.1**. Omicron patients recruited were significantly older than alpha and delta patients (p=0.0087, p=0.0107 respectively).

There was increased mortality in the omicron patients compared to the alpha cohort (p=0.05), with a trend to increased mortality in the delta cohort (p=0.08). Vaccination data was only collected for delta and omicron patients due to the timings of the roll out of the UK vaccination programme. Comparison of patients receiving two or more vaccines between delta and omicron variant patients was made as booster vaccinations were still being rolled out to the general public at this time. There was a significantly higher proportion of patients with two or more vaccinations in the omicron cohort than the delta cohort (p=0.0207).

	COVID-19 (ALL) n=87	COVID-19 (Alpha) n=41	COVID-19 (Delta) n=32	COVID-19 (Omicron) n=14	Significance
Male: Female	48:39	26:15	17:15	5:9	
White: Non-white	66:21	31:10	22:10	13:1	
COVID-19 Variant					
Mortality (%)	17 (19.5%)	10 (24%)	7 (22%)	0 (0%)	Alpha vs omicron p=0.05 Delta vs omicron p=0.08
Age	70.4 (57.0-84.3)	71.5 (58.0-84.0)	72 (51.8-83.0)	82 (72.5-93.8)	Delta vs omicron p=0.0107 Alpha vs omicron p=0.0087
BMI (kg/m^2)	28.6 (23.4-32.6)	26.4 (24.2-32.8)	26.9 (23.2-31.9)	29.3 (23.5-34.6)	
Vaccinations					
0			17 (53%)	1 (7%)	
1			0 (0%)	1 (7%)	
2			10 (31%)	0 (0%)	
2+ booster			4 (12.5%)	12 (85.7%)	>=2 vaccines Delta vs Omicron p=0.0207
Comorbidities					
Cardiovascular	28 (32.2%)	12 (29.3%)	9 (28.1%)	7 (50%)	
Respiratory	7 (8%)	1 (2.4%)	5 (15.6%)	1 (7%)	
Endocrine	39 (44.8%)	16 (39.0%)	17 (53.1%)	6 (42.9%)	
Hypertension	40 (46.0%)	19 (46.3%)	13 (40.6%)	8 (57.1%)	
Other	50 (57.5%)	24 (58.5%)	16 (50%)	10 (71.4%)	

Table 7.1 Demographics from recruited patients for alpha, delta and omicron COVID-19 variants, collected at time of enrolment. Statistical comparisons were made between variant cohorts, as shown in Significance column using a Chi squared test or Kruskal-Wallis test. Results shown as median (IQR). Other comorbidities were included if they caused a significant impact on patient quality of life or regular medication – this included but not limited to: severe peripheral vascular disease with ulceration, dementia, chronic kidney disease, stroke, childhood polio, obesity, diverticulosis, alcohol related liver disease, rheumatoid arthritis.

7.4.2 Biochemical correlations

Biochemically, differences were observed between the omicron cohort vs alpha and delta variants. There were no differences observed between the alpha and delta cohorts. Routine measures of inflammation were higher in omicron patients. WCC and neutrophil count were higher compared to delta patients (p=0.0404, p=0.0221 respectively, **Table 7.2**). C-reactive protein levels (CRP) were significantly lower in omicron patients compared to alpha (p=0.05). Markers originally correlated to disease severity at the beginning of the pandemic such as ferritin and NLR however were not significantly different between variant infections. High sensitivity troponin I levels were higher in omicron patients compared to delta (p=0.05) and d-dimer levels were higher in omicron compared to delta (p=0.0126).

Dexamethasone administration was not significantly different between patient cohorts. Guidance for dexamethasone administration at QEHB Trust during recruitment was for patients to receive dexamethasone if they were requiring supplemental oxygen to maintain saturations of >90%.

	COVID-19 (ALL) n=87	COVID-19 (Alpha) n=41	COVID-19 (Delta) n=32	COVID-19 (Omicron) n=14	Significance
Biochemistry					
WCC (x10^9/L)	10.3 (6.1-11.8)	8.2 (6.3-12.0)	6.7 (5.0-9.8)	10.1 (8.0-13.7)	Delta vs Omicron p=0.0404
Neutrophils (x10^9/L)	7.4 (4.3-8.8)	6.4 (4.4-8.6)	5.2 (3.6-8.7)	8.8 (6.4-12.1)	Delta vs Omicron p=0.0221
CRP (mg/L)	111.0 (43.3-160.3)	103.0 (63.0-165.0)	81.0 (41.0-336.0)	35.5 (24.5-59.8)	Alpha vs omicron p=0.05
NLR	9.4 (4.1-13.3)	5.4 (3.8-10.8)	6.1 (3.1-21.3)	12.9 (6.8-17.4)	
HS Troponin I (ng/L)	123.3 (7.5-36.5)	14.5 (5.0-31.3)	8.0 (5.3-282.0)	22.0 (22.0-26.0)	Delta vs omicron p=0.05
D-dimer (ng/mL)	2005.6 (252.3-837.0)	382.0 (218.0-829.5)	493.0 (241.3-833.0)	1365.5 (374.8-2496.0)	Delta vs omicron p=0.0126
Ferritin (µg/L)	1714.0 (285.3-1489.8)	1082 (428.3-1525.0)	353.5 (203.3-1752.0)	179.0 (133.0-207.5)	
Vitamin D (nmol/L)	49.1 (24.6-62.9)	35.6 (23.0-51.8)	37.8 (23.3-62.3)	51.9 (26.2-64.9)	
Dexamethasone	67 (77.0%)	38 (92.6%)	19 (59%)	10 (71%)	

Table 7.2 Biochemical data from recruited patients, collected at time of enrolment for alpha, delta and omicron COVID-19 patients. WCC- white cell count; CRP- C-reactive protein; NLR- neutrophil lymphocyte ratio; HS Troponin I- high sensitivity troponin I; Statistical comparisons were made between variant cohorts, as shown in Significance column using Kruskal Wallis test for not normally distributed data. Data shown as median (IQR Q1-Q3).

Severity scoring for patients recruited was carried out similarly to that done in **Chapter 5** for patients initially recruited. All patients here were class 5 WHO progression score as per previously recruited. 4C score was used for in-hospital mortality. There was no significant difference between the patients recruited and classified by COVID-19 variant. This was consistent with the calculated qSOFA and CURB-65 scores, **Table 7.3**.

	COVID-19 (ALL) n=87	COVID-19 (Alpha) n=41	COVID-19 (Delta) n=32	COVID-19 (Omicron) n=14	Significance
Admission					
Worst NEWS2	6.0 (4.0-7.0)	6.0 (5.0-7.0)	6.0 (3.0-12.0)	4.0 (4.0-7.8)	
4C	11.3 (9.0-14.0)	12.0 (9.0-14.0)	11.0 (5.8-13.2)	13.0 (10.3-14.0)	
qSOFA	1.0 (1.0-1.0)	1.0 (1.0-1.5)	1.0 (1.0-1.0)	1.0 (1.0-1.0)	
CURB-65	2.0 (1.0-3.0)	2.0 (1.0-3.0)	2.0 (2.0-3.0)	2.0 (2.0-3.0)	
Length of stay (days)	6.0 (3.0-12.0)	5.5 (3.0-12.0)	5.0 (3.0-11.5)	8.0 (5.0-11.8)	

Table 7.3 Clinical data from recruited patients, collected at time of enrolment for alpha, delta and omicron COVID-19 patients. NEWS2- National Early Warning Score 2, data collected was worst score in the 24 hours after admission; qSOFA- quick Sepsis-related Organ Failure Assessment Score; CURB-65- Mortality in community acquired pneumonia. Statistical comparisons were made between variant cohorts, as shown in Significance column using Kruskal Wallis test for not normally distributed data. Data shown as median (IQR Q1-Q3).

There was no significant difference in length of hospital admission between COVID-19 variants. Patients were followed up for outcome at 28 days, 3 months, 6 months and 12 months from recruitment. Readmissions at 28 days are shown in **Table 7.4** with reasons documented. There were no significant differences in mortality between patients admitted with different strains. In addition to patient outcome, radiological changes were reviewed at 6 months and 12 months to determine if any changes persisted.

Variant		In-hospital	28-day		3 month	6 month	12 month
			Mortality	Re-admission			
Alpha	Additional mortality	10/41 (24%)	0/31	2/31 (1 non-related infection, 1 worsening of symptoms)	1/31 (3%)	2/29 (7%)	1/27 (4%)
	Cumulative mortality	10/41 (24%)	10/41 (24%)		11/41 (27%)	13/41 (32%)	14/41 (34%)
Delta	Additional mortality	7/32 (22%)	0/25	5/25 (2 unrelated presentation, 2 with breathlessness	2/25 (8%)	2/23 (9%)	0/21
	Cumulative mortality	7/32 (22%)	7/32 (22%)		9/32 (28%)	11/32 (34%)	11/32 (34%)
Omicron	Additional mortality	0/14	0/14	3/14 (3 unrelated presentation)	1/14 (7%)	1/13 (8%)	1/12 (8%)
	Cumulative mortality	0/14	0/14		1/14 (7%)	2/14 (14%)	3/14 (21%)

Table 7.4 COVID-19 patient clinical outcome data for alpha, delta and omicron COVID-19 patients. Mortality shown as additional deaths at each follow-up time point and as cumulative mortality. Re-admission data was collected at 28 days only. Alpha readmissions: one non-related cellulitis infection and one patient with worsening of COVID-19 symptoms – patient was transferred to ICU care later on in admission. Delta readmissions: one fall, one generally unwell, two presentations with increased breathlessness not treated as COVID-19. Omicron readmissions one generally unwell, one fall, one AKI.

Both patients with follow up imaging at 6 months demonstrated longstanding ground-glass inflammatory changes on CXR. A further 4 patients had a CXR completed at one year after recruitment, with showed no persistent features of infection.

Patients were recruited within 48 hours of hospital admission, but there was considerable variation in date of symptom onset to presentation (alpha median time to presentation 7 days (range 0-19 days), delta 5.5 days (range 0-37 days), omicron 2.5 days (range 0-16 days). However, there was not any significant difference in the length of stay between the three cohorts. Median time to presentation across all cohorts is 6.0 days (3.0-12.0). Alpha variant patients presenting less than 6 days after symptom onset were older ($p=0.026$), had a higher CFS score ($p<0.0001$), lower vitamin D ($p=0.05$) and higher 4C score ($p=0.004$) at admission, as described in **Chapter 5**. These were not observed in delta or omicron patients. There were

no significant clinical biochemical differences in patients with different time to presentation for delta or omicron patients. There was no change to length of stay outcome.

7.5 Functional assays

7.5.1 Phagocytosis

Phagocytosis of labelled S. *pneumoniae* by neutrophils isolated from COVID-19 patients demonstrated significantly higher phagocytosis in delta variant patients compared to alpha and omicron (alpha MFI 6.83 (0.30), delta 15.91 (1.20), omicron 5.59 (1.11), alpha vs delta $p<0.0001$, omicron vs delta $p<0.0001$; alpha % phagocytosis 33.53% (1.96), delta 46.64% (3.37), omicron 37.53% (2.03), alpha vs delta $p=0.0012$, omicron vs delta $p=0.0209$, **Figure 7.1A, B**). There was no difference in cROS production between variants, **Figure 7.1C**. There was significantly reduced n/mROS production in omicron compared to alpha patients (MFI fold change alpha 1.18 (0.07), omicron 0.87 (0.06), $p=0.0014$, **Figure 7.1D**).

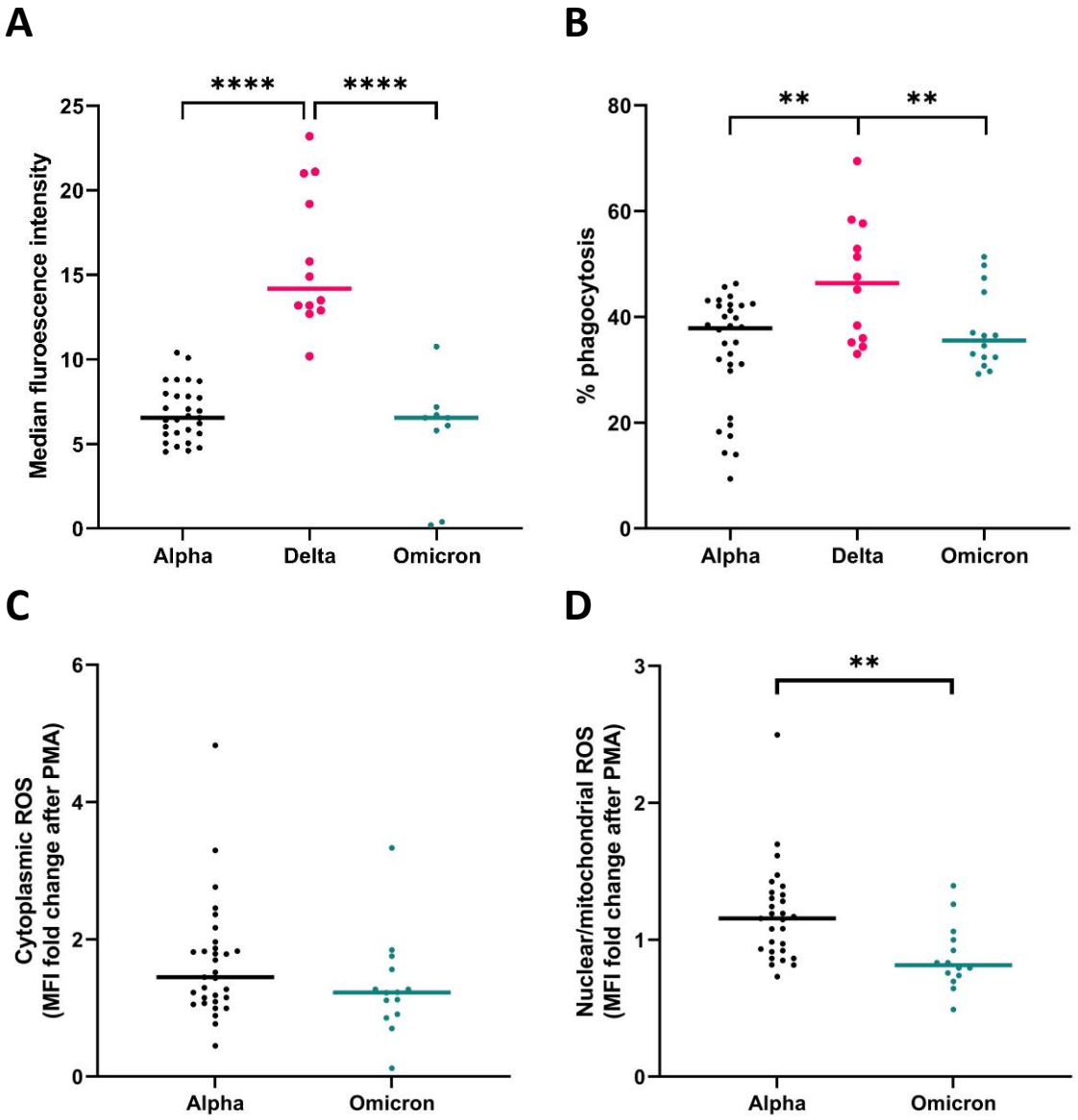

Figure 7.1 Isolated neutrophil phagocytosis of labelled S. pneumonia after 30 minutes compared between COVID-19 variants, alpha n=33, delta n=12, omicron n=14. Data shown as full data spread with median. Kruskal Wallis test used for statistical analysis or Mann Whitney U as data not normally distributed. **A.** phagocytosis MFI **B.** % phagocytosis. **C.** Cytoplasmic ROS generation compared between alpha and omicron COVID-19 patients. **D**. Nuclear/ mitochondrial ROS generation compared between alpha and omicron COVID-19 patients. *p≤0.05, **p≤0.01, ***p≤0.001, ****p≤0.0001

7.5.2 Transwell migration

Neutrophils isolated from omicron patients exhibited significantly reduced transmigration compared to those from alpha and delta patients (median fold change cells migrated alpha 31.7 (8.8-101.1), delta 22.0 (7.2-73.6), omicron 2.5 (1.4-8.5), alpha vs omicron p=0.0002, delta vs omicron p=0.0129, **Figure 7.2**).

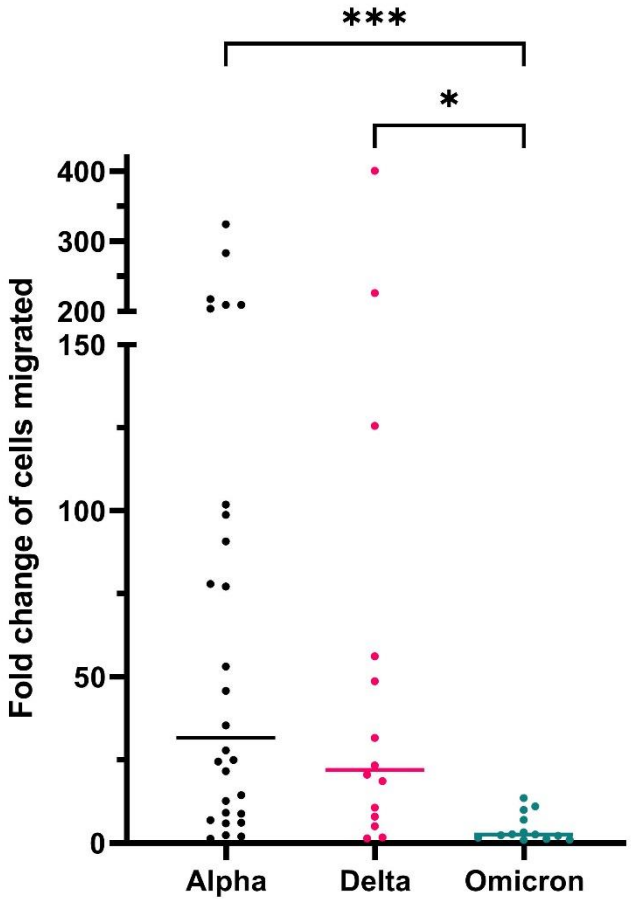

Figure 7.2 Neutrophil migration through a transwell membrane compared between alpha (n=28), delta (n=14), omicron (n=14) COVID-19 patients. Data shown as full data spread with median. Significance calculated using Kruskal-Wallis test for not normally distributed data. *p≤0.05, **p≤0.01, ***p≤0.001, ****p≤0.0001

7.5.3 NETosis

NET formation in response to PMA stimulation was significantly increased in alpha variant patients compared to all other variants (mean alpha NETosis fold change 164.0 (8.7), delta 126.7 (3.1), omicron 121.4 (10.6), alpha vs delta p=0.0043, alpha vs omicron p=0.0043, **Figure 7.3A**). Circulating cfDNA was not significantly different between variants, **Figure 7.3B**. DNase levels were not available for the delta or omicron patients due to prioritisation of experiments.

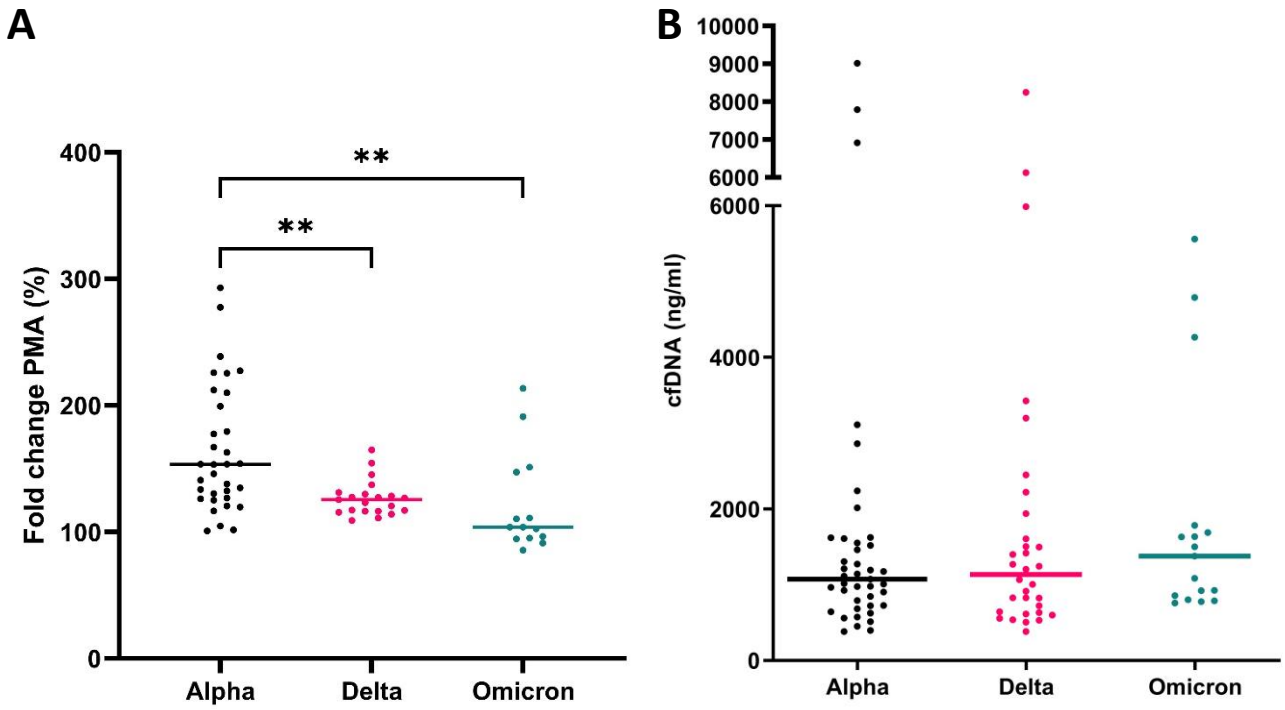

Figure 7.3 NETosis and circulating cfDNA compared between COVID-19 variants from isolated neutrophils, alpha n=36, delta n=25, omicron n=14. Data shown as full data spread with median. Kruskal Wallis test used for statistical analysis for not normally distributed data. **A**. NETosis after stimulation with PMA **B.** cfDNA measured was not significantly different between COVID-19 variants. *p≤0.05, **p≤0.01, ***p≤0.001, ****p≤0.0001

7.5.4 Circulating inflammatory mediators

Plasma concentrations of vascular endothelial growth factor (VEGF) were significantly lower in omicron patients compared to both alpha and delta variant patients (p=0.0002 and p=0.0284 respectively, **Figure 7.4A**). IL-6 concentrations were significantly higher in omicron patients compared to both alpha and delta variant patients (p=0.0037 and p=0.0020 respectively, **Figure 7.4B**). sTNFR1 levels were significantly lower in omicron patients compared to both alpha and delta variant patients (p=0.0027, p=0.0381 respectively, **Figure 7.4C**).

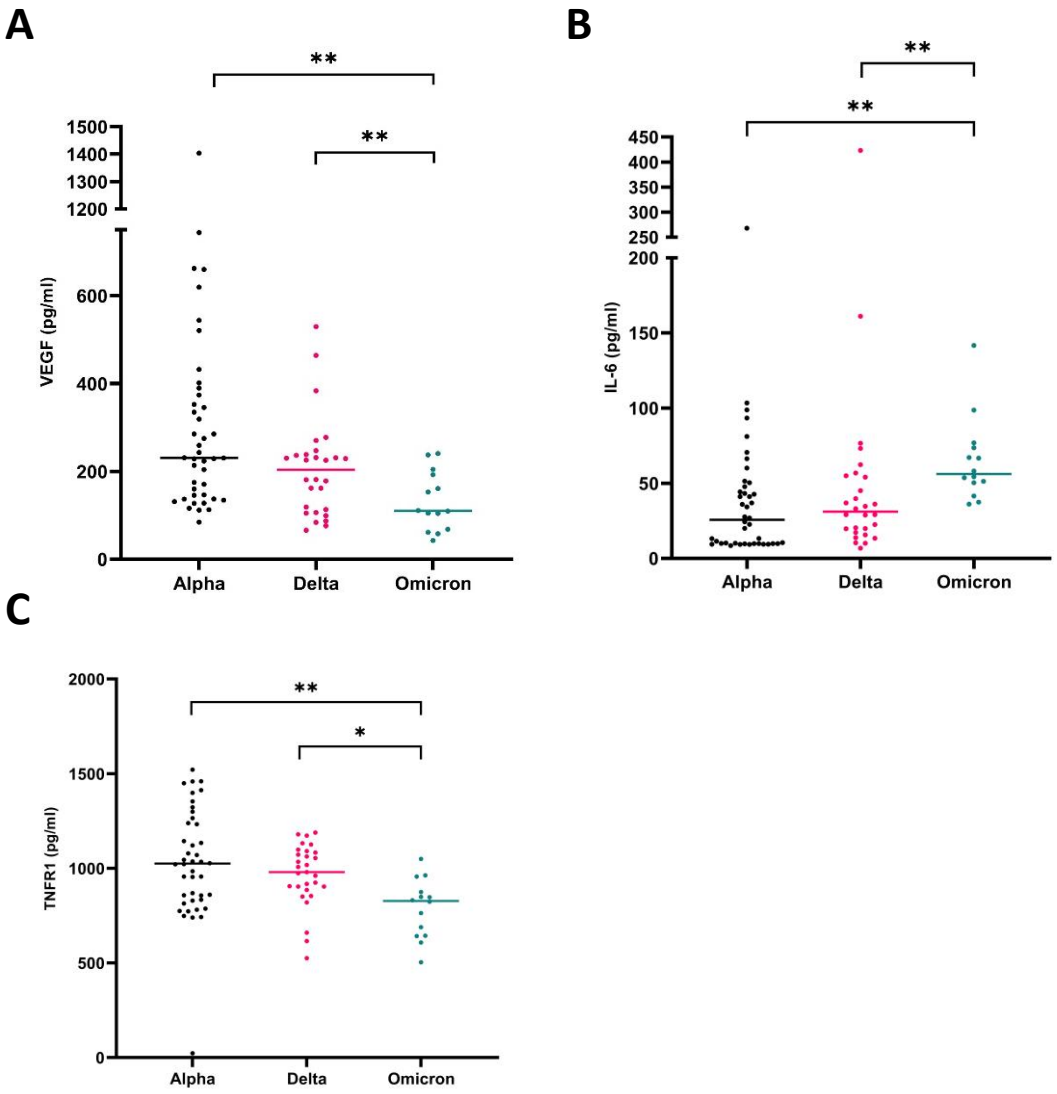

Figure 7.4 Circulating inflammatory mediators, measured by serum ELISA, compared between COVID-19 variants, alpha n=43, delta n=32, omicron n=14. Full data spread shown with median, one-way ANOVA used for statistical analysis of normally distributed data. **A.** VEGF **B**. IL-6 **C.** sTNFR1 *p≤0.05, **p≤0.01, ***p≤0.001, ****p≤0.0001

7.5.5 Surface marker phenotype

Surface marker expression conveying phenotype was compared between alpha and omicron patients. Expression was normalised to AMC cohort and expressed as fold change difference. Percentage receptor expression, MFI values and significance are shown in **Table 7.5**.

In omicron patients compared to alpha there was significantly reduced expression of CD10 (% expression alpha vs omicron p=0.0001, MFI p=0.0004), CD11b (% expression alpha vs omicron p=0.0081, MFI p=0.0607), CD62L (% expression alpha vs omicron p<0.0001, MFI p=0.0013), CXCR2 (% expression alpha vs omicron p=0.0126, MFI p=0.0001), and CD11c (% expression alpha vs omicron p=0.0008, MFI p<0.0001). There was a reduction in the percentage expression fold change of CXCR4 (% expression alpha vs omicron p<0.0001) and PD-L1 (percentage expression alpha vs omicron p=0.0002), but there was no significant difference in MFI fold change for these surface markers. MFI fold change of CD54 was significantly reduced in omicron (MFI alpha vs omicron p=0.0015).

Receptors	% Expression fold change from AMC			MFI fold change from AMC		
	Alpha (n=25)	Omicron (n=14)	p value	Alpha (n=25)	Omicron (n=14)	p value
CD10	1.00 (0.9-1.0)	0.47 (0.3-0.9)	0.0001	1.25 (1.0-1.7)	0.59 (0.5-0.8)	0.0004
CD11b	0.83 (0.6-1.1)	0.46 (0.3-0.8)	0.0081	0.11 (0.0-0.7)	0.38 (0.3-0.7)	0.0607
CD54	2.18 (1.8-2.4)	2.48 (1.7-3.0)	0.1374	3.44 (1.7-4.5)	1.4 (1.0-1.7)	0.0015
CD62L	1.57 (1.3-2.1)	0.39 (0.1-0.6)	<0.0001	1.5 (0.5-25)	0.4 (0.2-0.5)	0.0013
CXCR2	0.99 (1.0-1.0)	0.99 (1.0-1.0)	0.0126	0.82 (0.5-1.1)	1.49 (1.2-1.9)	0.0001
CXCR4	1.00 (0.9-1.0)	0.41 (0.3-0.8)	<0.0001	0.78 (0.59-2.5)	0.9 (0.8-1.1)	0.5340
CD66b	1.00 (0.9-1.0)	0.99 (0.9-1.0)	0.9865	0.72 (0.5-1.1)	0.65 (0.5-0.9)	0.6138
CD11c	1.00 (0.9-1.0)	0.65 (0.5-0.8)	0.0008	5.2 (4.1-7.1)	1.1 (0.8-1.3)	<0.0001
PD-L1	0.85 (0.7-1.2)	0.30 (0.2-0.5)	0.0002	0.45 (0.2-1.0)	1.47 (0.4-0.6)	0.8446

Table 7.5 Fold change of omicron COVID-19 surface receptor expression compared to alpha COVID-19 of percentage of cells expressing and MFI of isolated neutrophil cell surface markers as measured by flow cytometry in alpha (n=25) and omicron (n=14). Data displayed as median (IQR). Data analysed by individual One Way ANOVA with multiple comparisons. Green square indicates significance.

7.6 Relationship of clinical phenotype to function

7.6.1 Clinical outcomes

Length of hospital admission was used as the primary clinical outcome for comparison between COVID-19 cohorts. In-hospital mortality was not used for comparison as all omicron patients survived admission. Median length of stay across all COVID-19 variants was 6.0 days (3.0-12.0). Omicron patients admitted for 6 days or longer had significantly reduced neutrophil migration compared to alpha patients admitted for 6 days or longer (alpha median migration fold change 53.14 (12.7-209.1), omicron 2.67 (1.4-12.3), p=0.0360, **Figure 7.5B**). Otherwise, there was no significant difference between phagocytosis, transwell migration, NETosis or cfDNA levels between variants when separated by length of stay, **Figure 7.5**.

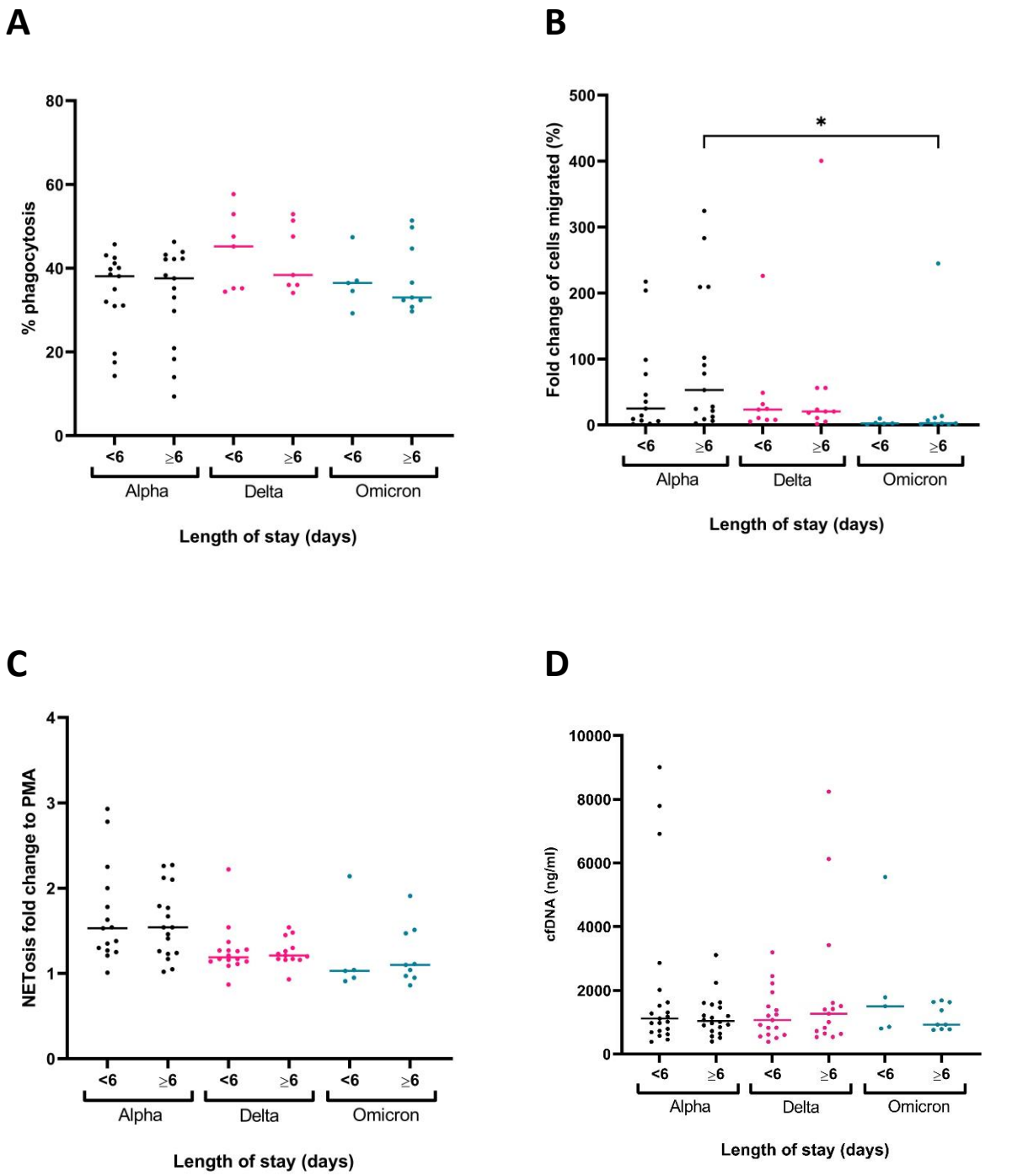

Figure 7.5 Neutrophil effector functions when stratified by length of stay, split between below median (<6 days) and above median (≥6 days) hospital admission for COVID-19 patients with different variant infection. Results shown as full data spread with median. Kruskal Wallis test used for statistical analysis of non parametric data. **A**. Phagocytosis of labelled *S. pneumoniae* after 30 minutes (alpha <6 n=15, ≥6 n=15; delta <6 n=7, ≥6 n=7; omicron <6 n=5, ≥6 n=9). **B**. Neutrophil transwell migration towards CXCL8 after 90 minutes (alpha <6 n=13, ≥6 n=15; delta <6 n=9, ≥6 n=10; omicron <6 n=5, ≥6 n=9). **C.** NETosis after PMA stimulation after 3 hours (alpha <6 n=15, ≥6 n=17; delta <6 n=16, ≥6 n=13; omicron <6 n=5, ≥6 n=9). **D**. Circulating cfDNA measured in serum (alpha <6 n=21, ≥6 n=20; delta <6 n=17, ≥6 n=15; omicron <6 n=5, ≥6 n=9).

Symptom onset

The mean time from symptom onset to presentation was 6 days (3.0-10.8) across all COVID-19 variants. NETosis was significantly lower in omicron patients presenting <6 days after symptom onset compared to alpha patients presenting in this time (alpha median NETosis fold change 1.54 (1.3-2.1), omicron 1.04 (0.9-1.5), p=0.0103, **Figure 7.6C**). There were no other significant neutrophil functional differences between variants when separated by time from symptom onset to presentation, **Figure 7.6A, B, D**.

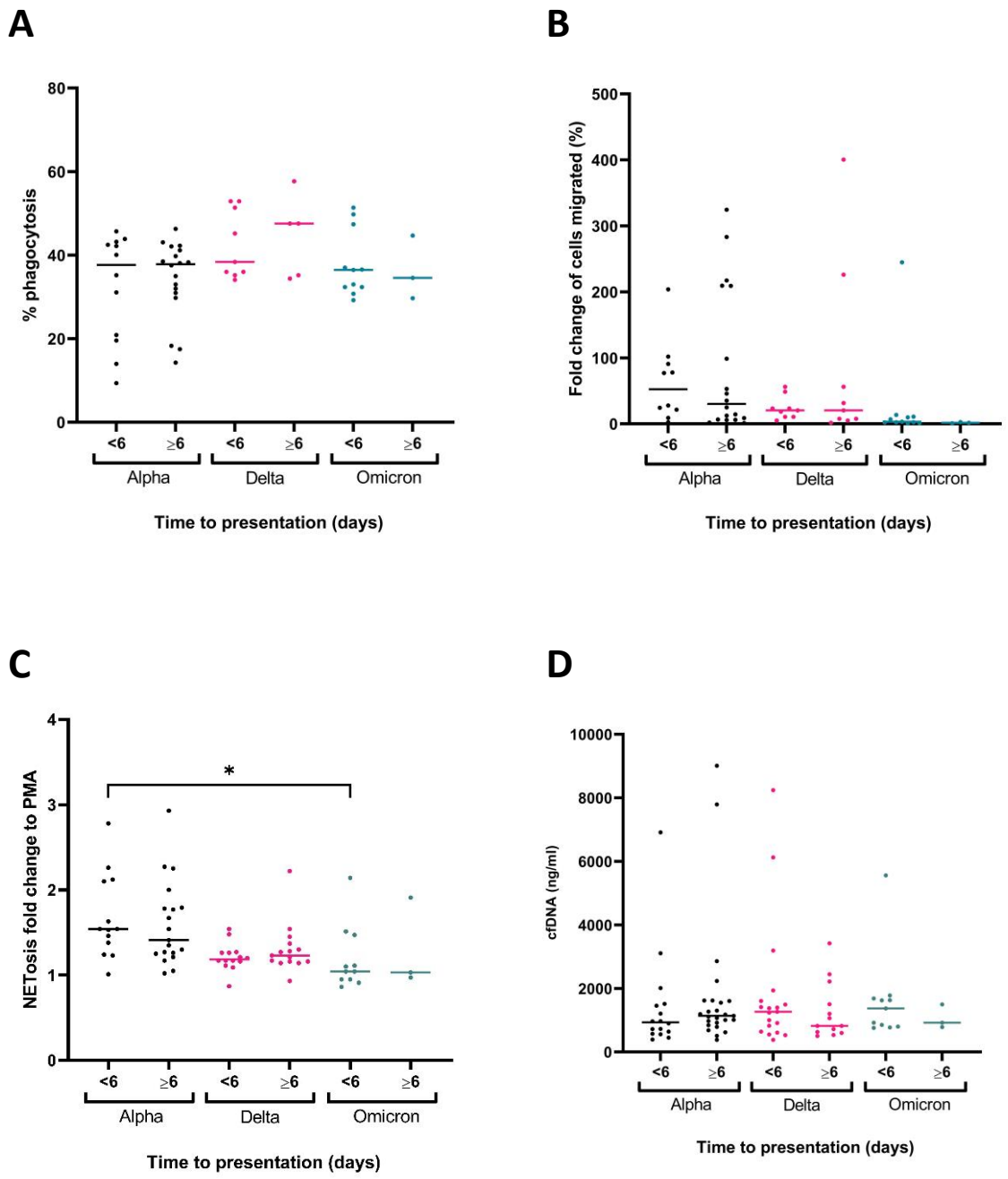

Figure 7.6 Differences in neutrophil effector functions from different COVID-19 variant infections when stratified by time from symptom onset to presentation, separated by median overall time to presentation split between below median (<6) and above median (≥6) days hospital admission. Results shown as full data spread with median. Kruskal Wallis test used for statistical analysis of not normally distributed data **A.** Phagocytosis of labelled *S. pneumoniae* after 30 minutes (alpha <6 n=12, ≥≥6 n=18; delta <6 n=9, ≥≥6 n=5; omicron <6 n=3, ≥≥6 n=11). **B.** Neutrophil transwell migration towards CXCL8 after 90 minutes (alpha <6 n=10, ≥≥6 n=18; delta <6 n=9, ≥≥6 n=9; omicron <6 n=3, ≥≥6 n=11) **C.** NETosis after PMA stimulation after 3 hours (alpha <6 n=13, ≥≥6 n=19; delta <6 n=14, ≥≥6 n=15; omicron <6 n=3, ≥≥6 n=11). **D.** Circulating cfDNA measured in serum (alpha <6 n=16, ≥≥6 n=25;

When stratified by time to presentation, circulating VEGF was higher in alpha patients presenting within 6 days compared to both delta and omicron patients (alpha median VEGF 267.2pg/mL (165.8-441.7), delta 123.6pg/mL (82.6-228.5), omicron 104.9pg/mL (61.3-161.3), alpha vs delta p=0.0284, alpha vs omicron p=0.0023, **Figure 7.7B**). sTNFR1 was significantly lower in omicron patients presenting within 6 days compared to both alpha and delta patients (alpha median sTNFR1 1187pg/mL (861.4-1410), delta 1005pg/mL (919.8-1162), omicron 763.5pg/mL (642.0-849.7), omicron vs alpha p=0.0005, omicron vs delta p=0.0113, **Figure 7.7A**). There was no significant difference in IL-6 levels between patients presenting within 6 days or longer than 6 days **Figure 7.7C**.

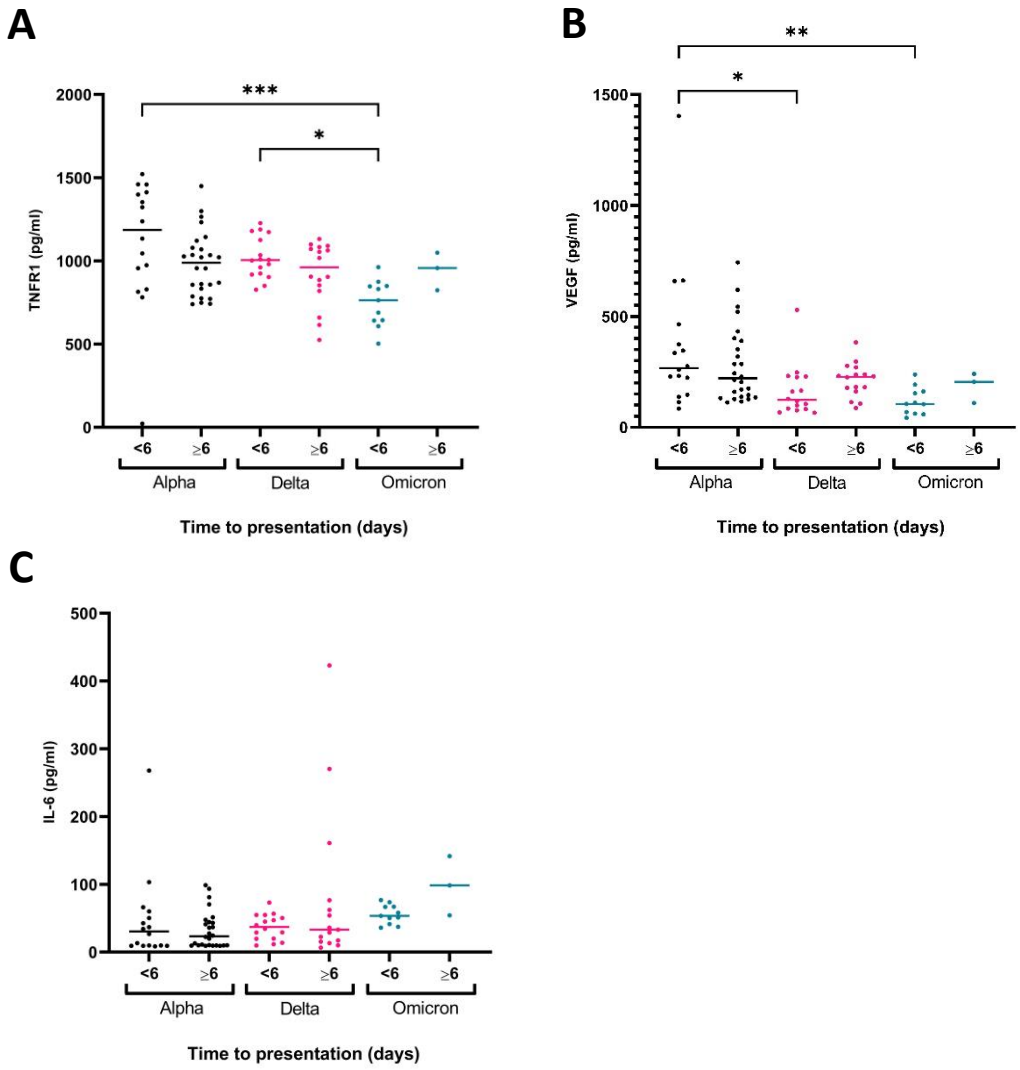

Figure 7.7 Differences in circulating inflammatory mediators from different COVID-19 variant infections when stratified by time from symptom onset, separated by median overall time to presentation, split between below median (<6 days) and above median (≥6 days) hospital admission (alpha <6 n=16, ≥6 n=26; delta <6 n=16, ≥6 n=16; omicron <6 n=3, ≥6 n=11). Full data spread shown with median. Kruskal Wallis test used for statistical analysis of not normally distributed data **A**. sTNFR1 **B.** VEGF **C**. IL-6

7.6.2 4C

Patients were stratified according to disease severity using the 4C score validated against initial COVID-19 disease caused by wild-type virus. Patients were classified as either high-or low-risk mortality based on score, <9 low-risk, ≥9 high-risk. There was no significant difference in neutrophil phagocytosis across variants when split by 4C score. Neutrophil migration was significantly reduced in high-risk omicron patients compared to high-risk alpha patients (median alpha fold change cells migrated 4C ≥9 36.88 (9.0-205.2), omicron 4C ≥9 2.67 (1.2-11.0), p=0.0256, **Figure 7.8B**). NETosis was increased in low-risk alpha patients compared to high-risk delta patients (median alpha NETosis 4C <9 1.78 (1.3-2.8), delta ≥9 1.20 (1.2-1.3), p=0.0318, **Figure 7.8C**). NETosis was significantly higher in both low- and high-risk alpha patients compared to high-risk omicron patients (median alpha NETosis 4C <9 1.78 (1.3-2.8), alpha ≥9 1.46 (1.2-1.8), omicron ≥9 1.04 (0.9-1.5), alpha 4C <9 vs omicron p=0.0060; alpha 4C ≥9 vs omicron p=0.0224). There were no significant differences in circulating cfDNA between variants or when sub-stratified by 4C score, **Figure 7.8D.**

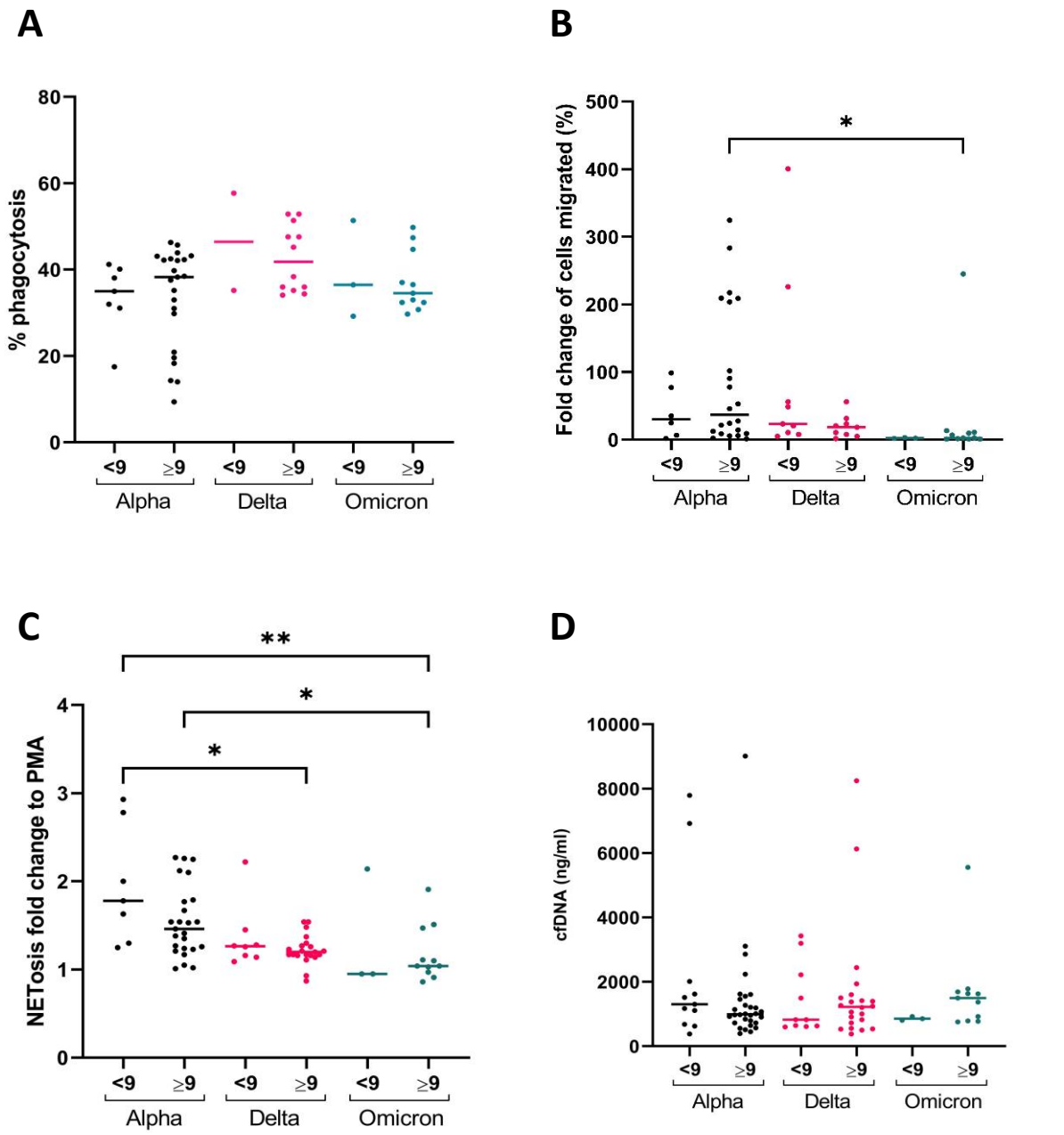

Figure 7.8 Differences in neutrophil effector functions from different COVID-19 variant infections when stratified by 4C in-hospital mortality risk, split 4C score <9 and ≥9. Results shown as full data spread with median. Kruskal Wallis test used for statistical analysis of not normally distributed data. **A.** Neutrophil phagocytosis to labelled *S. pneumoniae* (alpha 4C<9 n=7, 4C≥9 n=23; delta 4C<9 n=2, 4C≥9 n=12; omicron 4C<9 n=3, 4C≥9 n=11). **B.** Neutrophil transwell migration towards CXCL8. (alpha 4C<9 n=6, 4C≥9 n=22; delta 4C<9 n=9, 4C≥9 n=9; omicron 4C<9 n=3, 4C≥9 n=11. **C.** NETosis after 3 hours PMA stimulation, alpha 4C<9 n=7, 4C≥9 n=25; delta 4C<9 n=8, 4C≥9 n=21; omicron 4C<9 n=3, 4C≥9 n=11). **D.** Circulating cfDNA measured in the serum (alpha 4C<9 n=11, 4C≥9 n=30; delta 4C<9 n=10, 4C≥9 n=22; omicron 4C<9 n=3, 4C≥9 n=11)

7.6.3 Vaccination status

The UK vaccination program for COVID-19 was not rolled out during the alpha wave. At the time of recruitment of omicron patients those admitted had the same vaccination status. The delta wave of recruitment represents the only cohort where there is significant grouping of patients unvaccinated and vaccinated. Patients who received a vaccine were more likely to be Caucasian and older (p=0.0207 and p=0.0004 respectively), **Table 7.6**.

	COVID-19	
	No vaccine n=17	At least 1+ vaccine dose n=14
Male: Female	9:8	7:7
White: Non-white	9:8	13:1*
Age	56.0 (42.4-72.0)	81 (73.8-97.0)**
BMI (kg/m^2)	27.2 (22.1-32.4)	25.6 (23.3-31.2)
Died	9:8	7:7

Table 7.6 Table showing demographics of vaccinated vs unvaccinated patients. Data shown as median (IQR). Fisher's exact test and t-test used for not normally distributed categorical and normally distributed data respectively.

CRP was significantly higher in patients with 2 or more vaccinations (mean CRP no vaccine 48.5 mg/L (37.5-95.5), 2+ vaccinations 157 mg/L (72.3-210), p=0.0471,). CFS was significantly higher in patients with 2 or more vaccinations (median CFS no vaccine 1.0 (1.0-3.2), 2+ vaccinations 5.0 (2.0-5.5), p=0.0103,). 4C score was significantly higher in patients with 2 or more vaccinations (median 4C score no vaccine 7.0 (3.0-12), 2+ vaccinations 12.0 (10.0-16.0), p=0.0024,), **Table 7.7**. Circulating VEGF was significantly lower in patients with 2 vaccinations (mean VEGF no vaccine 218.7 pg/mL (24.9), 2+ vaccinations 143.2 pg/mL (19.0), p=0.0339,). There were no significant differences between unvaccinated and vaccinated patients in terms of neutrophil effector functions.

	COVID-19	
	No vaccine n=17	At least 1+ vaccine dose n=14
WCC (x10^9/L)	5.7 (4.8-6.7)	9.6 (7.3-15.3)*
Neutrophils (x10^9/L)	4.2 (3.4-5.3)	8.6 (4.6-10.4)*
CRP (mg/L)	48.5 (37.5-95.5)	157 (72.3-210.0)*
NLR	4.3 (2.6-8.6))	6.7 (4.8-14.5)
HS Troponin I (ng/L)	7.0 (4.5-12.5)	15.5 (6.8-90.0)
D-dimer (ng/mL)	462.0 (252.5-676.3)	490.0 (227.0-834.0)
Ferritin (ug/L)	1393.0 (230.8-15007)	298.5 (185.8-769.5)
Vitamin D (nmol/L)	30.1 (22.9-66.1)	38.0 (28.9-63.4)
4C	7.0 (3.0-12.0)	12.0 (10.0-16.0)*
Worst NEWS2	5.0 (3.0-7.5)	6.5 (3.0-10.0)
qSOFA	1.0 (1.0-1.0)	1.0 (1.0-2.0)*
Length of stay (days)	5.0 (3.0-11.5)	7.5 (2.8-21.0)

Table 7.7 Table showing biochemical and severity scoring data for vaccinated and unvaccinated COVID-19 patients. Data shown as median (IQR) and Mann Whitney U test used for statistical analysis of not normally distributed data.

7.7 Omicron comparison to AMC and CAP

Omicron patients compared to AMC were older (median age omicron 82 years (72.5-93.8), AMC 70 years (61.0-78.0), p=0.0009), and had a higher incidence of cardiovascular co-morbidities (omicron 7/14 (50%), AMC 4/26 (15%), p=0.0292), as in **Table 7.8**. Omicron patients had a higher incidence of endocrine comorbidities than CAP (omicron 6/14 (43%), CAP 3/26 (12%)).

Biochemically CRP was significantly higher in CAP compared to omicron (omicron median CRP 35.5 (24.5-59.8), CAP 119.0 (42.0-396.0), p=0.0715) and no CAP patients were administered dexamethasone, **Table 7.9**. There was no significant difference in scoring disease severity or length of stay between omicron and CAP patients, .

	COVID-19 (Omicron) n=14	AMC n=26	CAP n=26	Significance
Male: Female	5:9	10:16	15:11	
White: Non-white	13:1	24:2	23:3	
Mortality (%)	0 (0%)	0 (0%)	2 (8%)	
Age	82 (72.5-93.8)	70 (61.0-78.0)	67.5 (54.5-85.0)	Omicron vs AMC p=0.0009
BMI (kg/m^2)	29.3 (23.5-34.6)		27.9 (23.3-41.1)	
Vaccinations				
0	1 (7%)			
1	1 (7%)			
2	0 (0%)			
2+ booster	12 (85.7%)			
Comorbidities				
Cardiovascular	7 (50%)	4 (15.3%)	7 (26.9%)	Omicron vs AMC p=0.0292
Respiratory	1 (7%)	0 (0%)	4 (15.4%)	Omicron vs CAP p=0.0444
Endocrine	6 (42.9%)	10 (38.4%)	3 (11.5%)*	
Hypertension	8 (57.1%)	13 (50%)	10 (38.5%)	
Other	10 (71.4%)	11 (42.3%)	15 (57.7%)	

Table 7.8 Demographic data for omicron, AMC and CAP with significance shown. Data displayed as median (IQR) for non-parametric data. Statistics calculated using Kruskal Wallis test for multiple comparisons of not normally distributed data.

	COVID-19 (Omicron) n=41	CAP n=26	Significance
WCC (x10^9/L)	10.1 (8.0-13.7)	13.4 (10.7-16.4)	
Neutrophils (x10^9/L)	8.8 (6.4-12.1)	11.2 (7.8-13.6)	
CRP (mg/L)	35.5 (24.5-59.8)	119.0 (42.0-396.0)*	p=0.0715
NLR	12.9 (6.8-17.4)	8.5 (5.9-52.7)	
HS Troponin I (ng/L)	22.0 (22.0-26.0)	17.5 (4.0-318.0)	
D-dimer (ng/mL)	1365.5 (374.8-2496.0)	659.0 (270.5-1510.0)	
Ferritin (µg/L)	179.0 (133.0-207.5)	110.0 (78.8-225.3)	
Vitamin D (nmol/L)	51.9 (26.2-64.9)	45.3 (23.8-73.2)	

Table 7.9 Biochemical data for omicron and CAP patients with significance shown. Data displayed as median (IQR) for non-parametric data. Statistics calculated using Mann Whitney test for non-parametric data. No biochemical data was recorded for AMC.

	COVID-19 (Omicron) n=14	CAP n=26
Worst NEWS2	4.0 (4.0-7.8)	5.0 (3.0-12.0)
4C	13.0 (10.3-14.0)	11.0 (5.3-13.0)
qSOFA	1.0 (1.0-1.0)	1.0 (1.0-1.0)
CURB-65	2.0 (2.0-3.0)	2.0 (2.0-2.0)
Length of stay (days)	8.0 (5.0-11.8)	4.0 (3.0-7.5)

Table 7.10 Disease severity scoring and length of stay for omicron and CAP patients – no significance is shown as there is no significant difference in these parameters. Data displayed as median (IQR) for non-parametric data. Statistics calculated using Mann Whitney test for non-parametric data. No biochemical data was recorded for AMC.

Comparison of neutrophil functions showed no significant difference in % phagocytosis of labelled *S. pneumoniae*, but significantly higher MFI in omicron vs AMC (MFI omicron 6.55 (3.5-7.0), AMC 1.69 (1.1-2.4), p=0.0312, **Figure 7.9B**). n/mROS production was significantly higher in AMC compared to both omicron and CAP (n/mROS fold change omicron 0.81 (0.7-1.0), AMC 1.41 (1.3-1.7), CAP 0.93 (0.7-1.2), omicron vs AMC p<0.0001, CAP vs AMC p=0.0011, **Figure 7.9D**).

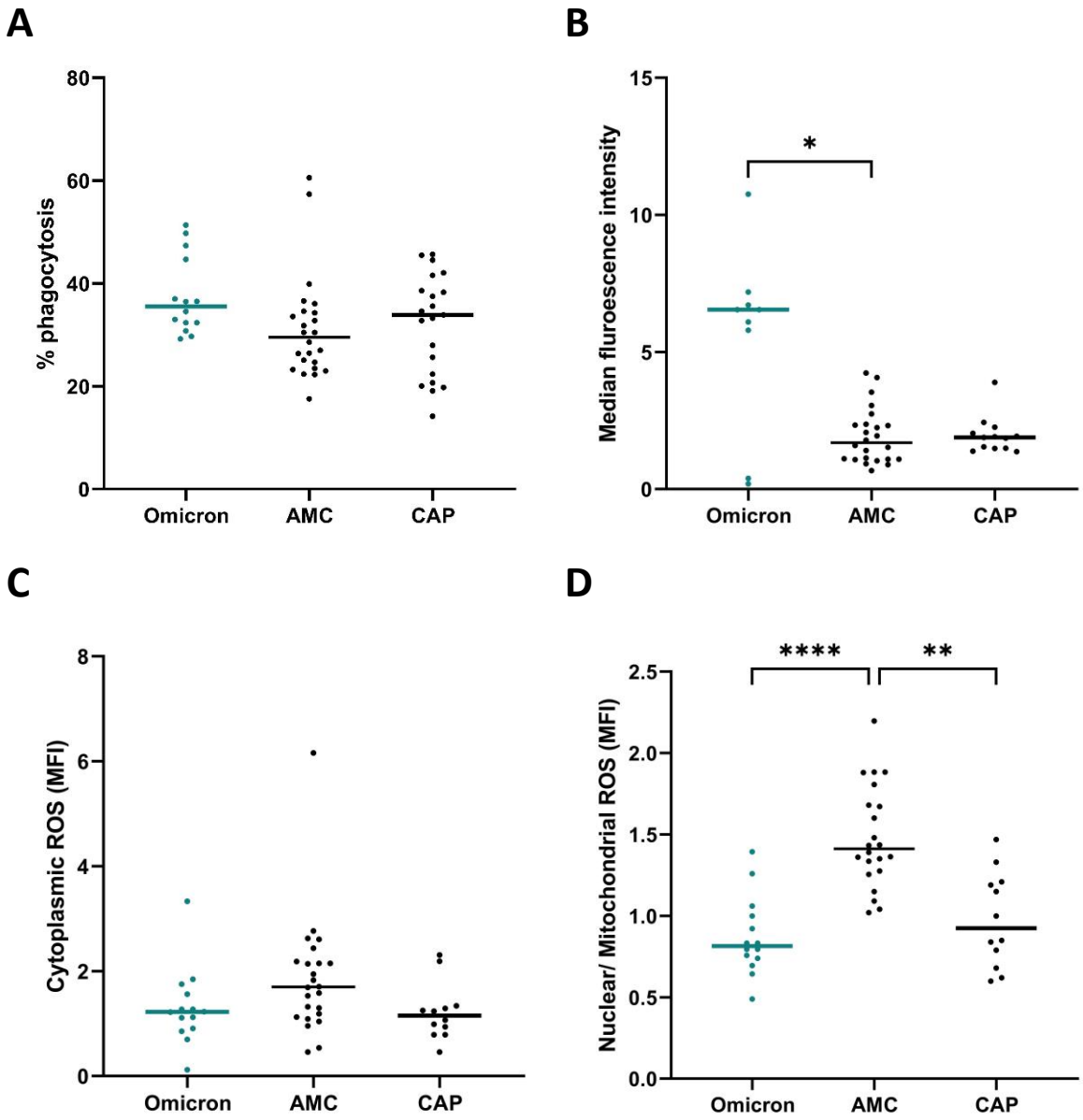

Figure 7.9 Neutrophil phagocytosis of labelled *S. pneumoniae* and reactive oxygen species (ROS) generation compared between omicron COVID-19, AMC and CAP, omicron n=14, AMC n=26, CAP n=26. Full data spread shown with median. Kruskal Wallis test used for statistical analysis of not normally distributed data**. A.** Neutrophil % phagocytosis of labelled *S. pneumoniae* after 30 minutes**. B.** Neutrophil phagocytosis MFI of labelled *S. pneumoniae* after 30 minutes, **C.** Cytoplasmic ROS production after 30 minutes phagocytosis. **D.** Nuclear/ mitochondrial ROS production after 30 minutes phagocytosis,

There was significantly reduced omicron neutrophil migration compared to AMC and CAP (omicron fold change migration 2.55 (1.4-8.5), CAP 20.29 (3.9-39.7), AMC 11.99 (4.4-51.8), omicron vs CAP p=0.0114, omicron vs AMC p=0.0051, **Figure 7.10A**). NETosis was

significantly decreased in omicron compared to AMC (omicron fold change NETosis 103.9 (95.1-148.4), AMC 127.9 (116.5-144.7), p=0.0290, **Figure 7.10B**. There was no significant difference in circulating cfDNA, **Figure 7.10C**. Circulating inflammatory mediators were significantly different in omicron compared to AMC and CAP as shown in **Table 7.11**.

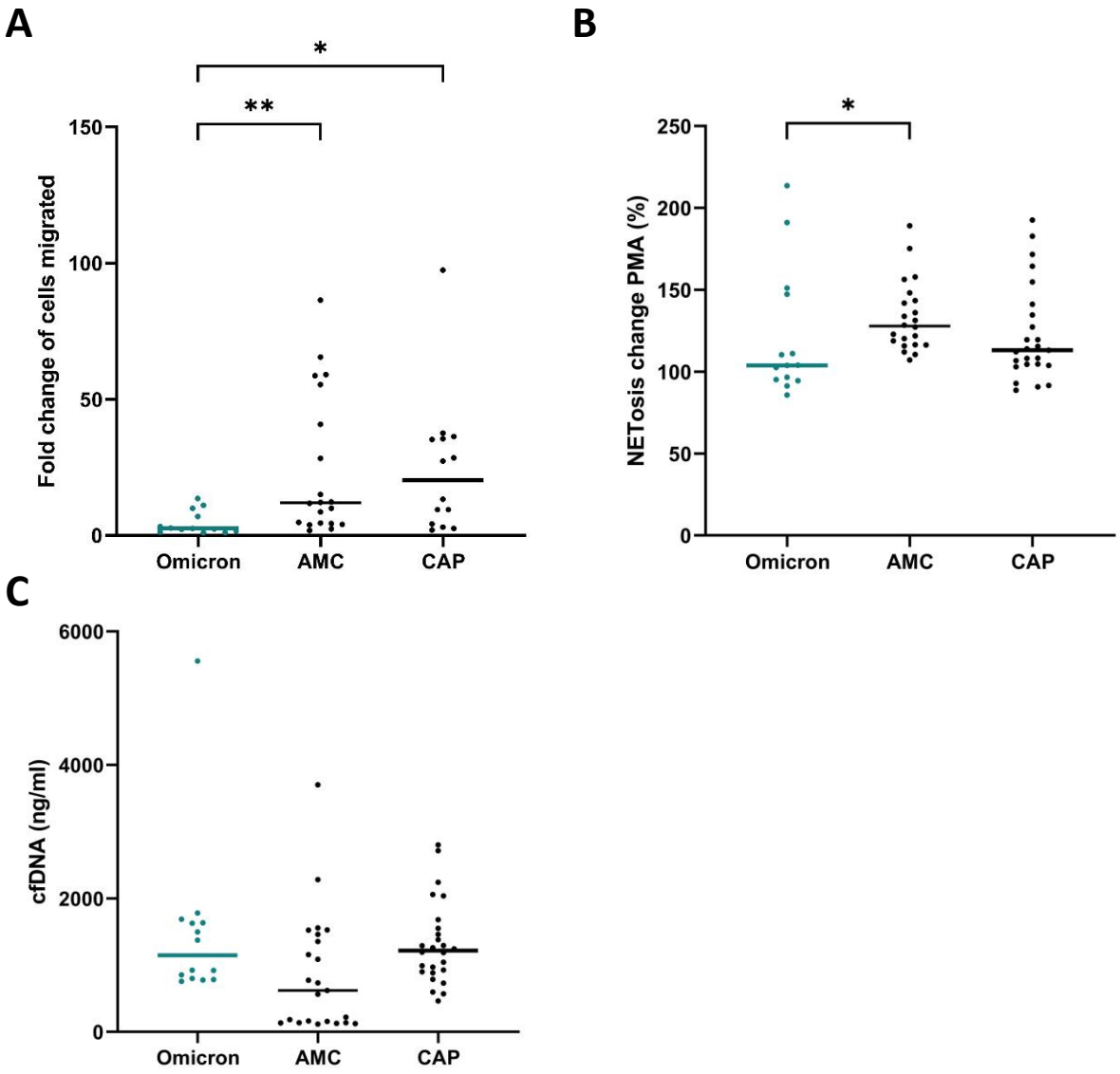

Figure 7.10 Neutrophil transwell migration, NETosis after PMA stimulation and serum cfDNA comparison between omicron COVID-19, AMC and CAP. Full data spread shown with median. Kruskal Wallis test used for statistical analysis of not normally distributed data **A.** Neutrophil transwell migration, Omicron n=14, AMC n=20, CAP n=15. **B.** NETosis after PMA stimulation for 3 hours, Omicron n=14, AMC n=24, CAP n=25. **C.** Circulating cfDNA measured by ELISA. Omicron n=14, AMC n=24, CAP n=25

	Omicron (n=14)	AMC (n=26)	CAP (n=26)	Significance
VEGF	110.2 (66.7-195.7)	118.5 (80.9-187.0)	223.0 (158.5-285.2)	Omicron vs CAP p=0.0078 AMC vs CAP p=0.0011
IL-6	56.2 (48.2-74.5)	10.39 (9.5-12.1)	26.48 (15.6-56.5)	Omicron vs AMC p<0.0001 AMC vs CAP p<0.0001
sTNFR1	827.7 (643.6-895.7)	620.7 (30.9-731.7)	980.9 (852.8-1151)	AMC vs CAP p<0.0001
MPO	46.4 (38.2-58.3)	80.4 (22.4-142.2)	103.2 (86.1-123.2)	Omicron vs CAP p=0.0003

Table 7.11 Circulating inflammatory mediators in omicron COVID-19, AMC and CAP as measured by ELISA. Data displayed as median (IQR). One-way ANOVA used for statistical analysis of normally distributed data**.**

Neutrophil surface marker expression in omicron patients was significantly different to AMC,

MFI and percentage expression with significance values shown in **Table 7.12**.

Receptors	% Expression fold change from AMC			MFI fold change from AMC		
	Omicron (n=14)	AMC (n=26)	p value	Omicron (n=14)	AMC (n=26)	p value
CD10	0.47 (0.3-0.9)	1.00 (0.9-1.0)	0.0003	0.59 (0.5-0.8)	1.00 (0.9-1.4)	0.0023
CD11b	0.46 (0.3-0.8)	1.00 (0.9-1.0)	<0.0001	0.38 (0.3-0.7)	0.99 (0.7-1.2)	0.0800
CD54	2.48 (1.7-3.0)	1.00 (0.6-1.6)	<0.0001	1.4 (1.0-1.7)	1.00 (0.6-2.1)	>0.9999
CD62L	0.39 (0.1-0.6)	1.00 (0.8-1.4)	0.0057	0.4 (0.2-0.5)	1.00 (0.8-1.4)	0.0102
CXCR2	0.99 (1.0-1.0)	1.00 (1.0-1.0)	0.0080	1.49 (1.2-1.9)	1.00 (0.7-1.2)	0.0180
CXCR4	0.41 (0.3-0.8)	1.00 (0.9-1.0)	0.0008	0.9 (0.8-1.1)	1.00 (0.6-2.3)	>0.9999
CD66b	0.99 (0.9-1.0)	1.00 (1.0-1.0)	>0.9999	0.65 (0.5-0.9)	1.00 (0.5-1.3)	0.4344
CD11c	0.65 (0.5-0.8)	1.00 (1.0-1.0)	0.0332	1.1 (0.8-1.3)	0.93 (0.5-1.9)	>0.9999
PD-L1	0.30 (0.2-0.5)	1.00 (0.8-1.2)	0.0003	1.47 (0.4-0.6)	1.00 (0.6-1.4)	0.1768

Table 7.12 Fold change of omicron COVID-19 surface receptor expression compared to AMC of percentage of cells expressing and MFI of isolated neutrophil cell surface markers as measured by flow cytometry in omicron (n=14) and AMC (n=26). Data displayed as median (IQR). Data analysed by individual One Way ANOVA with multiple comparisons. Green square indicates significance.

7.8 Discussion

7.8.1 Clinical outcomes

Omicron patients had lower mortality than either alpha or delta patients recruited, reflecting the observational literature of less severe omicron infection (OurWorldInData, 2022). This is despite an increased mean age compared to both alpha and delta cohorts. Most biochemical differences were between the omicron cohort and the alpha/ delta patients. Higher WCC, differential neutrophil count and lower CRP were noted in omicron patients.

Patients recruited to represent alpha, delta and omicron variant COVID-19 were well demographically matched, with an increased age noted for the omicron admissions. Collectively, the changes observed with COVID-19 variant progression suggest a milder inflammatory state in omicron infected patients compared to alpha. Although the severity of patients recruited according to the 4C score was not significantly different between the recruited cohorts, the overall mortality in the omicron cohort was significantly lower despite an overall older patient group. Validation of the 4C score has been repeated in omicron patients, which confirms its use with the current dominant strain (De Vito et al., 2023). However, mortality rates in each of the categories was reduced 22.5% lower (53.8% vs 47.1%) in the very high risk of death group (De Vito et al., 2023). This supports the data from the omicron cohort here.

7.8.2 Cellular outcomes

Neutrophil dysfunction in alpha COVID-19 has been documented in **Chapter 6**. Neutrophils isolated from these patients demonstrated significant changes across all effector functions, with decreased phagocytic capacity, increased migration, increased NETosis and altered surface marker expression (**Figure 7.11**). It is likely that neutrophil dysfunction played a role in the clinical outcomes that were observed with this variant infection. From clinical

observational data and epidemiological worldwide data, the subsequent omicron variant displays less severe COVID-19 infection. Examination of neutrophils from patients infected with omicron variant COVID-19 was therefore important to determine if infection severity may be linked to restoration of neutrophil function.

Phagocytosis in the delta variant patient was significantly increased compared to neutrophils isolated from both omicron and alpha patients. The delta variant was shown to have increased transmissibility compared to the previous alpha variant (Hart et al., 2022). Patients infected with the delta variant COVID-19 displayed a higher viral load during illness and potentially a different response to vaccination compared to other variants (Duong, 2021). There was no significant difference in neutrophil effector functions between patients who are vaccinated and unvaccinated in the delta cohort.

Impaired phagocytosis can lead to a prolonged secondary bacterial infection leading to associated tissue damage. This can cause more severe disease and lead to mortality. Phagocytosis in omicron patients was not significantly different to alpha patients but mortality was lower in the omicron cohort. Combining this with cytokine and neutrophil phenotype differences between these cohorts suggests there may be less host mediated tissue damage and therefore reduced impact and invasiveness of secondary bacterial infection.

Migration was reduced compared to alpha patients, which was higher than in AMC and CAP comparators. Although migration in omicron was lower than AMC and CAP, this may suggest more accurate neutrophil migration compared to the alpha cohort.

NETosis was significantly decreased compared to alpha variant neutrophils, which may account for the fewer thromboembolic events noted (Khalafallah et al., 2016, Cui et al., 2020). In addition, NETs play an important role in the amount of systemic inflammation, which again may be contributing to the overall dampened inflammatory phenotype of omicron infection. When compared to AMC and CAP, NET formation levels were more similar to those in CAP. Omicron COVID-19 as a milder lower respiratory tract infection phenotype would fit with this.

It was not possible to examine the effects of vaccination across all COVID-19 variants, due to the rollout of the vaccination program during recruitment. It was possible to examine the differences in vaccinated and unvaccinated patients in the delta cohort as this coincided with the rollout of vaccination. Vaccinated patients had a higher CFS score and 4C score compared to those unvaccinated. This reflects the targeted vaccination programme towards the elderly and those at risk or frailer. This would be in keeping with a successful vaccination effect as unvaccinated patients who are less frail requiring hospital admission would suggest a more severe infection response. Higher 4C scores in vaccinated patients might suggest that those who are vaccinated with lower scores had reduced clinical symptoms and therefore did not seek medical advice or require hospital admission. The most common presenting symptoms of COVID-19 have been reported as pyrexia, cough, shortness of breath (2020). Measurement of SpO_2/FiO_2 ratio was used as a surrogate for breathlessness and temperature on a mission was used as a surrogate for pyrexia. Patients who are unvaccinated had higher temperatures on admission compared to vaccinated patients, but there was no difference in SpO_2/FiO_2 ratio. This may mean that symptoms prior to admission are less severe in those vaccinated.

7.8.3 Compared to AMC and CAP

A summary of the changes observed between AMC, alpha COVID-19 and omicron COVID-19 is detailed in **Figure 7.11**. Neutrophil functions are clearly altered compared to both alpha and AMC neutrophils. Objectively there are fewer differences between omicron COVID-19 neutrophils and those from AMC, suggesting there is some restoration of function. However, the differences from AMC neutrophils suggest that there is an ongoing effect of the SARS-CoV-2 virus on underlying function.

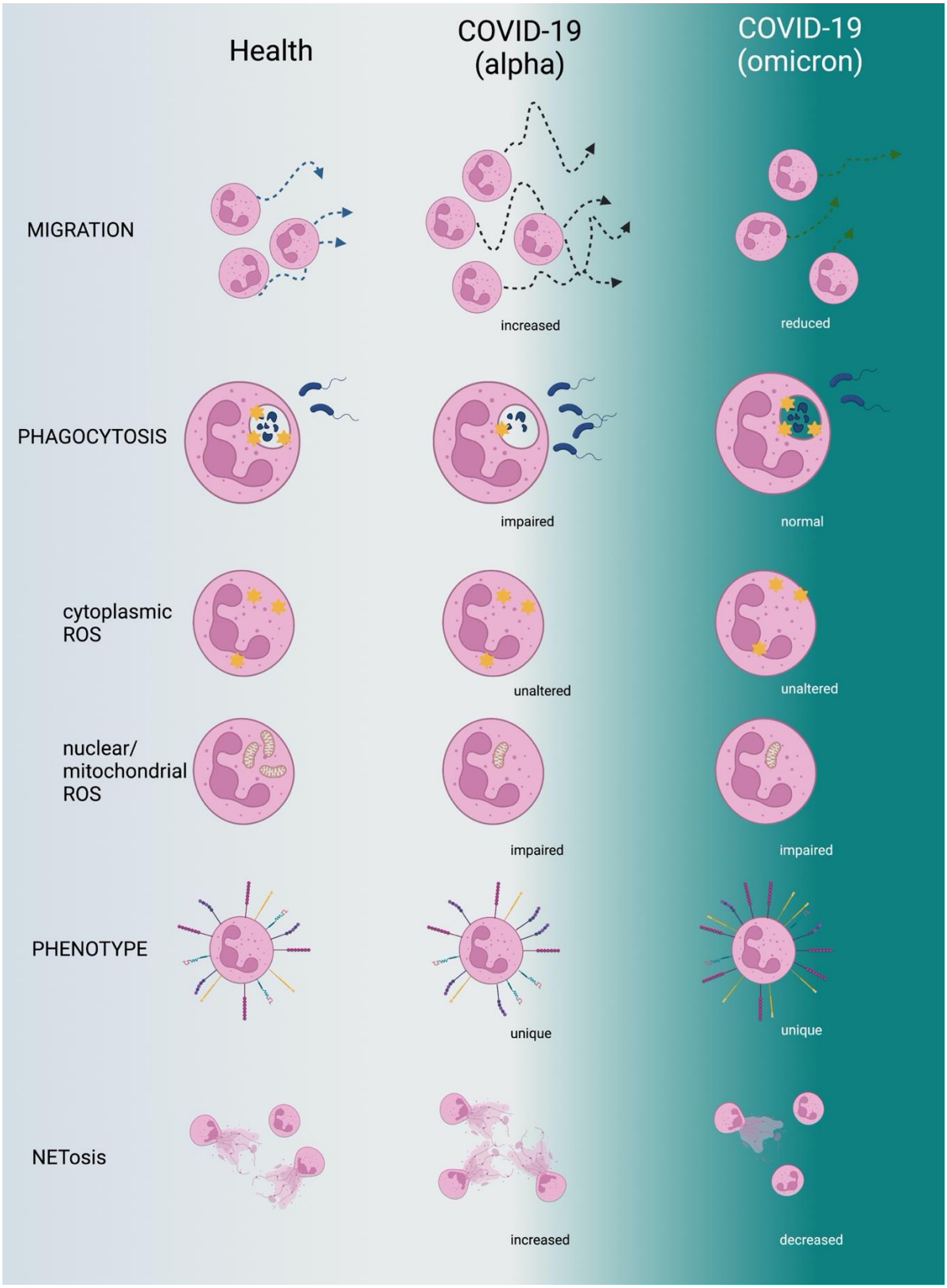

Figure 7.11 Summary of changes to cellular function. Compared to AMC, neutrophils from alpha and omicron COVID-19 demonstrated significantly altered neutrophil effector functions.

Comparison of omicron patients to AMC and CAP showed differences in demographics in terms of age and presence of cardiovascular disease. It was not possible to do further breakdown and analyse as per alpha patients due to a smaller omicron cohort size. Neutrophil effector function changes showed there was decreased n/mROS production compared to AMC and CAP. Percentage of neutrophils undergoing phagocytosis in omicron patients was similar to that of AMC and CAP, with a raised MFI. Neutrophils undergoing phagocytosis were therefore more efficient. Migration and NETosis was decreased in the omicron cohort. There was decreased circulating VEGF and MPO with increased IL-6 in omicron. Circulating MPO can be used as a marker of neutrophil degranulation, with lower levels suggesting decreased activation. It is possible that vaccination may lead to expansion of a neutrophil subset polarised towards antigen presentation, seen in a rhesus macaque SIV trial (Musich et al., 2018b). This would be in keeping with decreased phagocytosing fraction and circulating MPO. Decreased activation of phagocytic neutrophils would be in keeping with decreased VEGF and NETosis in omicron compared to AMC. NETs act as an endothelial scaffold for trapping erythrocytes and platelets to lead to thrombus formation (Savchenko et al., 2014). From this, platelet-derived thrombin can subsequently increase VEGF secretion (Maragoudakis et al., 2002).

Raised IL-6 in omicron patients compared to alpha, AMC and CAP may relate to overall systemic inflammation and an altered response after vaccination. IL-6 is also involved in the release of neutrophils from the bone marrow and can act as a chemoattractant in acute inflammation (Florentin et al., 2021), (Fielding et al., 2008). High IL-6 may be responsible for the increased neutrophil count seen in omicron patients. IL-6 itself has been targeted as a potential treatment in COVID-19, with tocilizumab approved by NICE. Tocilizumab can cause a transient neutropenia post administration, but effector functions are not affected by treatment (Wright et al., 2014). Decreasing neutrophil release may have reduced dysfunctional inflammation in alpha COVID-19, but the raised IL-6 in omicron infection may contribute to restoration of appropriate neutrophil migration.

7.8.4 Limitations

Method limitations regarding handling of COVID-19 samples have been discussed in **Chapter 3**.

For continuity and validity of comparison, delta and omicron variant patients recruited were ward-based, similar to that of alpha patients. As with alpha infection, these patients represent the majority of the in-patient burden and remain under-represented in research. Early intervention to prevent deterioration in this cohort remains important.

Differences in vaccination status between patients recruited representing different COVID-19 variants add an additional confounding factor to interpreting results. It is not possible to make direct comparisons between variants and the efficacy of the vaccines due to the timeframe of recruitment.

Owing to time and sample constraints, it was not possible to compare surface marker expression in the delta variant patients collected. However, as most of the significant changes in neutrophil function are most pronounced between alpha and omicron patients, and as omicron infections remain the prevailing strain, this comparison remains the most valid. Limited numbers of experiments were able to be carried out on a particular patient sample without compromising result integrity and due to time constrictions. As a result, further comparison between neutrophils to determine trends with ROS production would have been interesting to observe, but were not deemed a priority over investigating potential treatment and mechanisms of underlying disease documented in **Chapter 6**.

7.8.5 Conclusion

The disease caused by SARS-CoV-2 variants has clinically evolved along with the knowledge of effective treatments. Neutrophils from alpha COVID-19 patients demonstrated a unique

pattern of dysfunction. Comparison with neutrophils isolated from delta and omicron COVID-19 patients showed a shift in function with those from omicron having restored phagocytosis, reduced migration and NETosis with different surface marker expression. More accurate migration, effective phagocytosis and reduced NET formation could account for some of the decreased severity of clinical disease. Alterations in neutrophil function with changing variant infection suggests that neutrophils play a key role in SARS-CoV-2 host immune responses and dysfunctional responses can contribute to disease. Future viral disease pandemics should focus research on neutrophil function early for treatment targets to improve patient outcome.

CHAPTER 8
GENERAL DISCUSSION

8.1 Overall findings

This thesis aimed to describe and investigate a population of ward-based COVID-19 in-patients from both a clinical and neutrophil effector function perspective. In addition, it investigated neutrophil function as a potential underlying cause of the clinical changes observed with evolving COVID-19 variants. The COVID-19 pandemic represented a time of uncertainty with patient treatments and transmissibility of the virus. Thus, it was paramount to researcher safety for all experiments to be carried out in a category laboratory with appropriate safety precautions. The data in **Chapter 4** presents the alterations to standard working protocols required to do this. Some of these represent significant necessary changes that limited the investigations and data e.g. transwell migration vs our gold standard Insall chamber chemotaxis. However, validation of alternative methods demonstrated little difference in results compared to convention in healthy controls. Comparison of AMC, CAP and COVID-19 patients were also valid as all samples were processed in the same manner.

Data from **Chapter 6** showed that neutrophils isolated from non-ventilated COVID-19 patients demonstrated increased migration and NET formation, with impaired phagocytic capacity and decreased n/mROS production. These alterations in neutrophil function may lead to migration to healthy areas, and therefore increased tissue damage and inflammatory exudate. In addition, increased NET deposition is associated with immune thrombus formation, potentially contributing to the increased embolic phenomena seen in COVID-19 (Whyte et al., 2020, Papayannopoulos, 2018). Alterations to surface marker expression suggest a unique phenotype compared to those described in CAP, sepsis, and ageing. It is likely that altered neutrophil function may contribute to the clinical picture associated with COVID-19 and deterioration in certain patients. In an attempt to restore neutrophil function to that seen in AMC, investigation into PI3K pathway inhibition was investigated. PI3K inhibition reduced NET formation but did not restore other effector neutrophil functions. Addition of treatments which affect neutrophil enzymatic function also did not restore normal neutrophil effector function.

Investigation into different neutrophil responses to COVID-19 variant infections demonstrated that the dysfunction seen in alpha COVID-19 patients did not persist in neutrophils from patients with delta or omicron infection.

The data from this thesis generally supports the hypothesis that neutrophil dysfunction in COVID-19 contributes to the clinical symptoms observed in COVID-19 disease, with function normalising with the evolution of less severe subsequent strains. The wider immune response e.g. circulating IL-6 is likely due to systemic viral effects potentially affecting other immune cells. Treatments investigated here did not restore neutrophil function, and the changes do not appear to have been due to dysregulation of PI3Kinase pathway signalling.

8.1.1 Clinical

Patients recruited were all clinically managed in normal hospital wards and classified as Class 5 on the WHO severity scale. This is a unique cohort as the literature predominantly investigates patients managed on intensive care units. Severe ward-based patients have the potential to prevent deterioration and require advanced support if appropriate. Anti-inflammatory therapeutics such as dexamethasone, anti-IL6 and barcitinib have shown to improve clinical outcomes (Manoharan and Ying, 2022, Abani et al., 2021). Validation work determined that there was not a significant effect on the specific neutrophil functions examined in this thesis with dexamethasone treatment. It has been suggested that intracellular signalling of SARS-CoV-2 and the internalised glucocorticoid receptor are highly connected. This includes cytoskeletal rearrangement and cell cycle arrest at G2/M (V'kovski et al., 2021, Suryawanshi et al., 2021, Chrousos and Kino, 2005, Kino, 2018). Impediment of normal cellular processes would in theory prevent normal glucocorticoid signalling and thus improving outcomes rather than being immunosuppressive. Higher viral burden would amplify this e.g. in patients with an oxygen requirement.

Demographic and clinical associations with more severe disease were increasing age and CFS being associated with earlier hospital admission after symptom onset.

COVID-19 in-hospital mortality risk as derived from the 4C score was not significantly different between variants. However, observed mortality from the cohorts recruited demonstrated a significant decrease in the omicron variant despite an older patient group. This may be in part due to the uptake of COVID-19 vaccination between recruitment periods.

8.1.2 Neutrophil effector functions

Neutrophil phagocytosis is important to prevent development of severe secondary bacterial infections after initial injury (Brundage, 2006). The recruitment and design of this study did not allow for prolonged temporal follow up of recruited patients to examine the development of bacterial pneumonia. Due to restrictions with investigations and resources during the pandemic, not all patients had blood cultures taken on admission. As the time from symptom onset to presentation varied from one to 14 days, it is possible patients were co-infected with COVID-19 and CAP. In order to fully assess the effect of neutrophil dysfunction and secondary bacterial infections in COVID-19, separate study is required. Alpha variant patients demonstrated decreased phagocytic capacity compared to AMC. In omicron patients there was no significant difference in phagocytosis with AMC or CAP. Migration was increased in alpha patients which may suggest inaccurate migration leading to excessive host-mediated lung tissue damage. Reduced migratory accuracy has been associated with poor patient outcomes and increased tissue damage due to obligate proteolysis (Sapey et al., 2011). Migration was significantly lower in omicron variant patients, even when compared to AMC and CAP. The ARDS presentation seen during the early part of the COVID-19 pandemic has not been as clinically apparent in omicron infected patients (Van Goethem et al., 2022). This may

reflect more accurate neutrophil migration reducing excessive tissue inflammation and damage.

NET formation and release is associated with immune-thrombotic events, and embolic events were common in alpha COVID-19 (Skendros et al., 2020a). Along with the cohort recruited here, other studies documented increased NETosis in severe COVID-19 (Middleton et al., 2020, Skendros et al., 2020a, Veras et al., 2020). Reduction in NETosis in omicron patients in this cohort again correlates with the observed more favourable clinical outcomes for that variant (Bayrakçı, 2023).

8.1.3 Surface marker expression

Surface marker expression can convey the prevailing neutrophil phenotype at the time of blood collection. Neutrophils isolated from alpha variant patients displayed high levels of CD54 (associated with reverse transmigration) and reduction in CD11b (marker of neutrophil activation). These changes are not associated with neutrophil senescence or sepsis states. Neutrophils from omicron variant patients had decreased CD62L (shed during activation), with an increased expression of CXCR2 and decreased CXCR4 (indicative of bone marrow mobilisation). This phenotype is more in keeping with activation of neutrophils, although other markers of activation (CD10 and CD11b) were reduced in both alpha and omicron patients compared to AMC. Omicron patients had higher levels of circulating IL-6 compared to other SARS-CoV-2 variants, AMC and CAP. Higher IL-6 may be responsible for driving more targeted chemotaxis as well as neutrophil deployment from the bone marrow leading to the change in effector functions and surface marker expression (Florentin et al., 2021, Fielding et al., 2008). The change in surface marker expression on neutrophils with viral evolution is again suggestive of a less dysfunctional neutrophil response to infection and correlates with the clinical phenotype returning towards a response expected in severe lower respiratory tract infections.

8.1.4 Mechanisms and treatments

Based on results from the initial alpha cohort, PI3K pathway as a mechanism for COVID-19 mediated disruption of neutrophil function was examined. Inhibition has been shown to restore migration accuracy in the elderly, and signalling is related to NETosis (Sapey et al., 2014). However, addition of PI3K inhibitors to neutrophils from COVID-19 patients did not alter migration and did not fully reduce NETosis to that of AMC. NSP activity blockade through the use of the drugs metoprolol, brensocatib and AZD9668 failed to alter neutrophil effector functions suggesting that NSP dysfunction is not driving increased inflammation or decreased phagocytosis.

8.2 What does this study contribute to the field?

This study contributes insights into neutrophil dysfunction in the largest population of in-hospital patients affected with COVID-19 reported outside of the ITU setting. Severely unwell ward-based COVID-19 patients demonstrated minimal difference to those admitted to intensive care, suggesting the viral effect on neutrophils is established early in disease rather than evolving with disease progression. Furthermore, this study demonstrates that neutrophil dysfunction is not driven by PI3K disruption. This is the first time a comparison of neutrophils from different SARS-CoV-2 variants has been carried out and this thesis demonstrates that neutrophil response to infection associates with the change in clinical severity. There are further clinical implications from this which suggest that therapies that are currently used may need re-evaluating given the significant change observed in host response to different COVID-19 variant infection. This not only has implications in the acute setting but potentially on the longer-term changes in neutrophil effector function that may influence post infectious sequalae or post-COVID syndrome.

8.3 Clinical implications

Investigation of PI3K and NSP blockade as potential treatments in COVID-19 has implications for other diseases affecting neutrophil function. The randomised control trial of brensocatib vs placebo showed worse outcomes in the brensocatib arm; and here there was no effect on neutrophil function in COVID-19, suggesting a different underlying disease process to bronchiectasis (Chalmers et al., 2017).

Whilst COVID-19 does not present the same challenges to global healthcare as in March 2020, investigation of its ongoing evolution remains important. COVID-19 treatments remain largely unchanged from initial trials, yet both the observed clinical phenotype and the cellular phenotype described here have evolved with the virus. In order to ensure that treatments recommended by NICE and international health bodies remain valid and effective, ongoing research is required in current prevailing SARS-CoV-2 strains. Furthermore, the most likely patients to now be hospitalised are frail, elderly and co-morbid and therefore identifying potential targets for therapy to prevent further deterioration and death is of clinical importance.

8.4 Study strengths

Neutrophil *ex vivo* experiments require delicate technique with precision to prevent unintentional cell activation. The method of neutrophil isolation used here with dextran sedimentation followed by a Percoll® density gradient has been shown to reduce neutrophil disruption compared to the use of techniques requiring red blood cell lysis (Vuorte et al., 2001). This technique is widely used, and thus allowing for comparisons with other studies to be made. High yield, purity and viability were achieved through practice with healthy blood donors prior to any experimentation with samples from recruited patients and AMC.

This is the first COVID-19 study to examine neutrophil function in ward-based patients. Previous literature focuses on the intensive care patient population and preventing further deterioration. Hospital in-patients not treated in intensive care represented both the largest population of admitted patients with COVID-19 as well as the most likely to deteriorate and require intensive care treatment (Sapey et al., 2020). By investigating this cohort of patients, we can determine if the neutrophil dysfunction seen in ICU patients is driving COVID-19 or if this develops after deterioration occurs.

Treatments for COVID-19 were investigated on a clinical outcome basis, based on limited primary research into COVID-19. Outcomes based on clinical parameters usually occur after insight into underlying mechanisms, which was not possible with the COVID-19 pandemic. This thesis examined potential failed treatments in clinical practice to determine if the underlying therapeutic mechanism had basis for investigation into alternative related therapeutics. This study was able to test these therapeutics from cells isolated from patients with active COVID-19 infection and determine the poor clinical outcomes persisted to a cellular level.

Investigation into neutrophil dysfunction was able to be done in parallel with CAP control patients to examine the differences in other respiratory tract infections. AMC provide a good control group, but recruitment of CAP patients at the same time allowed for identical investigation procedures to be carried out in patients with a similar clinical disease severity.

8.5 Study limitations

Methodology limitations due to COVID-19 present the biggest limitations to this study. Validation work in **Chapter 4** has determined that the precautions taken for investigator safety largely do not compromise the validity of the results obtained. However, limitations of working with hazardous samples outside the CAT2 laboratory reduced the achievable amount of data e.g. Insall chamber chemotaxis.

The rapid pace of research into treatments for COVID-19, coupled with unprecedented vaccine development complicated patient recruitment and comparison of results from different COVID-19 variants. Patients were recruited prior to administration of novel therapies, but approval of drugs for the treatment of COVID meant that several patients were excluded having received immunomodulatory medications.

Investigation into the restoration of the dysfunction observed in neutrophils would be an interesting time point – which had ethical approval. However, patient follow-up in a healthcare setting during waves of infection where the public were encouraged to remain at home was not deemed morally correct.

The labelled *S. pneumoniae* used for phagocytosis experiments did show signal loss over the two years of patient recruitment of this thesis, but this was not statistically significant. Labelling fresh heat-killed bacteria may have prevented this signal loss but would have increased difficulty in batch variability. The use of labelled bioparticles such as pHrodo™ may have prevented this, but there are reports of inter-batch variability with these. In addition, they are less physiologically representative of bacterial phagocytosis compared to labelled heat-killed opsonised bacteria.

Due to the nature of the pandemic, it was not possible to investigate a known respiratory viral illness in parallel e.g. influenza and review the effects on neutrophil function. Recruitment of a fourth cohort of influenza patients was attempted in winter 2022, but there were insufficient patients to recruit who were not already treated with antiviral medication such as neuraminidase inhibitors (oseltamivir). These have been shown to affect neutrophil function in a murine model of COVID-19 (de Oliveira Formiga et al., 2020).

Investigation of neutrophil dysfunction in alpha patients is more informed after omicron recruitment and experiments. However, it is not possible to further investigate mechanisms of the effect of the virus on neutrophil function as there were no further alpha SARS-CoV-2 infections. In addition, neutrophil lifespan *ex vivo* is not sufficient to be able to have stored cells for further work. The rapidly evolving nature of both virus and treatments meant selection

of pathways and mechanisms to investigate was limited and it was not possible to explore all avenues.

8.6 Future directions

The work presented in this thesis details the neutrophil changes in patients with active COVID-19 infection. Whilst the acute danger from COVID-19 has cleared, there is a significant proportion of the population who have long term effects after infection. From the patients with follow up radiological imaging in this cohort, persistent physical changes to the lung parenchyma in the form of fibrosis or ground glass changes are not the norm (Diaz et al., 2022, Fabbri et al., 2023, Touman et al., 2022). There are no cellular or detailed clinical studies or trials in patients diagnosed with long-COVID. Investigation of underlying cellular immune causes may expose a treatable cause. Persistent neutrophil changes may suggest underlying alterations to immune cell development and activation (George et al., 2022). Recruitment of patients with long-COVID correlating qualitative and quantitative symptoms with biochemical and cellular experiments may provide insight into what is currently an unknown disease process.

Validation of experimental methods in potentially infectious samples will allow for future work to be done in samples where researcher safety must be taken into account. Demonstration that alternative methods can be used to reliably generate results when examining neutrophil effector functions. This is more crucial in neutrophil work due to the fragile nature of maintaining cell viability *ex vivo*.

Treatments investigated early in the pandemic focussed on treatments of systemic inflammation (Group, 2020, Wilkinson, 2020, Beigel et al., 2020). The investigation of neutrophils throughout different SARS-CoV-2 variant infections has shown that the observed dysfunction appears to be associated with disease severity. Future pandemics are inevitable, whether it be related to a known pathogen with a novel mutation e.g. influenza, new resistant bacterial species or subspecies or a zoonotic infection. The insights into the way the immune

system responds to respiratory viral infections can be used in the future to help more rapidly develop targeted treatments (Mahoney and Sridhar, 2023, Pericàs et al., 2023).

8.7 Conclusions

The SARS-CoV-2 pandemic represented an unprecedented time of global health burden, health research and collaboration. It enabled vast research to be conducted in record time and led to the development of a successful vaccination programme. In parallel to this, this thesis explored the cellular effects of the virus on neutrophil function, an innate immune cell key to the initiation and resolution of inflammation. Neutrophils from COVID-19 patients exhibited altered effector functions with decreased phagocytic capacity, increased NETosis and migration, and surface marker expression not in keeping with those previously described. Evolution of the virus and further patient recruitment demonstrated some resolution of neutrophil functions with decreased NETosis, migration and normalised phagocytic capacity. This correlates with the milder clinical phenotype of omicron patients; supported by systemic metabolomic data. Investigation of the PI3K pathway and NSP dysfunction as a mechanism of altered function did not demonstrate alteration to these pathways.

This thesis has validated neutrophil experimentation in hazardous samples, and highlighted the importance of early and on-going investigation into the innate immune system as an evolving target for treatment in future pandemics.

REFERENCES

2020. COVID-19 symptoms at hospital admission vary with age and sex: ISARIC multinational study. *medRxiv*.

ABANI, O., ABBAS, A., ABBAS, F., ABBAS, M., ABBASI, S., ABBASS, H., ABBOTT, A., ABDALLAH, N., ABDELAZIZ, A. & ABDELFATTAH, M. 2021. Tocilizumab in patients admitted to hospital with COVID-19 (RECOVERY): a randomised, controlled, open-label, platform trial. *The Lancet,* 397**,** 1637-1645.

ABU-RADDAD, L. J., CHEMAITELLY, H. & BUTT, A. A. 2021. Effectiveness of the BNT162b2 Covid-19 Vaccine against the B.1.1.7 and B.1.351 Variants. *N Engl J Med,* 385**,** 187-189.

ADROVER, J. M., CARRAU, L., DASSLE-PLENKER, J., BRAM, Y., CHANDAR, V., HOUGHTON, S., REDMOND, D., MERRILL, J. R., SHEVIK, M. & LYONS, S. K. 2022. Disulfiram inhibits neutrophil extracellular trap formation and protects rodents from acute lung injury and SARS-CoV-2 infection. *JCI insight,* 7.

AGARWAL, A., HUNT, B. J., STEGEMANN, M., ROCHWERG, B., LAMONTAGNE, F., SIEMIENIUK, R. A., AGORITSAS, T., ASKIE, L., LYTVYN, L., LEO, Y.-S., MACDONALD, H., ZENG, L., ALHADYAN, A., MUNA, A.-M., AMIN, W., DA SILVA, A. R. A., ARYAL, D., BARRAGAN, F. A. J., BAUSCH, F. J., BURHAN, E., CALFEE, C. S., CECCONI, M., CHACKO, B., CHANDA, D., DAT, V. Q., DE SUTTER, A., DU, B., FREEDMAN, S., GEDULD, H., GEE, P., HAIDER, M., GOTTE, M., HARLEY, N., HASHMI, M., HUI, D., ISMAIL, M., JEHAN, F., KABRA, S. K., KANDA, S., KIM, Y.-J., KISSOO, N., KRISHNA, S., KUPPALLI, K., KWIZERA, A., CASTRO-RIAL, M. L., LISBOA, T., LODHA, R., MAHAKA, I., MANAI, H., MENDELSON, M., BATTISTA MIGLIORI, G., MINO, G., NSUTEBU, E., PETER, J., PRELLER, J., PSHENICHNAYA, N., QADIR, N., RANGANATHAN, S. S., RELAN, P., RYLANCE, J., SABZWARI, S., SARIN, R., SHANKAR-HARI, M., SHARLAND, M., SHEN, Y., SOUZA, J. P., SWANSTROM, R., TSHOKEY, T., UGARTE, S., UYEKI, T., VAZQUEZ CURIEL, E., VENKATAPURAM, S., VUYISEKA, D., WIJEWICKRAMA, A., TRAN, L., ZERAATKAR, D., BARTOSZKO, J. J., GE, L., BRIGNARDELLO-PETERSEN, R., OWEN, A., GUYATT, G., DIAZ, J., KAWANO-DOURADO, L., JACOBS, M. & VANDVIK, P. O. 2020. A living WHO guideline on drugs for covid-19. *BMJ,* 370**,** m3379.

AHMED, A., ALDERAZI, S. A., ASLAM, R., BARKAT, B., BARKER, B. L., BHAT, R., CASSIDY, S., CROWLEY, L. E., DOSANJH, D. P. & EBRAHIM, H. 2022. Utility of severity assessment tools in COVID-19 pneumonia: a multicentre observational study. *Clinical Medicine,* 22**,** 63.

ALLARD, B., PANARITI, A. & MARTIN, J. G. 2018. Alveolar macrophages in the resolution of inflammation, tissue repair, and tolerance to infection. *Frontiers in immunology,* 9**,** 1777.

AMULIC, B., CAZALET, C., HAYES, G. L., METZLER, K. D. & ZYCHLINSKY, A. 2012. Neutrophil function: from mechanisms to disease. *Annu Rev Immunol,* 30**,** 459-89.

ANDREW, N. & INSALL, R. H. 2007. Chemotaxis in shallow gradients is mediated independently of PtdIns 3-kinase by biased choices between random protrusions. *Nat Cell Biol,* 9**,** 193-200.

ANTHONY GORDON, P. R. M., FARAH AL-BEIDH , KATHRYN M ROWAN , ALISTAIR D NICHOL , YASEEN M ARABI , DJILLALI ANNANE , ABI BEANE , WILMA VAN BENTUM-PUIJK , LINDSAY R BERRY , ZAHRA BHIMANI , MARC J M BONTEN , CHARLOTTE A BRADBURY , FRANK M BRUNKHORST , ADRIAN BUZGAU , ALLEN C CHENG , MICHELLE A DETRY , EAMON J DUFFY , LISE J ESTCOURT , MARK FITZGERALD , HERMAN GOOSSENS , RASHAN HANIFFA , ALISA M HIGGINS , THOMAS E HILLS , CHRISTOPHER M HORVAT , FRANCOIS LAMONTAGNE , PATRICK R LAWLER , HELEN L LEAVIS , KELSEY M LINSTRUM , EDWARD LITTON , ELIZABETH LORENZI , JOHN C MARSHALL , FLORIAN B MAYR , DANIEL F MCAULEY , ANNA MCGLOTHLIN , SHAY P MCGUINNESS , BRYAN J MCVERRY , STEPHANIE K MONTGOMERY , SUSAN C MORPETH , SRINIVAS MURTHY , KATRINA ORR , RACHAEL L PARKE , JANE C PARKER , ASAD E PATANWALA , VILLE PETTILÄ , EMMA RADEMAKER , MARLENE S SANTOS , CHRISTINA T SAUNDERS , CHRISTOPHER W SEYMOUR , MANU SHANKAR-HARI , WENDY I SLIGL , ALEXIS F TURGEON , ANNE M TURNER , FRANK L VAN DE VEERDONK , RYAN ZARYCHANSKI , CAMERON GREEN , ROGER J LEWIS , DEREK C ANGUS , COLIN J MCARTHUR , SCOTT BERRY , STEVE A WEBB , LENNIE P G DERDE 2021. Interleukin-6 Receptor Antagonists in Critically Ill Patients with Covid-19. *New England Journal of Medicine,* 384**,** 1491-1502.

APEL, F., ANDREEVA, L., KNACKSTEDT, L. S., STREECK, R., FRESE, C. K., GOOSMANN, C., HOPFNER, K.-P. & ZYCHLINSKY, A. 2021. The cytosolic DNA sensor cGAS recognizes neutrophil extracellular traps. *Science signaling,* 14**,** eaax7942.

ARGYROPOULOS, K. V., SERRANO, A., HU, J., BLACK, M., FENG, X., SHEN, G., CALL, M., KIM, M. J., LYTLE, A. & BELOVARAC, B. 2020. Association of initial viral load in severe acute respiratory syndrome coronavirus 2 (SARS-CoV-2) patients with outcome and symptoms. *The American journal of pathology,* 190**,** 1881-1887.

ASCHENBRENNER, A. C., MOUKTAROUDI, M., KRÄMER, B., OESTREICH, M., ANTONAKOS, N., NUESCH-GERMANO, M., GKIZELI, K., BONAGURO, L., REUSCH, N. & BASSLE, K. 2021. Disease severity-specific neutrophil signatures in blood transcriptomes stratify COVID-19 patients. *Genome medicine,* 13**,** 1-25.

AULAKH, G. K. 2018. Neutrophils in the lung: "the first responders". *Cell Tissue Res,* 371**,** 577-588.

AURIEMMA, C. L., ZHUO, H., DELUCCHI, K., DEISS, T., LIU, T., JAUREGUI, A., KE, S., VESSEL, K., LIPPI, M. & SEELEY, E. 2020. Acute respiratory distress syndrome-attributable mortality in critically ill patients with sepsis. *Intensive care medicine,* 46**,** 1222-1231.

BABIOR, B. M. 2004. NADPH oxidase. *Curr Opin Immunol,* 16**,** 42-7.

BACKER, J. M. 2016. The intricate regulation and complex functions of the Class III phosphoinositide 3-kinase Vps34. *Biochemical Journal,* 473**,** 2251-2271.

BAIN, W., YANG, H., SHAH, F. A., SUBER, T., DROHAN, C., AL-YOUSIF, N., DESENSI, R. S., BENSEN, N., SCHAEFER, C., ROSBOROUGH, B. R., SOMASUNDARAM, A., WORKMAN, C. J., LAMPENFELD, C., CILLO, A. R., CARDELLO, C., SHAN, F., BRUNO, T. C., VIGNALI, D. A. A., RAY, P., RAY, A., ZHANG, Y., LEE, J. S., METHÉ, B., MCVERRY, B. J., MORRIS, A. & KITSIOS, G. D. 2021. COVID-19 versus Non-COVID-19 Acute Respiratory Distress Syndrome: Comparison of Demographics, Physiologic Parameters, Inflammatory Biomarkers, and Clinical Outcomes. *Ann Am Thorac Soc,* 18**,** 1202-1210.

BANNENBERG, G. & SERHAN, C. N. 2010. Specialized pro-resolving lipid mediators in the inflammatory response: An update. *Biochimica et Biophysica Acta (BBA)-Molecular and Cell Biology of Lipids,* 1801**,** 1260-1273.

BARNES, C. O., WEST, A. P., JR., HUEY-TUBMAN, K. E., HOFFMANN, M. A. G., SHARAF, N. G., HOFFMAN, P. R., KORANDA, N., GRISTICK, H. B., GAEBLER, C., MUECKSCH, F., LORENZI, J. C. C., FINKIN, S., HÄGGLÖF, T., HURLEY, A., MILLARD, K. G., WEISBLUM, Y., SCHMIDT, F., HATZIIOANNOU, T., BIENIASZ, P. D., CASKEY, M., ROBBIANI, D. F., NUSSENZWEIG, M. C. & BJORKMAN, P. J. 2020. Structures of Human Antibodies Bound to SARS-CoV-2 Spike Reveal Common Epitopes and Recurrent Features of Antibodies. *Cell,* 182**,** 828-842.e16.

BARUCH, G., ROTHSCHILD, E., SADON, S., SZEKELY, Y., LICHTER, Y., KAPLAN, A., TAIEB, P., BANAI, A., HOCHSTADT, A. & MERDLER, I. 2022. Evolution of right and left ventricle routine and speckle-tracking echocardiography in patients recovering from coronavirus disease 2019: a longitudinal study. *European Heart Journal-Cardiovascular Imaging,* 23**,** 1055-1065.

BASU, S., HODGSON, G., KATZ, M. & DUNN, A. R. 2002. Evaluation of role of G-CSF in the production, survival, and release of neutrophils from bone marrow into circulation. *Blood, The Journal of the American Society of Hematology,* 100**,** 854-861.

BAUDIS, K., DE PAULA VIEIRA, R., CICKO, S., AYATA, K., HOSSFELD, M., EHRAT, N., GÓMEZ-MUÑOZ, A., ELTZSCHIG, H. K. & IDZKO, M. 2016. C1P Attenuates Lipopolysaccharide-Induced Acute Lung Injury by Preventing NF-κB Activation in Neutrophils. *J Immunol,* 196**,** 2319-26.

BAYRAKÇI, O. 2023. Outcomes of wuhan, alpha, delta, omicron and other variants in severe acute respiratory syndrome coronavirus-2.

BEAUVILLAIN, C., CUNIN, P., DONI, A., SCOTET, M., JAILLON, S., LOIRY, M. L., MAGISTRELLI, G., MASTERNAK, K., CHEVAILLER, A., DELNESTE, Y. & JEANNIN, P. 2011. CCR7 is involved in the migration of neutrophils to lymph nodes. *Blood,* 117**,** 1196-204.

BEDI, P., DAVIDSON, D. J., MCHUGH, B. J., ROSSI, A. G. & HILL, A. T. 2018. Blood neutrophils are reprogrammed in bronchiectasis. *American journal of respiratory and critical care medicine,* 198**,** 880-890.

BEIGEL, J. H., TOMASHEK, K. M., DODD, L. E., MEHTA, A. K., ZINGMAN, B. S., KALIL, A. C., HOHMANN, E., CHU, H. Y., LUETKEMEYER, A., KLINE, S., LOPEZ DE CASTILLA, D., FINBERG, R. W., DIERBERG,

K., TAPSON, V., HSIEH, L., PATTERSON, T. F., PAREDES, R., SWEENEY, D. A., SHORT, W. R., TOULOUMI, G., LYE, D. C., OHMAGARI, N., OH, M. D., RUIZ-PALACIOS, G. M., BENFIELD, T., FÄTKENHEUER, G., KORTEPETER, M. G., ATMAR, R. L., CREECH, C. B., LUNDGREN, J., BABIKER, A. G., PETT, S., NEATON, J. D., BURGESS, T. H., BONNETT, T., GREEN, M., MAKOWSKI, M., OSINUSI, A., NAYAK, S. & LANE, H. C. 2020. Remdesivir for the Treatment of Covid-19 - Final Report. *N Engl J Med,* 383**,** 1813-1826.

BELCHAMBER, K., THEIN, O., HAZELDINE, J., GRUDZINSKA, F., HUGHES, M., JASPER, A., YIP, K., SAPEY, E., PAREKH, D., THICKETT, D. & SCOTT, A. 2021. Altered neutrophil phenotype and function in non-ICU hospitalised COVID-19 patients correlated with disease severity. *medRxiv***,** 2021.06.08.21258535.

BELCHAMBER, K. B., THEIN, O. S., HAZELDINE, J., GRUDZINSKA, F. S., FANIYI, A. A., HUGHES, M. J., JASPER, A. E., YIP, K. P., CROWLEY, L. E. & LUGG, S. T. 2022. Dysregulated neutrophil phenotype and function in hospitalised non-ICU COVID-19 pneumonia. *Cells,* 11**,** 2901.

BELCHAMBER, K. B., WALKER, E. M., STOCKLEY, R. A. & SAPEY, E. 2020. Monocytes and macrophages in alpha-1 antitrypsin deficiency. *International journal of chronic obstructive pulmonary disease***,** 3183-3192.

BERNAL, J. L., ANDREWS, N., GOWER, C., GALLAGHER, E., SIMMONS, R., THELWALL, S., STOWE, J., TESSIER, E., GROVES, N. & DABRERA, G. 2021. Effectiveness of Covid-19 vaccines against the B. 1.617. 2 (Delta) variant. *New England Journal of Medicine*.

BEUMER, J., GEURTS, M. H., LAMERS, M. M., PUSCHHOF, J., ZHANG, J., VAN DER VAART, J., MYKYTYN, A. Z., BREUGEM, T. I., RIESEBOSCH, S., SCHIPPER, D., VAN DEN DOEL, P. B., DE LAU, W., PLEGUEZUELOS-MANZANO, C., BUSSLINGER, G., HAAGMANS, B. L. & CLEVERS, H. 2021. A CRISPR/Cas9 genetically engineered organoid biobank reveals essential host factors for coronaviruses. *Nat Commun,* 12**,** 5498.

BHATNAGAR, J., GARY, J., REAGAN-STEINER, S., ESTETTER, L. B., TONG, S., TAO, Y., DENISON, A. M., LEE, E., DELEON-CARNES, M., LI, Y., UEHARA, A., PADEN, C. R., LEITGEB, B., UYEKI, T. M., MARTINES, R. B., RITTER, J. M., PADDOCK, C. D., SHIEH, W. J. & ZAKI, S. R. 2021. Evidence of Severe Acute Respiratory Syndrome Coronavirus 2 Replication and Tropism in the Lungs, Airways, and Vascular Endothelium of Patients With Fatal Coronavirus Disease 2019: An Autopsy Case Series. *J Infect Dis,* 223**,** 752-764.

BHUIYAN, M. U., BLYTH, C. C., WEST, R., LANG, J., RAHMAN, T., GRANLAND, C., DE GIER, C., BORLAND, M. L., THORNTON, R. B. & KIRKHAM, L.-A. S. 2019. Combination of clinical symptoms and blood biomarkers can improve discrimination between bacterial or viral community-acquired pneumonia in children. *BMC pulmonary medicine,* 19**,** 1-9.

BILANGES, B., POSOR, Y. & VANHAESEBROECK, B. 2019. PI3K isoforms in cell signalling and vesicle trafficking. *Nature reviews Molecular cell biology,* 20**,** 515-534.

BONDEVA, T., PIROLA, L., BULGARELLI-LEVA, G., RUBIO, I., WETZKER, R. & WYMANN, M. P. 1998. Bifurcation of lipid and protein kinase signals of PI3Kγ to the protein kinases PKB and MAPK. *Science,* 282**,** 293-296.

BORELLA, R., DE BIASI, S., PAOLINI, A., BORALDI, F., LO TARTARO, D., MATTIOLI, M., FIDANZA, L., NERONI, A., CARO-MALDONADO, A., MESCHIARI, M., FRANCESCHINI, E., QUAGLINO, D., GUARALDI, G., BERTOLDI, C., SITA, M., BUSANI, S., GIRARDIS, M., MUSSINI, C., COSSARIZZA, A. & GIBELLINI, L. 2022. Metabolic reprograming shapes neutrophil functions in severe COVID-19. *Eur J Immunol,* 52**,** 484-502.

BORREGAARD, N. 2010. Neutrophils, from marrow to microbes. *Immunity,* 33**,** 657-670.

BRACCINI, L., CIRAOLO, E., CAMPA, C. C., PERINO, A., LONGO, D. L., TIBOLLA, G., PREGNOLATO, M., CAO, Y., TASSONE, B. & DAMILANO, F. 2015. PI3K-C2γ is a Rab5 effector selectively controlling endosomal Akt2 activation downstream of insulin signalling. *Nature communications,* 6**,** 7400.

BRINKMANN, V., REICHARD, U., GOOSMANN, C., FAULER, B., UHLEMANN, Y., WEISS, D. S., WEINRAUCH, Y. & ZYCHLINSKY, A. 2004. Neutrophil extracellular traps kill bacteria. *science,* 303**,** 1532-1535.

BRUNDAGE, J. F. 2006. Interactions between influenza and bacterial respiratory pathogens: implications for pandemic preparedness. *Lancet Infect Dis,* 6**,** 303-12.

BRUNDAGE, J. F. & SHANKS, G. D. 2008. Deaths from bacterial pneumonia during 1918-19 influenza pandemic. *Emerg Infect Dis,* 14**,** 1193-9.

BUEHLER, P. K., ZINKERNAGEL, A. S., HOFMAENNER, D. A., GARCIA, P. D. W., ACEVEDO, C. T., GÓMEZ-MEJIA, A., SHAMBAT, S. M., ANDREONI, F., MAIBACH, M. A. & BARTUSSEK, J. 2021. Bacterial pulmonary superinfections are associated with longer duration of ventilation in critically ill COVID-19 patients. *Cell Reports Medicine,* 2**,** 100229.

BUESCHER, E. S. & GALLIN, J. I. 1987. Effects of storage and radiation on human neutrophil function in vitro. *Inflammation,* 11**,** 401-416.

BURTON, J. L., KEHRLI JR, M. E., KAPIL, S. & HORST, R. L. 1995. Regulation of L-selectin and CD18 on bovine neutrophils by glucocorticoids: effects of cortisol and dexamethasone. *Journal of leukocyte biology,* 57**,** 317-325.

BUSCH, M. H., TIMMERMANS, S. A., NAGY, M., VISSER, M., HUCKRIEDE, J., AENDEKERK, J. P., DE VRIES, F., POTJEWIJD, J., JALLAH, B. & YSERMANS, R. 2020. Neutrophils and contact activation of coagulation as potential drivers of COVID-19. *Circulation,* 142**,** 1787-1790.

BUTCHER, S., CHAHAL, H., NAYAK, L., SINCLAIR, A., HENRIQUEZ, N., SAPEY, E., O'MAHONY, D. & LORD, J. 2001. Senescence in innate immune responses: reduced neutrophil phagocytic capacity and CD16 expression in elderly humans. *Journal of leukocyte biology,* 70**,** 881-886.

CARSANA, L., SONZOGNI, A., NASR, A., ROSSI, R. S., PELLEGRINELLI, A., ZERBI, P., RECH, R., COLOMBO, R., ANTINORI, S., CORBELLINO, M., GALLI, M., CATENA, E., TOSONI, A., GIANATTI, A. & NEBULONI, M. 2020. Pulmonary post-mortem findings in a series of COVID-19 cases from northern Italy: a two-centre descriptive study. *Lancet Infect Dis,* 20**,** 1135-1140.

CDC. 2021. *Delta Variant: What We Know about the Science* [Online]. Available: https://www.cdc.gov/coronavirus/2019-ncov/variants/delta-variant.html [Accessed].

CEVIK, M., BAMFORD, C. & HO, A. 2020. COVID-19 pandemic—a focused review for clinicians. *Clinical Microbiology and Infection,* 26**,** 842-847.

CHALMERS, J. D., HAWORTH, C. S., METERSKY, M. L., LOEBINGER, M. R., BLASI, F., SIBILA, O., O'DONNELL, A. E., SULLIVAN, E. J., MANGE, K. C., FERNANDEZ, C., ZOU, J. & DALEY, C. L. 2020. Phase 2 Trial of the DPP-1 Inhibitor Brensocatib in Bronchiectasis. *New England Journal of Medicine,* 383**,** 2127-2137.

CHALMERS, J. D., MOFFITT, K. L., SUAREZ-CUARTIN, G., SIBILA, O., FINCH, S., FURRIE, E., DICKER, A., WROBEL, K., ELBORN, J. S. & WALKER, B. 2017. Neutrophil elastase activity is associated with exacerbations and lung function decline in bronchiectasis. *American journal of respiratory and critical care medicine,* 195**,** 1384-1393.

CHAUDHRY, F., LAVANDERO, S., XIE, X., SABHARWAL, B., ZHENG, Y.-Y., CORREA, A., NARULA, J. & LEVY, P. 2020. Manipulation of ACE2 expression in COVID-19. *Open Heart,* 7**,** e001424.

CHEN, C. Y., TSAI, Y. F., HUANG, W. J., CHANG, S. H. & HWANG, T. L. 2018a. Propofol inhibits endogenous formyl peptide-induced neutrophil activation and alleviates lung injury. *Free Radic Biol Med,* 129**,** 372-382.

CHEN, K., MONTELEONE, M., BOUCHER, D., SOLLBERGER, G., RAMNATH, D., CONDON, N., VON PEIN, J., BROZ, P., SWEET, M. & SCHRODER, K. 2018b. Noncanonical inflammasome signaling elicits gasdermin D-dependent neutrophil extracellular traps. Sci Immunol 3 (26).

CHIKHALKAR, B., GOSAIN, D., GAIKWAD, S., DESHMUKH, R. & CHIKHALKAR, B. G. 2022. Assessment of national early warning score 2 as a tool to predict the outcome of COVID-19 patients on admission. *Cureus,* 14.

CHISHTI, A. D., SHENTON, B. K., KIRBY, J. A. & BAUDOUIN, S. V. 2004. Neutrophil chemotaxis and receptor expression in clinical septic shock. *Intensive Care Med,* 30**,** 605-11.

CHRISTOPHER, M. J., LIU, F., HILTON, M. J., LONG, F. & LINK, D. C. 2009. Suppression of CXCL12 production by bone marrow osteoblasts is a common and critical pathway for cytokine-induced mobilization. *Blood, The Journal of the American Society of Hematology,* 114**,** 1331-1339.

CHROUSOS, G. P. & KINO, T. 2005. Intracellular glucocorticoid signaling: a formerly simple system turns stochastic. *Science's STKE,* 2005**,** pe48-pe48.

CIPOLLA, D., ZHANG, J., KORKMAZ, B., CHALMERS, J. D., BASSO, J., LASALA, D., FERNANDEZ, C., TEPER, A., MANGE, K. C., PERKINS, W. R. & SULLIVAN, E. J. 2023. Dipeptidyl peptidase-1 inhibition with

brensocatib reduces the activity of all major neutrophil serine proteases in patients with bronchiectasis: results from the WILLOW trial. *Respiratory Research,* 24**,** 133.

CITU, C., GORUN, F., MOTOC, A., SAS, I., GORUN, O. M., BURLEA, B., TUTA-SAS, I., TOMESCU, L., NEAMTU, R. & MALITA, D. 2022. The predictive role of NLR, d-NLR, MLR, and SIRI in COVID-19 mortality. *Diagnostics,* 12**,** 122.

CLEMENTE-MORAGÓN, A., MARTÍNEZ-MILLA, J., OLIVER, E., SANTOS, A., FLANDES, J., FERNÁNDEZ, I., RODRÍGUEZ-GONZÁLEZ, L., CASTILLO, C. S. D., IOAN, A.-M., LÓPEZ-ÁLVAREZ, M., GÓMEZ-TALAVERA, S., GALÁN-ARRIOLA, C., FUSTER, V., PÉREZ-CALVO, C. & IBÁÑEZ, B. 2021. Metoprolol in Critically Ill Patients With COVID-19. *Journal of the American College of Cardiology,* 78**,** 1001-1011.

CRISFORD, H., SAPEY, E., ROGERS, G. B., TAYLOR, S., NAGAKUMAR, P., LOKWANI, R. & SIMPSON, J. L. 2021. Neutrophils in asthma: the good, the bad and the bacteria. *Thorax,* 76**,** 835-844.

CUI, S., CHEN, S., LI, X., LIU, S. & WANG, F. 2020. Prevalence of venous thromboembolism in patients with severe novel coronavirus pneumonia. *J Thromb Haemost,* 18**,** 1421-1424.

CURRIE, S. M., GWYER FINDLAY, E., MCFARLANE, A. J., FITCH, P. M., BÖTTCHER, B., COLEGRAVE, N., PARAS, A., JOZWIK, A., CHIU, C., SCHWARZE, J. & DAVIDSON, D. J. 2016. Cathelicidins Have Direct Antiviral Activity against Respiratory Syncytial Virus In Vitro and Protective Function In Vivo in Mice and Humans. *J Immunol,* 196**,** 2699-710.

DALE, D., LILES, W., LLEWELLYN, C., RODGER, E. & PRICE, T. 1998. Neutrophil transfusions: kinetics and functions of neutrophils mobilized with granulocyte-colony-stimulating factor and dexamethasone. *Transfusion,* 38**,** 713-721.

DANCEY, J., DEUBELBEISS, K. A., HARKER, L. A. & FINCH, C. A. 1976. Neutrophil kinetics in man. *The Journal of clinical investigation,* 58**,** 705-715.

DE BUHR, N., PARPLYS, A. C., SCHROEDER, M., HENNECK, T., SCHAUMBURG, B., STANELLE-BERTRAM, S., JARCZAK, D., NIERHAUS, A., HILLER, J., PEINE, S., KLUGE, S., KLINGEL, K., GABRIEL, G. & VON KÖCKRITZ-BLICKWEDE, M. 2022. Impaired Degradation of Neutrophil Extracellular Traps: A Possible Severity Factor of Elderly Male COVID-19 Patients. *J Innate Immun***,** 1-16.

DE OLIVEIRA FORMIGA, R., AMARAL, F. C., SOUZA, C. F., MENDES, D. A., WANDERLEY, C. W., LORENZINI, C. B., SANTOS, A. A., ANTÔNIA, J., FARIA, L. F. & NATALE, C. C. 2020. Neuraminidase inhibitors rewire neutrophil function in vivo in murine sepsis and ex vivo in COVID-19. *Biorxiv***,** 2020.11. 12.379115.

DE SANTIS, M. C., GULLUNI, F., CAMPA, C. C., MARTINI, M. & HIRSCH, E. 2019. Targeting PI3K signaling in cancer: Challenges and advances. *Biochimica et Biophysica Acta (BBA)-Reviews on Cancer,* 1871**,** 361-366.

DE VITO, A., COLPANI, A., SADERI, L., PUCI, M., ZAULI, B., MELONI, M. C., FOIS, M., BITTI, A., DI CASTRI, C., FIORE, V., MAIDA, I., BABUDIERI, S., SOTGIU, G. & MADEDDU, G. 2023. Is the 4C Score Still a Valid Item to Predict In-Hospital Mortality in People with SARS-CoV-2 Infections in the Omicron Variant Era? *Life,* 13**,** 183.

DEL VALLE, D. M., KIM-SCHULZE, S., HUANG, H. H., BECKMANN, N. D., NIRENBERG, S., WANG, B., LAVIN, Y., SWARTZ, T. H., MADDURI, D., STOCK, A., MARRON, T. U., XIE, H., PATEL, M., TUBALLES, K., VAN OEKELEN, O., RAHMAN, A., KOVATCH, P., ABERG, J. A., SCHADT, E., JAGANNATH, S., MAZUMDAR, M., CHARNEY, A. W., FIRPO-BETANCOURT, A., MENDU, D. R., JHANG, J., REICH, D., SIGEL, K., CORDON-CARDO, C., FELDMANN, M., PAREKH, S., MERAD, M. & GNJATIC, S. 2020. An inflammatory cytokine signature predicts COVID-19 severity and survival. *Nat Med,* 26**,** 1636-1643.

DELGADO-RIZO, V., MARTÍNEZ-GUZMÁN, M. A., IÑIGUEZ-GUTIERREZ, L., GARCÍA-OROZCO, A., ALVARADO-NAVARRO, A. & FAFUTIS-MORRIS, M. 2017. Neutrophil Extracellular Traps and Its Implications in Inflammation: An Overview. *Front Immunol,* 8**,** 81.

DIAZ, A., BUJNOWSKI, D., MCMULLEN, P., LYSANDROU, M., ANANTHANARAYANAN, V., HUSAIN, A. N., FREEMAN, R., VIGNESWARAN, W. T., FERGUSON, M. K. & DONINGTON, J. S. 2022. Pulmonary parenchymal changes in COVID-19 survivors. *The Annals of Thoracic Surgery,* 114**,** 301-310.

DOMIN, J. & WATERFIELD, M. 1997. Using structure to define the function of phosphoinositide 3-kinase family members. *FEBS letters,* 410**,** 91-95.

DOMON, H., MAEKAWA, T., ISONO, T., FURUTA, K., KAITO, C. & TERAO, Y. 2021. Proteolytic cleavage of HLA class II by human neutrophil elastase in pneumococcal pneumonia. *Scientific reports,* 11**,** 1-9.

DORWARD, D. A., RUSSELL, C. D., UM, I. H., ELSHANI, M., ARMSTRONG, S. D., PENRICE-RANDAL, R., MILLAR, T., LERPINIERE, C. E., TAGLIAVINI, G. & HARTLEY, C. S. 2021. Tissue-specific immunopathology in fatal COVID-19. *American journal of respiratory and critical care medicine,* 203**,** 192-201.

DREW, W., WILSON, D. V. & SAPEY, E. 2018. Inflammation and neutrophil immunosenescence in health and disease: Targeted treatments to improve clinical outcomes in the elderly. *Experimental gerontology,* 105**,** 70-77.

DUFFY, S. 2018. Why are RNA virus mutation rates so damn high? *PLoS Biol,* 16**,** e3000003.

DUNZENDORFER, S. & WIEDERMANN, C. J. 2000a. Modulation of Neutrophil Migration and Superoxide Anion Release by Metoprolol. *Journal of Molecular and Cellular Cardiology,* 32**,** 915-924.

DUNZENDORFER, S. & WIEDERMANN, C. J. 2000b. Neuropeptide-induced chemotaxis of eosinophils in pulmonary diseases. *Ann Med,* 32**,** 429-39.

DUONG, D. 2021. Alpha, Beta, Delta, Gamma: What's important to know about SARS-CoV-2 variants of concern? *Cmaj,* 193**,** E1059-e1060.

DUPONT, A., RAUCH, A., STAESSENS, S., MOUSSA, M., ROSA, M., CORSEAUX, D., JEANPIERRE, E., GOUTAY, J., CAPLAN, M. & VARLET, P. 2021. Vascular endothelial damage in the pathogenesis of organ injury in severe COVID-19. *Arteriosclerosis, thrombosis, and vascular biology,* 41**,** 1760-1773.

EASH, K. J., GREENBAUM, A. M., GOPALAN, P. K. & LINK, D. C. 2010. CXCR2 and CXCR4 antagonistically regulate neutrophil trafficking from murine bone marrow. *The Journal of clinical investigation,* 120**,** 2423-2431.

EBRAHIMI, F., GIAGLIS, S., HAHN, S., BLUM, C. A., BAUMGARTNER, C., KUTZ, A., VAN BREDA, S. V., MUELLER, B., SCHUETZ, P., CHRIST-CRAIN, M. & HASLER, P. 2018. Markers of neutrophil extracellular traps predict adverse outcome in community-acquired pneumonia: secondary analysis of a randomised controlled trial. *Eur Respir J,* 51.

EL KEBIR, D. & FILEP, J. G. 2010. Role of neutrophil apoptosis in the resolution of inflammation. *TheScientificWorldJournal,* 10**,** 1731-1748.

ERPENBECK, L., GRUHN, A. L., KUDRYASHEVA, G., GÜNAY, G., MEYER, D., BUSSE, J., NEUBERT, E., SCHÖN, M. P., REHFELDT, F. & KRUSS, S. 2019. Effect of Adhesion and Substrate Elasticity on Neutrophil Extracellular Trap Formation. *Front Immunol,* 10**,** 2320.

FABBRI, L., MOSS, S., KHAN, F. A., CHI, W., XIA, J., ROBINSON, K., SMYTH, A. R., JENKINS, G. & STEWART, I. 2023. Parenchymal lung abnormalities following hospitalisation for COVID-19 and viral pneumonitis: a systematic review and meta-analysis. *Thorax,* 78**,** 191-201.

FAES, C., ABRAMS, S., VAN BECKHOVEN, D., MEYFROIDT, G., VLIEGHE, E. & HENS, N. 2020. Time between Symptom Onset, Hospitalisation and Recovery or Death: Statistical Analysis of Belgian COVID-19 Patients. *Int J Environ Res Public Health,* 17.

FANIYI, A., THEIN, O., BELCHAMBER, K., PAREKH, D., SCOTT, A., SAPEY, E. & THICKETT, D. 2022. S95 Prolonged neutrophil dysfunction and phenotype in elderly hospitalised community acquired pneumonia patients. BMJ Publishing Group Ltd.

FELDMAN, C. & ANDERSON, R. 2021. The role of co-infections and secondary infections in patients with COVID-19. *Pneumonia,* 13**,** 1-15.

FIELDING, C. A., MCLOUGHLIN, R. M., MCLEOD, L., COLMONT, C. S., NAJDOVSKA, M., GRAIL, D., ERNST, M., JONES, S. A., TOPLEY, N. & JENKINS, B. J. 2008. IL-6 regulates neutrophil trafficking during acute inflammation via STAT3. *J Immunol,* 181**,** 2189-95.

FILLMORE, N., BELL, S., SHEN, C., NGUYEN, V., LA, J., DUBREUIL, M., STRYMISH, J., BROPHY, M., MEHTA, G., WU, H., LIEBERMAN, J., DO, N. & SANDER, C. 2021. Disulfiram use is associated with lower risk of COVID-19: A retrospective cohort study. *PLOS ONE,* 16**,** e0259061.

FITZSIMMONS, W. J., WOODS, R. J., MCCRONE, J. T., WOODMAN, A., ARNOLD, J. J., YENNAWAR, M., EVANS, R., CAMERON, C. E. & LAURING, A. S. 2018. A speed-fidelity trade-off determines the mutation rate and virulence of an RNA virus. *PLoS Biol,* 16**,** e2006459.

FLORENTIN, J., ZHAO, J., TAI, Y.-Y., VASAMSETTI, S. B., O'NEIL, S. P., KUMAR, R., ARUNKUMAR, A., WATSON, A., SEMBRAT, J., BULLOCK, G. C., SANDERS, L., KASSA, B., ROJAS, M., GRAHAM, B. B., CHAN, S. Y. & DUTTA, P. 2021. Interleukin-6 mediates neutrophil mobilization from bone marrow in pulmonary hypertension. *Cellular & Molecular Immunology,* 18**,** 374-384.

FORTIN, C. F., CLOUTIER, A., EAR, T., SYLVAIN-PRÉVOST, S., MAYER, T. Z., BOUCHELAGHEM, R. & MCDONALD, P. P. 2011. A class IA PI3K controls inflammatory cytokine production in human neutrophils. *Eur J Immunol,* 41**,** 1709-19.

FRUMAN, D. A., CHIU, H., HOPKINS, B. D., BAGRODIA, S., CANTLEY, L. C. & ABRAHAM, R. T. 2017. The PI3K pathway in human disease. *Cell,* 170**,** 605-635.

FUENFER, M. M., OLSON, G. E. & POLK, H. C. 1975. Effect of various corticosteroids upon the phagocytic bactericidal activity of neutrophils. *Surgery,* 78**,** 27-33.

GALANI, I. E. & ANDREAKOS, E. 2015. Neutrophils in viral infections: Current concepts and caveats. *J Leukoc Biol,* 98**,** 557-64.

GALVÁN-ROMÁN, J. M., RODRÍGUEZ-GARCÍA, S. C., ROY-VALLEJO, E., MARCOS-JIMÉNEZ, A., SÁNCHEZ-ALONSO, S., FERNÁNDEZ-DÍAZ, C., ALCARAZ-SERNA, A., MATEU-ALBERO, T., RODRÍGUEZ-CORTES, P., SÁNCHEZ-CERRILLO, I., ESPARCIA, L., MARTÍNEZ-FLETA, P., LÓPEZ-SANZ, C., GABRIE, L., DEL CAMPO GUEROLA, L., SUÁREZ-FERNÁNDEZ, C., ANCOCHEA, J., CANABAL, A., ALBERT, P., RODRÍGUEZ-SERRANO, D. A., AGUILAR, J. M., DEL ARCO, C., DE LOS SANTOS, I., GARCÍA-FRAILE, L., DE LA CÁMARA, R., SERRA, J. M., RAMÍREZ, E., ALONSO, T., LANDETE, P., SORIANO, J. B., MARTÍN-GAYO, E., FRAILE TORRES, A., ZURITA CRUZ, N. D., GARCÍA-VICUÑA, R., CARDEÑOSO, L., SÁNCHEZ-MADRID, F., ALFRANCA, A., MUÑOZ-CALLEJA, C. & GONZÁLEZ-ÁLVARO, I. 2021. IL-6 serum levels predict severity and response to tocilizumab in COVID-19: An observational study. *J Allergy Clin Immunol,* 147**,** 72-80.e8.

GANGOPADHYAY, K. K. 2020. "Does having diabetes increase chances of contracting COVID-19 infection?". *Diabetes Metab Syndr,* 14**,** 765-766.

GARCÍA-PRIETO, J., VILLENA-GUTIÉRREZ, R., GÓMEZ, M., BERNARDO, E., PUN-GARCÍA, A., GARCÍA-LUNAR, I., CRAINICIUC, G., FERNÁNDEZ-JIMÉNEZ, R., SREERAMKUMAR, V., BOURIO-MARTÍNEZ, R., GARCÍA-RUIZ, J. M., DEL VALLE, A. S., SANZ-ROSA, D., PIZARRO, G., FERNÁNDEZ-ORTIZ, A., HIDALGO, A., FUSTER, V. & IBANEZ, B. 2017. Neutrophil stunning by metoprolol reduces infarct size. *Nature Communications,* 8**,** 14780.

GEORG, P., ASTABURUAGA-GARCÍA, R., BONAGURO, L., BRUMHARD, S., MICHALICK, L., LIPPERT, L. J., KOSTEVC, T., GÄBEL, C., SCHNEIDER, M., STREITZ, M., DEMICHEV, V., GEMÜND, I., BARONE, M., TOBER-LAU, P., HELBIG, E. T., HILLUS, D., PETROV, L., STEIN, J., DEY, H. P., PACLIK, D., IWERT, C., MÜLLEDER, M., AULAKH, S. K., DJUDJAJ, S., BÜLOW, R. D., MEI, H. E., SCHULZ, A. R., THIEL, A., HIPPENSTIEL, S., SALIBA, A. E., EILS, R., LEHMANN, I., MALL, M. A., STRICKER, S., RÖHMEL, J., CORMAN, V. M., BEULE, D., WYLER, E., LANDTHALER, M., OBERMAYER, B., VON STILLFRIED, S., BOOR, P., DEMIR, M., WESSELMANN, H., SUTTORP, N., UHRIG, A., MÜLLER-REDETZKY, H., NATTERMANN, J., KUEBLER, W. M., MEISEL, C., RALSER, M., SCHULTZE, J. L., ASCHENBRENNER, A. C., THIBEAULT, C., KURTH, F., SANDER, L. E., BLÜTHGEN, N. & SAWITZKI, B. 2022. Complement activation induces excessive T cell cytotoxicity in severe COVID-19. *Cell,* 185**,** 493-512.e25.

GEORGE, P. M., REED, A., DESAI, S. R., DEVARAJ, A., FAIEZ, T. S., LAVERTY, S., KANWAL, A., ESNEAU, C., LIU, M. K. & KAMAL, F. 2022. A persistent neutrophil-associated immune signature characterizes post–COVID-19 pulmonary sequelae. *Science translational medicine,* 14**,** eabo5795.

GIRALDO, E., MARTIN-CORDERO, L., HINCHADO, M., GARCIA, J. & ORTEGA, E. 2010. Role of phosphatidylinositol-3-kinase (PI3K), extracellular signal-regulated kinase (ERK) and nuclear transcription factor kappa β (NF-kβ) on neutrophil phagocytic process of Candida albicans. *Molecular and cellular biochemistry,* 333**,** 115-120.

GOLDFINGER, L. E., HAN, J., KIOSSES, W. B., HOWE, A. K. & GINSBERG, M. H. 2003. Spatial restriction of α4 integrin phosphorylation regulates lamellipodial stability and α4β1-dependent cell migration. *The Journal of cell biology,* 162**,** 731-741.

GOTTS, J. E., BERNARD, O., CHUN, L., CROZE, R. H., ROSS, J. T., NESSELER, N., WU, X., ABBOTT, J., FANG, X. & CALFEE, C. S. 2019. Clinically relevant model of pneumococcal pneumonia, ARDS, and

nonpulmonary organ dysfunction in mice. *American Journal of Physiology-Lung Cellular and Molecular Physiology,* 317**,** L717-L736.

GROUP, R. C. 2021. Dexamethasone in hospitalized patients with Covid-19. *New England Journal of Medicine,* 384**,** 693-704.

GROUP, T. R. C. 2020. Dexamethasone in hospitalized patients with Covid-19—preliminary report. *The New England journal of medicine*.

GRUDZINSKA, F. S., BRODLIE, M., SCHOLEFIELD, B. R., JACKSON, T., SCOTT, A., THICKETT, D. R. & SAPEY, E. 2020. Neutrophils in community-acquired pneumonia: parallels in dysfunction at the extremes of age. *Thorax,* 75**,** 164-171.

GUAN, W.-J., NI, Z.-Y., HU, Y., LIANG, W.-H., OU, C.-Q., HE, J.-X., LIU, L., SHAN, H., LEI, C.-L., HUI, D. S. C., DU, B., LI, L.-J., ZENG, G., YUEN, K.-Y., CHEN, R.-C., TANG, C.-L., WANG, T., CHEN, P.-Y., XIANG, J., LI, S.-Y., WANG, J.-L., LIANG, Z.-J., PENG, Y.-X., WEI, L., LIU, Y., HU, Y.-H., PENG, P., WANG, J.-M., LIU, J.-Y., CHEN, Z., LI, G., ZHENG, Z.-J., QIU, S.-Q., LUO, J., YE, C.-J., ZHU, S.-Y. & ZHONG, N.-S. 2020. Clinical Characteristics of Coronavirus Disease 2019 in China. *New England Journal of Medicine*.

GUPTA, R. K., HARRISON, E. M., HO, A., DOCHERTY, A. B., KNIGHT, S. R., VAN SMEDEN, M., ABUBAKAR, I., LIPMAN, M., QUARTAGNO, M., PIUS, R., BUCHAN, I., CARSON, G., DRAKE, T. M., DUNNING, J., FAIRFIELD, C. J., GAMBLE, C., GREEN, C. A., HALPIN, S., HARDWICK, H. E., HOLDEN, K. A., HORBY, P. W., JACKSON, C., MCLEAN, K. A., MERSON, L., NGUYEN-VAN-TAM, J. S., NORMAN, L., OLLIARO, P. L., PRITCHARD, M. G., RUSSELL, C. D., SCOTT-BROWN, J., SHAW, C. A., SHEIKH, A., SOLOMON, T., SUDLOW, C., SWANN, O. V., TURTLE, L., OPENSHAW, P. J. M., BAILLIE, J. K., SEMPLE, M. G. & NOURSADEGHI, M. 2021. Development and validation of the ISARIC 4C Deterioration model for adults hospitalised with COVID-19: a prospective cohort study. *Lancet Respir Med,* 9**,** 349-359.

HÄGER, M., COWLAND, J. B. & BORREGAARD, N. 2010. Neutrophil granules in health and disease. *J Intern Med,* 268**,** 25-34.

HAGIO, T., KISHIKAWA, K., KAWABATA, K., TASAKA, S., HASHIMOTO, S., HASEGAWA, N. & ISHIZAKA, A. 2008. Inhibition of neutrophil elastase reduces lung injury and bacterial count in hamsters. *Pulmonary pharmacology & therapeutics,* 21**,** 884-891.

HANNIGAN, M., HUANG, C. & WU, D. 2004. Roles of PI3K in neutrophil function. *Phosphoinositides in Subcellular Targeting and Enzyme Activation***,** 165-175.

HART, W. S., MILLER, E., ANDREWS, N. J., WAIGHT, P., MAINI, P. K., FUNK, S. & THOMPSON, R. N. 2022. Generation time of the alpha and delta SARS-CoV-2 variants: an epidemiological analysis. *The Lancet Infectious Diseases,* 22**,** 603-610.

HARTENIAN, E., NANDAKUMAR, D., LARI, A., LY, M., TUCKER, J. M. & GLAUNSINGER, B. A. 2020. The molecular virology of coronaviruses. *Journal of Biological Chemistry,* 295**,** 12910-12934.

HAWKINS, P. & STEPHENS, L. 2015. PI3K signalling in inflammation. *Biochimica et Biophysica Acta (BBA)-Molecular and Cell Biology of Lipids,* 1851**,** 882-897.

HAYDEN, F. G., FRITZ, R., LOBO, M. C., ALVORD, W., STROBER, W. & STRAUS, S. E. 1998. Local and systemic cytokine responses during experimental human influenza A virus infection. Relation to symptom formation and host defense. *J Clin Invest,* 101**,** 643-9.

HAZELDINE, J., DINSDALE, R. J., HARRISON, P. & LORD, J. M. 2019. Traumatic injury and exposure to mitochondrial-derived damage associated molecular patterns suppresses neutrophil extracellular trap formation. *Frontiers in immunology,* 10**,** 685.

HAZELDINE, J., HARRIS, P., CHAPPLE, I. L., GRANT, M., GREENWOOD, H., LIVESEY, A., SAPEY, E. & LORD, J. M. 2014. Impaired neutrophil extracellular trap formation: a novel defect in the innate immune system of aged individuals. *Aging Cell,* 13**,** 690-8.

HAZRATI, E., GALEN, B., LU, W., WANG, W., OUYANG, Y., KELLER, M. J., LEHRER, R. I. & HEROLD, B. C. 2006. Human alpha- and beta-defensins block multiple steps in herpes simplex virus infection. *J Immunol,* 177**,** 8658-66.

HERNANDEZ, P. A., GORLIN, R. J., LUKENS, J. N., TANIUCHI, S., BOHINJEC, J., FRANCOIS, F., KLOTMAN, M. E. & DIAZ, G. A. 2003. Mutations in the chemokine receptor gene CXCR4 are associated with WHIM syndrome, a combined immunodeficiency disease. *Nature genetics,* 34**,** 70-74.

HIRSCH, E., KATANAEV, V. L., GARLANDA, C., AZZOLINO, O., PIROLA, L., SILENGO, L., SOZZANI, S., MANTOVANI, A., ALTRUDA, F. & WYMANN, M. P. 2000. Central role for G protein-coupled phosphoinositide 3-kinase γ in inflammation. *Science,* 287**,** 1049-1053.

HOCK, H., HAMBLEN, M. J., ROOKE, H. M., TRAVER, D., BRONSON, R. T., CAMERON, S. & ORKIN, S. H. 2003. Intrinsic requirement for zinc finger transcription factor Gfi-1 in neutrophil differentiation. *Immunity,* 18**,** 109-120.

HORBY, P., LIM, W. S., EMBERSON, J. R., MAFHAM, M., BELL, J. L., LINSELL, L., STAPLIN, N., BRIGHTLING, C., USTIANOWSKI, A., ELMAHI, E., PRUDON, B., GREEN, C., FELTON, T., CHADWICK, D., REGE, K., FEGAN, C., CHAPPELL, L. C., FAUST, S. N., JAKI, T., JEFFERY, K., MONTGOMERY, A., ROWAN, K., JUSZCZAK, E., BAILLIE, J. K., HAYNES, R. & LANDRAY, M. J. 2021a. Dexamethasone in Hospitalized Patients with Covid-19. *N Engl J Med,* 384**,** 693-704.

HORBY, P. W., PESSOA-AMORIM, G., PETO, L., BRIGHTLING, C. E., SARKAR, R., THOMAS, K., JEEBUN, V., ASHISH, A., TULLY, R. & CHADWICK, D. 2021b. Tocilizumab in patients admitted to hospital with COVID-19 (RECOVERY): preliminary results of a randomised, controlled, open-label, platform trial. *Medrxiv*.

HOUSTON, N., STEWART, N., SMITH, D. S., BELL, S. C., CHAMPION, A. C. & REID, D. W. 2013. Sputum neutrophils in cystic fibrosis patients display a reduced respiratory burst. *Journal of cystic fibrosis,* 12**,** 352-362.

HOWELL, M. D., JONES, J. F., KISICH, K. O., STREIB, J. E., GALLO, R. L. & LEUNG, D. Y. 2004. Selective killing of vaccinia virus by LL-37: implications for eczema vaccinatum. *J Immunol,* 172**,** 1763-7.

HUANG, Y., YANG, C., XU, X. F., XU, W. & LIU, S. W. 2020. Structural and functional properties of SARS-CoV-2 spike protein: potential antivirus drug development for COVID-19. *Acta Pharmacol Sin,* 41**,** 1141-1149.

HUFFORD, M. M., RICHARDSON, G., ZHOU, H., MANICASSAMY, B., GARCÍA-SASTRE, A., ENELOW, R. I. & BRACIALE, T. J. 2012. Influenza-infected neutrophils within the infected lungs act as antigen presenting cells for anti-viral CD8(+) T cells. *PLoS One,* 7**,** e46581.

JANKOWSKI, A., SCOTT, C. C. & GRINSTEIN, S. 2002. Determinants of the phagosomal pH in neutrophils. *J Biol Chem,* 277**,** 6059-66.

JANOFF, A. & SCHERER, J. 1968. Mediators of inflammation in leukocyte lysosomes: IX. Elastinolytic activity in granules of human polymorphonuclear leukocytes. *The Journal of experimental medicine,* 128**,** 1137-1155.

JASPER, A. E., MCIVER, W. J., SAPEY, E. & WALTON, G. M. 2019. Understanding the role of neutrophils in chronic inflammatory airway disease. *F1000Research,* 8.

JOHNSON, R. M. & VINETZ, J. M. 2020. Dexamethasone in the management of covid-19. British Medical Journal Publishing Group.

JUSS, J. K., HOUSE, D., AMOUR, A., BEGG, M., HERRE, J., STORISTEANU, D. M., HOENDERDOS, K., BRADLEY, G., LENNON, M. & SUMMERS, C. 2016a. Acute respiratory distress syndrome neutrophils have a distinct phenotype and are resistant to phosphoinositide 3-kinase inhibition. *American journal of respiratory and critical care medicine,* 194**,** 961-973.

JUSS, J. K., HOUSE, D., AMOUR, A., BEGG, M., HERRE, J., STORISTEANU, D. M., HOENDERDOS, K., BRADLEY, G., LENNON, M., SUMMERS, C., HESSEL, E. M., CONDLIFFE, A. & CHILVERS, E. R. 2016b. Acute Respiratory Distress Syndrome Neutrophils Have a Distinct Phenotype and Are Resistant to Phosphoinositide 3-Kinase Inhibition. *Am J Respir Crit Care Med,* 194**,** 961-973.

KAFIENAH, W. E., BUTTLE, J. D., BURNETT, D. & HOLLANDER, P. A. 1998. Cleavage of native type I collagen by human neutrophil elastase. *Biochemical Journal,* 330**,** 897-902.

KANSAS, G. S. 1996. Selectins and their ligands: current concepts and controversies.

KARSUNKY, H., ZENG, H., SCHMIDT, T., ZEVNIK, B., KLUGE, R., SCHMID, K. W., DÜHRSEN, U. & MÖRÖY, T. 2002. Inflammatory reactions and severe neutropenia in mice lacking the transcriptional repressor Gfi1. *Nature genetics,* 30**,** 295-300.

KATSURA, H., SONTAKE, V., TATA, A., KOBAYASHI, Y., EDWARDS, C. E., HEATON, B. E., KONKIMALLA, A., ASAKURA, T., MIKAMI, Y., FRITCH, E. J., LEE, P. J., HEATON, N. S., BOUCHER, R. C., RANDELL, S. H., BARIC, R. S. & TATA, P. R. 2020. Human Lung Stem Cell-Based Alveolospheres Provide Insights into SARS-CoV-2-Mediated Interferon Responses and Pneumocyte Dysfunction. *Cell Stem Cell,* 27**,** 890-904.e8.

KATZENSTEIN, A. L., BLOOR, C. M. & LEIBOW, A. A. 1976. Diffuse alveolar damage--the role of oxygen, shock, and related factors. A review. *Am J Pathol,* 85**,** 209-28.

KEIR, H. R., LONG, M. B., ABO-LEYAH, H., GIAM, Y. H., VADIVELOO, T., PEMBRIDGE, T., HULL, R. C., DELGADO, L., BAND, M. & MCLAREN-NEIL, F. 2022. Dipeptidyl peptidase-1 inhibition in patients hospitalised with COVID-19: a multicentre, double-blind, randomised, parallel-group, placebo-controlled trial. *The Lancet Respiratory Medicine*.

KENAWY, H. I., BORAL, I. & BEVINGTON, A. 2015. Complement-Coagulation Cross-Talk: A Potential Mediator of the Physiological Activation of Complement by Low pH. *Front Immunol,* 6**,** 215.

KENNY, E. F., HERZIG, A., KRÜGER, R., MUTH, A., MONDAL, S., THOMPSON, P. R., BRINKMANN, V., VON BERNUTH, H. & ZYCHLINSKY, A. 2017. Diverse stimuli engage different neutrophil extracellular trap pathways. *Elife,* 6**,** e24437.

KERBOUA, K. E. 2021. NLR: A cost-effective nomogram to guide therapeutic interventions in COVID-19. *Immunological Investigations,* 50**,** 92-100.

KERMANI, N. Z., SONG, W.-J., BADI, Y., VERSI, A., GUO, Y., SUN, K., BHAVSAR, P., HOWARTH, P., DAHLEN, S.-E. & STERK, P. J. 2021. Sputum ACE2, TMPRSS2 and FURIN gene expression in severe neutrophilic asthma. *Respiratory research,* 22**,** 1-10.

KHALAFALLAH, A. A., KIRKBY, B. E., WONG, S., FOONG, Y. C., RANJAN, N., LUTTRELL, J., MATHEW, R., CHILVERS, C. M., MAULDON, E., SHARP, C. & HANNAN, T. 2016. Venous thromboembolism in medical patients during hospitalisation and 3 months after hospitalisation: a prospective observational study. *BMJ Open,* 6**,** e012346.

KHAN, M. A., PHILIP, L. M., CHEUNG, G., VADAKEPEEDIKA, S., GRASEMANN, H., SWEEZEY, N. & PALANIYAR, N. 2018. Regulating NETosis: Increasing pH Promotes NADPH Oxidase-Dependent NETosis. *Front Med (Lausanne),* 5**,** 19.

KHAN, M. O., PARK, K. K. & LEE, H. J. 2005. Antedrugs: an approach to safer drugs. *Curr Med Chem,* 12**,** 2227-39.

KHAN, S. Y., KELHER, M. R., HEAL, J. M., BLUMBERG, N., BOSHKOV, L. K., PHIPPS, R., GETTINGS, K. F., MCLAUGHLIN, N. J. & SILLIMAN, C. C. 2006. Soluble CD40 ligand accumulates in stored blood components, primes neutrophils through CD40, and is a potential cofactor in the development of transfusion-related acute lung injury. *Blood,* 108**,** 2455-2462.

KIM, K. H. & SEDERSTROM, J. M. 2015. Assaying cell cycle status using flow cytometry. *Current protocols in molecular biology,* 111**,** 28.6. 1-28.6. 11.

KIM, W., ZHOU, J. Q., HORVATH, S. C., SCHMITZ, A. J., STURTZ, A. J., LEI, T., LIU, Z., KALAIDINA, E., THAPA, M. & ALSOUSSI, W. B. 2022. Germinal centre-driven maturation of B cell response to mRNA vaccination. *Nature,* 604**,** 141-145.

KINO, T. 2018. GR-regulating serine/threonine kinases: new physiologic and pathologic implications. *Trends in Endocrinology & Metabolism,* 29**,** 260-270.

KNIGHT, S. R., HO, A., PIUS, R., BUCHAN, I., CARSON, G., DRAKE, T. M., DUNNING, J., FAIRFIELD, C. J., GAMBLE, C., GREEN, C. A., GUPTA, R., HALPIN, S., HARDWICK, H. E., HOLDEN, K. A., HORBY, P. W., JACKSON, C., MCLEAN, K. A., MERSON, L., NGUYEN-VAN-TAM, J. S., NORMAN, L., NOURSADEGHI, M., OLLIARO, P. L., PRITCHARD, M. G., RUSSELL, C. D., SHAW, C. A., SHEIKH, A., SOLOMON, T., SUDLOW, C., SWANN, O. V., TURTLE, L. C., OPENSHAW, P. J., BAILLIE, J. K., SEMPLE, M. G., DOCHERTY, A. B. & HARRISON, E. M. 2020. Risk stratification of patients admitted to hospital with covid-19 using the ISARIC WHO Clinical Characterisation Protocol: development and validation of the 4C Mortality Score. *Bmj,* 370**,** m3339.

KOBAYASHI, S. D., MALACHOWA, N. & DELEO, F. R. 2018. Neutrophils and bacterial immune evasion. *Journal of Innate Immunity,* 10**,** 432-441.

KOLACZKOWSKA, E. & KUBES, P. 2013. Neutrophil recruitment and function in health and inflammation. *Nature reviews immunology,* 13**,** 159-175.

KORKMAZ, B., HORWITZ, M. S., JENNE, D. E. & GAUTHIER, F. 2010. Neutrophil elastase, proteinase 3, and cathepsin G as therapeutic targets in human diseases. *Pharmacological reviews,* 62**,** 726-759.

KRITIKOS, A., CARUANA, G., BROUILLET, R., MIROZ, J. P., ABED-MAILLARD, S., STIEGER, G., OPOTA, O., CROXATTO, A., VOLLENWEIDER, P., BART, P. A., CHICHE, J. D. & GREUB, G. 2021. Sensitivity of Rapid Antigen Testing and RT-PCR Performed on Nasopharyngeal Swabs versus Saliva Samples

in COVID-19 Hospitalized Patients: Results of a Prospective Comparative Trial (RESTART). *Microorganisms,* 9.

KTISTAKIS, N. T. & TOOZE, S. A. 2016. Digesting the expanding mechanisms of autophagy. *Trends in cell biology,* 26**,** 624-635.

KUEK, L. E. & LEE, R. J. 2020. First contact: the role of respiratory cilia in host-pathogen interactions in the airways. *American Journal of Physiology-Lung Cellular and Molecular Physiology,* 319**,** L603-L619.

KUHNS, D. B., PRIEL, D. A. L. & GALLIN, J. I. 1995. Loss of L-selectin (CD62L) on human neutrophils following exudation in vivo. *Cellular immunology,* 164**,** 306-310.

LACY, P. 2006. Mechanisms of degranulation in neutrophils. *Allergy Asthma Clin Immunol,* 2**,** 98-108.

LAMERS, M. M., MYKYTYN, A. Z., BREUGEM, T. I., WANG, Y., WU, D. C., RIESEBOSCH, S., VAN DEN DOEL, P. B., SCHIPPER, D., BESTEBROER, T., WU, N. C. & HAAGMANS, B. L. 2021. Human airway cells prevent SARS-CoV-2 multibasic cleavage site cell culture adaptation. *Elife,* 10.

LANIER, L. L. & WARNER, N. L. 1981. Paraformaldehyde fixation of hematopoietic cells for quantitative flow cytometry (FACS) analysis. *J Immunol Methods,* 47**,** 25-30.

LEE, A., WHYTE, M. K. & HASLETT, C. 1993. Inhibition of apoptosis and prolongation of neutrophil functional longevity by inflammatory mediators. *J Leukoc Biol,* 54**,** 283-8.

LEE, W. L., HARRISON, R. E. & GRINSTEIN, S. 2003. Phagocytosis by neutrophils. *Microbes Infect,* 5**,** 1299-306.

LEPPKES, M., KNOPF, J., NASCHBERGER, E., LINDEMANN, A., SINGH, J., HERRMANN, I., STÜRZL, M., STAATS, L., MAHAJAN, A. & SCHAUER, C. 2020. Vascular occlusion by neutrophil extracellular traps in COVID-19. *EBioMedicine,* 58**,** 102925.

LESCURE, F. X., HONDA, H., FOWLER, R. A., LAZAR, J. S., SHI, G., WUNG, P., PATEL, N. & HAGINO, O. 2021. Sarilumab in patients admitted to hospital with severe or critical COVID-19: a randomised, double-blind, placebo-controlled, phase 3 trial. *Lancet Respir Med,* 9**,** 522-532.

LEVY, B. D. & SERHAN, C. N. 2014. Resolution of acute inflammation in the lung. *Annual review of physiology,* 76**,** 467-492.

LEY, K., LAUDANNA, C., CYBULSKY, M. I. & NOURSHARGH, S. 2007. Getting to the site of inflammation: the leukocyte adhesion cascade updated. *Nature Reviews Immunology,* 7**,** 678-689.

LEY, K., SMITH, E. & STARK, M. A. 2006. IL-17A-producing neutrophil-regulatory Tn lymphocytes. *Immunologic research,* 34**,** 229-242.

LIM, W. S., BAUDOUIN, S. V., GEORGE, R. C., HILL, A. T., JAMIESON, C., LE JEUNE, I., MACFARLANE, J. T., READ, R. C., ROBERTS, H. J., LEVY, M. L., WANI, M., WOODHEAD, M. A. & PNEUMONIA GUIDELINES COMMITTEE OF THE, B. T. S. S. O. C. C. 2009. BTS guidelines for the management of community acquired pneumonia in adults: update 2009. *Thorax,* 64 Suppl 3**,** iii1-55.

LIM, W. S., VAN DER EERDEN, M. M., LAING, R., BOERSMA, W. G., KARALUS, N., TOWN, G. I., LEWIS, S. A. & MACFARLANE, J. T. 2003. Defining community acquired pneumonia severity on presentation to hospital: an international derivation and validation study. *Thorax,* 58**,** 377-82.

LIN, R. Y., ASTIZ, M. E., SAXON, J. C. & RACKOW, E. C. 1993. Altered leukocyte immunophenotypes in septic shock. Studies of HLA-DR, CD11b, CD14, and IL-2R expression. *Chest,* 104**,** 847-53.

LINDNER, D., FITZEK, A., BRÄUNINGER, H., ALESHCHEVA, G., EDLER, C., MEISSNER, K., SCHERSCHEL, K., KIRCHHOF, P., ESCHER, F., SCHULTHEISS, H. P., BLANKENBERG, S., PÜSCHEL, K. & WESTERMANN, D. 2020. Association of Cardiac Infection With SARS-CoV-2 in Confirmed COVID-19 Autopsy Cases. *JAMA Cardiol,* 5**,** 1281-1285.

LISMAN, T. 2018. Platelet-neutrophil interactions as drivers of inflammatory and thrombotic disease. *Cell Tissue Res,* 371**,** 567-576.

LIU, C. L., TANGSOMBATVISIT, S., ROSENBERG, J. M., MANDELBAUM, G., GILLESPIE, E. C., GOZANI, O. P., ALIZADEH, A. A. & UTZ, P. J. 2012. Specific post-translational histone modifications of neutrophil extracellular traps as immunogens and potential targets of lupus autoantibodies. *Arthritis Res Ther,* 14**,** R25.

LOMAS, D., IP, M., CHAMBA, A. & STOCKLEY, R. 1991. The effect of in vitro and in vivo dexamethasone on human neutrophil function. *Agents and actions,* 33**,** 279-285.

LONG, J. P., KOTUR, M. S., STARK, G. V., WARREN, R. L., KASOJI, M., CRAFT, J. L., ALBRECHT, R. A., GARCÍA-SASTRE, A., KATZE, M. G. & WATERS, K. M. 2013. Accumulation of CD11b+ Gr-1+ cells

in the lung, blood and bone marrow of mice infected with highly pathogenic H5N1 and H1N1 influenza viruses. *Archives of virology,* 158**,** 1305-1322.

LOPEZ-ILASACA, M., CRESPO, P., PELLICI, P. G., GUTKIND, J. S. & WETZKER, R. 1997. Linkage of G protein-coupled receptors to the MAPK signaling pathway through PI 3-kinase γ. *Science,* 275**,** 394-397.

LOYER, C., LAPOSTOLLE, A., URBINA, T., ELABBADI, A., LAVILLEGRAND, J. R., CHAIGNEAU, T., SIMOES, C., DESSAJAN, J., DESNOS, C., MORIN-BRUREAU, M., CHANTRAN, Y., AUCOUTURIER, P., GUIDET, B., VOIRIOT, G., AIT-OUFELLA, H. & ELBIM, C. 2022. Impairment of neutrophil functions and homeostasis in COVID-19 patients: association with disease severity. *Crit Care,* 26**,** 155.

MAFFUCCI, T., COOKE, F. T., FOSTER, F. M., TRAER, C. J., FRY, M. J. & FALASCA, M. 2005. Class II phosphoinositide 3-kinase defines a novel signaling pathway in cell migration. *The Journal of cell biology,* 169**,** 789-799.

MAHONEY, M. E. & SRIDHAR, S. S. 2023. Clinical trial reform in the post-COVID era. *Therapeutic Advances in Medical Oncology,* 15**,** 17588359231183676.

MANIK, M. & SINGH, R. K. 2022. Role of toll-like receptors in modulation of cytokine storm signaling in SARS-CoV-2-induced COVID-19. *Journal of medical virology,* 94**,** 869-877.

MANLEY, H. R., KEIGHTLEY, M. C. & LIESCHKE, G. J. 2018. The Neutrophil Nucleus: An Important Influence on Neutrophil Migration and Function. *Front Immunol,* 9**,** 2867.

MANOHARAN, S. & YING, L. Y. 2022. Baricitinib for the Management of SARS-CoV-2-Infected Patients: A Systematic Review and Meta-Analysis of Randomised Controlled Trials. *Can J Infect Dis Med Microbiol,* 2022**,** 8332819.

MARAGOUDAKIS, M., TSOPANOGLOU, N. & ANDRIOPOULOU, P. 2002. Mechanism of thrombin-induced angiogenesis. *Biochemical Society Transactions,* 30**,** 173-177.

MARINI, O., COSTA, S., BEVILACQUA, D., CALZETTI, F., TAMASSIA, N., SPINA, C., DE SABATA, D., TINAZZI, E., LUNARDI, C., SCUPOLI, M. T., CAVALLINI, C., ZORATTI, E., TINAZZI, I., MARCHETTA, A., VASSANELLI, A., CANTINI, M., GANDINI, G., RUZZENENTE, A., GUGLIELMI, A., MISSALE, F., VERMI, W., TECCHIO, C., CASSATELLA, M. A. & SCAPINI, P. 2017. Mature CD10(+) and immature CD10(-) neutrophils present in G-CSF-treated donors display opposite effects on T cells. *Blood,* 129**,** 1343-1356.

MARTIN, C., BURDON, P. C., BRIDGER, G., GUTIERREZ-RAMOS, J. C., WILLIAMS, T. J. & RANKIN, S. M. 2003. Chemokines acting via CXCR2 and CXCR4 control the release of neutrophils from the bone marrow and their return following senescence. *Immunity,* 19**,** 583-93.

MASSO-SILVA, J. A., MOSHENSKY, A., LAM, M. T., ODISH, M., PATEL, A., XU, L., HANSEN, E., TRESCOTT, S., NGUYEN, C. & KIM, R. 2021. Increased peripheral blood neutrophil activation phenotypes and NETosis in critically ill COVID-19 patients: a case series and review of the literature.

MEIZLISH, M. L., PINE, A. B., BISHAI, J. D., GOSHUA, G., NADELMANN, E. R., SIMONOV, M., CHANG, C.-H., ZHANG, H., SHALLOW, M. & BAHEL, P. 2021. A neutrophil activation signature predicts critical illness and mortality in COVID-19. *Blood advances,* 5**,** 1164-1177.

MENTER, T., HASLBAUER, J. D., NIENHOLD, R., SAVIC, S., HOPFER, H., DEIGENDESCH, N., FRANK, S., TUREK, D., WILLI, N., PARGGER, H., BASSETTI, S., LEUPPI, J. D., CATHOMAS, G., TOLNAY, M., MERTZ, K. D. & TZANKOV, A. 2020. Postmortem examination of COVID-19 patients reveals diffuse alveolar damage with severe capillary congestion and variegated findings in lungs and other organs suggesting vascular dysfunction. *Histopathology,* 77**,** 198-209.

MESSNER, C. B., DEMICHEV, V., WENDISCH, D., MICHALICK, L., WHITE, M., FREIWALD, A., TEXTORIS-TAUBE, K., VERNARDIS, S. I., EGGER, A. S., KREIDL, M., LUDWIG, D., KILIAN, C., AGOSTINI, F., ZELEZNIAK, A., THIBEAULT, C., PFEIFFER, M., HIPPENSTIEL, S., HOCKE, A., VON KALLE, C., CAMPBELL, A., HAYWARD, C., PORTEOUS, D. J., MARIONI, R. E., LANGENBERG, C., LILLEY, K. S., KUEBLER, W. M., MÜLLEDER, M., DROSTEN, C., SUTTORP, N., WITZENRATH, M., KURTH, F., SANDER, L. E. & RALSER, M. 2020. Ultra-High-Throughput Clinical Proteomics Reveals Classifiers of COVID-19 Infection. *Cell Syst,* 11**,** 11-24.e4.

METZEMAEKERS, M., CAMBIER, S., BLANTER, M., VANDOOREN, J., DE CARVALHO, A. C., MALENGIER-DEVLIES, B., VANDERBEKE, L., JACOBS, C., COENEN, S. & MARTENS, E. 2021. Kinetics of

peripheral blood neutrophils in severe coronavirus disease 2019. *Clinical & translational immunology,* 10**,** e1271.

MIDDLETON, E. A., HE, X.-Y., DENORME, F., CAMPBELL, R. A., NG, D., SALVATORE, S. P., MOSTYKA, M., BAXTER-STOLTZFUS, A., BORCZUK, A. C. & LODA, M. 2020. Neutrophil extracellular traps contribute to immunothrombosis in COVID-19 acute respiratory distress syndrome. *Blood,* 136**,** 1169-1179.

MIRALDA, I., URIARTE, S. M. & MCLEISH, K. R. 2017. Multiple phenotypic changes define neutrophil priming. *Frontiers in cellular and infection microbiology,* 7**,** 217.

MÓCSAI, A., WALZOG, B. & LOWELL, C. A. 2015. Intracellular signalling during neutrophil recruitment. *Cardiovascular research,* 107**,** 373-385.

MOKART, D., VAN CRAENENBROECK, T., LAMBERT, J., TEXTORIS, J., BRUN, J. P., SANNINI, A., CHOW-CHINE, L., HAMOUDA, S., FOUCHÉ, L., ETTORI, F., FAUCHER, M. & BLACHE, J. L. 2012. Prognosis of acute respiratory distress syndrome in neutropenic cancer patients. *Eur Respir J,* 40**,** 169-76.

MORRISSEY, S. M., GELLER, A. E., HU, X., TIERI, D., DING, C., KLAES, C. K., COOKE, E. A., WOESTE, M. R., MARTIN, Z. C. & CHEN, O. 2021. A specific low-density neutrophil population correlates with hypercoagulation and disease severity in hospitalized COVID-19 patients. *JCI insight,* 6.

MUINONEN-MARTIN, A. J., VELTMAN, D. M., KALNA, G. & INSALL, R. H. 2010. An improved chamber for direct visualisation of chemotaxis. *PloS one,* 5**,** e15309.

MULLER KOBOLD, A. C., TULLEKEN, J. E., ZIJLSTRA, J. G., SLUITER, W., HERMANS, J., KALLENBERG, C. G. & TERVAERT, J. W. 2000. Leukocyte activation in sepsis; correlations with disease state and mortality. *Intensive Care Med,* 26**,** 883-92.

MUSICH, T., RAHMAN, M. A., MOHANRAM, V., MILLER-NOVAK, L., DEMBERG, T., VENZON, D. J., FELBER, B. K., FRANCHINI, G., PAVLAKIS, G. N. & ROBERT-GUROFF, M. 2018a. Neutrophil Vaccination Dynamics and Their Capacity To Mediate B Cell Help in Rhesus Macaques. *J Immunol,* 201**,** 2287-2302.

MUSICH, T., RAHMAN, M. A., MOHANRAM, V., MILLER-NOVAK, L., DEMBERG, T., VENZON, D. J., FELBER, B. K., FRANCHINI, G., PAVLAKIS, G. N. & ROBERT-GUROFF, M. 2018b. Neutrophil Vaccination Dynamics and Their Capacity To Mediate B Cell Help in Rhesus Macaques. *The Journal of Immunology,* 201**,** 2287-2302.

NARASARAJU, T., YANG, E., SAMY, R. P., NG, H. H., POH, W. P., LIEW, A. A., PHOON, M. C., VAN ROOIJEN, N. & CHOW, V. T. 2011. Excessive neutrophils and neutrophil extracellular traps contribute to acute lung injury of influenza pneumonitis. *Am J Pathol,* 179**,** 199-210.

NARAYANA MOORTHY, A., NARASARAJU, T., RAI, P., PERUMALSAMY, R., TAN, K. B., WANG, S., ENGELWARD, B. & CHOW, V. T. 2013. In vivo and in vitro studies on the roles of neutrophil extracellular traps during secondary pneumococcal pneumonia after primary pulmonary influenza infection. *Front Immunol,* 4**,** 56.

NAUMENKO, V., TURK, M., JENNE, C. N. & KIM, S. J. 2018. Neutrophils in viral infection. *Cell Tissue Res,* 371**,** 505-516.

NEXTSTRAIN. 2023. Available: www.nextstrain.org [Accessed].

NICOD, L. 2005. Lung defences: an overview. *European Respiratory Review,* 14**,** 45-50.

NIIRO, H., OTSUKA, T., IZUHARA, K., YAMAOKA, K., OHSHIMA, K., TANABE, T., HARA, S., NEMOTO, Y., TANAKA, Y., NAKASHIMA, H. & NIHO, Y. 1997. Regulation by interleukin-10 and interleukin-4 of cyclooxygenase-2 expression in human neutrophils. *Blood,* 89**,** 1621-8.

NOMANI, M., VARAHRAM, M., TABARSI, P., HASHEMIAN, S. M., JAMAATI, H., MALEKMOHAMMAD, M., GHAZI, M., ADCOCK, I. M. & MORTAZ, E. 2021. Decreased neutrophil-mediated bacterial killing in COVID-19 patients. *Scandinavian Journal of Immunology,* 94**,** e13083.

OGANDO, N. S., DALEBOUT, T. J., ZEVENHOVEN-DOBBE, J. C., LIMPENS, R., VAN DER MEER, Y., CALY, L., DRUCE, J., DE VRIES, J. J. C., KIKKERT, M., BÁRCENA, M., SIDOROV, I. & SNIJDER, E. J. 2020. SARS-coronavirus-2 replication in Vero E6 cells: replication kinetics, rapid adaptation and cytopathology. *J Gen Virol,* 101**,** 925-940.

OH, H., SIANO, B. & DIAMOND, S. 2008. Neutrophil isolation protocol. *Journal of visualized experiments: JoVE*.

OKRENT, D. G., LICHTENSTEIN, A. K. & GANZ, T. 1990. Direct cytotoxicity of polymorphonuclear leukocyte granule proteins to human lung-derived cells and endothelial cells. *Am Rev Respir Dis,* 141**,** 179-85.

OPASAWATCHAI, A., AMORNSUPAWAT, P., JIRAVEJCHAKUL, N., CHAN-IN, W., SPOERK, N. J., MANOPWISEDJAROEN, K., SINGHASIVANON, P., YINGTAWEESAK, T., SURAAMORNKUL, S. & MONGKOLSAPAYA, J. 2019. Neutrophil activation and early features of NET formation are associated with dengue virus infection in human. *Frontiers in immunology,* 9**,** 3007.

ORR, Y., TAYLOR, J., BANNON, P., GECZY, C. & KRITHARIDES, L. 2005. Circulating CD10−/CD16low neutrophils provide a quantitative index of active bone marrow neutrophil release. *British journal of haematology,* 131**,** 508-519.

OURWORLDINDATA. 2022. *Coronavirus* [Online]. Available: https://ourworldindata.org/coronavirus [Accessed].

OVERMYER, K. A., SHISHKOVA, E., MILLER, I. J., BALNIS, J., BERNSTEIN, M. N., PETERS-CLARKE, T. M., MEYER, J. G., QUAN, Q., MUEHLBAUER, L. K., TRUJILLO, E. A., HE, Y., CHOPRA, A., CHIENG, H. C., TIWARI, A., JUDSON, M. A., PAULSON, B., BRADEMAN, D. R., ZHU, Y., SERRANO, L. R., LINKE, V., DRAKE, L. A., ADAM, A. P., SCHWARTZ, B. S., SINGER, H. A., SWANSON, S., MOSHER, D. F., STEWART, R., COON, J. J. & JAITOVICH, A. 2021. Large-Scale Multi-omic Analysis of COVID-19 Severity. *Cell Syst,* 12**,** 23-40.e7.

OWENS, A. P., 3RD & MACKMAN, N. 2010. Tissue factor and thrombosis: The clot starts here. *Thromb Haemost,* 104**,** 432-9.

PALMA, G., PASQUA, T., SILVESTRI, G., ROCCA, C., GUALTIERI, P., BARBIERI, A., DE BARTOLO, A., DE LORENZO, A., ANGELONE, T., AVOLIO, E. & BOTTI, G. 2020. PI3Kδ Inhibition as a Potential Therapeutic Target in COVID-19. *Front Immunol,* 11**,** 2094.

PAN, H., MA, Y., WANG, D., WANG, J., JIANG, H., PAN, S., ZHAO, B., WU, Y., XU, D., SUN, X., LIU, L. & XU, Z. 2013. Effect of IFN-α on KC and LIX expression: role of STAT1 and its effect on neutrophil recruitment to the spleen after lipopolysaccharide stimulation. *Mol Immunol,* 56**,** 12-22.

PAPAYANNOPOULOS, V. 2018. Neutrophil extracellular traps in immunity and disease. *Nature Reviews Immunology,* 18**,** 134-147.

PAPAYANNOPOULOS, V., METZLER, K. D., HAKKIM, A. & ZYCHLINSKY, A. 2010. Neutrophil elastase and myeloperoxidase regulate the formation of neutrophil extracellular traps. *J Cell Biol,* 191**,** 677-91.

PARK, A. & IWASAKI, A. 2020. Type I and type III interferons–induction, signaling, evasion, and application to combat COVID-19. *Cell host & microbe,* 27**,** 870-878.

PARTIDA-SANCHEZ, S., COCKAYNE, D. A., MONARD, S., JACOBSON, E. L., OPPENHEIMER, N., GARVY, B., KUSSER, K., GOODRICH, S., HOWARD, M. & HARMSEN, A. 2001. Cyclic ADP-ribose production by CD38 regulates intracellular calcium release, extracellular calcium influx and chemotaxis in neutrophils and is required for bacterial clearance in vivo. *Nature medicine,* 7**,** 1209-1216.

PATEL, J. M., SAPEY, E., PAREKH, D., SCOTT, A., DOSANJH, D., GAO, F. & THICKETT, D. R. 2018. Sepsis induces a dysregulated neutrophil phenotype that is associated with increased mortality. *Mediators of inflammation,* 2018.

PERICÀS, J. M., DERDE, L. P. & BERRY, S. M. 2023. Platform trials as the way forward in infectious disease'clinical research: the case of coronavirus disease 2019. *Clinical Microbiology and Infection,* 29**,** 277-280.

PERNG, D.-W., WU, Y.-C., TSAI, M.-C., LIN, C.-P., HSU, W.-H., PERNG, R.-P. & LEE, Y.-C. 2003. Neutrophil elastase stimulates human airway epithelial cells to produce PGE2 through activation of p44/42 MAPK and upregulation of cyclooxygenase-2. *American Journal of Physiology-Lung Cellular and Molecular Physiology,* 285**,** L925-L930.

PERRETTI, M. & FLOWER, R. J. 1993. Modulation of IL-1-induced neutrophil migration by dexamethasone and lipocortin 1. *The Journal of Immunology,* 150**,** 992-999.

PERRONE, L. A., PLOWDEN, J. K., GARCÍA-SASTRE, A., KATZ, J. M. & TUMPEY, T. M. 2008. H5N1 and 1918 pandemic influenza virus infection results in early and excessive infiltration of macrophages and neutrophils in the lungs of mice. *PLoS Pathog,* 4**,** e1000115.

PETERHANS, E. 1997. Reactive oxygen species and nitric oxide in viral diseases. *Biol Trace Elem Res,* 56**,** 107-16.

PHAM, T. & RUBENFELD, G. D. 2017. Fifty Years of Research in ARDS. The Epidemiology of Acute Respiratory Distress Syndrome. A 50th Birthday Review. *Am J Respir Crit Care Med,* 195**,** 860-870.

PHILLIPSON, M., HEIT, B., COLARUSSO, P., LIU, L., BALLANTYNE, C. M. & KUBES, P. 2006. Intraluminal crawling of neutrophils to emigration sites: a molecularly distinct process from adhesion in the recruitment cascade. *The Journal of experimental medicine,* 203**,** 2569-2575.

PHILLIPSON, M. & KUBES, P. 2011. The neutrophil in vascular inflammation. *Nature medicine,* 17**,** 1381-1390.

PILLAY, J., DEN BRABER, I., VRISEKOOP, N., KWAST, L. M., DE BOER, R. J., BORGHANS, J. A., TESSELAAR, K. & KOENDERMAN, L. 2010. In vivo labeling with 2H2O reveals a human neutrophil lifespan of 5.4 days. *Blood, The Journal of the American Society of Hematology,* 116**,** 625-627.

POSPIESZALSKA, M. K. & LEY, K. 2009. Dynamics of microvillus extension and tether formation in rolling leukocytes. *Cellular and molecular bioengineering,* 2**,** 207-217.

PRANATA, R., HENRINA, J., LIM, M. A., LAWRENSIA, S., YONAS, E., VANIA, R., HUANG, I., LUKITO, A. A., SUASTIKA, K., KUSWARDHANI, R. A. T. & SETIATI, S. 2021. Clinical frailty scale and mortality in COVID-19: A systematic review and dose-response meta-analysis. *Arch Gerontol Geriatr,* 93**,** 104324.

PRICE, T. & DALE, D. C. 1977. Neutrophil preservation: the effect of short-term storage on in vivo kinetics. *The Journal of Clinical Investigation,* 59**,** 475-480.

PRINTZ, C. 2021. Poor COVID-19 outcomes and deaths linked to advanced age and pre-existing conditions. *Cancer,* 127**,** 497-497.

PUELLES, V. G., LÜTGEHETMANN, M., LINDENMEYER, M. T., SPERHAKE, J. P., WONG, M. N., ALLWEISS, L., CHILLA, S., HEINEMANN, A., WANNER, N., LIU, S., BRAUN, F., LU, S., PFEFFERLE, S., SCHRÖDER, A. S., EDLER, C., GROSS, O., GLATZEL, M., WICHMANN, D., WIECH, T., KLUGE, S., PUESCHEL, K., AEPFELBACHER, M. & HUBER, T. B. 2020. Multiorgan and Renal Tropism of SARS-CoV-2. *N Engl J Med,* 383**,** 590-592.

QI, H., LIU, B., WANG, X. & ZHANG, L. 2022. The humoral response and antibodies against SARS-CoV-2 infection. *Nature Immunology,* 23**,** 1008-1020.

RADERMECKER, C., DETREMBLEUR, N., GUIOT, J., CAVALIER, E., HENKET, M., D'EMAL, C., VANWINGE, C., CATALDO, D., OURY, C. & DELVENNE, P. 2020. Neutrophil extracellular traps infiltrate the lung airway, interstitial, and vascular compartments in severe COVID-19. *Journal of Experimental Medicine,* 217.

RATCLIFFE, D. R., NOLIN, S. L. & CRAMER, E. B. 1988. Neutrophil interaction with influenza-infected epithelial cells. *Blood,* 72**,** 142-9.

RCP 2017. National Early Warning Score (NEWS) 2.

RICE, T. W., WHEELER, A. P., BERNARD, G. R., HAYDEN, D. L., SCHOENFELD, D. A. & WARE, L. B. 2007. Comparison of the Spo2/Fio2 Ratio and the Pao2/Fio2 Ratio in Patients With Acute Lung Injury or ARDS. *Chest,* 132**,** 410-417.

ROBINSON, J. J., WATSON, F., BUCKNALL, R. C. & EDWARDS, S. W. 1994. Role of Fc gamma receptors in the activation of neutrophils by soluble and insoluble immunoglobulin aggregates isolated from the synovial fluid of patients with rheumatoid arthritis. *Ann Rheum Dis,* 53**,** 515-20.

ROSAS, I. O., BRÄU, N., WATERS, M., GO, R. C., HUNTER, B. D., BHAGANI, S., SKIEST, D., AZIZ, M. S., COOPER, N., DOUGLAS, I. S., SAVIC, S., YOUNGSTEIN, T., DEL SORBO, L., CUBILLO GRACIAN, A., DE LA ZERDA, D. J., USTIANOWSKI, A., BAO, M., DIMONACO, S., GRAHAM, E., MATHARU, B., SPOTSWOOD, H., TSAI, L. & MALHOTRA, A. 2021. Tocilizumab in Hospitalized Patients with Severe Covid-19 Pneumonia. *N Engl J Med,* 384**,** 1503-1516.

ROSE JR, C. E., SUNG, S. S. J. & FU, S. M. 2003. Significant involvement of CCL2 (MCP-1) in inflammatory disorders of the lung. *Microcirculation,* 10**,** 273-288.

ROSENBLOOM, A. J., PINSKY, M. R., NAPOLITANO, C., NGUYEN, T. S., LEVANN, D., PENCOSKY, N., DORRANCE, A., RAY, B. K. & WHITESIDE, T. 1999. Suppression of cytokine-mediated beta2-integrin activation on circulating neutrophils in critically ill patients. *J Leukoc Biol,* 66**,** 83-9.

SADIK, C. D., KIM, N. D. & LUSTER, A. D. 2011. Neutrophils cascading their way to inflammation. *Trends Immunol,* 32**,** 452-60.

SALAHUDEEN, A. A., CHOI, S. S., RUSTAGI, A., ZHU, J., VAN UNEN, V., DE LA, O. S., FLYNN, R. A., MARGALEF-CATALÀ, M., SANTOS, A. J. M., JU, J., BATISH, A., USUI, T., ZHENG, G. X. Y., EDWARDS, C. E., WAGAR, L. E., LUCA, V., ANCHANG, B., NAGENDRAN, M., NGUYEN, K., HART, D. J., TERRY, J. M., BELGRADER, P., ZIRALDO, S. B., MIKKELSEN, T. S., HARBURY, P. B., GLENN, J. S., GARCIA, K. C., DAVIS, M. M., BARIC, R. S., SABATTI, C., AMIEVA, M. R., BLISH, C. A., DESAI, T. J. & KUO, C. J. 2020. Progenitor identification and SARS-CoV-2 infection in human distal lung organoids. *Nature,* 588**,** 670-675.

SAMARASINGHE, R. A., WITCHELL, S. F. & DEFRANCO, D. B. 2012. Cooperativity and complementarity: synergies in non-classical and classical glucocorticoid signaling. *Cell cycle,* 11**,** 2819-2827.

SAPEY, E., GALLIER, S., MAINEY, C., NIGHTINGALE, P., MCNULTY, D., CROTHERS, H., EVISON, F., REEVES, K., PAGANO, D. & DENNISTON, A. K. 2020. Ethnicity and risk of death in patients hospitalised for COVID-19 infection in the UK: an observational cohort study in an urban catchment area. *BMJ open respiratory research,* 7**,** e000644.

SAPEY, E., GREENWOOD, H., WALTON, G., MANN, E., LOVE, A., AARONSON, N., INSALL, R. H., STOCKLEY, R. A. & LORD, J. M. 2014. Phosphoinositide 3-kinase inhibition restores neutrophil accuracy in the elderly: toward targeted treatments for immunosenescence. *Blood,* 123**,** 239-48.

SAPEY, E., PATEL, J. M., GREENWOOD, H. L., WALTON, G. M., HAZELDINE, J., SADHRA, C., PAREKH, D., DANCER, R. C., NIGHTINGALE, P. & LORD, J. M. 2017. Pulmonary infections in the elderly lead to impaired neutrophil targeting, which is improved by simvastatin. *American journal of respiratory and critical care medicine,* 196**,** 1325-1336.

SAPEY, E., STOCKLEY, J. A., GREENWOOD, H., AHMAD, A., BAYLEY, D., LORD, J. M., INSALL, R. H. & STOCKLEY, R. A. 2011. Behavioral and structural differences in migrating peripheral neutrophils from patients with chronic obstructive pulmonary disease. *American journal of respiratory and critical care medicine,* 183**,** 1176-1186.

SAPEY, E. & STOCKLEY, R. A. 2014. Red, amber and green: the role of the lung in de-priming active systemic neutrophils. *Thorax,* 69**,** 606-8.

SAVCHENKO, A., MARTINOD, K., SEIDMAN, M., WONG, S., BORISSOFF, J., PIAZZA, G., LIBBY, P., GOLDHABER, S., MITCHELL, R. & WAGNER, D. 2014. Neutrophil extracellular traps form predominantly during the organizing stage of human venous thromboembolism development. *Journal of Thrombosis and Haemostasis,* 12**,** 860-870.

SCHAUER, C., JANKO, C., MUNOZ, L. E., ZHAO, Y., KIENHÖFER, D., FREY, B., LELL, M., MANGER, B., RECH, J. & NASCHBERGER, E. 2014. Aggregated neutrophil extracellular traps limit inflammation by degrading cytokines and chemokines. *Nature medicine,* 20**,** 511-517.

SCHOLZ, M., CINATL, J., SCHÄDEL-HÖPFNER, M. & WINDOLF, J. 2007. Neutrophils and the blood–brain barrier dysfunction after trauma. *Medicinal research reviews,* 27**,** 401-416.

SCHÖNRICH, G. & RAFTERY, M. J. 2016. Neutrophil Extracellular Traps Go Viral. *Front Immunol,* 7**,** 366.

SCHULTE-SCHREPPING, J., REUSCH, N., PACLIK, D., BASSLE, K., SCHLICKEISER, S., ZHANG, B., KRÄMER, B., KRAMMER, T., BRUMHARD, S. & BONAGURO, L. 2020. Severe COVID-19 is marked by a dysregulated myeloid cell compartment. *Cell,* 182**,** 1419-1440. e23.

SCHWARZENBERGER, P., HUANG, W., YE, P., OLIVER, P., MANUEL, M., ZHANG, Z., BAGBY, G., NELSON, S. & KOLLS, J. K. 2000. Requirement of endogenous stem cell factor and granulocyte-colony-stimulating factor for IL-17-mediated granulopoiesis. *The Journal of Immunology,* 164**,** 4783-4789.

SEEBACH, J. D., MORANT, R., RÜEGG, R., SEIFERT, B. & FEHR, J. 1997. The diagnostic value of the neutrophil left shift in predicting inflammatory and infectious disease. *Am J Clin Pathol,* 107**,** 582-91.

SEGAL, A. W., GEISOW, M., GARCIA, R., HARPER, A. & MILLER, R. 1981. The respiratory burst of phagocytic cells is associated with a rise in vacuolar pH. *Nature,* 290**,** 406-9.

SETTE, A. & CROTTY, S. 2021. Adaptive immunity to SARS-CoV-2 and COVID-19. *Cell,* 184**,** 861-880.

SEYMOUR, C. W., LIU, V. X., IWASHYNA, T. J., BRUNKHORST, F. M., REA, T. D., SCHERAG, A., RUBENFELD, G., KAHN, J. M., SHANKAR-HARI, M., SINGER, M., DEUTSCHMAN, C. S., ESCOBAR, G. J. & ANGUS, D. C. 2016. Assessment of Clinical Criteria for Sepsis: For the Third International Consensus Definitions for Sepsis and Septic Shock (Sepsis-3). *JAMA,* 315**,** 762-774.

SHACKELFORD, P. G. & FEIGIN, R. D. 1973. Periodicity of susceptibility to pneumococcal infection: influence of light and adrenocortical secretions. *Science,* 182**,** 285-7.

SHAH, R. D. & WUNDERINK, R. G. 2017. Viral Pneumonia and Acute Respiratory Distress Syndrome. *Clin Chest Med,* 38**,** 113-125.

SHEPPARD, F. R., KELHER, M. R., MOORE, E. E., MCLAUGHLIN, N. J., BANERJEE, A. & SILLIMAN, C. C. 2005. Structural organization of the neutrophil NADPH oxidase: phosphorylation and translocation during priming and activation. *Journal of leukocyte biology,* 78**,** 1025-1042.

SHIMOTAKAHARA, A., KUEBLER, J. F., VIETEN, G., KOS, M., METZELDER, M. L. & URE, B. M. 2008. Carbon dioxide directly suppresses spontaneous migration, chemotaxis, and free radical production of human neutrophils. *Surg Endosc,* 22**,** 1813-7.

SIGURDSSON, M. I., SIGVALDASON, K., GUNNARSSON, T. S., MOLLER, A. & SIGURDSSON, G. H. 2013. Acute respiratory distress syndrome: nationwide changes in incidence, treatment and mortality over 23 years. *Acta Anaesthesiol Scand,* 57**,** 37-45.

SINHA, P., DELUCCHI, K. L., MCAULEY, D. F., O'KANE, C. M., MATTHAY, M. A. & CALFEE, C. S. 2020. Development and validation of parsimonious algorithms to classify acute respiratory distress syndrome phenotypes: a secondary analysis of randomised controlled trials. *Lancet Respir Med,* 8**,** 247-257.

SKENDROS, P., MITSIOS, A., CHRYSANTHOPOULOU, A., MASTELLOS, D. C., METALLIDIS, S., RAFAILIDIS, P., NTINOPOULOU, M., SERTARIDOU, E., TSIRONIDOU, V. & TSIGALOU, C. 2020a. Complement and tissue factor–enriched neutrophil extracellular traps are key drivers in COVID-19 immunothrombosis. *The Journal of clinical investigation,* 130**,** 6151-6157.

SKENDROS, P., MITSIOS, A., CHRYSANTHOPOULOU, A., MASTELLOS, D. C., METALLIDIS, S., RAFAILIDIS, P., NTINOPOULOU, M., SERTARIDOU, E., TSIRONIDOU, V., TSIGALOU, C., TEKTONIDOU, M., KONSTANTINIDIS, T., PAPAGORAS, C., MITROULIS, I., GERMANIDIS, G., LAMBRIS, J. D. & RITIS, K. 2020b. Complement and tissue factor-enriched neutrophil extracellular traps are key drivers in COVID-19 immunothrombosis. *J Clin Invest,* 130**,** 6151-6157.

SSEMAGANDA, A., KINDINGER, L., BERGIN, P., NIELSEN, L., MPENDO, J., SSETAALA, A., KIWANUKA, N., MUNDER, M., TEOH, T. G., KROPF, P. & MÜLLER, I. 2014. Characterization of neutrophil subsets in healthy human pregnancies. *PLoS One,* 9**,** e85696.

STARR, T. N., GREANEY, A. J., DINGENS, A. S. & BLOOM, J. D. 2021. Complete map of SARS-CoV-2 RBD mutations that escape the monoclonal antibody LY-CoV555 and its cocktail with LY-CoV016. *Cell Rep Med,* 2**,** 100255.

STATISTICS, O. O. N. 2022. *Coronavirus (COVID-19) latest insights: Hospitals* [Online]. Available: https://www.ons.gov.uk/peoplepopulationandcommunity/healthandsocialcare/conditionsanddiseases/articles/coronaviruscovid19latestinsights/hospitals [Accessed 16/11/2022 2022].

STEPHENS, L., ELLSON, C. & HAWKINS, P. 2002. Roles of PI3Ks in leukocyte chemotaxis and phagocytosis. *Current opinion in cell biology,* 14**,** 203-213.

STEVENS, T., EKHOLM, K., GRÄNSE, M., LINDAHL, M., KOZMA, V., JUNGAR, C., OTTOSSON, T., FALK-HÅKANSSON, H., CHURG, A. & WRIGHT, J. L. 2011. AZD9668: pharmacological characterization of a novel oral inhibitor of neutrophil elastase. *Journal of Pharmacology and Experimental Therapeutics,* 339**,** 313-320.

STOCKLEY, J. A., WALTON, G. M., LORD, J. M. & SAPEY, E. 2013. Aberrant neutrophil functions in stable chronic obstructive pulmonary disease: the neutrophil as an immunotherapeutic target. *International immunopharmacology,* 17**,** 1211-1217.

SUMMERS, C., RANKIN, S. M., CONDLIFFE, A. M., SINGH, N., PETERS, A. M. & CHILVERS, E. R. 2010. Neutrophil kinetics in health and disease. *Trends Immunol,* 31**,** 318-24.

SURATT, B. T., PETTY, J. M., YOUNG, S. K., MALCOLM, K. C., LIEBER, J. G., NICK, J. A., GONZALO, J.-A., HENSON, P. M. & WORTHEN, G. S. 2004. Role of the CXCR4/SDF-1 chemokine axis in circulating neutrophil homeostasis. *Blood,* 104**,** 565-571.

SURYAWANSHI, R. K., KOGANTI, R., AGELIDIS, A., PATIL, C. D. & SHUKLA, D. 2021. Dysregulation of cell signaling by SARS-CoV-2. *Trends in microbiology,* 29**,** 224-237.

TAK, T., TESSELAAR, K., PILLAY, J., BORGHANS, J. A. & KOENDERMAN, L. 2013. What's your age again? Determination of human neutrophil half-lives revisited. *Journal of leukocyte biology,* 94**,** 595-601.

TATE, M. D., DENG, Y. M., JONES, J. E., ANDERSON, G. P., BROOKS, A. G. & READING, P. C. 2009. Neutrophils ameliorate lung injury and the development of severe disease during influenza infection. *J Immunol,* 183**,** 7441-50.

TATE, M. D., IOANNIDIS, L. J., CROKER, B., BROWN, L. E., BROOKS, A. G. & READING, P. C. 2011. The role of neutrophils during mild and severe influenza virus infections of mice. *PloS one,* 6**,** e17618.

TCHALLA, E. Y. I., BHALLA, M., WOHLFERT, E. A. & BOU GHANEM, E. N. 2020. Neutrophils Are Required During Immunization With the Pneumococcal Conjugate Vaccine for Protective Antibody Responses and Host Defense Against Infection. *J Infect Dis,* 222**,** 1363-1370.

THOMPSON, A. B., DAUGHTON, D., ROBBINS, R. A., GHAFOURI, M. A., OEHLERKING, M. & RENNARD, S. I. 1989. Intraluminal airway inflammation in chronic bronchitis. *Am Rev Respir Dis,* 140**,** 1527-1537.

THUKKANI, A. K., ALBERT, C. J., WILDSMITH, K. R., MESSNER, M. C., MARTINSON, B. D., HSU, F.-F. & FORD, D. A. 2003. Myeloperoxidase-derived reactive chlorinating species from human monocytes target plasmalogens in low density lipoprotein. *Journal of Biological Chemistry,* 278**,** 36365-36372.

TJABRINGA, G. S., RABE, K. F. & HIEMSTRA, P. S. 2005. The human cathelicidin LL-37: a multifunctional peptide involved in infection and inflammation in the lung. *Pulm Pharmacol Ther,* 18**,** 321-7.

TORJESEN, I. 2021. Covid-19: Delta variant is now UK's most dominant strain and spreading through schools. British Medical Journal Publishing Group.

TOUMAN, A., KAHYAT, M., BULKHI, A., KHAIRO, M., ALYAMANI, W., ALDOBYANY, A. M., GHALEB, N., ASHI, H., ALSOBAIE, M. & ALQURASHI, E. 2022. Post COVID-19 chronic parenchymal lung changes. *Cureus,* 14.

TRIPATHI, S., VERMA, A., KIM, E. J., WHITE, M. R. & HARTSHORN, K. L. 2014. LL-37 modulates human neutrophil responses to influenza A virus. *J Leukoc Biol,* 96**,** 931-8.

TUMPEY, T. M., GARCÍA-SASTRE, A., TAUBENBERGER, J. K., PALESE, P., SWAYNE, D. E., PANTIN-JACKWOOD, M. J., SCHULTZ-CHERRY, S., SOLÓRZANO, A., VAN ROOIJEN, N., KATZ, J. M. & BASLER, C. F. 2005. Pathogenicity of influenza viruses with genes from the 1918 pandemic virus: functional roles of alveolar macrophages and neutrophils in limiting virus replication and mortality in mice. *J Virol,* 79**,** 14933-44.

UK, O. O. N. S. 2023. *Prevalence of ongoing symptoms following coronavirus (COVID-19 infection in the UK* [Online]. Available: https://www.ons.gov.uk/peoplepopulationandcommunity/healthandsocialcare/conditionsanddiseases/bulletins/prevalenceofongoingsymptomsfollowingcoronaviruscovid19infectionintheuk/1april2021 [Accessed].

URIBE-QUEROL, E. & ROSALES, C. 2020. Phagocytosis: our current understanding of a universal biological process. *Frontiers in immunology,* 11**,** 1066.

V'KOVSKI, P., KRATZEL, A., STEINER, S., STALDER, H. & THIEL, V. 2021. Coronavirus biology and replication: implications for SARS-CoV-2. *Nature Reviews Microbiology,* 19**,** 155-170.

VAN DEN BERG, C. W., TAMBOURGI, D. V., CLARK, H. W., HOONG, S. J., SPILLER, O. B. & MCGREAL, E. P. 2014. Mechanism of neutrophil dysfunction: neutrophil serine proteases cleave and inactivate the C5a receptor. *The Journal of Immunology,* 192**,** 1787-1795.

VAN DOREMALEN, N., BUSHMAKER, T., MORRIS, D. H., HOLBROOK, M. G., GAMBLE, A., WILLIAMSON, B. N., TAMIN, A., HARCOURT, J. L., THORNBURG, N. J. & GERBER, S. I. 2020. Aerosol and surface stability of SARS-CoV-2 as compared with SARS-CoV-1. *New England journal of medicine,* 382**,** 1564-1567.

VAN GOETHEM, N., CHUNG, P. Y. J., MEURISSE, M., VANDROMME, M., DE MOT, L., BRONDEEL, R., STOUTEN, V., KLAMER, S., CUYPERS, L., BRAEYE, T., CATTEAU, L., NEVEJAN, L., VAN LOENHOUT, J. A. F. & BLOT, K. 2022. Clinical Severity of SARS-CoV-2 Omicron Variant Compared with Delta among Hospitalized COVID-19 Patients in Belgium during Autumn and Winter Season 2021–2022. *Viruses,* 14**,** 1297.

VAN KEYMEULEN, A., WONG, K., KNIGHT, Z. A., GOVAERTS, C., HAHN, K. M., SHOKAT, K. M. & BOURNE, H. R. 2006. To stabilize neutrophil polarity, PIP3 and Cdc42 augment RhoA activity at the back as well as signals at the front. *The Journal of cell biology,* 174**,** 437-445.

VAN LOCHEM, E. G., VAN DER VELDEN, V. H., WIND, H. K., TE MARVELDE, J. G., WESTERDAAL, N. A. & VAN DONGEN, J. J. 2004. Immunophenotypic differentiation patterns of normal hematopoiesis in human bone marrow: reference patterns for age-related changes and disease-induced shifts. *Cytometry B Clin Cytom,* 60**,** 1-13.

VAN OVERVELD, F. J., DEMKOW, U. A., GÓRECKA, D., ZIELINSKI, J. & DE BACKER, W. A. 2003. Inhibitory capacity of different steroids on neutrophil migration across a bilayer of endothelial and bronchial epithelial cells. *Eur J Pharmacol,* 477**,** 261-7.

VAN STRIJP, J. A., VAN KESSEL, K. P., VAN DER TOL, M. E., FLUIT, A. C., SNIPPE, H. & VERHOEF, J. 1989. Phagocytosis of herpes simplex virus by human granulocytes and monocytes. *Arch Virol,* 104**,** 287-98.

VANHAESEBROECK, B., GUILLERMET-GUIBERT, J., GRAUPERA, M. & BILANGES, B. 2010. The emerging mechanisms of isoform-specific PI3K signalling. *Nature reviews Molecular cell biology,* 11**,** 329-341.

VANICHAKARN, P., BLAIR, P., WU, C., FREEDMAN, J. E. & CHAKRABARTI, S. 2008. Neutrophil CD40 enhances platelet-mediated inflammation. *Thrombosis research,* 122**,** 346-358.

VERAS, F. P., PONTELLI, M. C., SILVA, C. M., TOLLER-KAWAHISA, J. E., DE LIMA, M., NASCIMENTO, D. C., SCHNEIDER, A. H., CAETITÉ, D., TAVARES, L. A. & PAIVA, I. M. 2020. SARS-CoV-2–triggered neutrophil extracellular traps mediate COVID-19 pathology. *Journal of Experimental Medicine,* 217.

VIRCHOW, R. 2022. *Gesammelte abhandlungen zur wissenschaftlichen medicin*, BoD–Books on Demand.

VITTE, J., DIALLO, A. B., BOUMAZA, A., LOPEZ, A., MICHEL, M., ALLARDET-SERVENT, J., MEZOUAR, S., SEREME, Y., BUSNEL, J.-M. & MILOUD, T. 2020. A granulocytic signature identifies COVID-19 and its severity. *The Journal of infectious diseases,* 222**,** 1985-1996.

VOLS, S., SIONOV, R. V. & GRANOT, Z. 2017. Always Look On the Bright Side: Anti-Tumor Functions of Neutrophils. *Curr Pharm Des,* 23**,** 4862-4892.

VOROBJEVA, N. & CHERNYAK, B. 2020. NETosis: molecular mechanisms, role in physiology and pathology. *Biochemistry (Moscow),* 85**,** 1178-1190.

VUORTE, J., JANSSON, S. E. & REPO, H. 2001. Evaluation of red blood cell lysing solutions in the study of neutrophil oxidative burst by the DCFH assay. *Cytometry,* 43**,** 290-6.

WALSH, K. A., JORDAN, K., CLYNE, B., ROHDE, D., DRUMMOND, L., BYRNE, P., AHERN, S., CARTY, P. G., O'BRIEN, K. K., O'MURCHU, E., O'NEILL, M., SMITH, S. M., RYAN, M. & HARRINGTON, P. 2020. SARS-CoV-2 detection, viral load and infectivity over the course of an infection. *J Infect,* 81**,** 357-371.

WANG, F. 2009. The signaling mechanisms underlying cell polarity and chemotaxis. *Cold Spring Harbor perspectives in biology,* 1**,** a002980.

WANG, Y., QU, K., LU, W., ZHAO, P., WANG, Z., CUI, C., LIU, Y., YANG, M., YU, Y. & WANG, L. 2022. Neutrophils recruited to immunization sites initiating vaccine-induced antibody responses by locally expressing BAFF. *iScience,* 25**,** 104453.

WATANABE, Y., HASHIMOTO, Y., SHIRATSUCHI, A., TAKIZAWA, T. & NAKANISHI, Y. 2005. Augmentation of fatality of influenza in mice by inhibition of phagocytosis. *Biochem Biophys Res Commun,* 337**,** 881-6.

WEIJTENS, O., VAN DER SLUIJS, F. A., SCHOEMAKER, R. C., LENTJES, E. G., COHEN, A. F., ROMIJN, F. P. & VAN MEURS, J. C. 1997. Peribulbar corticosteroid injection: vitreal and serum concentrations after dexamethasone disodium phosphate injection. *Am J Ophthalmol,* 123**,** 358-63.

WHO 2020. Clinical Management of severe acute respiratory infection (SARI) when COVID-19 disease is suspected.

WHO. 2023a. *COVID-19 epidemiological update - 22 December 2023* [Online]. Available: https://www.who.int/publications/m/item/covid-19-epidemiological-update---22-december-2023 [Accessed].

WHO. 2023b. *WHO Coronavirus (COVID-19) Dashboard* [Online]. Available: https://covid19.who.int/ [Accessed February 2023 2023].

WHYTE, M. B., KELLY, P. A., GONZALEZ, E., ARYA, R. & ROBERTS, L. N. 2020. Pulmonary embolism in hospitalised patients with COVID-19. *Thrombosis research,* 195**,** 95-99.

WILK, A. J., RUSTAGI, A., ZHAO, N. Q., ROQUE, J., MARTÍNEZ-COLÓN, G. J., MCKECHNIE, J. L., IVISON, G. T., RANGANATH, T., VERGARA, R. & HOLLIS, T. 2020. A single-cell atlas of the peripheral immune response in patients with severe COVID-19. *Nature medicine,* 26**,** 1070-1076.

WILKINSON, E. 2020. RECOVERY trial: the UK covid-19 study resetting expectations for clinical trials. *Bmj,* 369.

WILLSON, J. A., ARIENTI, S., SADIKU, P., REYES, L., COELHO, P., MORRISON, T., RINALDI, G., DOCKRELL, D. H., WHYTE, M. K. & WALMSLEY, S. R. 2022. Neutrophil HIF-1α stabilization is augmented by mitochondrial ROS produced via the glycerol 3-phosphate shuttle. *Blood, The Journal of the American Society of Hematology,* 139**,** 281-286.

WOODFIN, A., BEYRAU, M., VOISIN, M. B., MA, B., WHITEFORD, J. R., HORDIJK, P. L., HOGG, N. & NOURSHARGH, S. 2016. ICAM-1-expressing neutrophils exhibit enhanced effector functions in murine models of endotoxemia. *Blood,* 127**,** 898-907.

WOODFIN, A., VOISIN, M.-B., IMHOF, B. A., DEJANA, E., ENGELHARDT, B. & NOURSHARGH, S. 2009. Endothelial cell activation leads to neutrophil transmigration as supported by the sequential roles of ICAM-2, JAM-A, and PECAM-1. *Blood, The Journal of the American Society of Hematology,* 113**,** 6246-6257.

WOODFIN, A., VOISIN, M. B., BEYRAU, M., COLOM, B., CAILLE, D., DIAPOULI, F. M., NASH, G. B., CHAVAKIS, T., ALBELDA, S. M., RAINGER, G. E., MEDA, P., IMHOF, B. A. & NOURSHARGH, S. 2011. The junctional adhesion molecule JAM-C regulates polarized transendothelial migration of neutrophils in vivo. *Nat Immunol,* 12**,** 761-9.

WRIGHT, H. L., CROSS, A. L., EDWARDS, S. W. & MOOTS, R. J. 2014. Effects of IL-6 and IL-6 blockade on neutrophil function in vitro and in vivo. *Rheumatology,* 53**,** 1321-1331.

WU, M., CHEN, Y., XIA, H., WANG, C., TAN, C. Y., CAI, X., LIU, Y., JI, F., XIONG, P. & LIU, R. 2020. Transcriptional and proteomic insights into the host response in fatal COVID-19 cases. *Proceedings of the National Academy of Sciences,* 117**,** 28336-28343.

YACOUB, A. T., MOJICA, L., JONES, L., KNAB, A., ALRABAA, S. & GREENE, J. 2014. The Role of Corticosteroids in Adult Respiratory Distress Syndrome caused by Viridans Group Streptococci Bacteremia in Neutropenic Patients. *Mediterr J Hematol Infect Dis,* 6**,** e2014055.

YAGO, T., SHAO, B., MINER, J. J., YAO, L., KLOPOCKI, A. G., MAEDA, K., COGGESHALL, K. M. & MCEVER, R. P. 2010. E-selectin engages PSGL-1 and CD44 through a common signaling pathway to induce integrin αLβ2-mediated slow leukocyte rolling. *Blood, The Journal of the American Society of Hematology,* 116**,** 485-494.

YAMADA, K., YANAGIHARA, K., ARAKI, N., HARADA, Y., MORINAGA, Y., IZUMIKAWA, K., KAKEYA, H., YAMAMOTO, Y., HASEGAWA, H. & KOHNO, S. 2011. In vivo efficacy of KRP-109, a novel elastase inhibitor, in a murine model of severe pneumococcal pneumonia. *Pulmonary Pharmacology & Therapeutics,* 24**,** 660-665.

YANG, A.-P., LIU, J.-P., TAO, W.-Q. & LI, H.-M. 2020. The diagnostic and predictive role of NLR, d-NLR and PLR in COVID-19 patients. *International immunopharmacology,* 84**,** 106504.

YANG, C. W., STRONG, B. S., MILLER, M. J. & UNANUE, E. R. 2010. Neutrophils influence the level of antigen presentation during the immune response to protein antigens in adjuvants. *J Immunol,* 185**,** 2927-34.

YASUI, S., NAGAI, A., AOSHIBA, K., OZAWA, Y., KAKUTA, Y. & KONNO, K. 1995. A specific neutrophil elastase inhibitor (ONO-5046. Na) attenuates LPS-induced acute lung inflammation in the hamster. *European Respiratory Journal,* 8**,** 1293-1299.

YATIM, N., BOUSSIER, J., CHOCRON, R., HADJADJ, J., PHILIPPE, A., GENDRON, N., BARNABEI, L., CHARBIT, B., SZWEBEL, T.-A. & CARLIER, N. 2021. Platelet activation in critically ill COVID-19 patients. *Annals of intensive care,* 11**,** 1-12.

ZENTAY, Z., SHARAF, M., QADIR, M., DRAFTA, D. & DAVIDSON, D. 1999. Mechanism for dexamethasone inhibition of neutrophil migration upon exposure to lipopolysaccharide in vitro: role of neutrophil interleukin-8 release. *Pediatric research,* 46**,** 406-406.

ZHANG, G., HU, C., LUO, L., FANG, F., CHEN, Y., LI, J., PENG, Z. & PAN, H. 2020a. Clinical features and short-term outcomes of 221 patients with COVID-19 in Wuhan, China. *Journal of Clinical Virology,* 127**,** 104364.

ZHANG, H., ZHOU, P., WEI, Y., YUE, H., WANG, Y., HU, M., ZHANG, S., CAO, T., YANG, C. & LI, M. 2020b. Histopathologic changes and SARS-CoV-2 immunostaining in the lung of a patient with COVID-19. *Annals of internal medicine,* 172**,** 629-632.

ZHANG, R. & MYLONAKIS, E. 2021. In inpatients with COVID-19, none of remdesivir, hydroxychloroquine, lopinavir, or interferon β-1a differed from standard care for in-hospital mortality. *Ann Intern Med,* 174**,** Jc17.

ZHOU, F., YU, T., DU, R., FAN, G., LIU, Y., LIU, Z., XIANG, J., WANG, Y., SONG, B., GU, X., GUAN, L., WEI, Y., LI, H., WU, X., XU, J., TU, S., ZHANG, Y., CHEN, H. & CAO, B. 2020. Clinical course and risk factors for mortality of adult inpatients with COVID-19 in Wuhan, China: a retrospective cohort study. *Lancet,* 395**,** 1054-1062.

ZHU, C. L., XIE, J., ZHAO, Z. Z., LI, P., LIU, Q., GUO, Y., MENG, Y., WAN, X. J., BIAN, J. J., DENG, X. M. & WANG, J. F. 2022. PD-L1 maintains neutrophil extracellular traps release by inhibiting neutrophil autophagy in endotoxin-induced lung injury. *Front Immunol,* 13**,** 949217.

ZHU, X., GE, Y., WU, T., ZHAO, K., CHEN, Y., WU, B., ZHU, F., ZHU, B. & CUI, L. 2020. Co-infection with respiratory pathogens among COVID-2019 cases. *Virus Res,* 285**,** 198005.

ZUO, Y., YALAVARTHI, S., SHI, H., GOCKMAN, K., ZUO, M., MADISON, J. A., BLAIR, C., WEBER, A., BARNES, B. J. & EGEBLAD, M. 2020. Neutrophil extracellular traps in COVID-19. *JCI insight,* 5.

ZUO, Y., ZUO, M., YALAVARTHI, S., GOCKMAN, K., MADISON, J. A., SHI, H., WOODARD, W., LEZAK, S. P., LUGOGO, N. L. & KNIGHT, J. S. 2021. Neutrophil extracellular traps and thrombosis in COVID-19. *Journal of Thrombosis and Thrombolysis,* 51**,** 446-453.